

RECEIVED
MAR 02 2010
Texas Water Development Board

Texas Water Development Board Report

Final

Hydrostratigraphy of the Gulf Coast Aquifer from the Brazos River to the Rio Grande

by
Steven C Young, Ph.D., P.E., P.G.
Trevor Budge, Ph.D
URS Corporation

Paul R. Knox, P.G.
Robert Kalbouss
Baer Engineering and Environmental Consulting, Incorporated

Ernie Baker, P. G.

Scott Hamlin, Ph.D., P.G.

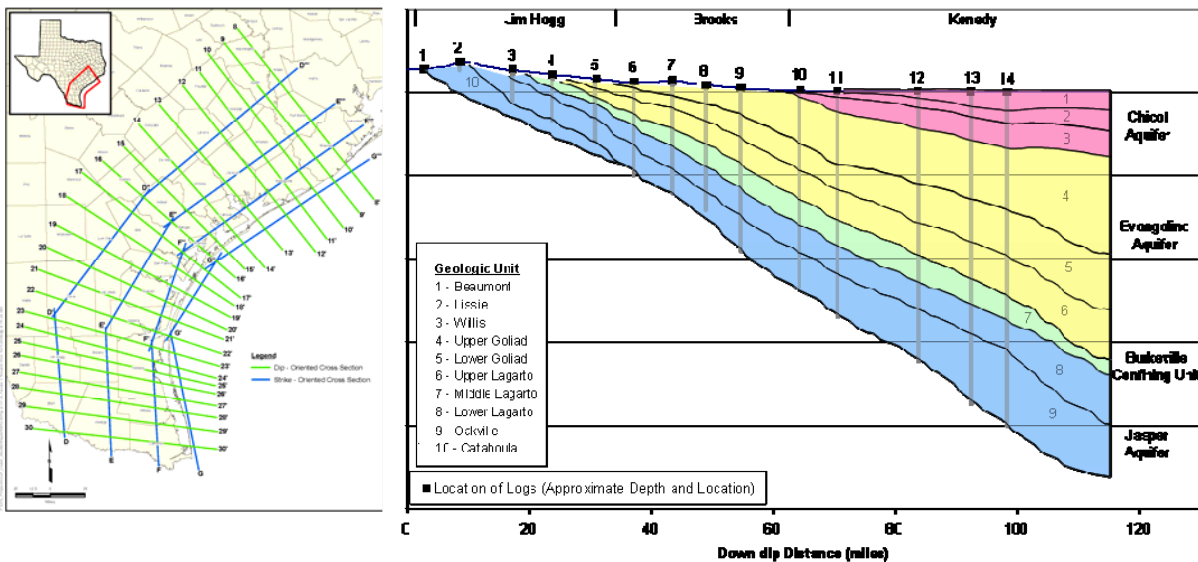
Bill Galloway, Ph.D., P.G.,

Neil Deeds, Ph.D, P.E.
INTERA, Incorporated

February 2010

Final

Hydrostratigraphy of the Gulf Coast Aquifer from the Brazos River to the Rio Grande



Report ###

by

Steven C. Young, Ph.D., P.E., P.G.

Paul R. Knox, P.G.

Ernie Baker, P.G.

Trevor Budge, Ph.D.

Scott Hamlin, Ph.D, P.G.

Bill Galloway, Ph.D., P.G.

Rob Kalbouss

Neil Deeds, Ph.D, P.E.

Texas Water Development Board

P.O. Box 13231, Capitol Station, Austin, TX 78711-3231

February 2010

Texas Water Development Board Report

Final

Hydrostratigraphy of the Gulf Coast Aquifer from the Brazos River to the Rio Grande

by
Steven C Young, Ph.D., P.E., P.G.
Trevor Budge, Ph.D
URS Corporation

Paul R. Knox, P.G.
Robert Kalbouss
Baer Engineering and Environmental Consulting, Incorporated

Ernie Baker, P. G.

Scott Hamlin, Ph.D., P.G.

Bill Galloway, Ph.D., P.G.,

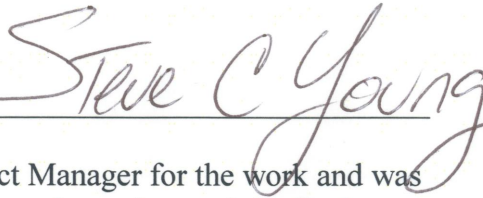
Neil Deeds, Ph.D, P.E.
INTERA, Incorporated

February 2010

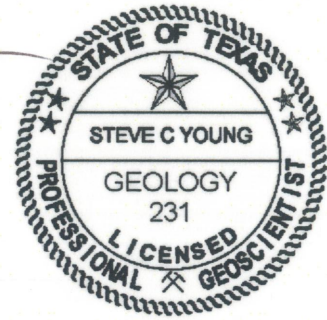
Geoscientist seal

This report documents the work of the following Licensed Geoscientists:

Steve C. Young, P.G.



Dr. Young was the Project Manager for the work and was responsible for oversight on the project and the final interpretation of the lithologic and water quality analysis of the geophysical logs.



Paul R. Knox, P.G.



Mr. Knox was primarily responsible for developing the chronostratigraphy of the Gulf Coast Aquifer and mapping the depositional facies.

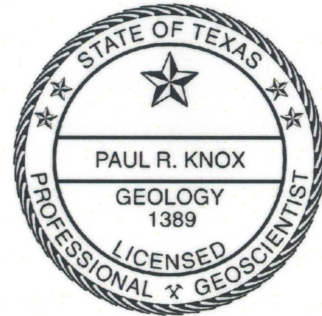


Table of Contents

1	Executive summary.....	1
2	Introduction.....	3
2.1	Approach for defining stratigraphy	3
2.2	Approach for defining lithology and generating sand maps	4
3	Gulf Coast Aquifer geologic setting.....	7
3.1	Overview	7
3.2	Structural features.....	9
3.3	Depositional systems	10
3.4	Depositional history.....	11
4	Stratigraphic and hydrogeologic framework	17
4.1	Previous studies	17
4.2	Fleming Group: Oakville and Lagarto Formations	19
4.3	Goliad Formation.....	22
4.4	Willis Formation.....	25
4.5	Lissie Formation.....	25
4.6	Beaumont Formation	26
4.7	Holocene deposits.....	27
5	Information sources	37
5.1	Geophysical logs	37
5.2	Approach for obtaining geophysical logs.....	40
5.3	Literature review	42
5.4	Geological faults.....	43
5.5	Paleontology data	43

6	Approach for stratigraphic interpretation.....	47
6.1	Chronostratigraphic conceptual framework	47
6.2	Methodology.....	49
7	Gulf Coast Aquifer stratigraphy.....	54
7.1	Chronostratigraphic surfaces and aquifer boundaries	54
7.2	Structural configuration of surfaces	55
8	Approach for lithologic interpretation	81
8.1	Lithology classification	81
8.2	Depositional facies classification	82
9	Gulf Coast Aquifer lithology	89
9.1	Sand thickness and percent.....	89
9.2	Depositional facies	91
10	Gulf Coast water quality	117
10.1	Terminology	117
10.2	Analysis of geophysical logs	118
10.3	Analysis of water well measurements	120
11	References.....	128
12	Appendix A Geophysical logs listing, including location and use	139
13	Appendix B Listing of geophysical logs stratigraphic contacts.....	167
14	Appendix C Estimated total sand thickness (ft) at each geophysical log location	181
15	Appendix D TWDB comments on draft hydrostratigraphy report and responses.....	197
15.1	General comments	197
15.2	Specific Comments.....	198

List of Figures

Figure 2-1.	Map of the study area showing the locations of the dip-oriented and strike-oriented cross-sections used to develop the stratigraphic surfaces.....	6
Figure 3-1.	Map of the Gulf of Mexico basin showing major structural elements and stratigraphic provinces. Modified from Ewing (1991).	13
Figure 3-2.	Regional dip-oriented cross section of Cenozoic strata on the northwestern margin of the Gulf of Mexico basin. Modified from Galloway et al. (1991) and Sharp et al. (1991).	13
Figure 3-3.	Map showing major growth fault zones and shallow salt domes in the onshore part of the Texas coastal zone. Modified from Ewing (1990) and Hamlin (2006).	14
Figure 3-4.	Schematic diagram showing a fluvial depositional system with its component depositional environments and resulting genetic facies. Modified from Galloway et al. (1979).	14
Figure 3-5.	Schematic drawing of Quaternary depositional systems of the Texas Coastal Plain. Modified from Winker (1979) and Galloway et al. (1986).	15
Figure 3-6.	Positions of principal fluvial-deltaic depocenters and interdeltic shorelines for selected depositional episodes, northwest GOM. Modified from Galloway (1989b) and Galloway et al. (2000).	15
Figure 3-7.	Chronostratigraphic chart of Miocene to Holocene depositional episodes, northwest GOM.	16
Figure 4-1.	Geologic map of the Texas Coastal Plain. Source: Barnes (1992).	28
Figure 4-2.	Schematic dip cross section showing relationships between outcropping formations and subsurface stratigraphy, central coastal plain, Texas. Modified from Doering (1956).	29
Figure 4-3.	Schematic cross section of lower Miocene stratigraphy showing depositional sequences and lithostratigraphic and biostratigraphic boundaries. Source: Galloway et al. (1986).	29
Figure 4-4.	Net-sandstone isopach map of the Oakville Formation also showing depositional systems. Red dotted line separates updip fluvial systems from downdip delta and shore-zone systems. Modified from Galloway et al. (1986). 30	
Figure 4-5.	Net-sandstone isopach map of the Lagarto Formation also showing depositional systems. Red dotted line separates updip fluvial systems from downdip delta and shore-zone systems. Modified from Galloway et al. (1986). 30	
Figure 4-6.	Schematic cross section of middle-upper Miocene stratigraphy showing depositional sequences and lithostratigraphic and biostratigraphic boundaries. From Morton et al. (1988).	31
Figure 4-7.	Percent sandstone maps of Goliad and equivalent middle-upper Miocene sequences. From Hoel (1982) and Morton et al. (1988).	32
Figure 4-8.	Sand content map of the Willis Formation, central coastal plain, Texas.	33
Figure 4-9.	Sand content map of the Lissie Formation, central coastal plain, Texas.	34
Figure 4-10.	Simplified environmental geologic map of the Port Lavaca, Texas area, showing Pleistocene and Holocene depositional surfaces. From McGowen et al. (1976).	35
Figure 4-11.	Sand content map of the Beaumont Formation, central coastal plain, Texas.	36

Figure 5-1.	Idealized SP and resistivity curve showing the responses corresponding to alternating sand and clay strata that are saturated with groundwater that has significant increases in total dissolved concentrations with depth. Modified from Driscoll (1986).	44
Figure 5-2.	Schematic showing the location of the Kelly Bushing relative to the ground level and the oil rig.	45
Figure 5-3.	Example of a geophysical well log that uses the American Petroleum Institute format.	45
Figure 5-4.	Location of the 915 logs used to characterize the stratigraphy and lithology of the Gulf Coast Aquifer from the Brazos to the Rio Grande.	46
Figure 6-1.	Schematic cross section showing small-scale depositional cycles (parasequences) and larger-scale sequence bounded by maximum flooding surfaces.	52
Figure 6-2.	Schematic cross section showing correlation strategies.	52
Figure 6-3.	Schematic cross section comparing (a) chronostratigraphic correlation to (b) lithostratigraphic correlation.	53
Figure 7-1.	Stratigraphic column showing correlations among age, geologic formations, hydrogeologic units, paleomarkers, and relative change of coastal onlap.	59
Figure 7-2.	Contours for the Oakville geologic unit showing: (a) base elevation and (b) thickness.	60
Figure 7-3.	Vertical cross-section of the geological units near dip section 9 in Figure 2-1.	61
Figure 7-4.	Vertical cross-section of the geological units near dip section 13 in Figure 2-1.	62
Figure 7-5.	Vertical cross-section of the geological units near dip section 16 in Figure 2-1.	63
Figure 7-6.	Vertical cross-section of the geological units near dip section 21 in Figure 2-1.	64
Figure 7-7.	Vertical cross-section of the geological units near dip section 26 in Figure 2-1.	65
Figure 7-8.	Vertical cross-section of the geological units near dip section 29 in Figure 2-1.	66
Figure 7-9.	Vertical cross-section of the geological units near strike section E-E'-E"-E"'	67
Figure 7-10.	Contours for the upper Lagarto geologic unit showing: (a) base elevation and (b) thickness.	68
Figure 7-11.	Contours for the Jasper Aquifer showing: (a) base elevation and (b) thickness.	69
Figure 7-12.	Contours for the Burkeville Confining Unit and the middle Lagarto Formation showing: (a) base elevation and (b) thickness.	70
Figure 7-13.	Contours for the upper Lagarto geologic unit showing: (a) base elevation and (b) thickness.	71
Figure 7-14.	Contours for the lower Goliad geologic unit showing: (a) base elevation and (b) thickness.	72
Figure 7-15.	Contours for the upper Goliad geologic unit showing: (a) base elevation and (b) thickness.	73
Figure 7-16.	Contours for the Evangeline Aquifer showing: (a) base elevation and (b) thickness.	74
Figure 7-17.	Contours for the Willis geologic unit showing: (a) base elevation and (b) thickness.	75
Figure 7-18.	Contours for the Lissie geologic unit showing: (a) base elevation and (b) thickness.	76
Figure 7-19.	Contours for the Beaumont geologic unit showing: (a) base elevation and (b) thickness.	77

Figure 7-20.	Contours for the Chicot Aquifer showing: (a) base elevation and (b) thickness.	78
Figure 7-21.	Schematic showing outcrop and subcrop locations of geologic units in a three-dimensional block (a) and in a map view (b).	79
Figure 7-22.	Surface geology map from Barnes (1992) showing the estimated locations of the subcrop of selected geologic units.	80
Figure 8-1.	Example calculation of net and percent sand from a spontaneous potential (SP) log curve.	85
Figure 8-2.	Example analysis of a geophysical log showing a binary and four-phase classification of lithology (taken from Young and Kelley, 2006).	86
Figure 8-3.	Example analysis of a geophysical log showing a binary and four-phase classification of lithology (taken from Young and Kelley, 2006).	87
Figure 8-4.	Example analysis of a geophysical log showing a binary and four-phase classification of lithology (taken from Young and Kelley, 2006).	88
Figure 9-1.	Map of the Chicot Aquifer showing total sand thickness.	96
Figure 9-2.	Map of the Beaumont geologic unit showing: (a) percentage sand coverage and (b) depositional facies.	97
Figure 9-3.	Map of the Beaumont geologic unit showing total sand thickness.	98
Figure 9-4.	Map of the Lissie geologic unit showing: (a) percentage sand coverage and (b) depositional facies.	99
Figure 9-5.	Map of the Lissie geologic unit showing total sand thickness.	100
Figure 9-6.	Map of the Willis geologic unit showing: (a) percentage sand coverage and (b) depositional facies.	101
Figure 9-7.	Map of the Willis geologic unit showing total sand thickness.	102
Figure 9-8.	Map of the Evangeline Aquifer showing total sand thickness.	103
Figure 9-9.	Map of the upper Goliad geologic unit showing: (a) percentage sand coverage and (b) depositional facies.	104
Figure 9-10.	Map of the upper Goliad geologic unit showing total sand thickness.	105
Figure 9-11.	Map of the lower Goliad geologic unit showing: (a) percentage sand coverage and (b) depositional facies.	106
Figure 9-12.	Map of the lower Goliad geologic unit showing total sand thickness.	107
Figure 9-13.	Map of the upper Lagarto geologic unit showing: (a) percentage sand coverage and (b) depositional facies.	108
Figure 9-14.	Map of the upper Lagarto geologic unit showing total sand thickness.	109
Figure 9-15.	Map of the Burkeville Confining Unit (middle Lagarto geologic unit) showing: (a) percentage sand coverage and (b) depositional facies.	110
Figure 9-16.	Map of the Burkeville Confining Unit (middle Lagarto geologic unit) showing total sand thickness.	111
Figure 9-17.	Map of the Jasper Aquifer showing total sand thickness.	112
Figure 9-18.	Map of the lower Lagarto geologic unit showing: (a) percentage sand coverage and (b) depositional facies.	113
Figure 9-19.	Map of the lower Lagarto showing total sand thickness.	114
Figure 9-20.	Map of the Oakville geologic unit showing: (a) percentage sand coverage and (b) depositional facies.	115
Figure 9-21.	Map of the Oakville geologic unit showing total sand thickness.	116
Figure 10-1.	Specific conductivity of salt solutions (modified from Moore, 1966).	122

Figure 10-2.	Fraction of the Chicot Aquifer estimated to be fresh water with a TDS concentration less than 1,000 ppm, as determined by the analysis of geophysical logs.....	123
Figure 10-3.	Fraction of the Evangeline Aquifer estimated to be fresh water with a TDS concentration less than 1,000 ppm, as determined by the analysis of geophysical logs.....	124
Figure 10-4.	Fraction of the Burkeville Confining Unit estimated to be fresh water with a TDS concentration less than 1,000 ppm, as determined by the analysis of geophysical logs.....	125
Figure 10-5.	Fraction of the Jasper Aquifer estimated to be fresh water with a TDS concentration less than 1,000 ppm, as determined by the analysis of geophysical logs.....	126
Figure 10-6.	Map of water well locations with at least one measurement of TDS concentrations.	127

List of Tables

Table 3-1.	Simplified stratigraphic and hydrogeologic chart of the northwestern Gulf of Mexico basin, Texas coastal zone (Galloway et al., 1991; Sharp et al., 1991).	8
Table 4-1.	Fleming Group depositional facies (Galloway et al., 1982, 1986).	20
Table 4-2.	Fleming Group depositional systems (Spradlin, 1980; Galloway, et al., 1982, 1986).	21
Table 4-3.	Goliad Formation depositional facies (Hoel, 1982).....	23
Table 4-4.	The Goliad Formation fluvial depositional systems (Hoel, 1982; Morton et al., 1988).	24
Table 5-1.	Types of log header data.....	39
Table 5-2.	Selected tables and fields from the Microsoft Access database used to manage information on the 892 well logs used for the study.	42
Table 8-1.	Description of the four textural classes used to characterize the lithology of the LSWP wells	82
Table 8-2.	Depositional Facies Definition and Predicted Flow Characteristics [modified from Table 3.1.3 in Young and Kelley (2006)]	83
Table 10-1.	Groundwater classifications based on TDS (from Collier, 1993).....	117
Table 10-2.	Relationship among TDS, specific conductivity, and resistivity (from Collier, 1993).	119
Table 10-3.	General criteria used by Mr. Baker to estimate the TDS from the geophysical logs.....	119
Table 10-4.	Aquifer codes used in Gulf Coast query.....	121

1 Executive summary

This report documents the development of the structure, lithology, and depositional framework for the Gulf Coast Aquifer system from the Brazos River to the Rio Grande. The project is part of a long-term plan to update the Groundwater Availability Models (GAMs) for the central and southern parts of the Gulf Coast Aquifer.

The structure of the Gulf Coast Aquifer system is comprised of, from shallowest to deepest, the Chicot Aquifer, the Evangeline Aquifer, the Burkeville Confining Unit, and the Jasper Aquifer, with parts of the Catahoula Formation acting as the Catahoula Confining System. In this study, aquifer units have been subdivided on the basis of chronostratigraphic correlation to yield subaquifer layers. The boundaries for the geologic units were traced from outcrop formation boundaries to identifiable flooding surfaces in the deeper subsurface, where paleontological control constrained geologic ages of surfaces at nearshore and offshore geophysical log locations.

The Chicot Aquifer subaquifer layers include, from the shallowest to deepest, the Beaumont and Lissie Formations of Pleistocene age and the Pliocene-age Willis Formation. The Evangeline Aquifer subaquifer layers include the upper Goliad Formation of earliest Pliocene and late Miocene age, the lower Goliad Formation of middle Miocene age, and the upper unit of the Lagarto Formation (a member of the Fleming Group) of middle Miocene age. The Burkeville Confining Unit is defined as the middle unit of the Lagarto Formation of middle and early Miocene age, which is the chronostratigraphic layer with the most widespread clayey interval between the Evangeline and Jasper Aquifers. For this study, the Jasper Aquifer includes the lower Lagarto unit of early Miocene age, the early Miocene Oakville sandstone member of the Fleming Group, and the sandy intervals of the Oligocene-age Catahoula Formation. Elevations from the established base Jasper surface in the Source Water Assessment Program dataset were used close to the outcrop and were merged with the chronostratigraphic base of the Oakville Sandstone defined in this study.

More than 900 geophysical logs were analyzed to define the structure and/or lithology of the Gulf Coast Aquifer system. Four hundred and fifty-seven of the logs were used in the chronostratigraphic correlations to define the surfaces for 10 of the geologic units previously listed. An appendix provides the surfaces for these geologic units along 23 dip-oriented cross-sections and 4 strike-oriented cross-sections.

With 706 geophysical logs, a continual profile of lithology was generated through the stratigraphic column for the Gulf Coast Aquifer system using a four-class system consisting of: 1) sand; 2) clay; 3) sand-with-clay; and 4) clay-with-sand. The four-class system provides more specificity than the commonly used "binary" system, which aggregates deposits into an alternating series of clay beds and sand beds. Based on the lithology, maps of sand percentages and total sand thickness maps were constructed for the Chicot, Evangeline, and Jasper Aquifers and their respective subaquifer layers.

To assist in the development of hydraulic conductivity distributions for each geologic unit, depositional facies maps were developed. The deposition facies provide information on factors

that affect groundwater flow such as the sorting, arrangement, and sizes of the particles in a deposit and how the deposit is or is not interconnected to similar and different deposits.

For each of the 706 geophysical logs used for the lithologic interpretation, an estimate of the water quality was made for each interval assigned a lithology classification. For each of these intervals, the water quality was classified as fresh, slightly saline, or moderately saline. These classifications are based on the concentration of Total Dissolved Solids (TDS). Fresh water is defined as having a TDS concentration less than 1,000 ppm. Slightly saline water has a TDS between 1,000 and 3,000 ppm, and moderately saline water has a TDS between 3,000 and 10,000 ppm.

2 Introduction

The current groundwater availability models (GAMs) for the northern region (Kasmarek and Robinson, 2004), the central region (Chowdhury and others, 2004), and the southern region (Chowdhury and Mace, 2007) of the Gulf Coast Aquifer are based on stratigraphy developed from the Source Water Assessment and Protection (SWAP) Program. For these GAMs, the Gulf Coast Aquifer includes the Chicot Aquifer, the Evangeline Aquifer, the Burkeville Confining System, and the Jasper Aquifer. One of the obstacles to improving the GAMs predictive accuracy is that the SWAP database contains limited stratigraphic and lithologic information at the scale of the geologic formations that comprise the aquifers. In a continual effort to improve the GAMs, the Texas Water Development Board (TWDB) has determined that additional stratigraphic and lithologic information beyond what is available from the SWAP data would be beneficial for improving the predictive accuracy of future GAMs.

The primary objective of this study is to provide the stratigraphic surfaces and sand thickness maps of the geological formations that compose the Gulf Coast Aquifer system from the Brazos River to the Rio Grande. For this study, the Chicot Aquifer includes, from the shallowest to deepest, the Beaumont and Lissie Formations of Pleistocene age and the Pliocene-age Willis Formation. The Evangeline Aquifer includes the upper Goliad Formation of earliest Pliocene and late Miocene age, the lower Goliad Formation of middle Miocene age, and the upper unit of the Lagarto Formation (a member of the Fleming Group) of middle Miocene age. The Burkeville Confining Unit is defined as the middle unit of the Lagarto Formation of middle and early Miocene age, which is the chronostratigraphic layer with the most widespread clayey interval between the Evangeline and Jasper Aquifers. The Jasper Aquifer includes the lower Lagarto unit of early Miocene age, the early Miocene Oakville sandstone member of the Fleming Group, and the sandy intervals of the Oligocene-age Catahoula Formation.

2.1 Approach for defining stratigraphy

Investigations of the Gulf Coast Aquifer began in the late 1880's. Since that time, numerous studies have contributed toward our understanding of the formations in that aquifer. Central to our approach are the selected studies that provide an overarching stratigraphic framework.

With regard to naming conventions, we rely on the founding work of Doering (1935), who was perhaps the first to use the nomenclature most commonly used today (from the surface downward), the Beaumont, Lissie, Willis, Goliad, Lagarto, and Oakville. With regard to nomenclature, we also reference Baker (1979). He was among the first to establish an accurate stratigraphic framework using a lithostratigraphic correlation of the Gulf Coast Aquifer that relied on good understanding of geologic processes.

With regard to defining the stratigraphy surfaces, our analysis is based on chronostratigraphic rather than lithostratigraphic correlation techniques. Lithostratigraphic correlations rely on the interpretation from well logs of formation lithologies and boundaries between different lithologies (e.g., mud on sand) and then correlating those boundaries between wells. Prior to the 1980s, lithofacies correlations were the most common technique to define stratigraphy. Since the 1980's, an improved understanding of depositional processes has shown that

lithostratigraphic correlations are more suspect for mischaracterizing the continuity and size of a formation than are chronostratigraphic correlations. Chronostratigraphic correlations focus on identifying clay-dominated flooding surfaces of the same age that form the boundaries of episodes that deposit the coarse sediment of an aquifer. As part of our approach, we used depositional facies modeling, including an analysis of depositional cyclicity, to better construct a regional framework for the flooding surfaces and the spatial variation of the aquifer-matrix properties.

Where appropriate, our sequence stratigraphy and chronostratigraphic correlations are based on the concepts and methods used by the Gulf Basin Depositional Synthesis Project (GBDS) and the LCRA-SAWS Water Project (LSWP). The GBDS project, whose principal investigator is Dr. Bill Galloway, is funded by a consortium of petroleum companies to characterize the Cenozoic depositional history of the Gulf of Mexico Basin. Among the key papers that explains some of these concepts and methods are Galloway (1989b), Galloway and others (2000), and Galloway (2005). The LSWP project included a chronostratigraphic analysis of the Chicot and Evangeline Aquifers across a 10-county region intersected by the Colorado River. Among the key papers that provide the results of the LSWP are Knox and others (2006) and Young and Kelley (2006).

Mr. Paul Knox is the geologist primarily responsible for developing the stratigraphic surfaces. He constructed the surfaces using a total of 457 logs that were arranged in 23 dip-oriented and three strike-oriented cross sections, which are shown in Figure 2-1. To establish the base of the Miocene-age deposits, Mr. Knox used the cross sections and data developed by Dodge and Posey (1981). Where available, biostratigraphic markers were used to check the age of correlations. Throughout the project, Mr. Knox consulted with Dr. Bill Galloway to resolve potential problems regarding the interpretation of the geophysical logs and the depositional history of the formations.

2.2 Approach for defining lithology and generating sand maps

Lithologic analyses were performed independently of the stratigraphic correlations. A total of 706 geophysical logs were analyzed using four textural classes instead of the traditional "binary" system of classifying lithology from geophysical logs. The "binary" system classifies lithology into either sand beds or clays beds based on the "kicks" provided by the spontaneous potential log or the resistivity log. The four textural classes used are (1) sand, basically; (2) clay, basically; (3) sand and clay but basically sand; and, (4) clay and sand but basically clay. This classification scheme is used to provide a more accurate representation of the lithology for vertical intervals where sands and clays are alternating and have individual bed thicknesses of less than 20 feet.

Our textural classes are the same as those used by Young and Kelley (2006) to characterize the Evangeline and Chicot Aquifers for a 10-county area that encompasses the lower Colorado River. In fact, the lithologic profiles from Young and Kelley (2006) are included in our analysis. To ensure consistency among all of the lithologic analyses, Mr. Ernie Baker performed all of lithologic analyses for this study. Also, Mr. Baker is the geologist who made all of the lithologic picks used by Young and Kelley (2006).

The boundaries between the four textural classes are based on the "kicks" in the resistivity logs and are supplemented by "kicks" in the spontaneous potential logs. Resistivity logs record an apparent electrical resistance in and within the vicinity of the borehole at different depths. Spontaneous potential (SP) logs record naturally occurring electrical potentials (voltages) that occur in the borehole at different depths.

The sand maps generated by this study are based on a continuous lithology profile for 706 logs. These maps were generated for selected lithostratigraphic units based on interpolation of the total sand thickness generated at each geophysical log. Interpolation of the sand thickness values was performed using ordinary kriging. Where appropriate, the generated contours were adjusted based on our interpretation of the depositional history and environments responsible for the sand distributions.

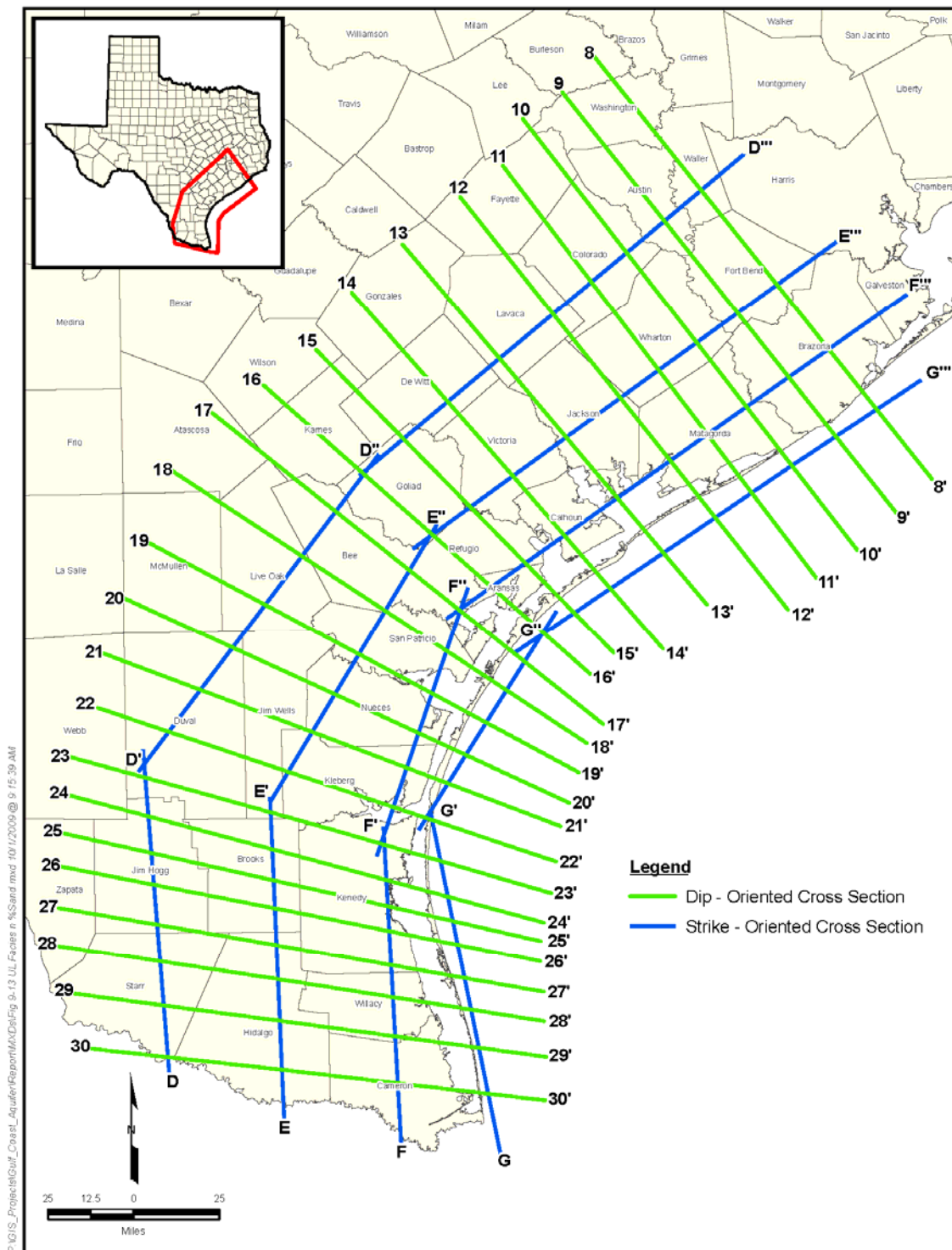


Figure 2-1. Map of the study area showing the locations of the dip-oriented and strike-oriented cross-sections used to develop the stratigraphic surfaces

3 Gulf Coast Aquifer geologic setting

3.1 Overview

The Gulf of Mexico (GOM) is a small semi-enclosed ocean basin surrounded by continental shelves and coastal plains (Bryant et al., 1991). The GOM is a circular structural basin, 940 miles in diameter, and filled with 0 to 9.4 miles of sediments ranging from Triassic to Holocene in age (Salvador, 1991) (Figure 3-1). The GOM basin probably originated in the Triassic time from rifting within the North American plate as it was drifting away from the African and South American plates (Salvador, 1991). Intermittent marine flooding of the proto-GOM rift valley formed extensive evaporite deposits (mainly salt) during the Jurassic period. Early Cretaceous carbonate platforms and shelf margins rimmed the GOM and provided a foundation for subsequent terrigenous clastic sedimentation during the Cenozoic period (Winker and Buffler, 1988). In the north and west parts of the GOM, Cenozoic sediments form thick sequences of sandstones and mudstones that overlie Cretaceous carbonates and extend basinward to the base of the modern continental slope (Figure 3-2). GOM stratigraphy is generalized in Table 3-1.

Three major stratigraphic-structural margins surround the deep ocean basin that forms the center of the GOM: 1) northern and northwestern margin of terrigenous clastic sedimentation; 2) western and southwestern structurally modified margin; and 3) eastern and southeastern carbonate-evaporite margin (Ewing, 1991; Galloway et al., 1991) (Figure 3-1). The eastern carbonate margin includes the Florida and Yucatan platforms and is characterized by low subsidence and limited clastic sediment input. The Floridian carbonate aquifer system is the main groundwater resource in the U.S. part of the eastern carbonate province (Miller, 1986). The western structurally modified margin of the Gulf Coast in Mexico includes a relatively narrow clastic coastal plain and continental shelf that have been affected by Laramide (early Cenozoic) compressional deformation. Sandy coastal aquifer systems similar to those in Texas are not well developed in Mexico (Sharp et al., 1991). The northern and northwestern clastic margin (northwest GOM) spans coastal Texas, coastal Louisiana, and adjacent offshore areas (Figure 3-1). The northwest GOM includes the major sand and sandstone aquifer systems of the Gulf Coast (Weiss, 1992; Chowdhury and Turco, 2006) of which one, the Gulf Coast Aquifer, is the focus of this report.

The northwest GOM includes two broad zones that parallel the basin margins: the interior zone and the coastal zone (Ewing, 1991). The interior zone defines the updip margin of the basin and extends downdip to the relict Early Cretaceous shelf margin (Figure 3-1). The interior zone is dominated by Cretaceous carbonates and Paleogene terrigenous clastics (Figure 3-2). The Edwards (Balcones Fault Zone), Carrizo-Wilcox, Queen City-Sparta, and Yegua-Jackson Aquifers occur in the northwest GOM interior zone (Table 3-1). The coastal zone extends from the Early Cretaceous shelf margin to the base of the modern continental slope (Figure 3-1). Basinward of the stable Cretaceous carbonate platform, subsidence increases greatly, and Cenozoic clastic sequences become much thicker. In the onshore part of the coastal zone, Paleogene sediments are dominated by deltaic, shore-zone, and marine depositional systems below the base of fresh water. Overlying Neogene sediments are dominantly nonmarine depositional systems. The Gulf Coast Aquifer of Texas is located within these onshore Neogene sediments (Table 3-1, Figure 3-2).

Table 3-1. Simplified stratigraphic and hydrogeologic chart of the northwestern Gulf of Mexico basin, Texas coastal zone (Galloway et al., 1991; Sharp et al., 1991).

ERA	Period		Epoch	Age (M.Y.)	Stratigraphic Unit	Dominant Lithology	Hydrogeologic Unit		
Cenozoic	Quaternary		Holocene	0.02	Alluvium	sand	Alluvium/Beaumont Aquifer	Gulf Coast Aquifer	
			Pleistocene		Beaumont	sand			
	Tertiary	Neogene	Pliocene	1.8 5.3	Lissie/Alta Loma	sand	Chicot Aquifer		
			Miocene		Goliad	sand	Evangeline Aquifer		
			Paleogene	Oligocene	23.9	Fleming/Lagarto	mud		Burkeville Aquitard
						Fleming/Oakville	sand		Jasper Aquifer
				Eocene	33.9	Catahoula/Frio/Anahuac	sand and mud		aquitard
						Vicksburg	mud		aquitard
		Jackson			sand and mud	Yegua-Jackson Aquifer			
		Yegua			sand and mud				
		Sparta	sand		Queen City-Sparta Aquifer				
		Queen City	sand and mud						
		Paleocene	55.8	Upper Wilcox/Carrizo	sand	Carrizo-Wilcox Aquifer			
				Middle Wilcox	mud				
Lower Wilcox/Simsboro	sand and mud								
Midway	mud		aquitard						
Mesozoic	Cretaceous	Upper	65.5		carbonate				
		Lower		Edwards	carbonate	Edwards (BFZ) Aquifer			
	Jurassic	Upper	145.5		carbonate				
		Middle		Louann salt	evaporite	salt domes			
	Triassic		201.6						

The northwest GOM encompasses several second-order structural elements inherited from the early formation of the basin. The Rio Grande embayment is an area of enhanced subsidence and greater sediment thickness centered on the modern Rio Grande River in South Texas and northeastern Mexico. The Burgos Basin in northeastern Mexico forms the south part of the Rio Grande embayment (Ewing, 1991; Hernandez-Mendoza et al., 2008). The Houston embayment is a similar subsidence trough centered in southeast Texas (Figure 3-1). The Mississippi embayment is a larger synclinal feature coinciding with the modern lower Mississippi River valley and delta. Although these embayments began in the Mesozoic as active tectonic structures, they became passive loading-induced depocenters during the Cenozoic (Ewing, 1991). In the coastal zone of the northwest GOM, these embayments are distinguished by enhanced subsidence and greater cumulative sediment thickness. The San Marcos arch separates the Rio Grande and Houston embayments in coastal Texas, forming a broad area of relatively lower subsidence and thinner cumulative sediment thickness (Figure 3-1).

The northwest GOM coastal zone is composed of terrigenous clastic sediments and sedimentary rocks that dip gently and thicken toward the center of the GOM. Older sediments are more indurated and dip more steeply than younger sediments (Figure 3-2). These stratigraphic patterns reflect increasing subsidence toward the central GOM and progradational deposition (infilling incrementally from the margin). Paleo-shoreline positions typically oscillated broadly in response to relative sea-level fluctuations, but continental margin outbuilding was progressive so that each successive major stratigraphic interval (e.g., Carrizo-Wilcox) extends basinward of the underlying interval. Minor stratigraphic intervals (e.g., Queen City-Sparta) typically do not extend basinward but instead stack vertically (aggradational deposition) upon underlying intervals (Figure 3-2).

3.2 Structural features

Geologic structures related mainly to sediment loading and gravity tectonics disrupt and deform Cenozoic sediments in the northwest GOM. Growth faults are syndepositional normal faults that form mainly by gravitational failure during rapid sediment loading along an unstable shelf margin and upper slope (Winker and Edwards, 1983). Coast-parallel growth fault zones mark shelf-margin positions of major Cenozoic depositional episodes, which get younger basinward (Figure 3-3). Sediments deposited during active growth faulting typically thicken on the downthrown sides of the faults because downward and basinward displacement creates local subsidence troughs and increased accommodation space. The greatest displacement and sediment thickening occur in shelf margin and upper-slope depositional settings. Growth fault displacement decreases upward, and overlying coastal-plain sediments are minimally offset (Galloway, 1981). Minor stratigraphic thickening on the downthrown sides of growth faults, however, does persist upward into coastal-plain sediments (Kreitler et al., 1977; Hoel, 1982).

Salt domes and other salt structures are also produced by gravity tectonics and sediment loading. Salt structures grow and develop as sediments are being deposited around them (Seni and Jackson, 1984). The salt originally formed as bedded evaporite deposits during the Jurassic period (Table 3-1). Salt, which is a low-density, ductile mineral, is gravitationally mobilized by sediment loading, forming a variety of upwelling structures, one of which is the cylindrical salt dome. Salt mobilization begins during initial progradation of thick sediment wedges into the

deepwater GOM. Salt structures continue to grow as coastal plain sediments are deposited around them. The growth of salt structures, in turn, influences the structure and stratigraphy of surrounding sediments and sedimentary rocks. Uplift and upward drag occur against the salt stock and over its crest. Steeply dipping strata terminate against the salt stock, and shallower layers arch over the dome crest. The zone of uplift near the dome is surrounded by areas of subsidence and downwarping. Faults and fractures are also common features of salt dome growth.

The northwest GOM coastal zone in Texas includes two salt dome provinces that coincide with the Rio Grande and Houston embayments (Figure 3-3). Shallow salt domes, with tops ranging from 0 to 2,000 feet deep, extend upward into the Gulf Coast Aquifer (Hamlin, 2006). The Houston embayment contains 35 shallow salt domes onshore and an equal number offshore under the modern continental shelf. The Houston embayment also contains many deeper salt structures that do not extend into the Gulf Coast Aquifer. The Rio Grande embayment includes three shallow salt domes (Figure 3-3).

3.3 Depositional systems

A depositional system is a three-dimensional body of sediment deposited in a contiguous suite of process-related sedimentary environments (Fisher and McGowen, 1967). Each sedimentary environment produces specific genetic facies (Figure 3- 4). Neogene Formations of the onshore northwest GOM coastal zone, which includes the Gulf Coast Aquifer, are mainly composed of nonmarine alluvial (fluvial) depositional systems. Because Miocene through Quaternary coastal plains had similar shoreline trends, climate gradients, physiography, and sediment source areas, Quaternary depositional systems that are exposed at the surface provide a good analog for underlying Neogene coastal plain depositional systems (Galloway, 1981).

The Quaternary coastal plain of Texas encompasses a mosaic of fluvial systems of various types, sizes, and sediment composition (Morton and McGowen, 1980; Galloway, 1981; Blum and Price, 1998; Anderson and Fillon, 2004) (Figure 3-5). Extrabasinal rivers have large drainage basins that extend well beyond the coastal plain, whereas basin-fringe and intrabasinal rivers have drainage basins marginal to and within the coastal plain. Extrabasinal rivers have persistently occupied the major embayments and still do so today; the Rio Grande, Houston, and Mississippi embayments are occupied by the Rio Grande, Colorado/Brazos, and Mississippi rivers, respectively. The point of entry of an extrabasinal river onto the coastal plain is stable owing to valley entrenchment across the slightly uplifted margin of the coastal zone (Winker, 1979). Basinward from the entry point, fluvial systems are free to migrate laterally, constructing alluvial aprons composed of sand-rich channel-fill facies and mud-rich floodplain facies (3- 5). In a fluvial channel, the proportion of bed load (sand and gravel) to suspended load (silt and clay) influences channel morphology and resulting sand-body geometry (Schumm, 1977). Bed-load channel systems form broad belts of sandstone with good lateral connectivity, whereas mixed- and suspended-load channel systems are more lenticular and isolated in mud-rich floodplain facies (Galloway, 1981). Superposition of channel systems in extrabasinal rivers results in sand bodies that are thicker than original channel depths.

Quaternary alluvial aprons grade basinward into deltaic and shore-zone depositional systems. On the modern Texas Coastal Plain, sand-rich deltaic headlands are constructed by major extrabasinal rivers in the Rio Grande and Houston embayments, while basin-fringe and intrabasinal rivers feed bay-head deltas on the San Marcos arch (Figure 3-5). This pattern persisted throughout the Neogene with some important exceptions (see Section 3.4, Depositional history). Bay, lagoon, barrier island, and shelf depositional systems fringe the onshore and near-offshore parts of the northwest GOM coastal zone. Most transported sediment bypasses these coastal plain systems to be stored permanently in shelf-margin and continental slope depositional systems (Galloway et al., 2000). Neogene shelf-margin and slope systems, however, are located offshore under the modern continental shelf and thus are not part of the Gulf Coast Aquifer.

3.4 Depositional history

Cenozoic sediments of the northwest GOM are monotonous sequences of interbedded sandstones and shales that lack distinctive lithostratigraphic units of regional extent (Galloway et al., 1991). Stratigraphic subdivision relies on a combination of: 1) biostratigraphic zonation; 2) depositional models based on Quaternary examples; and 3) regionally cyclic depositional episodes (Galloway et al., 2000). Biostratigraphic zonation is based primarily on extinction points of foraminifera (fossil protozoa) and other marine microfossils (Galloway et al., 1991; Lawless et al., 1997; Fillon and Lawless, 2000). Because marine fossils are not available in alluvial sediments, stratigraphic subdivision typically is extended updip to outcrop using lithologic boundaries, well log correlation techniques, and limited nonmarine (vertebrate faunas) biostratigraphy (Tedford and Hunter, 1984; Baskin and Hulbert, 2008).

A depositional episode is a period of focused deposition and progradation of the shoreline followed by nondeposition and transgression (marine flooding) of the coastal plain (Galloway et al., 1991, 2000). The physical product of a depositional episode is a genetic stratigraphic sequence (Galloway, 1989a). At any one time, active deposition is localized, while adjacent areas receive little or no sediment. Thus, a genetic stratigraphic sequence forms a stratigraphically and geographically distinct body of sediment bounded by surfaces of transgression or nondeposition (Frazier, 1974; Galloway, 1989a). The location of deposition (depocenter) shifts through time owing to geographic variations in sediment supply, which are controlled by tectonic events in the sediment source area (Winker, 1982). The timing and cyclicity of progradational and transgressive events depends upon the interplay of sediment supply, subsidence, and sea-level change (Galloway, 1989b). In the northwest GOM, genetic stratigraphic sequences typically consist of one or more major extrabasinal fluvial systems that supply progradational deltaic systems. Smaller intrabasinal fluvial systems and interdeltic shore-zone systems separate deltaic headlands (Galloway et al., 1991) (Figure 3-5).

Early Cenozoic (Paleogene, Table 3-1) depositional episodes in the northwest GOM were responses first to mountain building in the southern Rocky Mountains and later to explosive volcanism in West Texas and Mexico (Winker, 1982; Morton and Galloway, 1991; Galloway, 2005). Large volumes of sand, silt, and clay were delivered to the northwest GOM. In response, extrabasinal fluvial-deltaic systems developed first in the Houston embayment and then in the Rio Grande embayment (Figure 3-6). Abundant sediment supply in the Paleogene overwhelmed sea-level fluctuations and controlled sequence development (Morton and Galloway, 1991). In

the Neogene (Miocene-Pliocene), however, continental glaciers began forming in Antarctica (Fillon and Lawless, 2000), and the resulting high-amplitude sea-level fluctuations began exerting greater influence on sequence formation (Galloway et al., 1986; Morton et al., 1988) (Figure 3-7). Miocene genetic stratigraphic sequences are bounded by transgressive surfaces that can usually be related to glacio-eustatic highstands (global sea-level rises attributable to melting glaciers), but tectonic activity in the source areas was still controlling locations of sediment input into the northwest GOM. Tectonic development of the Rio Grande Rift in New Mexico disrupted drainage systems feeding the Rio Grande and Houston embayments so that large extrabasinal fluvial systems began shifting northeast into the Mississippi embayment (Winker, 1982) (Figure 3-6). Uplift of the Edwards Plateau along the Balcones Fault Zone in Central Texas supplied abundant Cretaceous calcareous detritus to smaller Miocene fluvial systems on the Texas Coastal Plain (Galloway et al., 1986; Morton et al., 1988). The principal middle-late Miocene fluvial-deltaic system in Texas was located on the San Marcos Arch (Figure 3-6). During the Plio-Pleistocene (Table 3-1), tectonic quiescence and high-frequency glacio-eustatic fluctuations (this time from northern hemisphere glaciation) resulted in multiple cross-cutting and superimposed alluvial valley fills and preservation of thin sequences on the Texas Coastal Plain (Blum and Price, 1998).

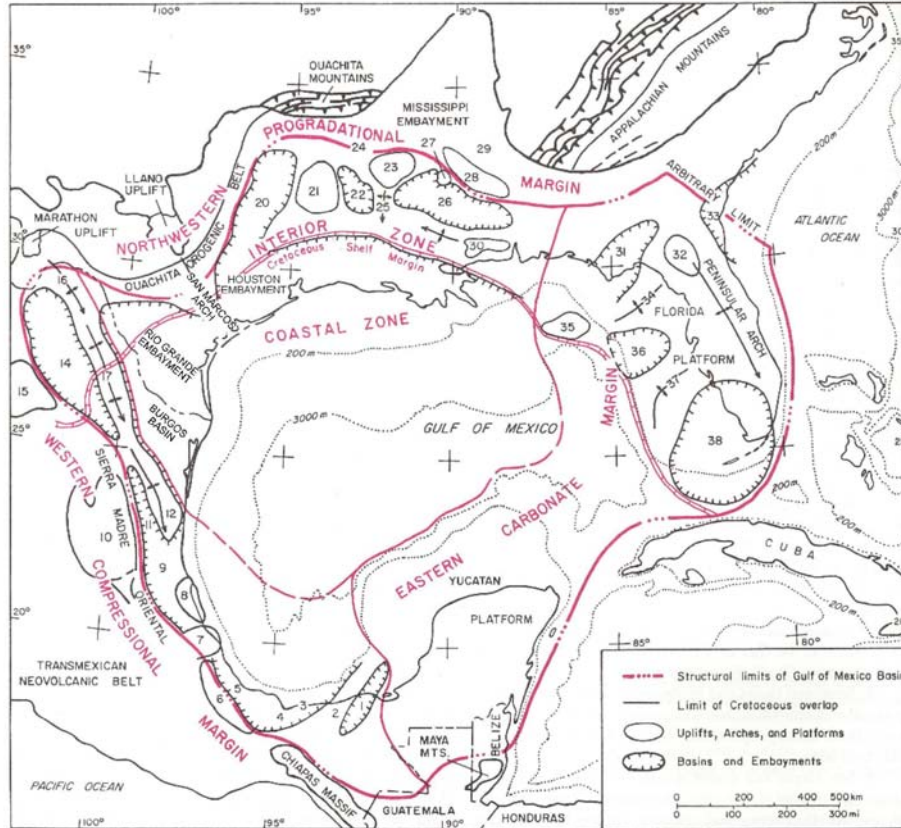


Figure 3-1. Map of the Gulf of Mexico basin showing major structural elements and stratigraphic provinces. Modified from Ewing (1991).

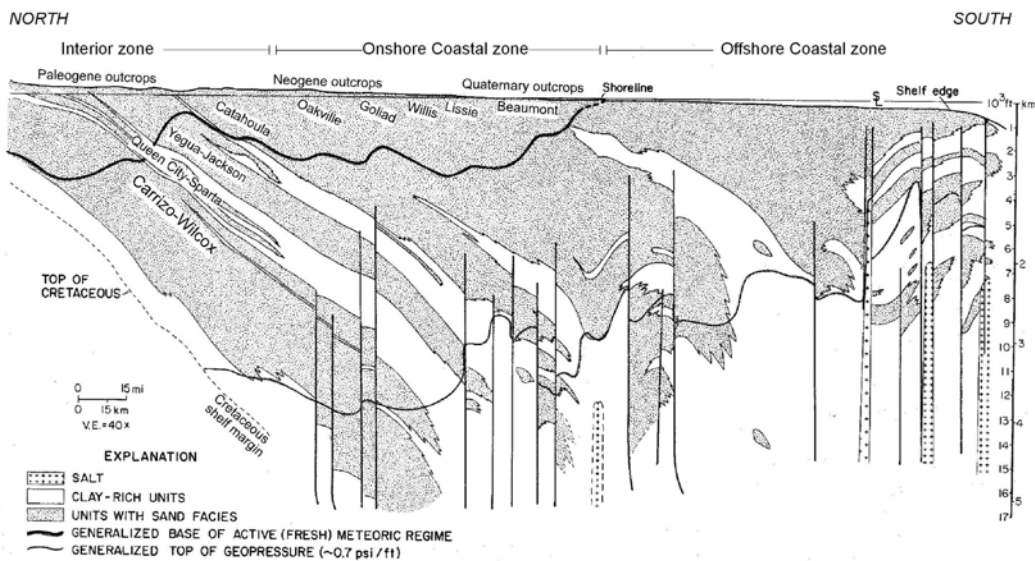


Figure 3-2. Regional dip-oriented cross section of Cenozoic strata on the northwestern margin of the Gulf of Mexico basin. Modified from Galloway et al. (1991) and Sharp et al. (1991).

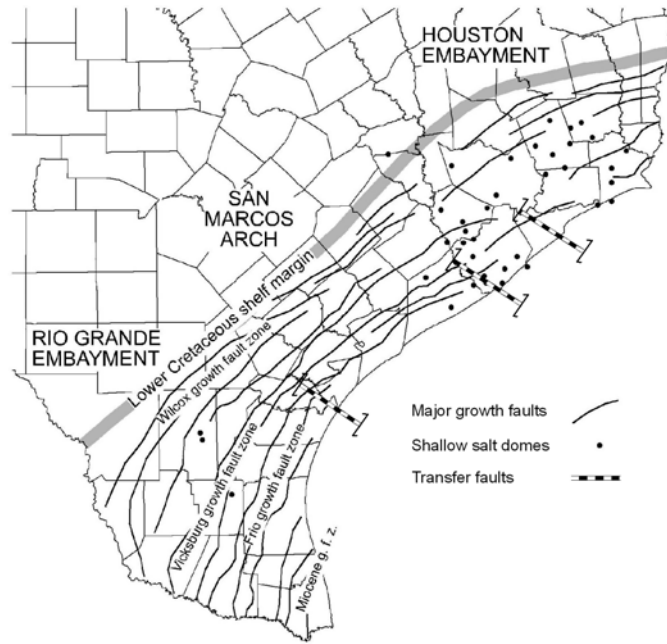


Figure 3-3. Map showing major growth fault zones and shallow salt domes in the onshore part of the Texas coastal zone. Modified from Ewing (1990) and Hamlin (2006).

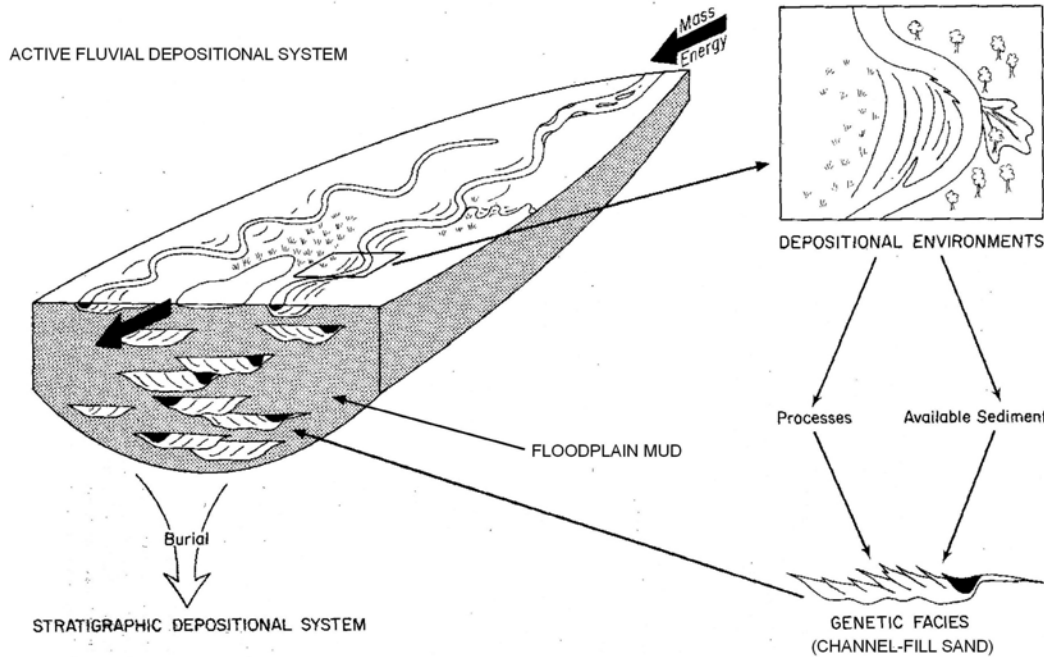


Figure 3-4. Schematic diagram showing a fluvial depositional system with its component depositional environments and resulting genetic facies. Modified from Galloway et al. (1979).

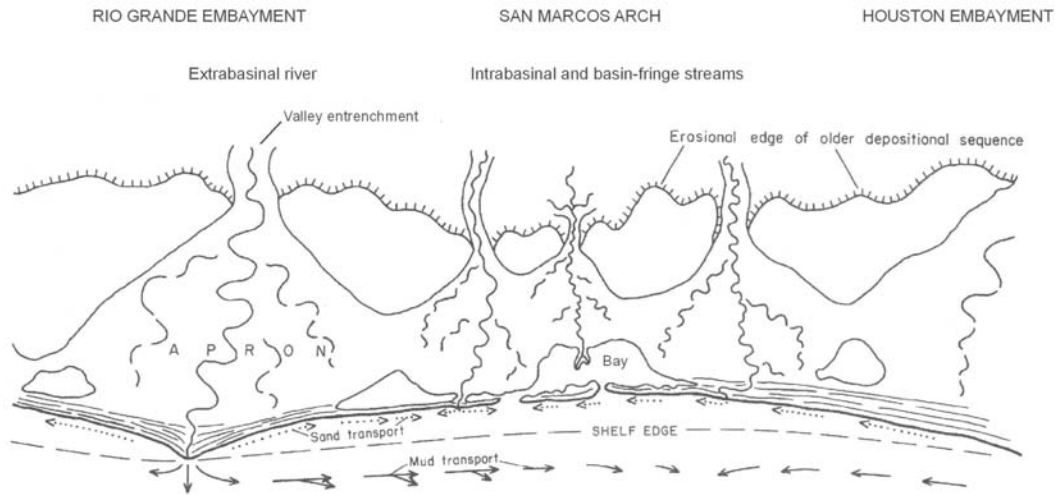


Figure 3-5. Schematic drawing of Quaternary depositional systems of the Texas Coastal Plain. Modified from Winker (1979) and Galloway et al. (1986).

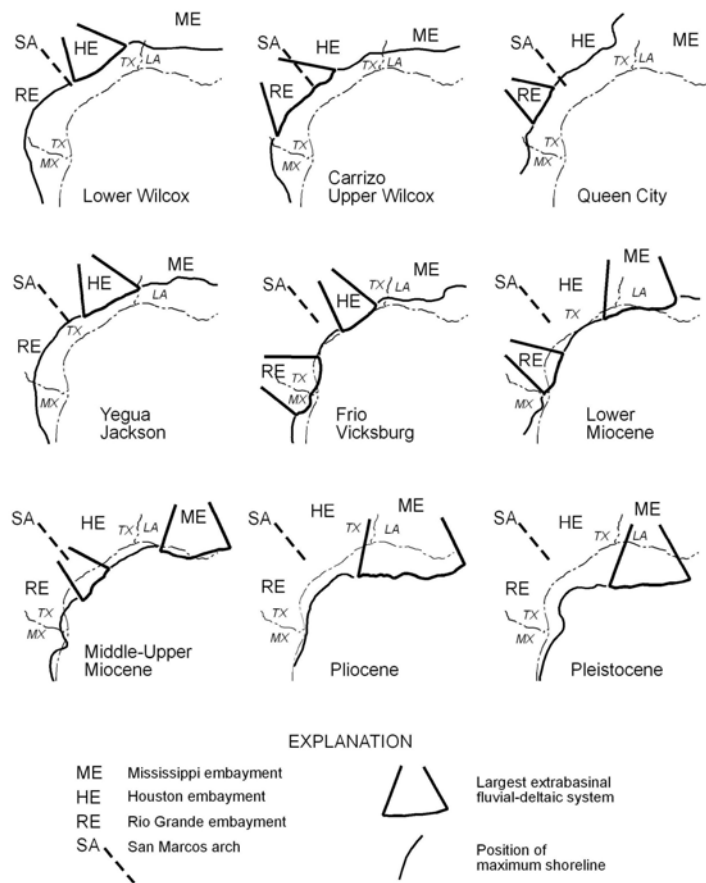


Figure 3-6. Positions of principal fluvial-deltaic depocenters and interdeltatic shorelines for selected depositional episodes, northwest GOM. Modified from Galloway (1989b) and Galloway et al. (2000).

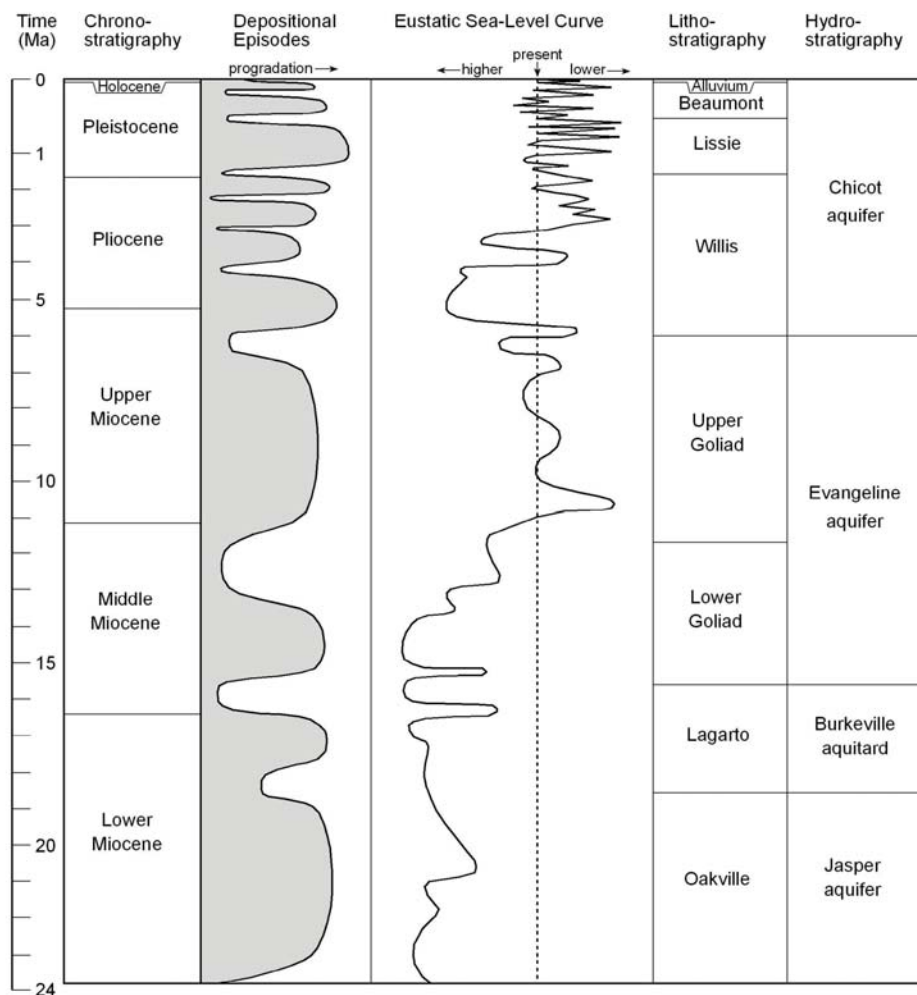


Figure 3-7. Chronostratigraphic chart of Miocene to Holocene depositional episodes, northwest GOM. Lithostratigraphic and hydrostratigraphic boundaries are approximate. Depositional episodes from Galloway et al. (2000) and sea-level curve from Haq et al. (1987). Geologic ages in millions of years ago (Ma) from Berggren et al. (1995).

4 Stratigraphic and hydrogeologic framework

The Gulf Coast Aquifer in Texas encompasses all stratigraphic units above the Vicksburg Formation (Ashworth and Hopkins, 1995) (Table 3-1). The lowermost stratigraphic unit is the Catahoula Formation (including the Frio and Anahuac in the deep subsurface), which is an aquitard everywhere except near the outcrop (Wood et al., 1963). In the overlying Fleming Group, the Oakville Sandstone is approximately equivalent to the Jasper Aquifer and the Lagarto Clay to the Burkeville Aquitard (Wesselman, 1967; Baker, 1979) (Figure 3-7). The Goliad, Willis, and Lissie Formations, which contain most of the fresh-water resources in the Gulf Coast Aquifer (Wood et al., 1963), are the focus of this description. The Goliad Formation is approximately equivalent to the Evangeline Aquifer, although the Evangeline includes some underlying Fleming sands locally (Baker, 1979). The Chicot Aquifer comprises all sands between the top of the Evangeline and the land surface (Baker, 1979) (Figure 3-7). Although Pliocene-Pleistocene stratigraphy in the shallow subsurface of the Texas Coastal Plain is complex, the primary components of the Chicot Aquifer are the Willis, Lissie, and Beaumont Formations (Ashworth and Hopkins, 1995). In southeast Texas, the Montgomery and Bentley Formations are approximately equivalent to the Lissie Formation (Baker, 1979; Dutton and Richter, 1990).

4.1 Previous studies

The earliest geologic studies focused on outcrop description and correlation (Deussen, 1914, 1924; Barton, 1930; Trowbridge, 1932; Plummer, 1932; Price, 1933, 1934; Weeks, 1933, 1945; Doering, 1935, 1956; Bernard and LeBlanc, 1965). Outcrop mapping culminated in the publication by the Bureau of Economic Geology (BEG) of the *Geologic Atlas of Texas (GAT)* (Aronow and Barnes, 1968; Shelby and others, 1968; Proctor and others, 1974; Aronow and Barnes, 1975; Aronow and others, 1975; Brewton and others, 1976a; Brewton and others, 1976b) (Figure 4-1). The BEG also published the *Environmental Geologic Atlas of the Texas Coastal Zone* (Brown et al., 1976, 1977, 1980; McGowen et al., 1976a,b). These studies demonstrated that outcropping Miocene to Holocene Formations are composed of unconformity-bounded, seaward dipping, nonmarine clastic wedges. In updip areas, each formation erosionally truncates and onlaps the underlying formation (Figure 4-2). Thin erosional remnants, isolated terraces, onlapping veneers, and Holocene alluvial cover make it difficult to establish regional correlations between outcropping and subsurface stratigraphic intervals (Winker, 1979; DuBar et al., 1991).

Subsurface stratigraphic analysis of the Texas Gulf Coast was originally developed for petroleum exploration but became an essential tool for characterization of aquifer composition, correlation, and structure. Subsurface mapping was initially based on analysis of rock cuttings and fossils produced during the well drilling process. However, by the 1930s, geophysical (electrical) well logs provided a major source of data for formation identification and correlation. Early subsurface studies focused on the stratigraphic and structural framework of Gulf Coast Formations (e.g., Applin et al., 1925; Barton et al., 1933; Bornhauser, 1947, 1958; Williamson, 1959; Murray, 1961). Subsequent studies developed the concepts of depositional systems and facies (e.g., Boyd and Dyer, 1964; Rainwater, 1964; Fisher and McGowen, 1967). More recently, the concepts and techniques of sequence stratigraphy and chronostratigraphic

correlation have been used to refine the stratigraphic framework and depositional history of the GOM (Galloway, 1989b; Lawless et al., 1997; Fillon and Lawless, 2000; Galloway et al., 2000; Hernandez-Mendoza et al., 2008). Gulf Coast subsurface stratigraphy, depositional systems, and structure are summarized in a series of well log cross sections published by BEG (Dodge and Posey, 1981; Morton et al., 1985; Galloway et al., 1994).

Subsurface analysis in Texas groundwater studies began early and has been an equal partner with petroleum studies in the development of our understanding of Gulf Coast stratigraphy. Early publications by the Texas Board of Water Engineers and the U.S. Geological Survey (USGS) used well logs to delineate aquifer boundaries and sand distribution in the subsurface (e.g., Rose, 1943; Lang et al., 1950; Jones et al., 1956). Numerous countywide and regional studies of geology and groundwater resources by the Texas Water Commission (later the Texas Water Development Board) refined aquifer stratigraphy (e.g., Baker, 1964; Wesselman, 1967). Building on stratigraphic interpretations from both petroleum and groundwater resources, Baker (1979) published a series of well log cross sections covering the entire Texas Gulf Coast, which became the standard reference for aquifer stratigraphy in the region.

The USGS conducts regional studies of major aquifer systems for resource evaluation and management. As part of their Regional Aquifer-System Analysis (RASA) Program, the USGS published a series of reports on major aquifer systems across the Gulf Coastal Plain from Texas to Florida (Grubb, 1984, 1987; Ryder, 1988; Weiss, 1992; Hosman, 1996; Williamson and Grubb, 2001; Ryder and Ardis, 2002). These reports assemble hydrogeologic data and interpretations and present the results of numerical simulations. The hydrostratigraphic units developed for the RASA Program, however, have generally not been adopted in recent Texas-based studies. Instead, the Chicot and Evangeline Aquifer designations that were established regionally by Baker (1979) have been retained (e.g., Chowdhury and Turco, 2006; Knox et al., 2006; Young et al., 2006).

A second USGS program, the Source Water Assessment and Protection (SWAP) Program, developed a computer-based data set of surfaces (stratigraphic boundaries) for the Chicot and Evangeline Aquifers. The primary source data set to generate the SWAP surfaces consist of digitized points taken from the surface contours for the Chicot and Evangeline Aquifers found in Carr and others (1985). Carr and others (1985) do not provide control points for these contours, nor do they explain the method used to develop the contours. Thus, the uncertainty associated with the original contours is largely unknown. In developing its SWAP data set, the USGS blended the information from Carr et al. (1985) with information from Jorgensen (1975), Baker (1979, 1986), and geologic outcrops mapped on BEG's GAT sheets. The outcrop information provided by the GAT sheets was used to estimate the updip region of the aquifers. The information from Baker (1979, 1986) was used to smoothly transition between the more detailed works of Jorgensen (1975) in the Houston area with the general framework established by Carr et al. (1985). The SWAP aquifer surfaces were used in developing conceptual models for TWDB groundwater availability models (GAMs) of the Gulf Coast Aquifer (Chowdhury and Mace, 2003; Chowdhury et al., 2004; Kasmarek and Robinson, 2004). The SWAP data, however, are based on stratigraphic studies conducted in the 1970s and 1980s, which are being superseded by more recent studies using sequence stratigraphic techniques and ties to offshore chronostratigraphy (Knox et al., 2006; Young et al., 2006).

4.2 Fleming Group: Oakville and Lagarto Formations

The Fleming Group of the Texas Coastal Plain is early Miocene in age and comprises the Oakville and Lagarto Formations (Galloway et al., 1986) (Figure 3-7, Table 3-1). The Fleming Group is bounded by regional marine shales in downdip areas and by the bases of massive fluvial sandstones updip. Fleming boundaries were traced updip through the nonmarine interval to outcrop using correlation, projection, lithology, and minor datum changes (Galloway et al., 1986) (Figure 4-3). The lower boundary was delineated by correlating between the Anahuac Shale downdip and the base of massive Oakville sandstone updip and in outcrop, and the upper boundary was delineated by similarly connecting the Amphistegina B Shale downdip with the base of massive Goliad sandstone updip. The Oakville and Lagarto Formations together compose a major fluvial-deltaic depositional episode in which the Oakville forms the lower progradational part, and the Lagarto forms the upper retrogradational part. In the onshore area, the Oakville is generally sand-rich, whereas the Lagarto is relatively more mud-rich. The Oakville and Lagarto Formations are separated by a marine transgressive shale downdip and a lithologic boundary updip (Figure 4-3).

The Fleming Group crops out across the entire Texas coastal plain except in South Texas where it is overlapped by a thin interval of Goliad gravel and caliche (Galloway et al., 1986) (Figure 4-3). The Oakville Formation ranges from 300 to 700 feet thick at outcrop to 1,000 to 2,000 feet thick near the modern shoreline, whereas the Lagarto Formation ranges from 700 to 1,400 feet thick at outcrop to 2,000 to 3,000 feet thick near the coast (Baker, 1979; Galloway et al., 1982, 1986). The Fleming Group dips coastward 50 to 60 feet per mile (Wood et al., 1963). Oakville sandstone is thickest (>900 feet) across a broad area in South Texas (Figure 4-4). The Lagarto Formation also contains thick sandstone in South Texas but in a more restricted area (Figure 4-5). Both formations contain thick sandstone in the far northeast part of the Texas coast, and both contain thick sandstone in the near offshore area (Figures 4-4 and 4-5). Across the broad middle coast from Nueces County in the southwest to Chambers County in the northeast, both formations contain relatively less sandstone, and several large regions in and near outcrop are marked by low sandstone (<200 feet) in both formations (Figures 4-4 and 4-5). Although net sandstone is low locally near outcrop in the Oakville Formation, sandstone percent is high because the gross Oakville interval is thin (Galloway et al., 1986). Across much of the outcrop and near outcrop area, the Oakville forms a thinner high-sand interval, and the overlying Lagarto forms a thicker low-sand interval.

The Fleming Group comprises several large fluvial systems that grade downdip into equally large delta and shore-zone systems (Rainwater, 1964; Doyle, 1979; Spradlin, 1980; DuBar, 1983; Galloway et al., 1982, 1986). The fluvial systems include conglomeratic bed-load channel-fill sandstones and finer-grained mixed-load channel-fill sandstones (Table 4-1). Channel-fill sandstones range from 500 feet to 5 miles wide and 3 to 30 feet thick. Broad, dip-oriented, sand-rich belts near outcrop and in mid-dip areas are composed of superposed and laterally amalgamated channel-fill and channel-margin splay facies (Figures 4-4 and 4-5). Channel belts are encased in mud-dominated floodplain facies. Down-dip near the modern shoreline, coastal-barrier and beach-ridge facies form thick sequences of strike-aligned, massive sandstone in both formations.

Table 4-1. Fleming Group depositional facies (Galloway et al., 1982, 1986).

Facies	Composition grain size	Sedimentary structures	Thickness	Width	Vertical trend (log pattern)	Depositional systems
Conglomeratic bed-load channel	Medium to coarse sand, gravel up to pebble size, mud clasts	Planar bedding, low-angle tabular cross-bedding, trough cross-bedding	3–15 ft	1000–5000 ft	Blocky, irregular	Santa Cruz fluvial system, southwest part of Moulton/Point Blank streamplain system
Sandy bed-load channel	Fine to coarse sand, local gravel, mud clasts	Planar bedding, trough and tabular cross-bedding	10–20 ft	1–5 mi	Blocky, irregular	Santa Cruz fluvial system
Mixed-load channel	Fine to coarse sand, silt, mud, mud clasts	Trough cross-bedding, planar bedding, ripple and wavy lamination	15–30 ft	500–2500 ft	Fining upward	Moulton/Point Blank streamplain system
Amalgamated small channel and splay	Very fine to coarse sand, silt	Trough cross-bedding, planar bedding, ripple and wavy lamination	10–25 ft	1–3 mi	Irregular to fining upward	Moulton/Point Blank streamplain system
Crevasse splay and sheet splay	Fine to coarse sand, silt, sandy mud, mud clasts	Planar lamination, ripples, small-scale cross bedding	3–15 ft	1000–5000 ft	Interbedded fine and coarse	All fluvial systems
Floodplain, coastal bays and lagoons	Silt, clay, sandy mud, caliche	Massive, horizontal lamination, roots, burrows	Variable	Fill inter-channel areas (miles)	No trend (shale baseline)	All fluvial systems
Coastal barrier and beach ridge	Fine to coarse sand	Not reported	Individual units not reported	Several miles wide, tens of miles long	Blocky, massive	North Padre delta system, Matagorda barrier/strandplain system, Calcasieu delta system

Major extrabasinal fluvial channel belts in the Fleming Group are located in South Texas and in the northeast near the Louisiana border (Figures 4-4 and 4-5). In South Texas, the Santa Cruz fluvial system (Table 4-2) is composed of coarse sand and gravel and is partly covered at outcrop by similarly coarse facies in the Goliad Formation (Galloway et al., 1982, 1986). Most Santa Cruz fluvial sandstones occur in the Oakville Formation; except for a few areas, the Lagarto Formation is dominated by mud-rich interchannel (floodplain) facies. In the northeast corner of the Texas coastal plain, the Newton fluvial system (Table 4-2) is just a small part of a large, lower Miocene fluvial-deltaic depocenter in Louisiana (Figure 3-6). Across the broad middle coast, the Moulton/Point Blank streamplain system (Table 4-2) comprises numerous small fluvial

channel and splay sandstones encased in floodplain mudstones (Spradlin, 1980; Galloway et al., 1986).

Table 4-2. Fleming Group depositional systems (Spradlin, 1980; Galloway, et al., 1982, 1986).

Depositional system	Location (Gulf Coast GAMs)	Principal facies	Sandstone geometry	Oakville sand content	Lagarto sand content
Santa Cruz fluvial	southern GC GAM, southwest part of central GC GAM	bed-load channel fill, sheet splay, floodplain	multiple dip-oriented low-sinuosity channel belts	200–900 ft, 40–80 %	mostly <500 ft, 20–40 %
Moulton/Point Blank streamplain	central GC GAM, southwest part northern GC GAM	amalgamated small channel and splay, floodplain, bed-load channel (Oakville)	thin sinuous channel and splay belts encased in floodplain mudstone	mostly <300 ft, local pockets of >500 ft, 20–60 %, increasing southwest	<300 ft, <40 %, increasing northeast
Newton fluvial	northeast part northern GC GAM	mixed-load channel, crevasse splay, floodplain	coalesced channel and splay belts, minor floodplain	300–900 ft, 40–80 %	300–900 ft, 40–80 %
North Padre delta (onshore part)	southern GC GAM, southwest part of central GC GAM	coastal barrier and beach ridge, coastal bays and lagoons	strike-aligned, vertically stacked	500–1000 ft, 20–50 %	200–900 ft, 10–40 %
Matagorda barrier/strandplain (onshore part)	central GC GAM, southwest part northern GC GAM	coastal barrier and beach ridge, coastal bays and lagoons	strike-aligned, vertically stacked	300–900 ft, 20–40 %	300–500 ft (10–40 %) updip, >900 ft (40–60 %) along present shoreline
Calcasieu delta	northeast part northern GC GAM	coastal barrier and beach ridge, coastal bays and lagoons	strike-aligned, vertically stacked	300–700 ft, 20–40 %	900–1100 ft, 40–60 %

Delta systems in the Fleming Group display strongly strike-aligned sandstone orientations (Figures 4-4 and 4-5). Redistribution of sand along strike away from deltaic headlands by shore-zone waves and currents resulted in strike-elongate stacks of massive sandstone in downdip areas (Galloway et al., 1986) (Figure 3-5). The North Padre delta system (Table 4-2) is the seaward extension of the Santa Cruz fluvial system in South Texas. Much of the sand delivered to the North Padre delta system was redistributed to the northeast into the Matagorda barrier/strandplain system (Table 4-2), especially in near offshore areas (Figures 4-4 and 4-5). The Calcasieu delta system (Table 4-2) is the seaward extension of the Newton fluvial system in the northeast. Calcasieu deltaic sandstones are thickest in the Lagarto Formation.

Fleming Group depositional systems constructed a framework of dip-oriented fluvial sandstone belts updip to mid-dip and strike-oriented shore-zone sandstone belts downdip. Fluvial and shore-zone sandstones are well interconnected only in South Texas and far northeast coastal

Texas. Across the broad middle coast, shore-zone sandstones are more isolated, grading updip into mud-dominated lagoonal and floodplain facies (Figures 4-4 and 4-5). Furthermore, much of Fleming shore-zone sandstone lies seaward of the modern shoreline. In South Texas, Lagarto sandstones generally thin downdip, whereas Oakville sandstones thicken downdip. The Oakville is distinctly sandier than the Lagarto in South Texas. Along the middle coast, thick Lagarto sandstones form a strike-aligned belt in coastal areas of Matagorda and Brazoria Counties, but this sandstone belt grades landward into low-sandstone areas (Figure 4-5). The Oakville is relatively sand-poor along the coast in Matagorda and Brazoria Counties but is somewhat sandier than the Lagarto in adjacent mid-dip areas (Figure 4-4). The Lagarto is generally sandier than the Oakville along the upper coast.

4.3 Goliad Formation

The Goliad Formation of the Texas Coastal Plain is primarily middle-to-late Miocene in age (Morton et al., 1988) (Figure 3-7, Table 3-1). The Goliad includes vertebrate fossils ranging in age from middle Miocene to earliest Pliocene (Baskin and Hulbert, 2008). At outcrop and in the shallow subsurface, the Goliad Formation is bounded by regional unconformities at the base of massive fluvial sandstones, but downdip, the Goliad is bounded by marine transgressive shales (Figure 4-6). A minor datum change is required to tie downdip marine paleontologic markers to updip lithologic markers (Morton et al., 1988). The lithostratigraphic Goliad Formation occurs only in the onshore part of the Texas Coastal Plain, where it is defined by nonmarine depositional systems and facies (Solis, 1981; Hoel, 1982). In extreme South Texas and northeastern Mexico (Burgos basin), however, the Goliad-equivalent interval is composed of shore-zone and marine depositional systems (Morton et al., 1988). In the modern offshore area, middle-upper Miocene sequences include fluvial, deltaic, and marine depositional systems (Doyle, 1979; Morton et al., 1988; Galloway et al., 2000).

The Goliad Formation ranges in thickness from 200 feet at outcrop to about 1,400 feet near the modern shoreline. The Goliad does not display significant thickness changes attributable to differential subsidence across the San Marcos arch and into adjacent embayments but does thicken (15–20%) locally across the major growth fault zones shown in Figure 3-3 (Hoel, 1982). Goliad strata dip coastward about 10 to 20 feet per mile. Net sandstone thicknesses range from 100 to 800 feet, and sandstone content decreases regionally to the southwest (Morton et al., 1988). Sandstones in the upper Goliad typically are less conglomeratic and thinner bedded than are those in the lower Goliad (Hoel, 1982; Morton et al., 1988).

Goliad fluvial depositional systems comprise channel-fill and interchannel facies (Hoel, 1982) (Table 4-1). Fluvial channel-fill facies are composed mainly of medium- to coarse-grained sand and gravel, displaying large-scale cross-bedding. Hoel (1982) recognized both bed-load and mixed-load channel-fill facies in Goliad outcrops (Table 4-1). Gravelly coarse sand, sandy gravel, and pebble-to-cobble-sized gravel dominate bed-load channel-fill facies. Vertical stratigraphic successions in bed-load channel-fill facies are irregular, and grain size and sorting vary greatly. Mixed-load channel-fill facies, however, commonly display fining-upwards vertical grain-size trends. Coarse sand and sandy gravel are overlain by medium-to-fine sand, and very fine sand and silt cap the mixed-load channel-fill succession. Electric log responses

reflect vertical grain-size trends: bed-load channel-fill facies cause blocky log patterns whereas mixed-load channel-fill facies cause fining-upwards log patterns.

Interchannel facies include sandy crevasse splays, and muddy floodplain and playa lake facies. Crevasse-splay facies formed where flood waters breached channel levees and deposited broad aprons of sandy sediment on the floodplain (Table 4-1). Crevasse splays associated with mixed-load channels are finer grained than those associated with bed-load channels (Hoel, 1982). Floodplain facies surround channel-fill and crevasse-splay facies and were deposited across interchannel areas during floods. Mottled red clays dominate floodplain successions, and secondary calichification and pedogenesis are pervasive (Hoel, 1982). Playa facies have been identified only in Brooks and San Patricio Counties (Hoel, 1982). In playa facies, gypsum occurs as interbeds and interstitial precipitates. The environment of deposition of playa facies was probably an arid-region evaporitic lake (inland sabkha facies of Hoel [1982]).

Table 4-3. Goliad Formation depositional facies (Hoel, 1982).

Facies	Composition grain size	Sedimentary structures	Thickness	Width	Vertical trend (log pattern)	Fluvial systems
Bed-load channel	Coarse sand, gravel up to cobble size, mud clastics	Large planar and trough cross-bedding	25–60 ft	~103 ft	Blocky, irregular	Realitos, Tomball
Mixed-load channel	Medium-coarse sand, gravelly sand, mud clasts	Large and small trough cross-bedding, low-angle planar bedding	30–60 ft	~103–104 ft	Fining upward	Eagle Lake
Crevasse splay	Medium-fine sand, silt, gravel lags	Ripple, wavy and parallel lamination	10–30 ft	~103–104 ft	Fining upward	All
Floodplain	Silt, clay, caliche	Massive, horizontal lamination, roots, burrows	Variable	Fill interchannel areas (miles)	No trend (shale baseline)	All
Playa lake	Gypsum, sand, silt, clay	Horizontal lamination, ripples, chaotic	30–60 ft	Miles	Thin fining upward cycles	Realitos

The Goliad Formation includes three large extrabasinal fluvial systems (Hoel, 1982; Morton et al., 1988). Each Goliad fluvial system contained multiple channel axes that formed an integrated drainage network. Channels preferentially reoccupied the same locations on the coastal plain, resulting in vertical stacking of sand bodies (Morton et al., 1988). Owing to an arid paleoclimate and lack of bank-stabilizing vegetation, Goliad fluvial channels had poorly developed levees, channel migration was relatively unconstrained, and channel-fill deposits tended to coalesce laterally (Hoel, 1982). Thus, Goliad channel-fill sand bodies form broad belts that are much thicker and wider than the river channels in which they were deposited.

Goliad fluvial systems vary in overall composition and sandstone development, and generally become sandier to the northeast (Table 4-1, Figure 4-7). The Realitos fluvial system occupies the Rio Grande embayment. This fluvial system includes spectacular pebble- and cobble-sized gravels in outcrop (Plummer, 1932; Hoel, 1982), but in mid-dip positions, Realitos channel belts are narrow and include relatively less aggregate net sand than the other Goliad fluvial systems (Figure 4-7, Table 4-2). Realitos gravels include volcanic rock fragments, Permian limestone, and other compositions reflecting extrabasinal source areas in West Texas and beyond (Hoel, 1982). The Realitos fluvial system feeds small deltaic and barrier-lagoon depositional systems that are located under the modern South Texas shoreline and adjacent offshore area.

The Eagle Lake fluvial system is located (atypically) on the San Marcos arch and the adjacent southwestern part of the Houston embayment. Fluvial axes of the Eagle Lake system are broader and sandier than those of the Realitos system (Figure 4-7, Table 4-2). Individual channel-fill sand bodies in the Eagle Lake system are slightly thicker than those in the other Goliad fluvial systems. Eagle Lake sand bodies are most developed in the upper part of the Goliad Formation (Hoel, 1982; Knox et al., 2006). The Eagle Lake fluvial system was the primary middle-late Miocene drainage conduit for the Texas part of the northwest GOM and supplied sediment to the South Brazos delta system located well offshore (Morton et al., 1988). The largest northwest GOM fluvial-deltaic drainage system in the middle-late Miocene was located in the Mississippi embayment (Figure 3-6).

Table 4-4. The Goliad Formation fluvial depositional systems (Hoel, 1982; Morton et al., 1988).

Depositional system	Location	Channel-belt composition	Channel-belt width	Stratigraphic position of maximum sand	Interchannel composition	Source area	Overall sand content (rank)
Realitos bed-load fluvial	Rio Grande embayment	≤400 ft sand, 40–50% sand	5–15 miles	lower and upper Goliad	calcareous mudstone, <20% sand	West Texas, northern Mexico	third (lowest sand content)
Eagle Lake mixed-load fluvial	North flank San Marcos arch	≤500 ft sand, 40–60% sand	10–20 miles	upper Goliad	calcareous mudstone, <20% sand	Central Texas	second
Tomball bed-load fluvial	Houston embayment	≤600 ft sand, 40–60% sand	10–30 miles	lower and upper Goliad	mudstone and sandstone, >25% sand	East Texas	first (highest sand content)

The Tomball fluvial system is located in the Houston embayment. Even though it was not the primary extrabasinal drainage conduit in Texas, the Tomball system is the sandiest of the three Goliad fluvial systems (Figure 4-1, Table 4-2). Tomball channel belts are broad and sand-rich, but interchannel areas are unusually sandy as well because of the abundance of crevasse-splay facies (Morton et al., 1988). During the middle Miocene, tectonic activity in the source areas disrupted drainage networks and shifted the axis of sedimentation northward from the Rio Grande embayment to the Houston and Mississippi embayments (Morton et al., 1988). For this reason, Tomball rivers transported larger volumes of sediment than more southerly rivers, and

this large sediment influx was sustained through both middle and late Miocene depositional episodes. Tomball rivers supplied sediment to form the thick sand-rich, shore-zone facies of the Galveston Strandplain system in the southeast Texas offshore area (Morton et al., 1988).

4.4 Willis Formation

The Willis Formation is approximately Pliocene in age (Galloway, 1989b). At outcrop, the Willis erosionally downcuts and locally truncates the underlying Goliad Formation and is in turn eroded and locally overlapped by the overlying Lissie Formation (Doering, 1935) (Figure 4-2). The Willis outcrop consists of cuesta-forming erosional remnants in the Houston Embayment and on the San Marcos Arch (Figure 4-1). The Willis does not outcrop in the Rio Grande Embayment, although Pliocene-age deposits are present there in the subsurface. Along the south and central Texas coast, Willis-equivalent strata have been mapped with the Lissie (Doering, 1956) or with the Goliad (Solis, 1981). Similar to the Goliad, the Willis is dominated by nonmarine, fluvial depositional systems in the onshore part of the Texas Coastal Plain (Guevara-Sanchez, 1974; Solis, 1981; Galloway et al., 2000). At outcrop, the Willis is composed of gravelly coarse sand in several upward-fining successions that are interpreted as incised valley fills overlain by transgressive deposits (Morton and Galloway, 1991). Near the modern shoreline and offshore, Willis deltaic and marine systems record four cyclic depositional episodes bounded by transgressive shales (Galloway et al., 2000) (Figure 3-7). The paleo Red River extended across the upper Texas Coastal Plain. This major Pliocene extrabasinal river for deltaic and continental margin progradation extends offshore from Houston. The ancestral Mississippi River in Louisiana was the second main source of sediment input during the Pliocene. Although the coastal plain in Texas included several smaller rivers, preserved sandy sediment in the Willis decreases southward.

The Willis Formation ranges in thickness from about 100 feet at outcrop to 500 feet near the coast and also thickens northeastward (Knox et al., 2006). The Willis dips coastward about 15 to 20 feet per mile and is 1,000 to 2,000 feet deep at the modern shoreline (Doering 1935; Knox et al., 2006). Willis fluvial systems include dip-oriented, sand-rich channel-fill facies and sand-poor interchannel areas, which grade toward the coast into shore-parallel deltaic and shore-zone sands and interdeltic muddy bay deposits (Figure 4-8). Individual Willis sands vary widely in thickness from about 20 to 200 feet and are separated by muds of similar thickness (Knox et al., 2006). Along the central coast, the abundance of sand in the Willis decreases downdip from 70% to 90% in the fluvial system to 30% to 70% in the deltaic and shore-zone systems (Solis, 1981). Fluvial channel sands thin and become more isolated in interchannel muds southward along the central coast (Figure 4-8).

4.5 Lissie Formation

The Lissie Formation is approximately early Pleistocene in age (DuBar et al., 1991). Pleistocene fossils have been found in the Lissie at several locations on the Texas Coastal Plain (Plummer, 1933). The Lissie outcrop is continuous except where cut by modern river valleys or where covered by Holocene windblown deposits in South Texas (Figure 4-1). North of the Brazos River, the Lissie Formation has been mapped at the surface as the Montgomery and Bentley Formations. At outcrop, the Lissie is composed of fine-grained sand and sandy clay and

unconformably overlies and onlaps the Willis (Morton and Galloway, 1991). In the subsurface, the Lissie is defined as the interval between the Willis and the Beaumont (Figure 4-2). The Lissie is dominated by nonmarine depositional systems in the onshore part of the Texas Coastal Plain, although shore-zone facies are prominent in some coastal counties (Guevara-Sanchez, 1974; Solis, 1981) (Figure 4-9). Lissie deposition was strongly influenced by glacial-interglacial cycles on the North American continent. High-frequency, glacio-eustatic, sea-level fluctuations resulted in shorter depositional episodes, thinner genetic sequences, and greater erosional downcutting (Figures 3-7 and 4-2).

The Lissie Formation ranges in thickness from about 100 feet at outcrop to greater than 700 feet at the coast (Knox et al., 2006). The Lissie dips coastward about 5 to 20 feet per mile and is 500 to 1,000 feet deep at the modern shoreline (Doering, 1935; Knox et al., 2006). Lissie depositional facies patterns are similar to those of the Willis: dip-oriented fluvial channel sands separated by interchannel muds and grading downdip into shore-parallel sands and muds (Figure 4-9). In Lissie fluvial systems, individual sand bodies are 20 to 100 feet thick, whereas interbedded muds are generally less than 20 feet thick (Knox et al., 2006). Shore-zone and marine systems downdip, however, include much thicker muddy intervals. In general, the Lissie is less sandy than the Willis. Along the central coast, the Lissie is 50% to 75% sand in updip fluvial systems and 30% to 70% sand in downdip shore-zone systems (Solis, 1981).

4.6 Beaumont Formation

The Beaumont Formation is late Pleistocene in age (DuBar et al., 1991). Pleistocene-age fossils have been found in the Beaumont at numerous locations on the Texas Coastal Plain (Maury, 1920, 1922; Plummer, 1933; Price, 1934). The Beaumont outcrop covers a large part of the lower coastal plain except where cut by modern river valleys or covered by Holocene wind-blown sand in south Texas (Figure 4-1). The Beaumont is composed of clay-rich sediments transected by sandy fluvial and deltaic-distributary channels. The Beaumont also includes isolated segments of coast-parallel, sandy beach ridges known as the Ingleside barrier/strandplain system (Price, 1958) (Figure 4-10). The Beaumont depositional episode records a continuation of patterns that developed during deposition of the Lissie: high-frequency, glacio-eustatic, sea-level fluctuations (Figure 3-7) and dominant fluvial sediment input located in Louisiana (Galloway et al., 2000). Much of the original depositional morphology of Beaumont fluvial, deltaic, and marginal-marine systems, such as abandoned channels and relict beach ridges, can be seen at the surface in aerial photographs (Figure 4-10). At sea-level highstand, the position of the Beaumont shoreline approximately coincided with that of the modern shoreline (Solis, 1981; Knox et al., 2006). During sea-level lowstand, Beaumont-incised valleys extended many miles seaward of the present shoreline (Morton and Galloway, 1991).

South of the Brazos River, the Beaumont Formation ranges in thickness from a thin veneer in updip areas to about 500 feet near the modern coast, and thickens to the northeast (Solis, 1981). The Beaumont dips coastward from 1 to 10 feet per mile (Solis, 1981). Individual sands range from 20 to 50 feet thick, stacking locally to reach 150 feet in thickness (Knox et al., 2006). Interbedded muddy intervals are generally of similar thickness to the sands. Thicknesses of individual sands increase updip, whereas thicknesses of individual shales increase downdip. Fluvial channels display dip-oriented, meandering, and distributary patterns at the surface

(Figure 4-10) and on subsurface sand maps (Figure 4-11). Within the channel belts, the Beaumont is 50% to 65% sand (Solis, 1981). Channel belts are separated by sand-poor floodplain, delta-plain, and bay-lagoon systems.

4.7 Holocene deposits

Holocene sediments were deposited within the last 18,000 years and consist mainly of isolated river valley fills that merge coastward with bays, lagoons, and barrier islands (DuBar et al., 1991). Holocene depositional systems record the final period of sea-level rise following the last North American glaciation, a rise that was punctuated by numerous stillstands and small reversals (McGowen et al., 1976). The base of the Holocene is an erosional surface that formed during sea-level lowstand at the end of the Pleistocene. River valleys were deeply incised into the pre-existing Beaumont coastal plain and filled slowly with bay-estuary muds as the sea level rose. Subsequently, fluvial-deltaic systems prograded seaward, filling the updip parts of the valleys with sandy alluvial deposits. Only the Colorado, Brazos, and Rio Grande Rivers have completely filled their valleys to the coast. The other Texas coastal river valleys are still partly occupied by bays and lagoons (Figure 4-10). Holocene fluvial sands of significant thickness are associated mainly with the Rio Grande and Brazos Rivers where they reach 30 feet in thickness locally (Wood et al., 1963). Holocene deltaic sands mixed with silts and clays are 100 to 300 feet thick near the mouth of the Rio Grande River (Brown et al., 1980). In south Texas, Holocene eolian deposits, wind-blown sand sheets, and dunes cover large areas and reach 30 feet in thickness locally in Kenedy County (Wood et al., 1963) (Figure 4-1).

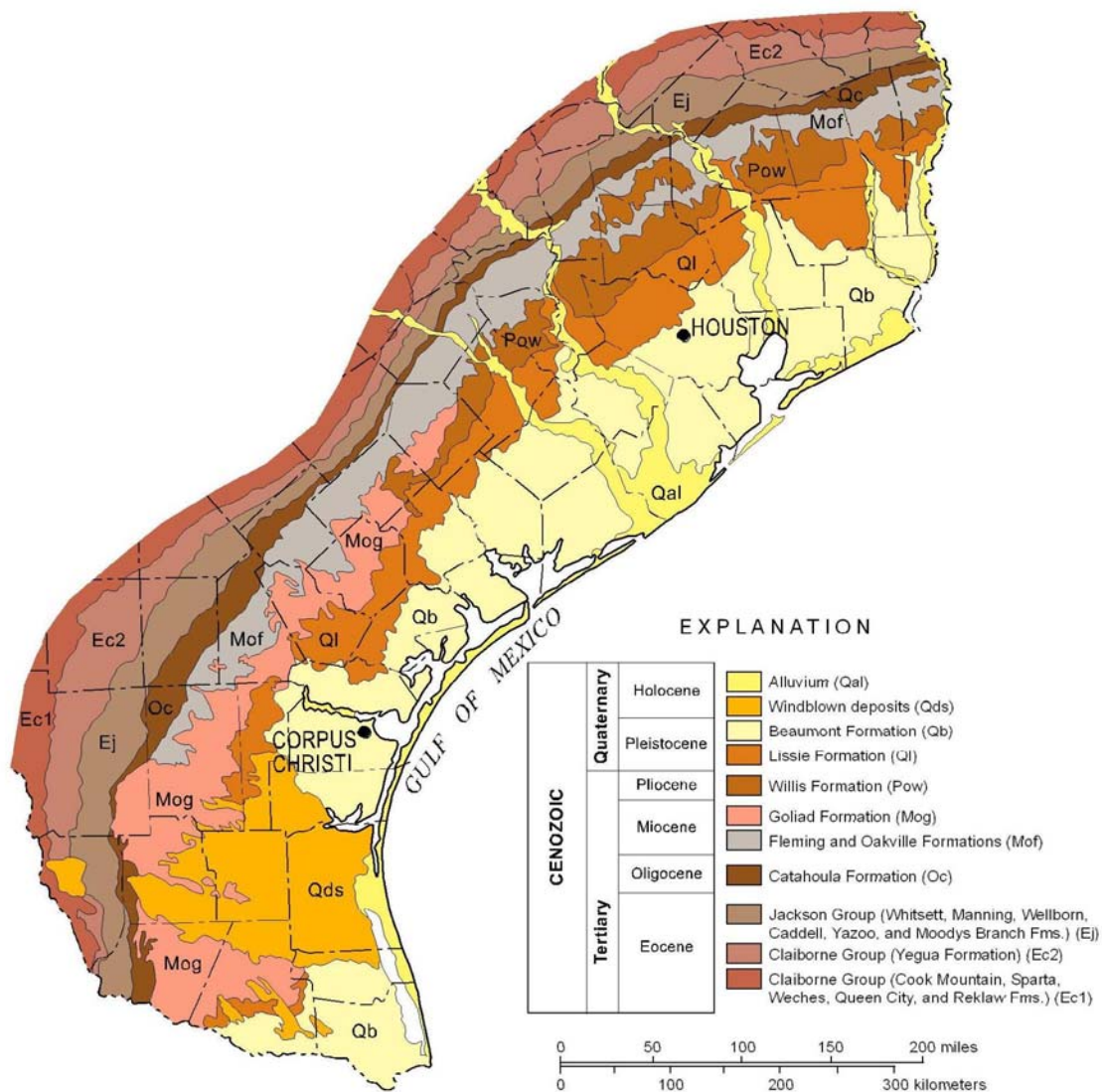


Figure 4-1. Geologic map of the Texas Coastal Plain. Source: Barnes (1992).

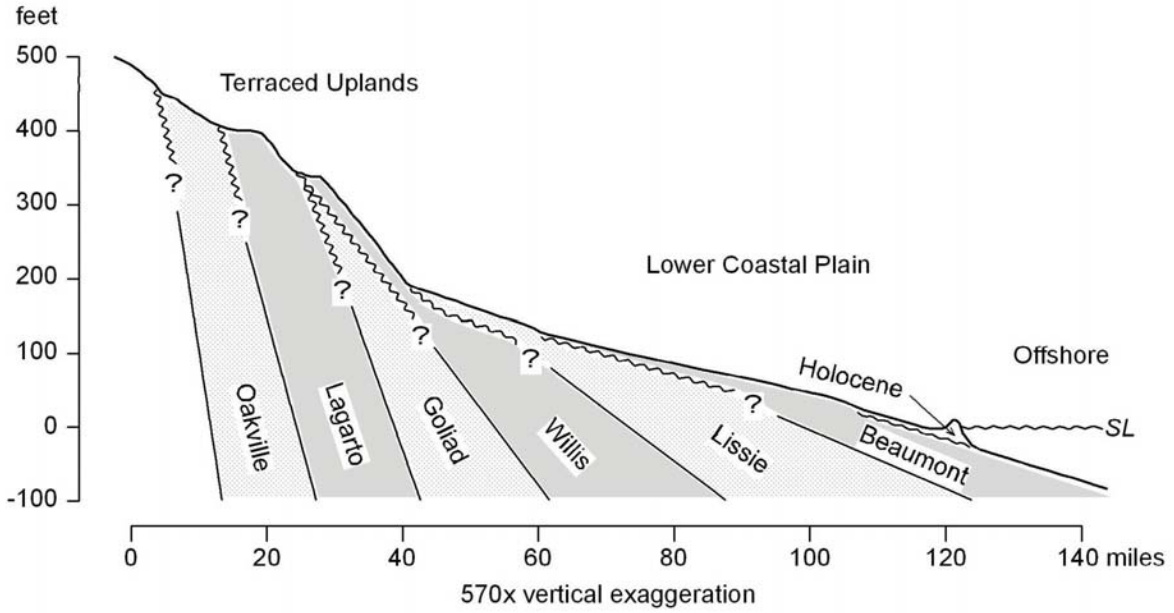


Figure 4-2. Schematic dip cross section showing relationships between outcropping formations and subsurface stratigraphy, central coastal plain, Texas. Modified from Doering (1956).

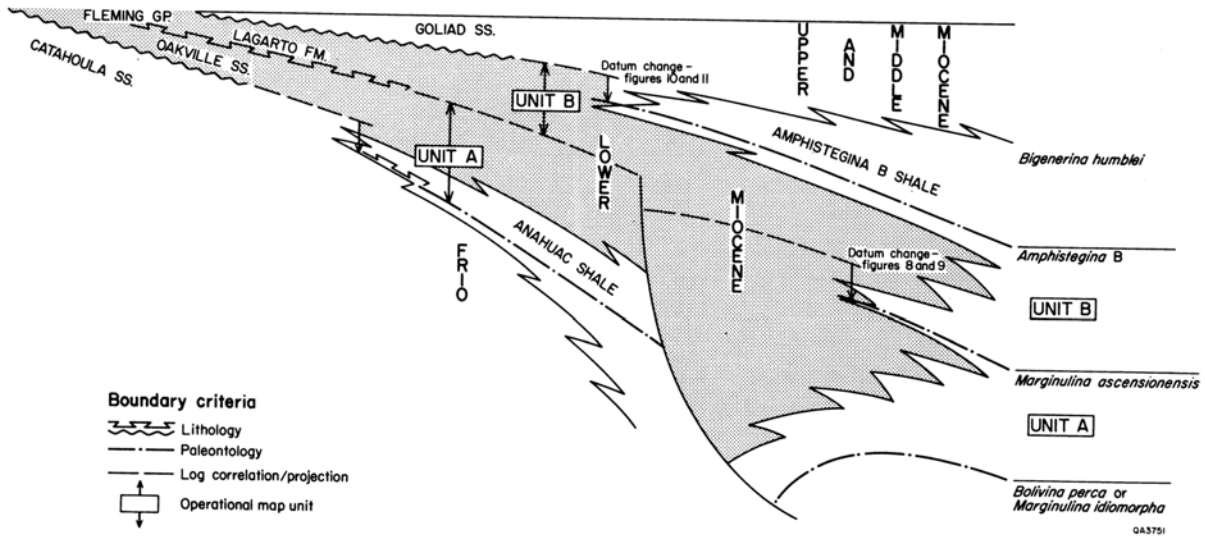


Figure 4-3. Schematic cross section of lower Miocene stratigraphy showing depositional sequences and lithostratigraphic and biostratigraphic boundaries. Source: Galloway et al. (1986).

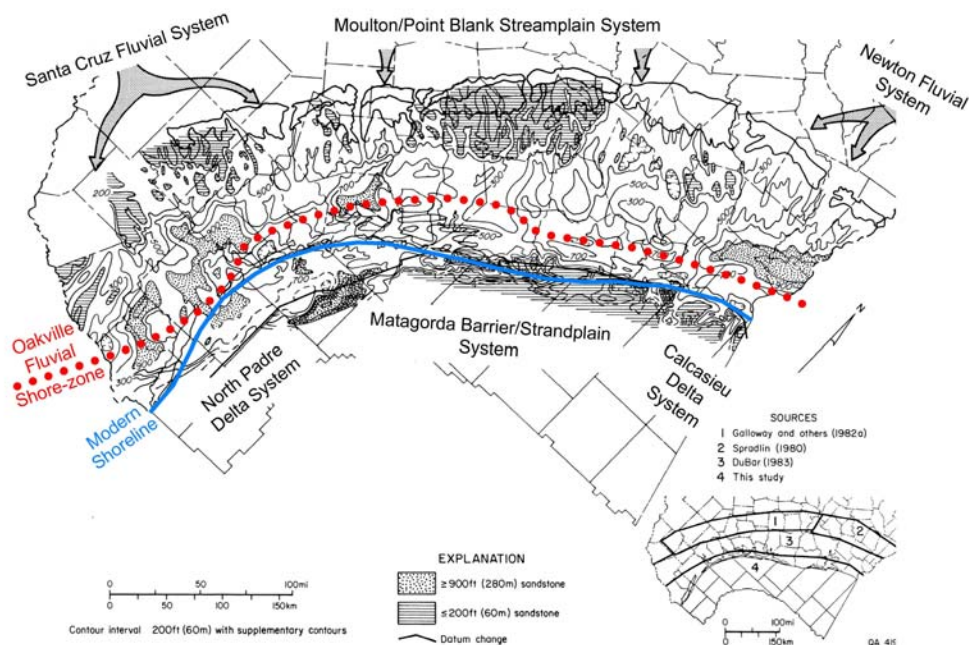


Figure 4-4. Net-sandstone isopach map of the Oakville Formation also showing depositional systems. Red dotted line separates updip fluvial systems from downdip delta and shore-zone systems. Modified from Galloway et al. (1986).

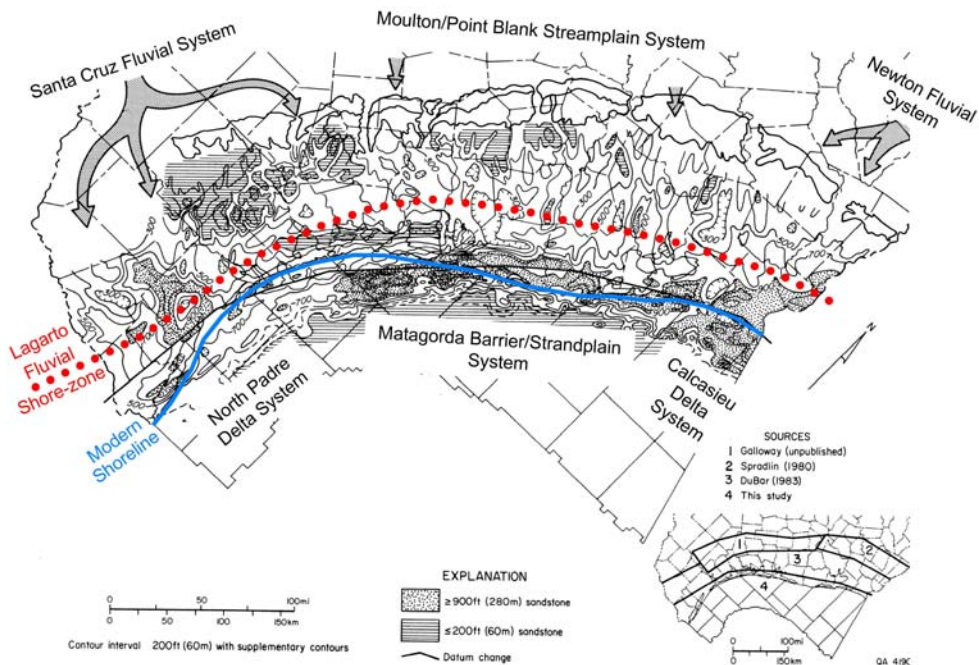


Figure 4-5. Net-sandstone isopach map of the Lagarto Formation also showing depositional systems. Red dotted line separates updip fluvial systems from downdip delta and shore-zone systems. Modified from Galloway et al. (1986).

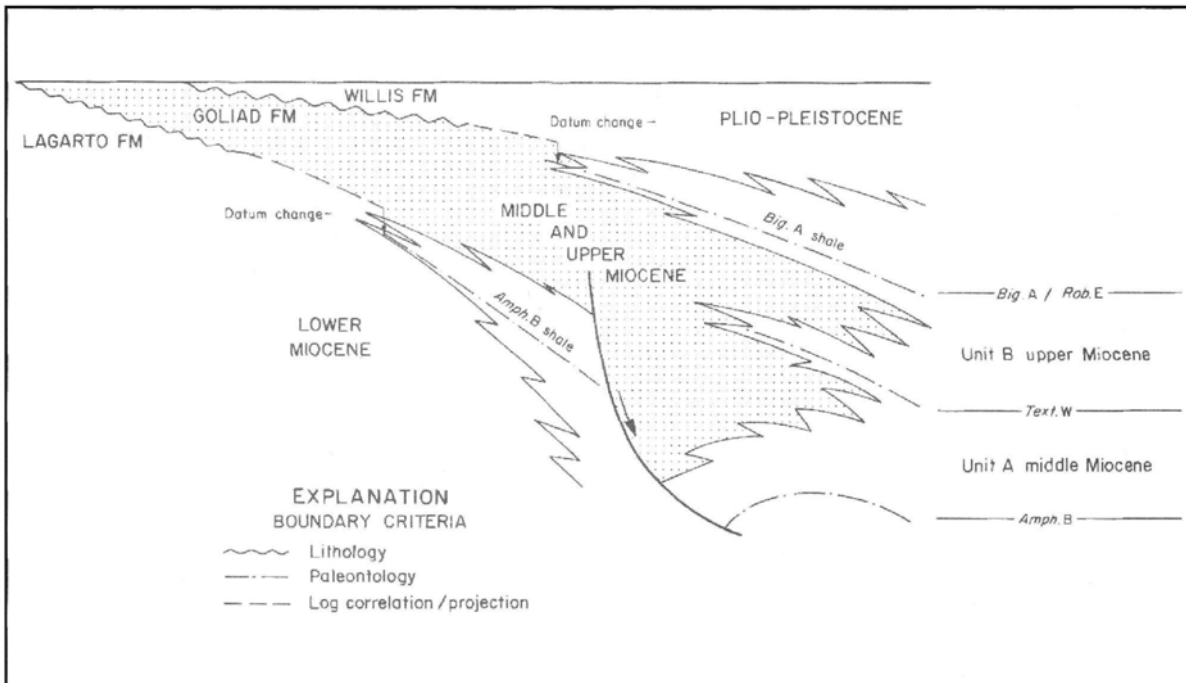


Figure 4-6. Schematic cross section of middle-upper Miocene stratigraphy showing depositional sequences and lithostratigraphic and biostratigraphic boundaries. From Morton et al. (1988).

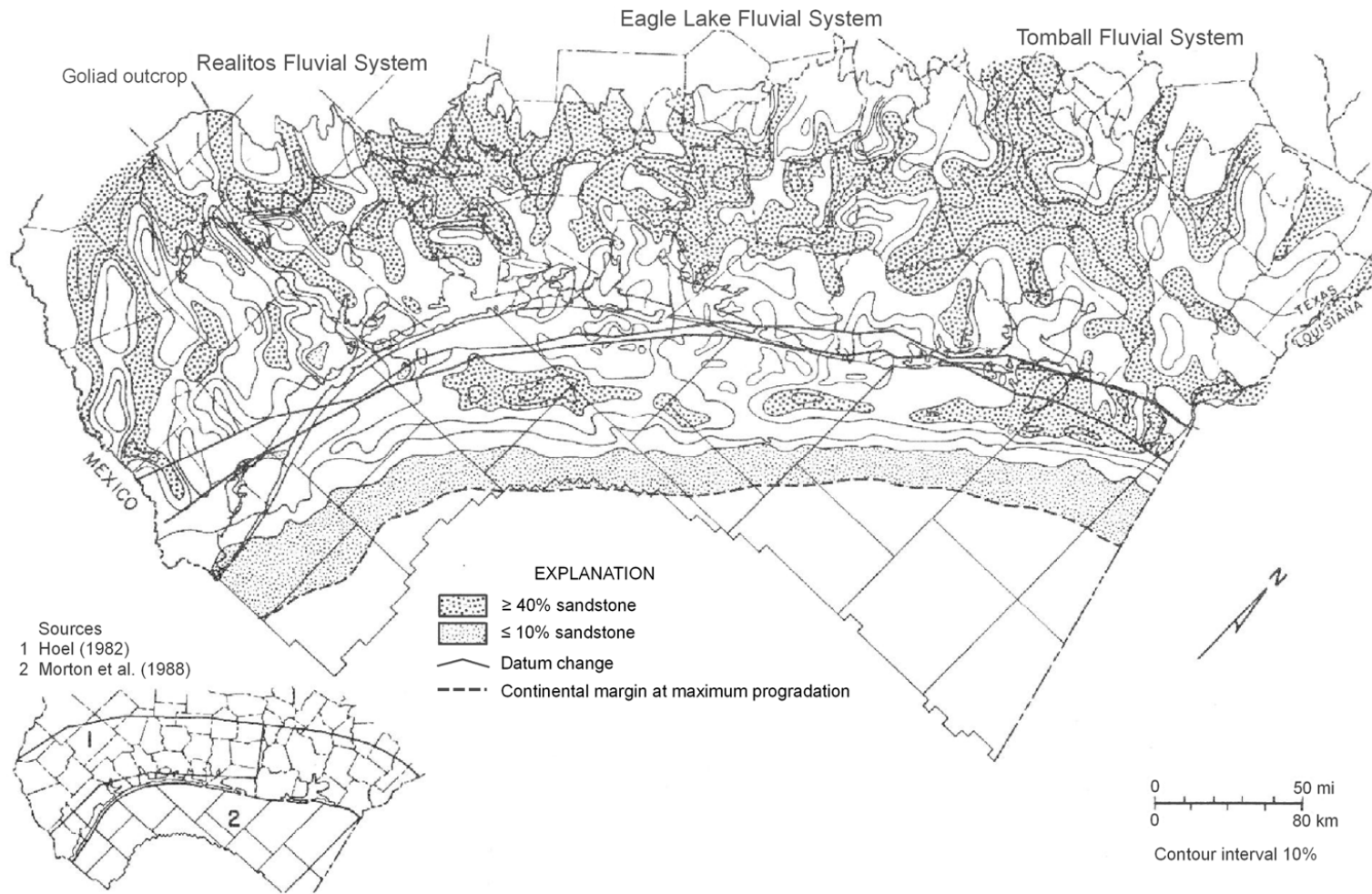


Figure 4-7. Percent sandstone maps of Goliad and equivalent middle-upper Miocene sequences. From Hoel (1982) and Morton et al. (1988).

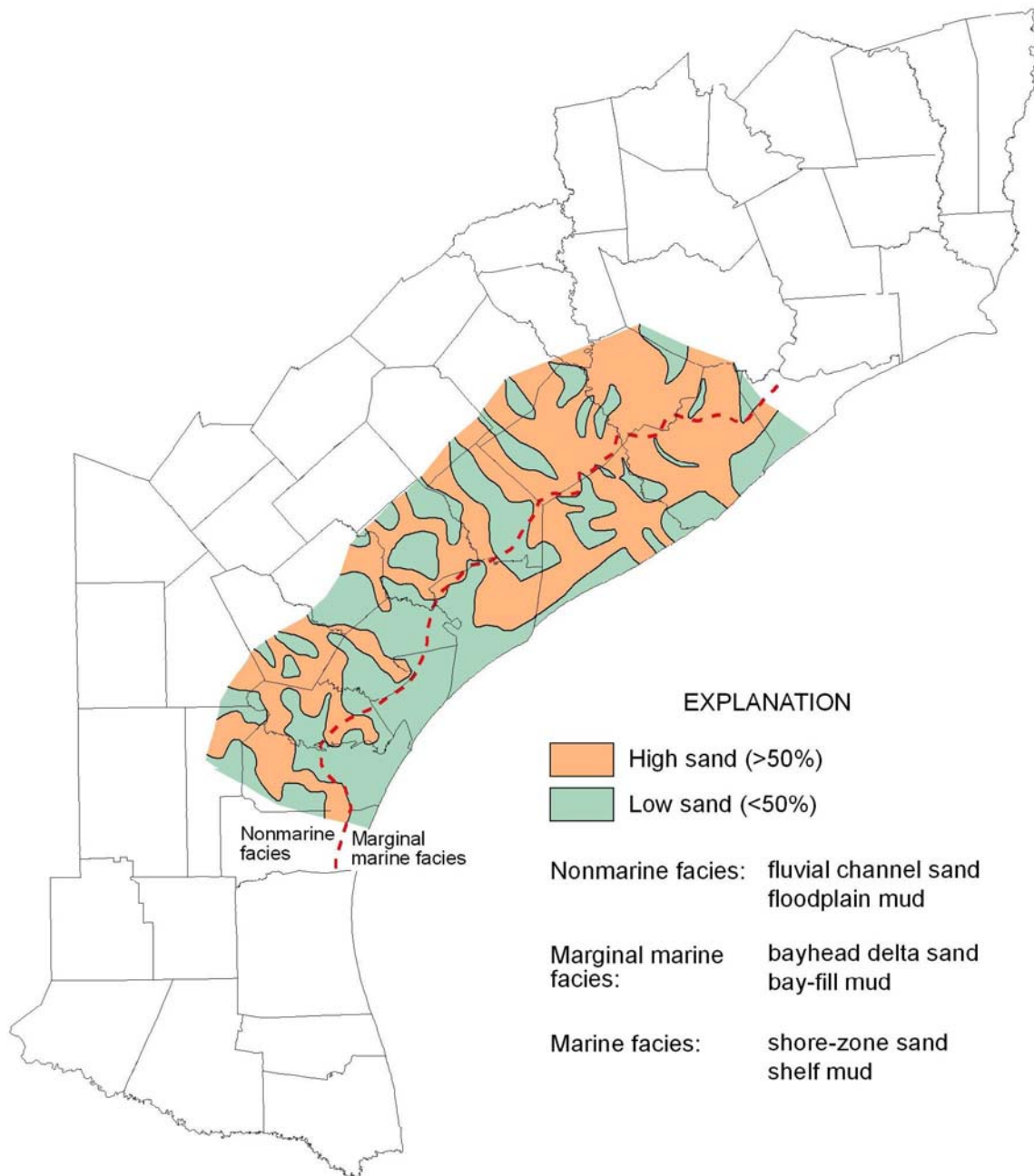


Figure 4-8. Sand content map of the Willis Formation, central coastal plain, Texas.

The red dashed line marks the approximate boundary between nonmarine and marginal marine depositional facies. Modified from Solis (1981) and Knox et al. (2006).

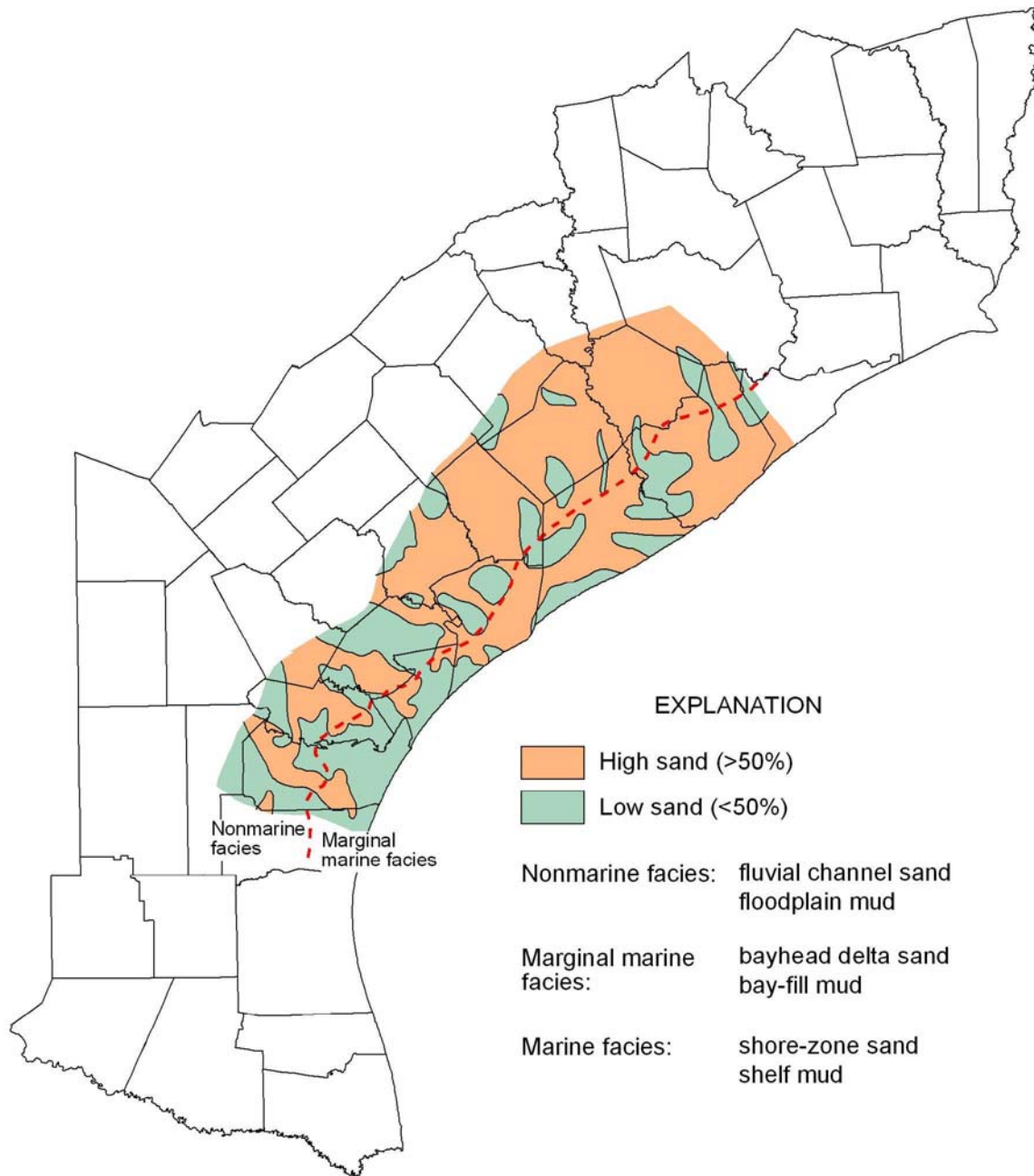


Figure 4-9. Sand content map of the Lissie Formation, central coastal plain, Texas.

The red dashed line marks the approximate boundary between nonmarine and marginal marine depositional facies. Modified from Solis (1981) and Knox et al. (2006).

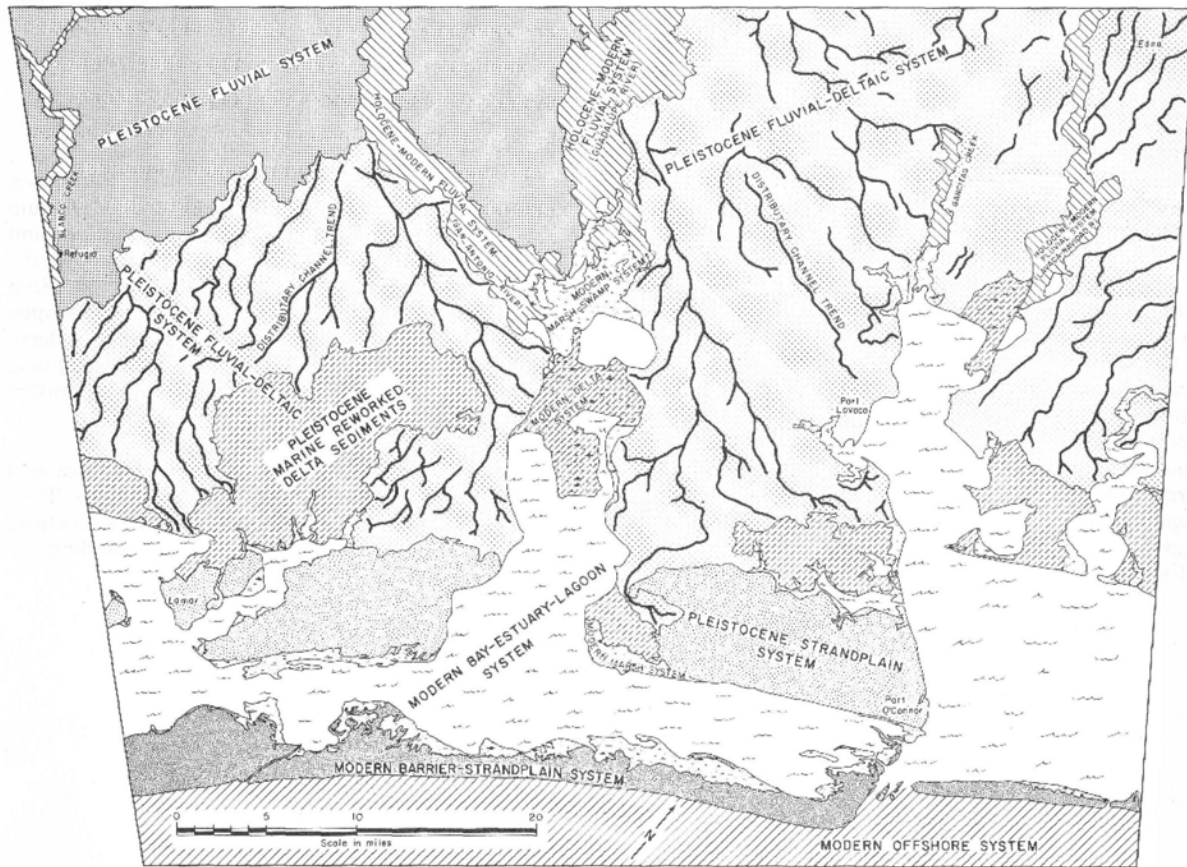


Figure 4-10. Simplified environmental geologic map of the Port Lavaca, Texas area, showing Pleistocene and Holocene depositional surfaces. From McGowen et al. (1976).

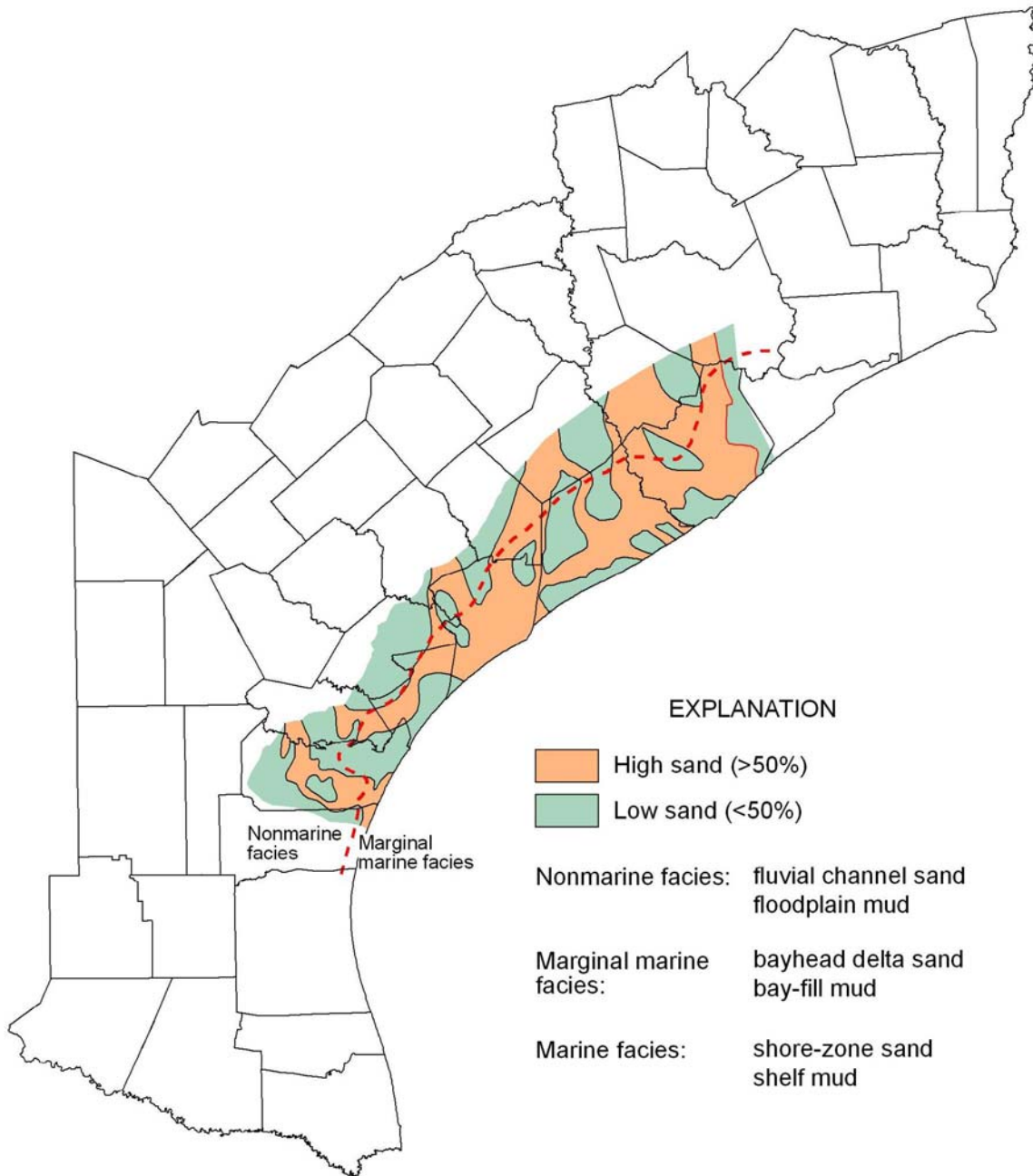


Figure 4-11. Sand content map of the Beaumont Formation, central coastal plain, Texas.
 The red dashed line marks the approximate boundary between nonmarine and marginal marine depositional facies.
 Modified from Solis (1981) and Knox et al. (2006).

5 Information sources

The information used to develop the hydrostratigraphy of the Gulf Coast Aquifer can be divided into two data groups. One group consists of geophysical logs, and the other consists of the information used to help guide the analysis of the geophysical logs. This section describes the type of information associated with each data group used to characterize the chronostratigraphy and lithology of the Gulf Coast Aquifer.

5.1 Geophysical logs

Extensive investigation of the subsurface conducted by the petroleum industry in the state of Texas has yielded a considerable number of geophysical logs that can be used to characterize the subsurface deposits. At the time of this writing, the Texas Railroad Commission was monitoring over 385,000 oil and gas wells in the state of Texas. The Texas Gulf Coast, particularly within the upper Cenozoic stratigraphy that includes the Gulf Coast Aquifer system, contains one of the largest concentrations of petroleum in the world (Nehring, 1991).

Geophysical logs are generated by lowering a measuring device into a borehole and taking a series of continuous measurements of the physical properties of the wellbore environment. A geophysical log typically contains a number of different curves acquired prior to completion of the well. Common geophysical logs include caliper, gamma, single-point resistance, normal resistivity, spontaneous potential, electromagnetic induction, fluid resistivity, temperature, flowmeter, television, and acoustic televiewer. The combination of a resistivity log and a spontaneous potential log are often referred to as electrical logs.

For this study, electrical logs were determined to be the most appropriate type of logs, and were sought exclusively due to their widespread use on the Gulf Coast for over 70 years and their particular utility in analyzing sequences of clastic sediments. Data from the shallow subsurface, as little as 100 ft below the ground surface, are critical to aquifer studies. Most wells drilled after the 1970s, when a wider array of logs became more common, do not record the shallow section of the borehole.

5.1.1 Resistivity logs

Resistivity logs record an apparent electrical resistance in and within the vicinity of the borehole at different depths. The unit of resistivity measurement is the ohm-meter² per meter. The reciprocal of resistivity is conductivity, which is measured in mhos per meter.

To generate a resistivity log, one or more electrodes are suspended on a cable and lowered into a borehole. An electric current is then forced to flow between an electrode at the surface and one or more electrodes that are downhole. The changes in the current losses are then recorded as the locations of the electrodes are moved up and down the borehole. The variations in the resistivity with depth are caused primarily by differences in the porosity and composition of the subsurface deposits and by the mineral content of the water contained in the strata and in the borehole.

The resistivity logs that were most commonly analyzed for this study consist of two electrodes downhole. When the separation of the electrodes is 16 inches or less, the configuration is called a short normal. If the two electrodes are separated by 64 inches, the configuration is called a long normal. The larger the spacing between the two downhole electrodes, the deeper the penetration of the measurement into the formation.

Dry formations will have very high resistivities because they are poor conductors of electricity. Saturation of a deposit reduces its resistivity because water is an electrical conductor. In general, saturated subsurface materials with low resistivity include silts, clays, and shales. Fresh water deposits composed of sands and gravel tend to have high resistivities. The resistivity of a formation will vary inversely with the total dissolved solids concentrations in its pore water. One of the reasons that clays tend to have low apparent resistivities is because their interstitial waters are often highly mineralized. On the other hand, sands and gravels saturated with fresh water tend to have high apparent resistivities because their surfaces are relatively inert and tend to release few minerals into solution.

Figure 5-1 illustrates how apparent resistivity can vary with differences in subsurface material and total dissolved solid concentrations in groundwater. In fresh water, the difference in the apparent resistivity between sandy and clayey deposits is considerably greater than in very brackish water. In fact, in salt water, the difference in apparent resistivity between a clay and a sand is subtle. In situations that involve heterogeneous deposit types and vertical variations in water quality, analysis of the resistivity logs should be performed in concert with the analysis of other logs that provide independent information on either the characteristics of the deposits or the water quality.

Because the borehole fluids affect the resistivity measurement, the borehole diameters should be kept as small as possible. In a large-diameter hole or with short spacings between the electrodes, the resistivity will be heavily influenced by the drilling fluid. This is because the "zone of influence" of the electrodes may not extend very far into the formation (Driscoll, 1986). If the drilling fluid is quite clayey or salty (highly conductive), the formation resistivity may serve to partially mask the resistance of relatively thin sandy aquifers.

5.1.2 Spontaneous potential logs

Spontaneous potential (SP) logs record naturally occurring electrical potentials (voltages) that occur in the borehole at different depths. The SP log primarily measures the electrochemical potential between a stationary reference at the surface and a moving electrode in the borehole. The circuitry between the surface and the downhole electrode does not include an external source for an electric current. The electrochemical potential is generated by ions moving between the borehole fluid and the formation water. If there is no contrast in the ionic concentrations of the borehole fluid and the formation water, there is no electrochemical potential, and the SP potential is zero. The downhole electrode usually has a lower (more negative) potential than the surface electrode. SP logs only record relative values rather than the absolute values of resistivity tools.

The examples in Figure 5-1 illustrate the type of SP responses that can be expected in formations containing fresh water, brackish water, and salt water when the drilling fluid is composed of

fresh water. As shown in Figure 5-1, at shallow depths where there may be little difference in the concentration of ions between the drilling fluids and the aquifer, the analysis of the SP log may be difficult because of the lack of deflections. However, at deeper depths where the formation waters are more mineralized than the drilling fluids, the leftward deflections (more negative values) in the SP logs are useful for identifying permeable strata. Despite the fact that the SP logs can provide potentially useful information on the location of permeable zones, there is no direct relationship between the magnitude of the SP deflection and either permeability or porosity because just a fraction of a millidarcy of permeability is sufficient to support the ionic movement required to generate a SP deflection. The deflections associated with sands and gravels are more associated with their mineralogical differences than their permeability difference with clays and shales.

The analysis of an SP log begins with developing a "baseline" by connecting the potentials associated with the impermeable beds such as clays and shales. Deflections to the left of this baseline are usually associated with beds of coarse-grained deposits such as sands and gravels. If no clay layers are present in the lithologic profile, the SP log may not provide much useful information.

5.1.3 American Petroleum Institute format

The standard format for geophysical logs used by the petroleum industry is set by the American Petroleum Institute (API). The API format includes a header file and a set of log curves. Table 5-1 summarizes categories of data contained in the API headers.

Table 5-1. Types of log header data

Data Categories	Description	Use
Measurement Datum / Log Datum	Elevation from which logged depths are measured	Allows referencing of curve measurements to a selected datum such as sea level
Kelly Bushing (KB)	An oil rig design component, specifically the device that transfers the torque of the rotary table to the drill stem	Elevation of KB is commonly used as the measurement datum by the logging engineer. Often given as height above GL
Ground Level (GL)	Elevation of surface of ground at the well head	Allows measured depths to be converted to absolute depths
Top of Logged Interval (TLI)	Shallowest measured depth	Determines whether the log covers the relevant stratigraphic interval
Bottom of Logged Interval (BLI)	Deepest measured depth	Determines whether the log covers the relevant stratigraphic interval
Operator / Company	The person or company, either proprietor lessee, actually operating an oil well or lease	A searchable term used to identify and locate wells
Lease	A parcel of land on which mineral exploration rights have been granted by the landowner to a lessee	A searchable term used to identify and locate wells

Data Categories	Description	Use
Well Number	A numbering system within a lease or other unit	A searchable term used to identify and locate wells
Well Field	A region encompassing several leases in which proven reserves exist	A searchable term used to identify and locate wells
Permit Date or Completion Date	Date after which well installation is permitted, date of complete of well construction for production	A searchable term used to identify and locate wells

The Kelly Bushing is an adapter that connects the drilling rig rotary table to the drill string. As shown in Figure 5-2, the Kelly Bushing exists near the elevation of the drill rig floor. The elevation of the Kelly Bushing is important because it is used as the measurement datum referenced by the log curves. Accurate datums for well log records are important because they establish the relationship between depths of stratigraphic events in the well and a universal datum – sea level. The well log header usually contains both the elevation of the Kelly Bushing and the ground level at the wellbore. Often, the height of the datum above ground level is provided.

For some of the log headers, no elevation information is available for either the ground level or the Kelly Bushing. To estimate the elevation of the Kelly Bushing in those instances, a computer script was written to estimate the ground elevation at the well bore location from the USGS Digital Elevation Model (DEM) of the Gulf Coast and then to add an additional 14.9 ft, which is the average height of the Kelly Bushing above ground level based on the headers of logs used in this study having completed elevation data.

Beneath the header, the main body of the geophysical log contains the log curves. Figure 5-3 shows an example header and set of log curves for a geophysical log used for this study. The logs are plotted on three tracks with a depth column dividing tracks 1 and 2. The vertical-scale plotting depth is always linear and is usually scaled as 1, 2, or 5 inches per 100 feet of depth. The three tracks for the logs can have different scales and are reserved for specific types of logs. Among the logs that are plotted on track 1 are SP, gamma ray, and caliper. Track 1 always uses a linear scale, whereas the other two tracks can use either a linear or logarithmic scale. Porosity and resistivity logs are always shown in track 2 or 3. At the top of each track, the scale and log types are shown.

5.2 Approach for obtaining geophysical logs

The approach for obtaining geophysical logs focused on gathering information along a series of dip- and strike-oriented lines to develop stratigraphic cross-sections. Where appropriate, we used the same logs as previous stratigraphic studies. Key information gathered from previous studies included analysis of paleontology data, estimates of age of deposition, mapping of depositional systems, identification of flooding surfaces (explained in Section 6), and delineation of geologic formations. As the logs were being collected along the dip-oriented and strike-oriented lines, additional logs were collected between the lines to fill in areas to benefit the generation of sand and facies maps and the correlation of stratigraphic surfaces across the study area.

A primary consideration in our log selection was a starting depth above 300 feet below ground surface. This consideration significantly reduced the number of candidate well logs because many drilling operations are not interested in characterizing the zone of fresh water that is cased off during the construction of an oil well.

5.2.1 Geophysical logs' sources

At the beginning of the project, the initial search for suitable logs focused on the logs that had been used as part of five previous aquifer studies. Two of these studies are considered to be among the landmark studies of the Texas Gulf Coast Cenozoic. These studies were performed by Dodge and Posey (1981), whose study focused on the Tertiary-age deposits, and by Morton and others (1985), whose study focused on Miocene-age deposits. A third study provided a detailed chronostratigraphic analysis of the Chicot and Evangeline Aquifers. This study was performed by Knox and others (2006) as part of a larger study of the groundwater system of the lower Colorado River Basin (Young and Kelley, 2006). A fourth study provided a detailed chronostratigraphic analysis of the Yegua and Jackson Aquifers (Knox and others, 2006). The fifth study provided a set of logs that were analyzed as part of a groundwater investigation performed by Goliad Sand, Ltd. in Bee and Refugio Counties. The log analysis for the fifth study was performed by retired USGS professional Ernest Baker. Mr. James Dodson, president of Goliad Sands, Ltd., provided us with the log information.

All of the logs selected from the five previous studies were combined with additional logs from our generalized search through the professional literature. Our search for logs included a review of maps and databases from the BEG, TWDB, the Texas Commission on Environmental Quality (TCEQ), and the U.S. Mineral Management Service (MMS). As the geophysical logs were identified through application of selection criteria, personnel from our team visited the archive where the logs were stored to retrieve and review the logs for quality control purposes. We then employed a third-party vendor to produce scanned raster images of the logs at a resolution of 400 dots per square inch (dpi). As scans were obtained, specific logs were selected for digitization to facilitate their use in stratigraphic correlation. Log scans were transmitted to a third-party vendor who digitized the images and generated a file with a 0.5-foot sample spacing, using the Log ASCII Standard (LAS) format.

5.2.2 Geophysical logs selected for the study

Figure 5-4 shows the locations for the 892 logs that were used for our study. For 706 of these logs, the lithology was identified and tabulated. In general, a uniform coverage was sought across the study domain for lithology. The higher density of logs analyzed for lithology occurs in the northern part of the study because of the lithologic information available from the Lower Colorado Water Project study by Young and Kelley (2006). Stratigraphic picks were made for 457 logs. of those 457 logs, 157 logs were associated with the dip-oriented cross-sections, and 443 logs were associated with the strike-oriented cross-sections, with 86 of the logs being associated with both sets of cross-sections. To interpolate the stratigraphic surfaces between these cross-sections, stratigraphic picks were made at 74 log locations in between the dip and

strike cross-sections. At 45 log locations, paleontology data were available and were used to check and guide the stratigraphic correlations.

Appendix A provides the information listed in Table 5-2 for the log locations shown in Figure 5-4.

Table 5-2. Selected tables and fields from the Microsoft Access database used to manage information on the 892 well logs used for the study.

Field Name	Description
API number	American Petroleum Institute (API) identification number.
NAD27 latitude	Latitude based on North American Datum 1927.
NAD27 longitude	Longitude based on North American Datum 1927.
Dip section/position	If blank, the log is not associated with a dip cross-section. Otherwise, the dip number is listed, and the position of the log is counted from a northwest-to-southeast sequence.
Strike section/position	If blank, the log is not associated with a strike cross-section. Otherwise, the strike number is listed, and the position of the log is counted from a southwest-to-northeast sequence.
Company	Company operating the oil or gas lease.
Lease	Land parcel being leased for use of the oil or gas well.
County	County in which the lease is located.
Lithology and water quality data	Indicates whether lithology picks and water quality interpretations were performed on the well log.
Paleo data	Indicates whether paleo data are associated with the log.

5.3 Literature review

A review of existing literature uncovered some key studies important to this investigation. The GAT maps, compiled as the Geologic Map of Texas (Barnes, 1992) and available in digital form (Estep, 2004), provided surface outcrop data. Stratigraphic unit geometries and approximate depths were obtained from the cross-section sets of Dodge and Posey (1981), Morton and others (1985), and Morton and Jirik (1989). General structural features for the Gulf coast were obtained from the Tectonic Map of Texas (Ewing, 1991) and from papers within Jones and Freed (1996). More specific structural information was obtained from Galloway et al. (1982; 1986). Numerous stratigraphic studies were valuable in assessing depositional setting, facies, and systems, including Galloway et al. (1986), Morton et al. (1988), Hoel (1982), Coleman (1990), Solis (1981), Knox et al. (2006), Hernández-Mendoza (2008), and Galloway et al. (2000). Aquifer studies that were reviewed included Baker (1979) and county water resource studies by USGS and TWDB, including Rogers (1967), Shafer (1960, 1965, 1968, 1974), Loshkot et al. (1982), Hammond (1969), Preston (1963), Marvin, Shafer, Dale (1962), Harris (1965), Thompson (1966), Peckham (1965), Anders and Baker (1961), Anders (1957), Dale (1952),

Mason (1963), Shafer (1960), Myers and Dale (1961), Shafer and Baker (1973), Reeves (1967), Myers and Dale (1967), Baker, R.C., and Dale (1961), McCoy (1990), and Chowdhury and Mace (2007). Paleontological and chronological data from Paleo-Data, Inc. (2009) and from Galloway et al. (2000) were referenced to establish the chronostratigraphic framework for this study.

5.4 Geological faults

Generalized fault locations and locations of salt features were taken from the Tectonic Map of Texas (Ewing, 1991). However, fault patterns at specific horizons were also incorporated from specific studies. Faults at the top of the Frio Formation were taken from Galloway et al. (1982). Fault patterns at a lower Miocene level were taken from Galloway et al. (1986). Younger faults near the shoreline and in the offshore area were taken from Al-Ghamdi and Watkins (1996), Huh et al. (1996), and Watkins et al. (1996).

5.5 Paleontology data

Paleontologic data are critical for defining geologic ages of stratigraphic intervals and surfaces. These data are collected during the drilling of oil and gas wells, and are more commonly associated with exploration drilling. Because the stratigraphic interval of the Gulf Coast Aquifer only produces hydrocarbons in the area beyond the current shoreline, the most useful data come from wells near the Texas shore and beyond. A collection of paleontologic data in digital form was obtained from the BEG, The University of Texas at Austin. The data are from wells drilled before 1980 either on land or within Texas submerged lands, which includes bays and the offshore area within 3 miles of the shoreline. For wells drilled beyond this area, data were collected from the MMS. These data are available digitally from the MMS website.

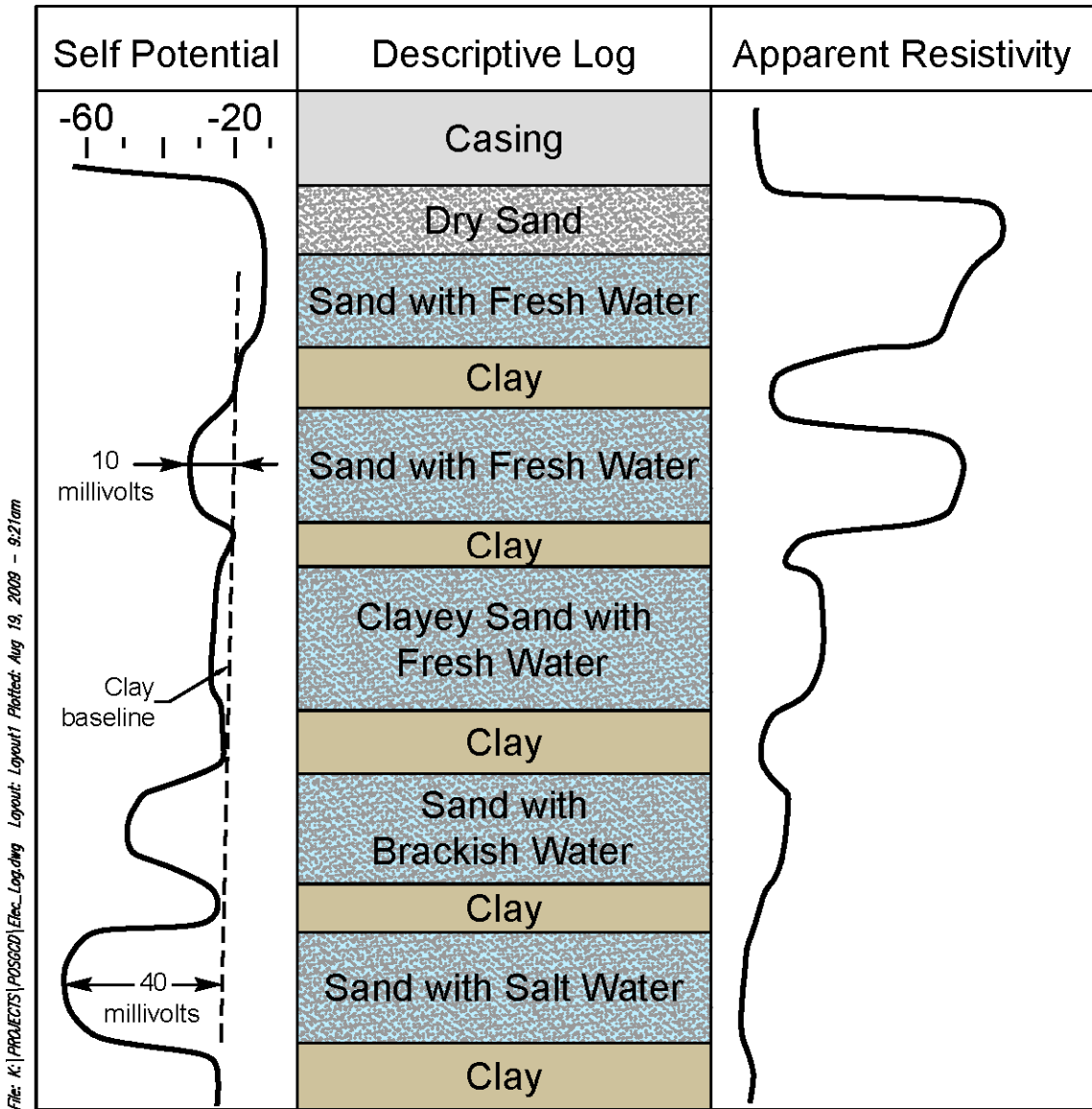


Figure 5-1. Idealized SP and resistivity curve showing the responses corresponding to alternating sand and clay strata that are saturated with groundwater that has significant increases in total dissolved concentrations with depth. Modified from Driscoll (1986).

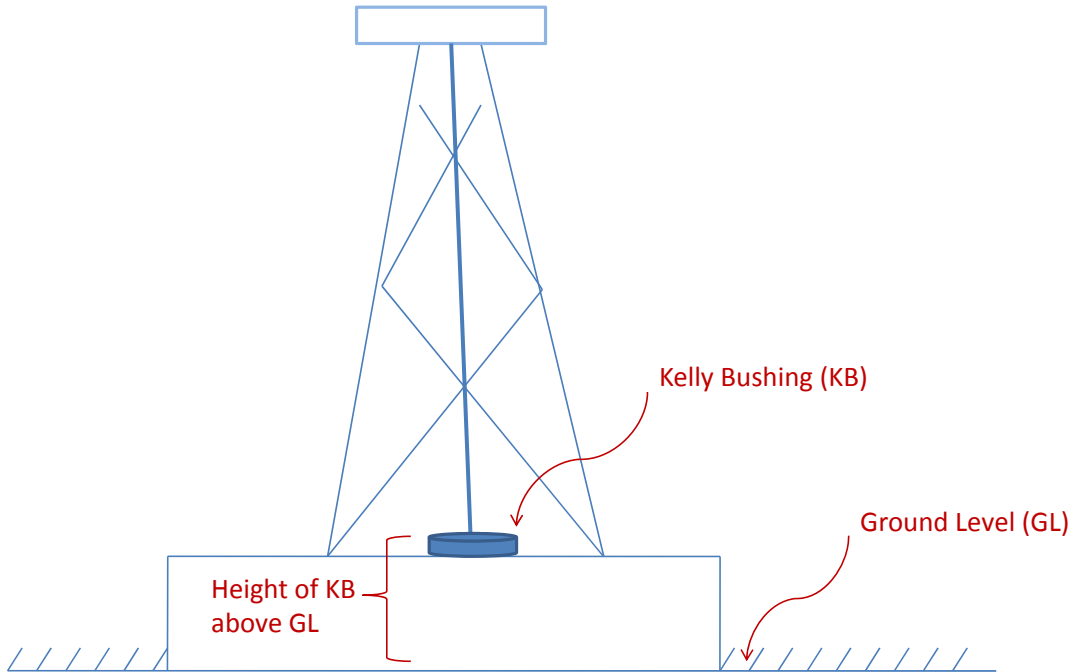


Figure 5-2. Schematic showing the location of the Kelly Bushing relative to the ground level and the oil rig.

FINAL LOG Schlumberger		DUAL INDUCTION-SFL WITH LINEAR CORRELATION LOG	
COUNTY HIDALGO	WELL NAME WEST JEFFRESS	COMPANY COASTAL OIL & GAS CORPORATION	WELL NO. MED-L (2" - 100') API # 215-31708
LOCALITY YTURRIA LAND & CATTLE CO. #3	FIELD JEFFRESS, W. (Vicksburg V)	WELL YTURRIA SAND & WATER CO. #3	STATE TEXAS
WELL CO. #3	COUNTY HIDALGO - 04	DATE 8/15/86	LOG NO. 660827272
APPROXIMATE LOCATION 5825' ENCL & 660' ENCL OF THE ANTONIO M. GANO SURVEY, A-81		Other Services: LOGOM LSS/WAVEFORM CYBERLOOK HDT, CBL/VDL	
Permeability Datum: G.L., Elev. 320.9		Elev.: K.B. 348.6	
Log Measured From: K.B., 27.7 Ft. Above Perm. Datum		D.P. 347.6	
Drilling Measured From: K.B.,		G.L. 320.9	
Date	13-SEPT-86	27-SEPT-86	10-OCT-86
Run No.	ONE	TWO	THREE
Depth-Driller	6446	10906	12500
Depth-Logger (Schl.)	6452	10442	12507
Run Log Interval	6446	10436	12501
Top Log Interval	3024	6430	10553
Casing-Driller	13-378 3025	9-62 6446	7-578 @ 10554
Casing-Logger	3024	6430	10553
Bit Size	12-1/4	8-7/8	6-3/4
Type Fluid in Hole	G.S.	OIL BASE	OIL
Depth - Visc.	12.8 139.0	16.3 146.0	17.0 152.0
pH - Field Log	10.5 6.2 ml		
Source of Sample	CIRC PIT		OILBASE
Run @ Meas. Temp.	46.3 @ 120°		
Run @ Meas. Temp.	54.0 @ 75°		
Run @ Meas. Temp.	1.11 @ 75°		
Source: Kerf / Misc	PRESS CHART		NOT AVAIL.
Run @ BH	311 @ 182°		@ 291°
Calculation Stopped	12:00 9/13 01:00 9/22 15:30 10/10		
Logger on Bottom	15:30 9/13 10:00 9/22 21:00 10/10		
Meas. Rec. Temp.	204	252	299
Equip. Location	8406 EDIN.	8246 EDIN.	8406 EDIN.
Recorded by	P. BERRIE	RIGG	BERRIE
Witnessed by	W. SANDEFUR	SANDEFUR	JAMES SANDEFUR

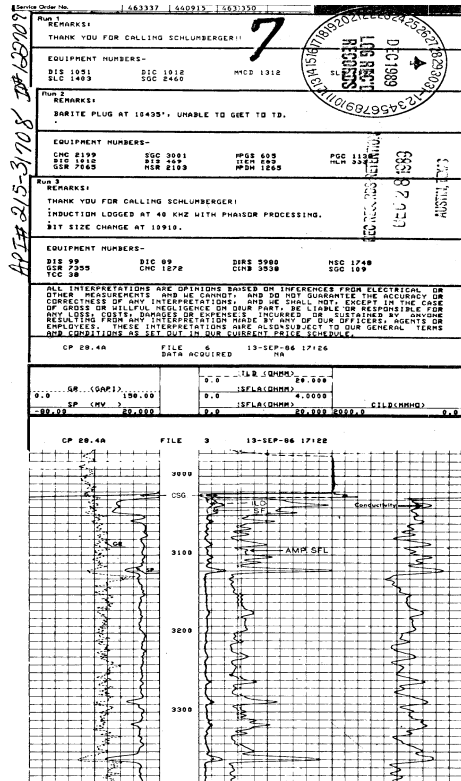


Figure 5-3. Example of a geophysical well log that uses the American Petroleum Institute format.

6 Approach for stratigraphic interpretation

This section identifies the geologic units that comprise the Chicot, Evangeline, and Jasper Aquifers and the Burkeville Confining Unit. For each of these units the maps of the base elevations and total thickness is provided.

6.1 Chronostratigraphic conceptual framework

Modern techniques for stratigraphic correlation and mapping are based on the principles of sequence stratigraphy, which integrate depositional systems with chronostratigraphically significant surfaces (Van Wagoner et al., 1990). Chronostratigraphy (time-stratigraphy) deals with the age relationships of stratigraphic layers and surfaces. Sequence stratigraphy emphasizes surfaces of widespread extent that bound sedimentary packages (sequences) formed during a specific time period in related depositional environments. An example of related depositional environments would be a fluvial system connected to a delta with flanking bay-lagoon systems (e.g., Figure 3-5). Chronostratigraphic surfaces typically are not precisely synchronous throughout their extents, but they do separate layers of differing ages and depositional environments. Within the discipline of sequence stratigraphy, there are various interpretive models, but the fundamental components – related depositional facies bounded by chronostratigraphic surfaces – are determined objectively and are common to all models (Catuneanu et al., 2009).

For the purpose of defining layers in the Gulf Coast Aquifer, there are two key chronostratigraphic surfaces: erosional unconformities and marine flooding surfaces. In sequence stratigraphy, unconformities are surfaces separating younger from older strata along which there is evidence of erosional truncation or down cutting (Van Wagoner et al., 1990). In the Gulf Coast Aquifer, most unconformities are formed where fluvial systems have eroded valleys into older sediments (incised valleys). Marine flooding surfaces are created by relative sea-level rise and transgression of the coastal plain. Marine transgressions, which may also be erosive, are generally accompanied by interruption in the supply of sandy sediment and formation of muddy marine facies (Galloway and Hobday, 1996). The maximum flooding surface is a special type of marine flooding surface that marks the most widespread extent of coastal transgression (Figure 6-1).

Marine flooding surfaces make good boundaries for aquifer layers. Flooding surfaces are enclosed in mud-dominated layers (marine facies), are laterally extensive, and produce distinctive signatures on well logs. Marine facies associated with flooding surfaces commonly contain fossils with well-documented extinction times, which are useful for global chronostratigraphic correlation (biostratigraphic zonation). Flooding surfaces bound genetic stratigraphic sequences formed during progradational depositional episodes (see Section 3.4, Depositional history). In the Gulf Coast Aquifer, progradational systems are dominated by fluvial sand and related nonmarine facies (Figure 6-1). Thus, flooding surfaces lie within regionally correlative, mud-dominated layers that enclose sand-prone layers. Sand bodies may be interconnected within these layers but are rarely interconnected across flooding-surface boundaries. Marine flooding surfaces, however, are not perfect aquifer layer boundaries. Transgression and marine flooding often do not extend across the entire coastal plain. Fluvial

depositional systems may persist uninterrupted in one area while marine transgression is occurring in another area. Furthermore, all marine flooding surfaces have limits to their landward extents (Figure 6-1).

Although marine flooding surfaces are useful for tracing aquifer layer boundaries, depositional facies modeling and mapping are needed to characterize hydrogeologic properties within layers. The depositional environment controls intrinsic aquifer-matrix properties – porosity, permeability, and mineral composition – as well as larger-scale aquifer storage and flow properties related to sand-body size, shape, orientation, and interconnectivity. In a fluvial depositional system, for example, channel-fill sand bodies are elongated in the direction of depositional dip (coastward) (Figure 3-4). In the Gulf Coast Aquifer, regional structural dip and hydraulic gradient parallel fluvial sand-body elongation, enhancing the potential for coastward groundwater flow. In sand-dominated fluvial systems, such as those in the Goliad Formation, sand bodies are highly interconnected, whereas in sand-poor fluvial systems, such as those in the Beaumont Formation, sand bodies are more isolated in floodplain muds. In marine shore-zone depositional systems, strand-plain and barrier-island sand bodies are elongated perpendicular to the regional hydraulic gradient and are located at the interface between meteoric fresh waters and marine saline waters. Thus, shore-zone sand bodies are commonly sites of groundwater mixing and saltwater intrusion. Post-depositional controls – compaction and intergranular cementation – modify aquifer properties inherited from the depositional environment. The Gulf Coast Aquifer, however, which is relatively young geologically and not deeply buried, has not been affected significantly by post-depositional processes.

Within sequence stratigraphy, the concept of depositional cyclicity provides a framework for regional stratigraphic correlation and layer definition. Deposition is inherently episodic, periods of coastal plain progradation alternating with relative sea-level rise and marine transgression (see Section 3.4, Depositional history). Depositional cyclicity is controlled by the interplay of varying sediment supply, sea-level fluctuation, climate, and subsidence. In the Gulf Coast Aquifer, a relatively constant rate of coastward increasing subsidence provided space for younger sediments to accumulate above older sediments without major interruption. The climate of the Texas Coastal Plain also has not varied greatly during the depositional history of the Gulf Coast Aquifer. Uplift of the Rocky Mountains and other tectonic events provided a relatively continuous supply of sediment for rivers to transport to the coast, although the location of sediment input onto the coastal plain varied (Figure 3-6). Sea-level fluctuation, on the other hand, has been cyclic, rising and falling at rates in response to the formation and melting of glaciers. For the Gulf Coast Aquifer, the combination of localized sediment input and sea-level fluctuation has created systematic depositional cycles of sand-prone progradational facies alternating with mud-dominated transgressive facies (Figure 6-1).

Depositional cycles occur at various scales. A geologically brief depositional cycle, commonly called a parasequence, records a single, usually localized, progradational event followed by transgression (Van Wagoner et al., 1990; Galloway and Hobday, 1996). Parasequences range in thickness from about 10 to 200 feet and in lateral extent from about 10 to 2,000 square miles (Van Wagoner et al., 1990). A parasequence is composed of beds of sand or mud, each a few feet to a few tens of feet thick, which record single depositional events produced by storms or floods. Sandy beds within a parasequence extend progressively farther seaward as the

fluvial-deltaic system progrades the shoreline. Rising sea level and diminished sediment supply combine to halt shoreline progradation and drown the coastal plain, capping the parasequence with a veneer of transgressive mud. Commonly, parasequence deposition is terminated when the fluvial-deltaic system moves to an adjacent part of the coastal plain. The process of lateral migration of fluvial-deltaic systems eventually creates a regionally continuous wedge of coastal plain sediments composed of amalgamated parasequences.

Parasequences stack to form sequences of increasing scale and duration. Large, long-term sequences record the entire GOM Tertiary fill, but the most commonly described sequences span 1 to 5 million years, range widely in thickness from about 30 to 5,000 feet, and cover 500 to 30,000 square miles (Van Wagoner et al., 1990). The Gulf Coast Aquifer encompasses about 10 such sequences, corresponding to major depositional episodes and covering a time span of about 24 million years (Galloway et al., 2000) (Figure 3-7). The duration of Gulf Coast sequences generally decreases through time in response to increasingly high-frequency sea-level fluctuations (Figure 3-7). As defined by Galloway and others (Galloway, 1989b; Galloway et al., 2000), Gulf Coast sequences are bounded by maximum flooding surfaces and are composed of sets of parasequences displaying alternating progradational and retrogradational (transgressive) stacking patterns (Figure 6-1). Sequences are hierarchical – shorter, more localized sequences group to form longer more widespread sequences – and the conceptual framework of sequence stratigraphy can be adapted to fit the scale of resolution allowed by the available data (Catuneanu et al., 2009). The upper Goliad sequence, for example, may be further subdivided based on distinctive parasequence stacking patterns, similarity of depositional systems, and/or areal extents of flooding surfaces.

6.2 Methodology

The methodology that we used to define and characterize layers in the Gulf Coast Aquifer is based on chronostratigraphic correlation and well log lithologic determination and has been developed and refined in similar studies of Texas coastal aquifer systems (Knox et al., 2006, 2007; Young and Kelley, 2006; Young et al., 2006). The basic work flow involves: 1) identification and correlation of flooding surfaces; 2) ranking of flooding surfaces and selection of aquifer layer boundaries; 3) systematic correlation of layers throughout the study area using a grid of cross sections; and 4) facies-based sand mapping within aquifer layers.

The task of identification and correlation of flooding surfaces started with the large scale and progressed toward smaller scales and higher resolutions (more numerous and thinner layers). Geophysical well logs were the basic data for stratigraphic correlation and lithologic interpretation. First we reviewed previous studies in the geologic literature (see Section 4, Stratigraphic and hydrogeologic framework) and used their correlations and sequence interpretations as a starting point. Then we identified and correlated the most laterally extensive flooding surfaces, such as those that bound the major depositional episodes (Figure 3-7). Using well log pattern recognition and trial and error, we searched out additional flooding surfaces to further subdivide the sequences into aquifer layers. To systematize and control the quality of this process, we constructed a grid of dip- and strike-oriented cross sections across the study area (Figure 2-1). The goal was to select the optimal number of chronostratigraphic surfaces that would subdivide the aquifer into manageable and hydrogeologically meaningful layers for

numerical modeling. Ideally, the layers should be continuous throughout the study area, internally consistent (composed of related facies), and separate (bounded by fine-grained facies).

Marine flooding surfaces, as previously discussed, are rarely as continuous as we would like, and so techniques must be applied to extend correlations beyond their limits. Near the coast and offshore, Miocene to Holocene sequences contain abundant marine facies and flooding surfaces, in which biostratigraphic zonation is well defined (Lawless et al., 1997; Fillon and Lawless, 2000). As we correlate these flooding surfaces landward, however, they grade into nonmarine facies and lose their distinctive well log signatures as well as marine biostratigraphic age control (Figure 6-2). In fluvial systems updip, depositional episodes commonly begin with erosion, followed by deposition of amalgamated channel sands (Galloway et al., 1986). Following the technique of Galloway and Morton (Galloway et al., 1986; Morton et al., 1988), we correlated the basal flooding surfaces updip as far as possible and then extended correlations toward the outcrop along the bases of major channel sands. In the Gulf Coast Aquifer, basal channel sands represent the initial pulse of a progradational sequence following marine transgression, even though no record of the transgression remains in updip areas.

The final step in the correlation process was to trace boundaries to outcrop. As we discussed in Section 4.1, Previous studies, subsurface-to-surface correlations are difficult and still uncertain after many decades of geologic investigation (DuBar et al., 1991). Outcrop mapping is based on lithologic changes, soil characteristics, and topographic expression, whereas our subsurface correlations are based on chronostratigraphy and depositional systems. Nevertheless, we tied layer boundaries from the subsurface to outcrop contacts by: 1) referring to previous studies that established the general correspondence between outcrop and subsurface; 2) projecting correlations updip from the wells closest to the outcrop while maintaining inclinations (dips) established in the subsurface; and 3) projecting outcrop contacts downdip using dips measured at the surface (Figure 6-2).

A discussion of the differences between chronostratigraphic and lithostratigraphic correlation techniques is in order. Until the 1980s, most well log correlation was lithostratigraphic, but with the advent of sequence stratigraphy, new conceptual tools became available to correlate layers that may display varying lithologies but were deposited during a specific time interval under distinct environmental conditions. Such chronostratigraphic layers are more likely to be internally integrated, hydrogeologic systems. Lithostratigraphic correlation relies on the interpretation from well logs of formation lithologies and boundaries between different lithologies (mud on sand, for example) and then correlating those boundaries between wells. A thick marine shore-zone sand, for example, would be correlated to other thick marine sands based on lithology and position within the vertical profile (Figure 6-3). It is now known that, owing to depositional cyclicity and the offlapping nature of many facies, sands that apparently form a continuous sheet are actually separated laterally by thin fine-grained layers or veneers (Figure 6-3). Thus, lithostratigraphic correlation may result in overestimation of sand-body continuity and/or miscorrelation of sand bodies of differing ages. In general and in practice, however, the differences between the two techniques are more subtle than the extreme case illustrated in Figure 6-3, and in some cases lithologic boundaries coincide with chronostratigraphic surfaces. Pioneering work by Baker (1979) and others (see Section 4.1,

Previous Studies) established accurate stratigraphic frameworks using lithostratigraphic correlation combined with a good understanding of geologic processes.

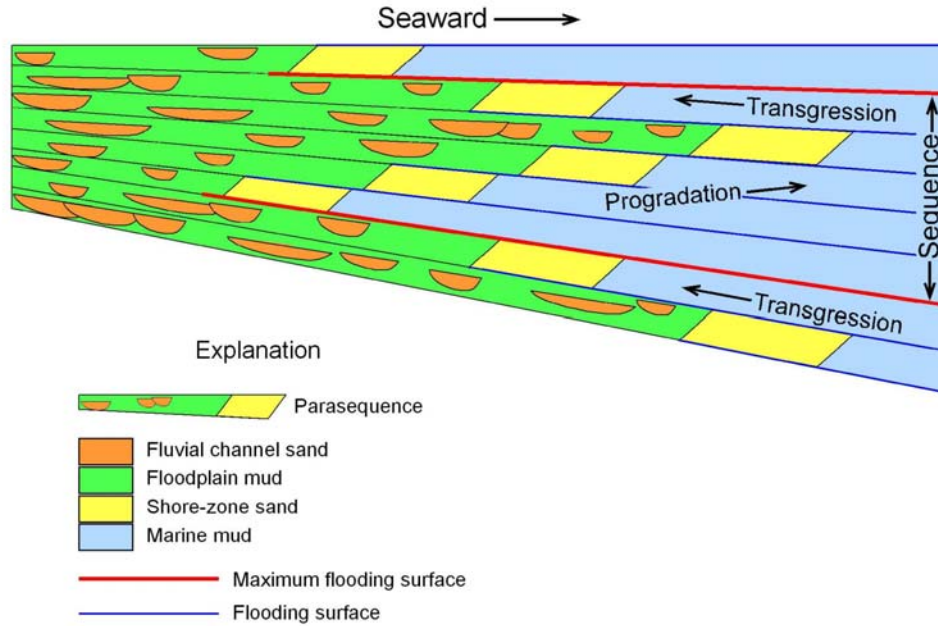


Figure 6-1. Schematic cross section showing small-scale depositional cycles (parasequences) and larger-scale sequence bounded by maximum flooding surfaces.

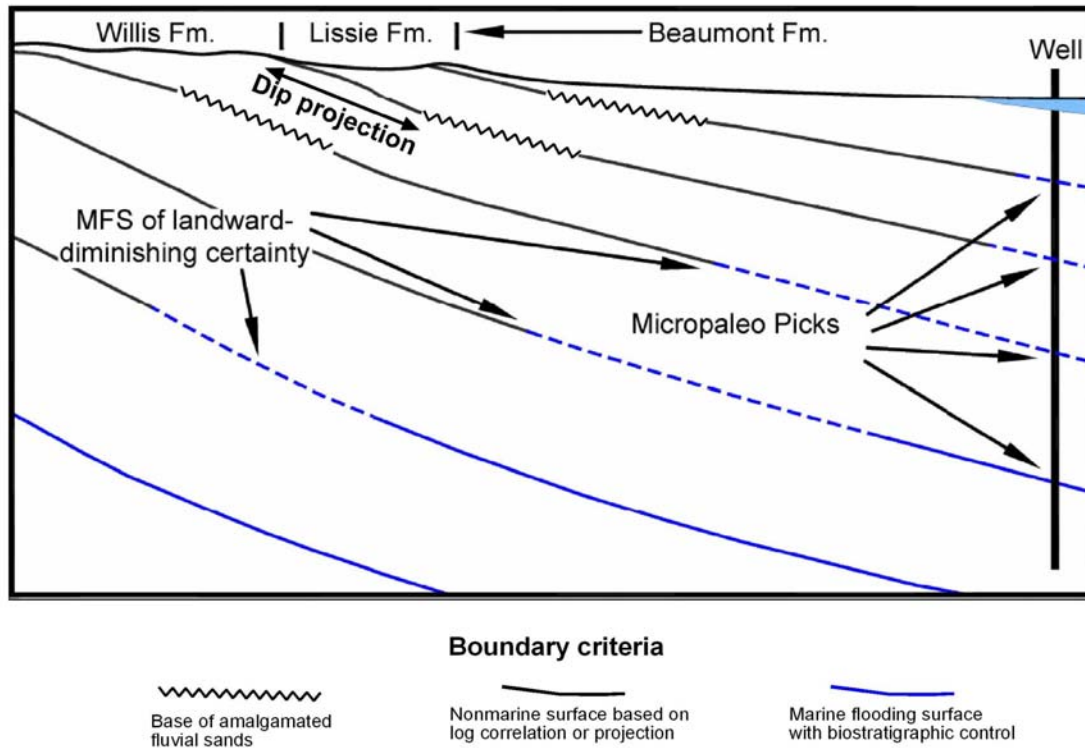


Figure 6-2. Schematic cross section showing correlation strategies.

Maximum flooding surfaces (MFS) are the correlation boundaries of choice in the marine region but must be replaced in the nonmarine region with well log correlation, tracing channel bases, and dip projection. Modified from Knox et al. (2006).

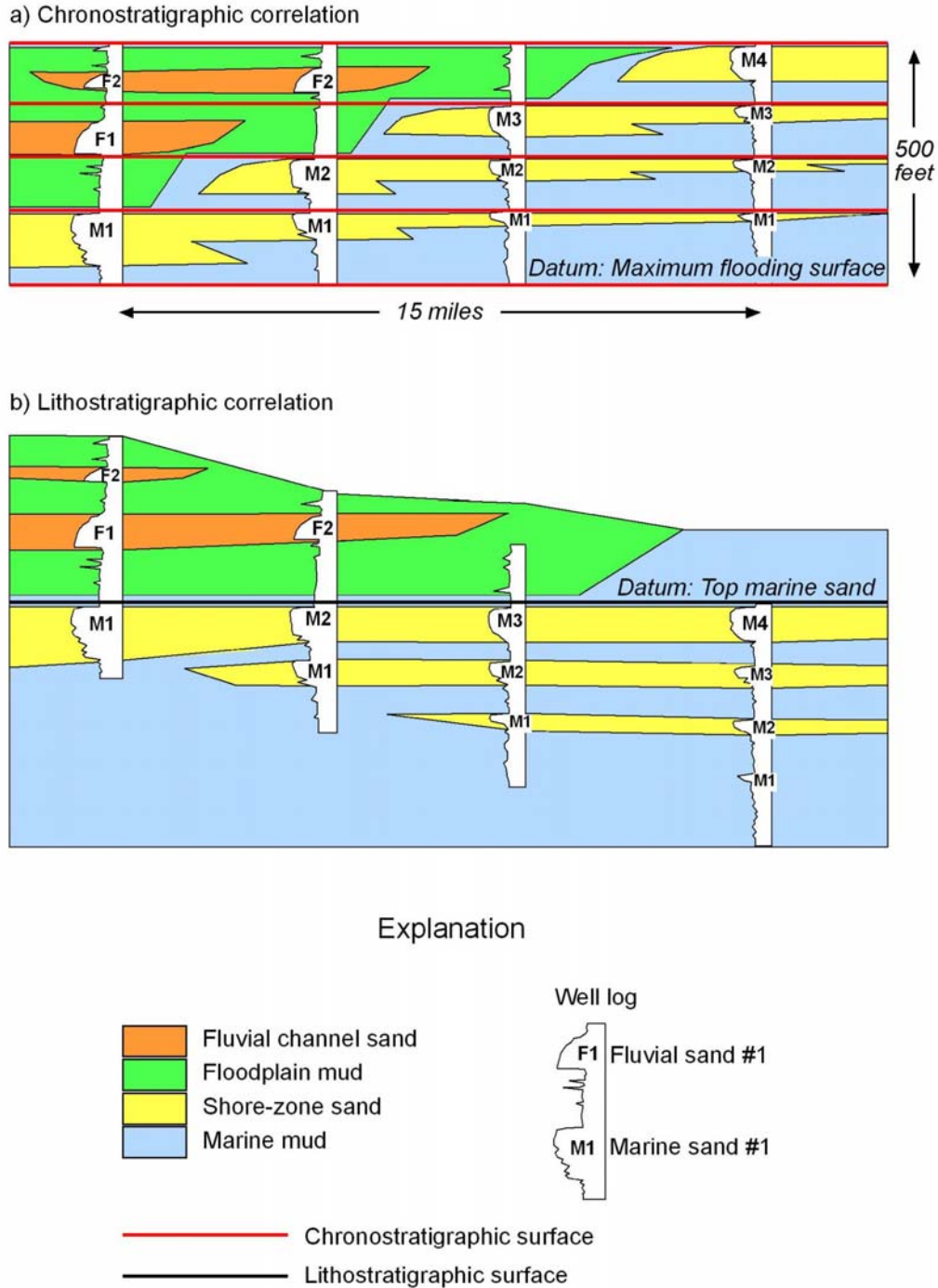


Figure 6-3. Schematic cross section comparing (a) chronostratigraphic correlation to (b) lithostratigraphic correlation.

Identical (hypothetical) well logs are used in both sections, but their vertical positions are shifted to line up correlated sands. Sands are numbered to show the correct correlations. Using lithostratigraphic correlation, the top of the thickest marine sand is incorrectly assumed to be a continuous surface, whereas chronostratigraphic correlation uses marine flooding surfaces in a progradational context to correctly correlate the sands. Modified from Van Wagoner et al. (1990).

7 Gulf Coast Aquifer stratigraphy

This section presents the geologic units that comprise the Chicot, Evangeline, and Jasper Aquifers and the Burkeville Confining Unit. For each of these units the maps of the base elevations and total thickness is provided.

7.1 Chronostratigraphic surfaces and aquifer boundaries

The Gulf Coast Aquifer is comprised of, from shallowest to deepest, the Chicot Aquifer, the Evangeline Aquifer, the Burkeville Confining System, and the Jasper Aquifer. In this study, aquifer units have been further subdivided on the basis of chronostratigraphic correlation to yield subaquifer layers. These layers are bounded by clay-dominated facies deposited during a sequence or parasequence flooding event. The layers consist of formations or parts of formations that have been historically considered part of a given aquifer. Formation boundaries were traced from outcrop boundaries provided by Barnes (1992) to identifiable flooding surfaces in the deeper subsurface, where paleontologic control constrained geologic ages of surfaces.

Figure 7-1 shows the relationship of chronostratigraphic units used in this study with respect to aquifer boundaries, paleontologic markers, geologic age, and epoch. The Chicot Aquifer includes, from the shallowest to deepest, the Beaumont and Lissie Formations of Pleistocene age and the Pliocene-age Willis Formation.

The Evangeline Aquifer includes the upper Goliad Formation of earliest Pliocene and late Miocene age, the lower Goliad Formation of middle Miocene age, and the upper unit of the Lagarto Formation (a member of the Fleming Group) of middle Miocene age.

The Burkeville Aquitard historically has been defined by lithology – the interval of lowest sand content between the Evangeline and Jasper Aquifers. This definition is difficult to apply objectively and crosses chronostratigraphic units. For this study, the Burkeville is defined as the chronostratigraphic layer with the most widespread clayey interval. That layer consists of the middle unit of the Lagarto Formation of middle and early Miocene age.

The Jasper Aquifer, as defined by Baker (1979) and reiterated by Chowdhury and Mace (2007), includes a sandy clay section below the highly clayey section of the Burkeville Confining System, the Oakville Sandstone of the Fleming Group, and sandy sections of the Catahoula Tuff and Catahoula Sandstone. For this study, the Jasper Aquifer is defined as including the lower Lagarto unit of early Miocene age, the early Miocene Oakville sandstone member of the Fleming Group, and the sandy intervals of the Oligocene-age Catahoula Formation. Elevations from the established base Jasper surface in the SWAP dataset were used close to the outcrop and were merged with the chronostratigraphic base of the Oakville Sandstone defined in this study.

The lowermost clayey unit of the Catahoula Formation, sometimes mapped in outcrop as the Frio Clay and equivalent in age to the Vicksburg Formation of the subsurface (Galloway, personal communication, 2009), is treated in this report as part of the Catahoula Confining System and is therefore not part of the Jasper Aquifer.

7.2 Structural configuration of surfaces

Geologic units on the Gulf Coast Aquifer system dip east or southeast toward the coast at a direction roughly perpendicular to the local shoreline. Consequently, the strike of geologic units is approximately parallel to the shoreline. Units also thicken toward the coast. Older units dip more steeply because of the accumulated subsidence and tilting since their deposition. Growth faults occur frequently in Gulf Coast geologic units and are most pronounced near the paleo-shelf margin of a geologic unit (the geomorphic shelf edge as the unit was being deposited). The shelf margin has grown toward the center of the Gulf of Mexico over time, so that growth faults of older units are well inland, and growth faults in units being deposited today are several tens of miles offshore (see Figures 3-2 and 4-2). Growth faults do not significantly impact the freshwater portions of the Gulf Coast Aquifer but may offset deeper parts of the Jasper Aquifer. Some older growth faults have continued to move slightly, and units within the Gulf Coast Aquifer may be impacted by localized changes in dip angle. Salt and shale movement and diapirism also modify structure under the Gulf Coast Aquifer system. Some salt and shale activity has had no effect on Gulf Coast Aquifer layers, while other activities may have created localized high areas in the lower layers of the aquifer. Still other salt and shale movement significantly impacts localized areas of the aquifer to a very shallow depth (Hamlin, 2006).

This study identified additional structural features that modify the gradual coastward dip. These features are most prominent on the deepest surface correlated – that of the base of the Oakville Formation, which corresponds roughly to the base of the Jasper Aquifer, except near the outcrop. Figure 7-2 shows the structural contour map of the base of the Oakville Formation and the total thickness of the Oakville Formation. Near its outcrop, the Oakville Formation can have relatively large changes in thickness over relatively small distances. These changes are attributed to the steep dip of the formation, the variability in the land surface elevations, and the relatively small contour intervals in the up-dip area. In Figure 7-2 dips near the outcrop are approximately 100 feet per mile (Figure 7-3) and are consistent from the Brazos River south to Live Oak County (Figures 7-4, 7-5, and 7-6). South of this, dips locally steepen to almost 200 feet per mile (Figures 7-7 and 7-8).

In the downdip to middip area from Matagorda County to Victoria, Refugio, San Patricio, Nueces, and Kleburg Counties, averaged dips flatten to less than 80 feet per mile and are locally reversed (Figures 7-4, 7-5, and 7-6). This feature is most pronounced in its southernmost extent and is mapped by Ewing (1990) as separate, somewhat circular, fault-bounded grabens in Kleburg, Nueces, and San Patricio Counties. A similar "shelf" appears subtly as a series of more widely spaced contours on the Top Frio structure map in Galloway et al. (1982). A seismic section published in a dissertation by Coleman (1990, Plate 5) shows a dip reversal above the Vicksburg Formation that extends high into the units above. It is unclear at this time whether this feature is the result of salt or shale movement, or a late-stage reactivation of deeper faults, or both.

At the downdip limit of data offshore from Matagorda, Calhoun, and Aransas Counties, dips steepen abruptly. This area coincides with the Lunker fault zone mapped from offshore data (Watkins et al., 1996) and lies subparallel to the shoreline, coming onshore at the mouth of Matagorda Bay as it trends toward the northeast.

Salt features have a minor impact on structural contours. One clear exception is the Shepherd's Mott dome near the boundary of Matagorda and Brazoria Counties (Figure 3-3).

Structural contours and fault trends in the Jackson Group and below along the Gulf Coast typically are mapped as parallel to the shoreline. Strike changes from northeast trending in east and central Texas to north trending in south Texas. Contours on the base of the Oakville (Figure 7-2) indicate a northwest-southeast trending fold in south Texas that plunges toward the southeast with a southern limb that reaches considerable depths along the Rio Grande axis. At least two smaller subparallel folds lie to the north of the major fold. Strike-oriented cross section E (Figure 7-9) shows these folds in profile. Similarly oriented folds are mapped by Ewing (1990). These include the Cinco de Mayo anticline in Zapata County and the Picachos and Papagayos anticlines in the Nueve Leon province of northern Mexico.

The folds at the level of the Oakville, like most of the structural features mentioned above, become progressively more subtle in shallower units. However, the surface expression of the folds may be reflected in the outcropping geology (Barnes, 1992) by extensive northwest-trending sand sheets that extend inland from the shore and coincide with synclines between mapped anticlines (Figure 4-1).

Structural contours on the base of the lower Lagarto unit (Figure 7-10) show similar trends to those at the base of the Oakville Formation. The contour interval highlights the area of flatter slopes across the central Texas coast. As discussed previously, the lower Lagarto, Oakville, and part of the Catahoula Formations comprise the Jasper Aquifer. Figure 7-11 shows the structural contours on the base of, as well as the total thickness of, the Jasper Aquifer. Structural contours are similar to those of the base Oakville Formation, except in the updip area where they have been merged with contours from the base of the Jasper Aquifer as mapped in the SWAP dataset.

The structural contours in Figure 7-12 on the base of the Burkeville Confining System (equivalent to the middle unit of the Lagarto Formation) as well as the total thickness of the Burkeville are similar to those of the underlying units.

Structural contours and total thicknesses of the three layers of the Evangeline – the upper Lagarto, lower Goliad, and the upper Goliad – are shown in Figures 7-13, 7-14, and 7-15, respectively. The base of the Evangeline Aquifer, which corresponds to the base of the upper unit of the Lagarto Formation, as well as the total thickness of the Evangeline are shown in Figure 7-16. These structural features are similar to those in underlying units but are generally smoother. This suggests that deeper structures decreased in movement through time. Exceptions include folds in south Texas and the flatter area of the central Texas coast. Contours for the upper Goliad (Figure 7-15) show a localized low in Kleburg County, documenting reversals of the typical eastward dip.

Figures 7-17, 7-18, and 7-19 show these data for the components of the Chicot – the Willis, Lissie, and Beaumont Formations. Figure 7-20 provides structural contours on the base of the Chicot Aquifer as well as the total thickness of the aquifer. Outcrop boundaries of these units, especially in south Texas, are difficult to locate accurately because they are overlain by

shallower units that have onlapped them through processes of erosion, followed by a rise in relative sea level. Consequently, zero-thickness boundaries and very shallow contours have more potential for error in details of the updip area. Structural contours do show that deeper features gradually lose their expression from the Willis upward to the Beaumont. Folds in south Texas, however, are still apparent in Beaumont contours, supporting the theory that modern surface sand distribution is tied to these deeper structures.

Because of the changes in subsidence rates (both through time and across the study area), eustatic sea level, and sediment supply, deposition of the various stratigraphic units of the Gulf Coast Aquifer do not have parallel outcrop patterns. Instead, erosional truncation of some units prior to the deposition of overlying units creates the condition of "subcrop." Bates and Jackson (1983) define a "subcrop" and an "outcrop" as:

Outcrop – that part of a geological formation or structure that appears at the surface of the earth; also, bedrock that is covered only by surficial deposits such as alluvium.

Subcrop – An occurrence of strata in contact with the undersurface of an inclusive stratigraphic unit that succeeds an important unconformity on which overstep is conspicuous; a "subsurface outcrop" that describes the areal limit of a truncated rock unit at a buried surface of unconformity. (b) An area within which a formation occurs directly beneath an unconformity.

Figure 7-21 illustrates the occurrence of a subcrop where the second youngest geologic unit pinches out to a zero thickness below an overlying unit. This occurs because an up-dip portion of the second youngest unit was eroded truncated, then covered by the deposition of an overlying geologic unit. In map view (looking downward upon the surface), a dashed line in Figure 7-21 marks the location where the second youngest unit pinches out beneath the youngest surface.

Among the limitations that constrained the ability to delineate subcrop locations are that most of the geophysical logs lack coverage within 200 feet of the ground surface and that the thicknesses of deposits associated with the mapped outcrop locations (Barnes, 1992) are generally unknown. This problem becomes most acute where the geological units flatten and are suspected of becoming relatively thin near the surface and where thin veneers of alluvium or wind-blown deposits exist at ground surface. In both situations, the approach for mapping the outcrops is to associate the region covered by the thin deposits to the geological unit that the veneer overlies.

Figure 7-22 shows the location of subcrops and outcrops for the geological formations that comprise the Gulf Coast Aquifer. Lengths of bolder lines mark areas where that particular boundary subcrops. Relationships in profile are shown in dip-oriented cross sections (Figures 7-3 through 7-8). In south Texas, Goliad units erode and onlap the Lagarto, Oakville, and Catahoula Formations, and the Lissie Formation erodes and mildly onlaps the Willis Formation. In the northern part of the study area, the Willis Formation erodes and overlaps the Goliad units. This can be seen in an area of DeWitt County and from Colorado County to the northeastern boundary of the study area. This relationship between the Lagarto and Goliad units differs from that described in Young et al. (2006a) where the Goliad was interpreted as laterally equivalent to

the Fleming (Lagarto) north of Colorado County. The current interpreted relationship between the Goliad and Willis units also differs from that of Hoel (1982), in which the Willis and Goliad Formations were considered to be time-equivalent units. The interpretation presented here has the advantage of a wider study area in which to trace and understand stratigraphic relationships than the area used in Young et al. (2006a). The current study also incorporates micropaleontologic information in the downdip areas, which Hoel (1982) lacked, to provide accurate chronologic separation of the adjacent Willis and Goliad Formations.

Inherent in the current interpretations of the outcrop and subcrop boundaries in Figure 7-22 is the occurrence of unconformities (where subcrops are mapped) that occur between Lagarto and Goliad Formations, between the Goliad and Willis Formations, and between the Willis and Lissie Formations. The unconformity between the Lagarto and Goliad Formations is most obvious in the Rio Grande Embayment, where the unconformity lies in the very shallow subsurface, and across the San Marco Arch. This unconformity becomes far less significant in the Houston embayment.

The unconformity between the Goliad and Willis Formations is subtle and localized in the Rio Grande Embayment, where it is not great enough to cause subcrop of mapped unit boundaries. Erosion along this unconformable surface increases northward across the San Marcos Arch, appearing to locally increase in relief near river valleys. In the Houston Embayment, this unconformity becomes very significant, appearing to result in the subcrop of the entire Goliad Formation.

The unconformity between the Willis and Lissie Formations appears to be widespread and minor in the Rio Grande Embayment and across the San Marcos Arch, becoming negligible in the Houston Embayment. Although the boundaries of all units at their updip depositional limits are likely unconformable, these three unconformities are the only ones significant enough to create subcrops of mapped boundaries.

Included in Figure 7-22 is the outcrop for the Catahoula mapped by Knox et al., (2009) as part of a TWDB project to define the geology of the Yegua-Jackson Aquifer and the outcrop for the Jasper Aquifer associated with the SWAP dataset. The area covered between the SWAP-based outcrop for the Jasper Aquifer and the outcrop for the Oakville represents the portion of Catahoula outcrop that has been added to the Oakville Formation to form our Jasper Aquifer. As shown in Figure 7-22, the base of the Jasper aquifer does not always coincide with the top of the Jackson Formation because the SWAP dataset does not associate all of the Catahoula Formation with the Jasper Formation.

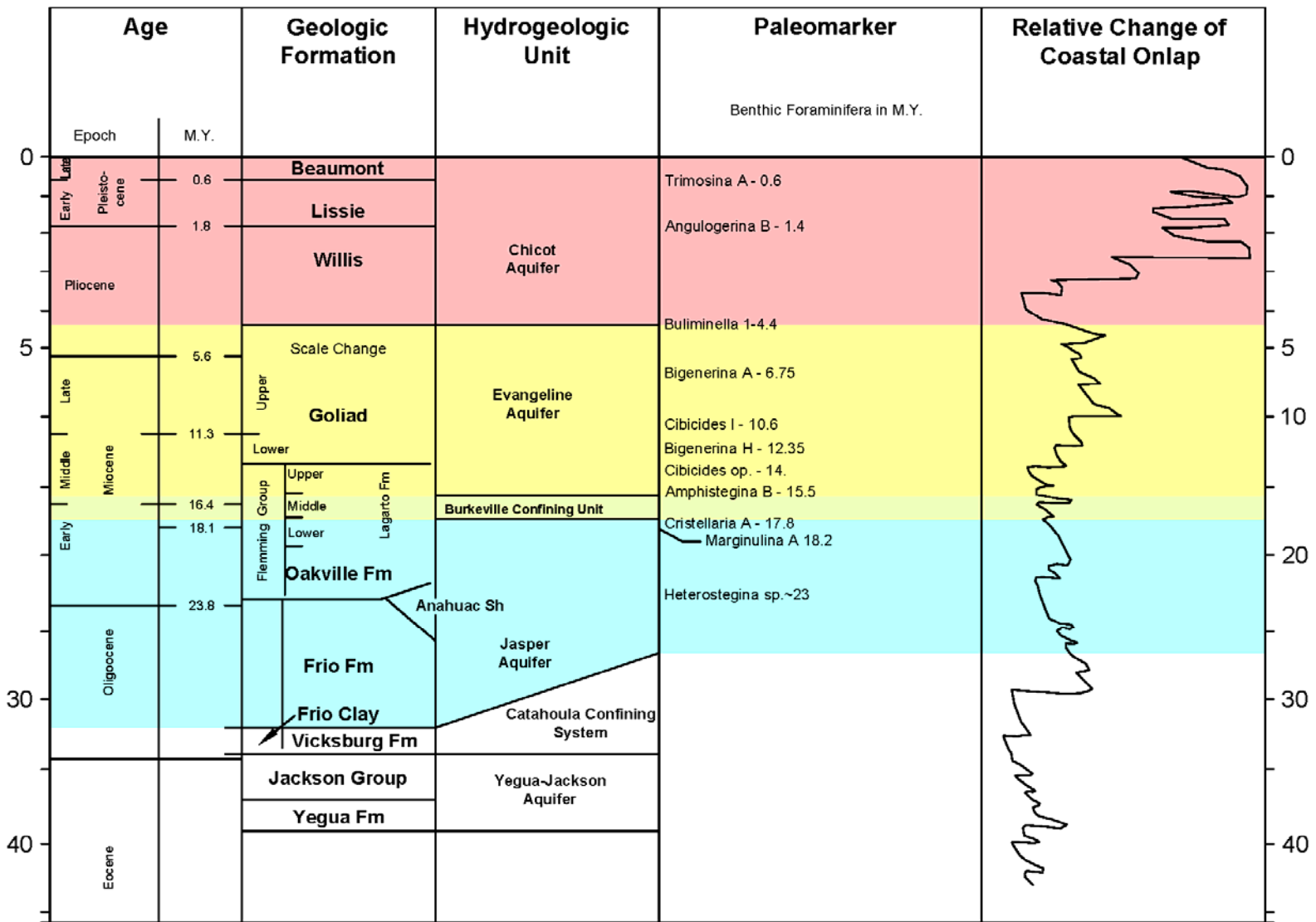


Figure 7-1. Stratigraphic column showing correlations among age, geologic formations, hydrogeologic units, paleomarkers, and relative change of coastal onlap.

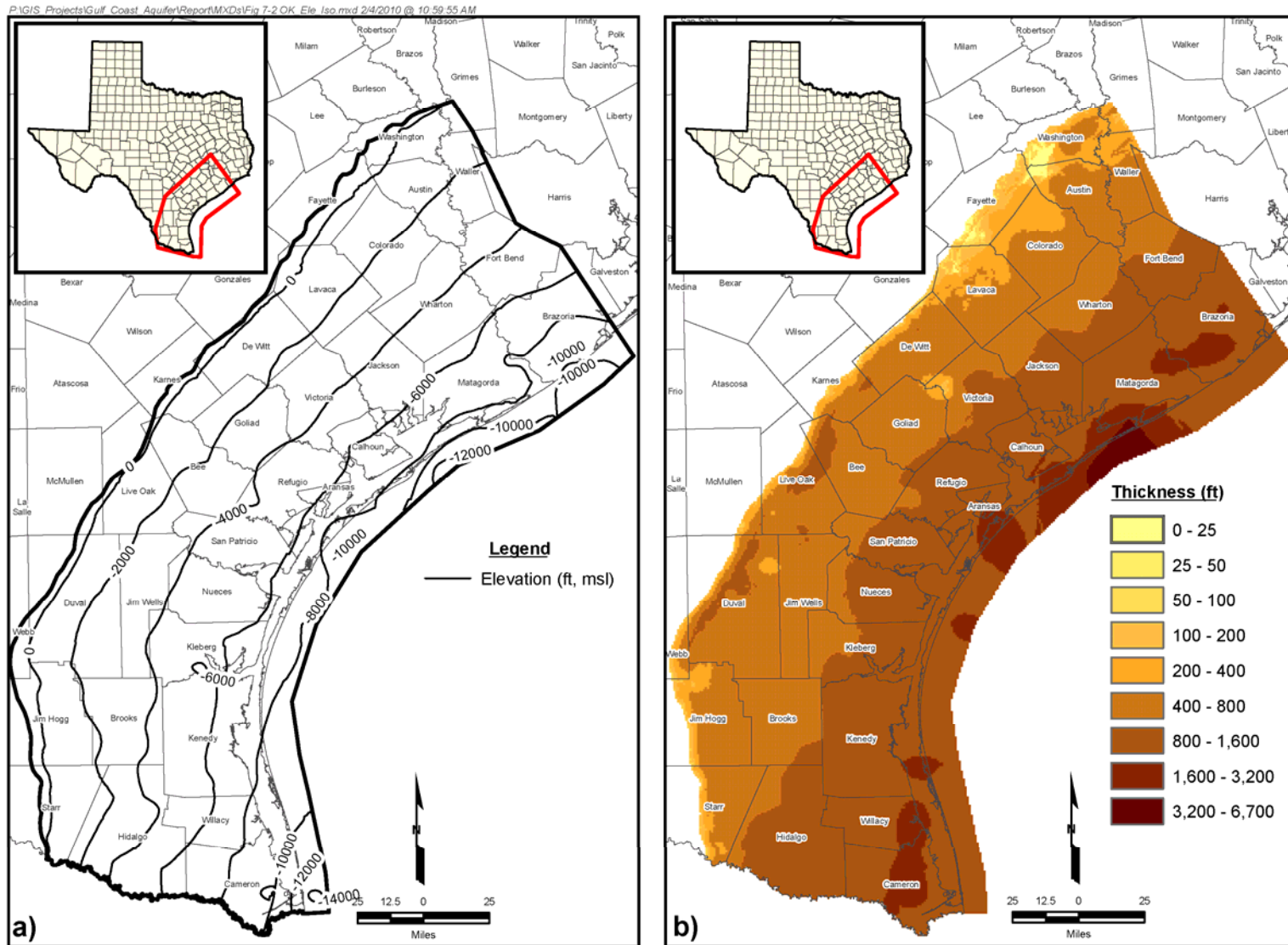


Figure 7-2. Contours for the Oakville geologic unit showing: (a) base elevation and (b) thickness.

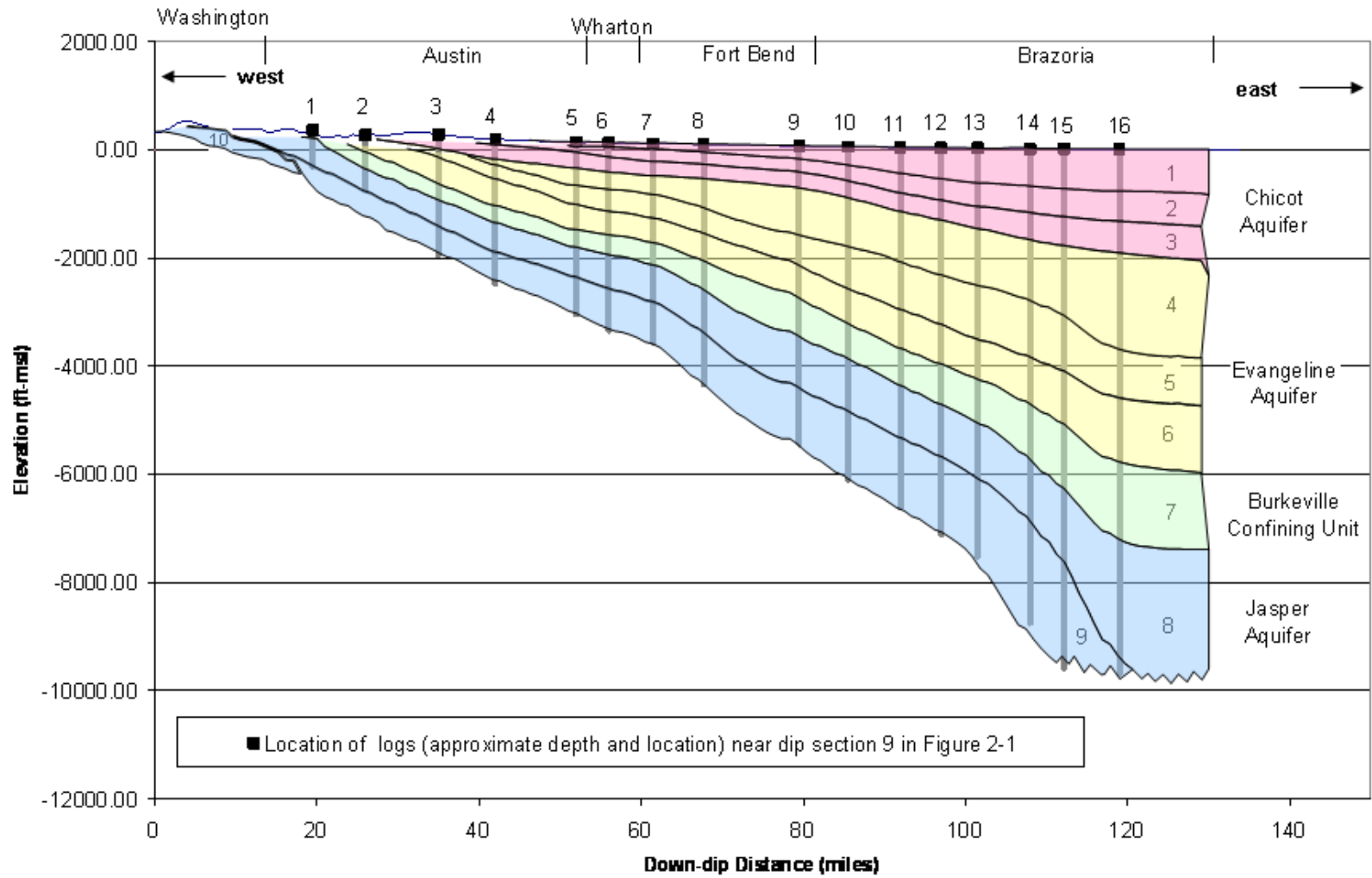


Figure 7-3. Vertical cross-section of the geological units near dip section 9 in Figure 2-1.

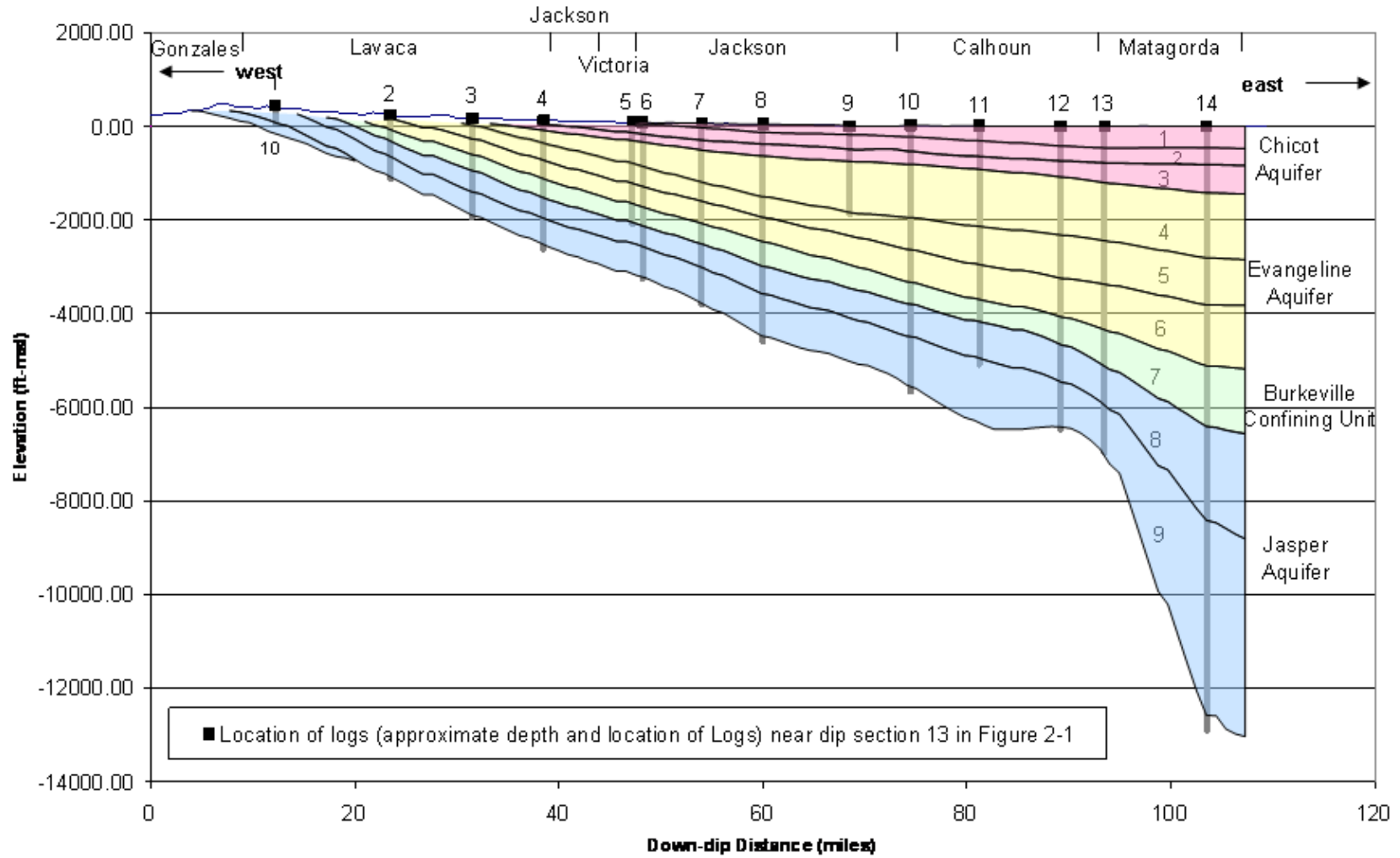


Figure 7-4. Vertical cross-section of the geological units near dip section 13 in Figure 2-1.

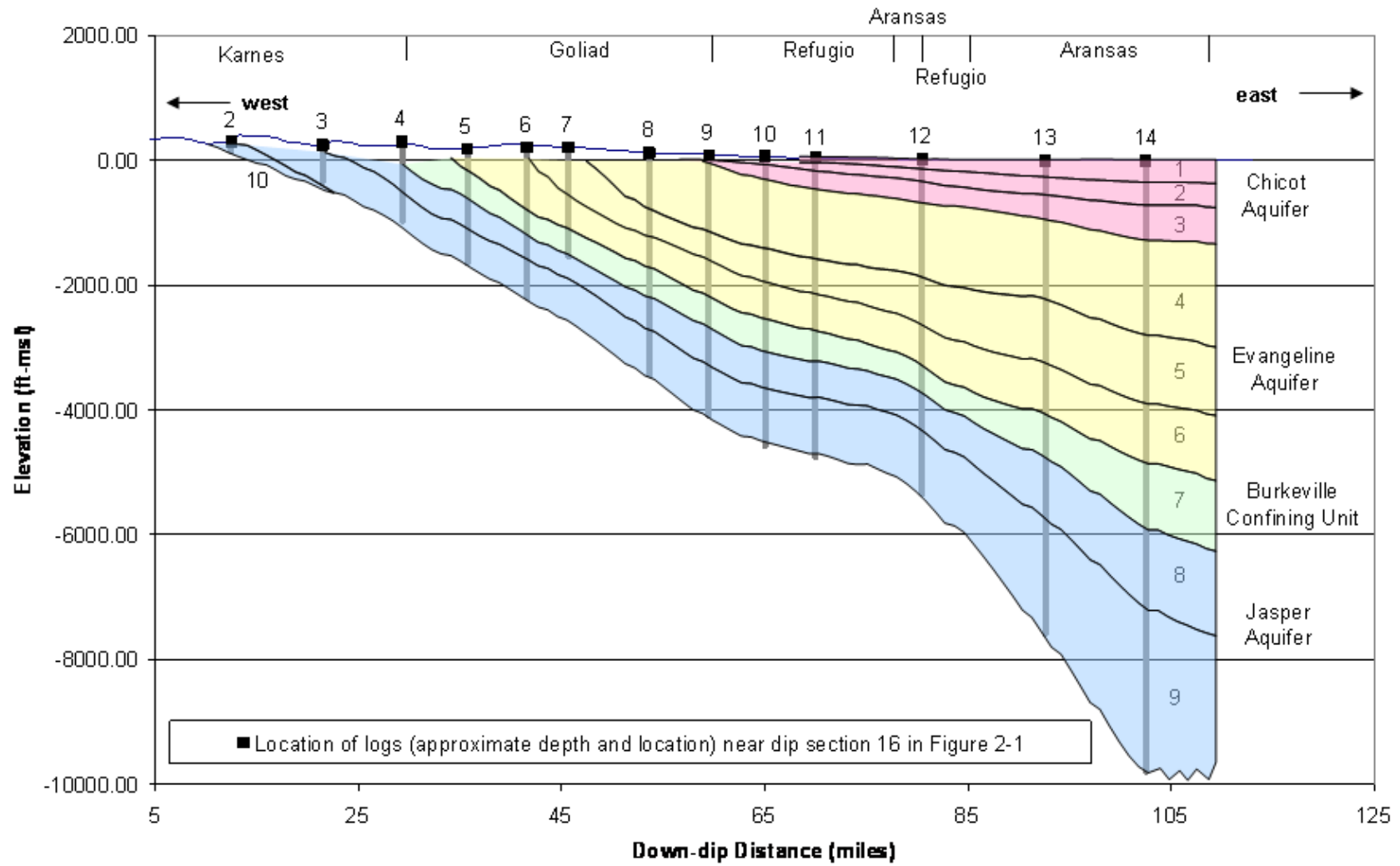


Figure 7-5. Vertical cross-section of the geological units near dip section 16 in Figure 2-1.

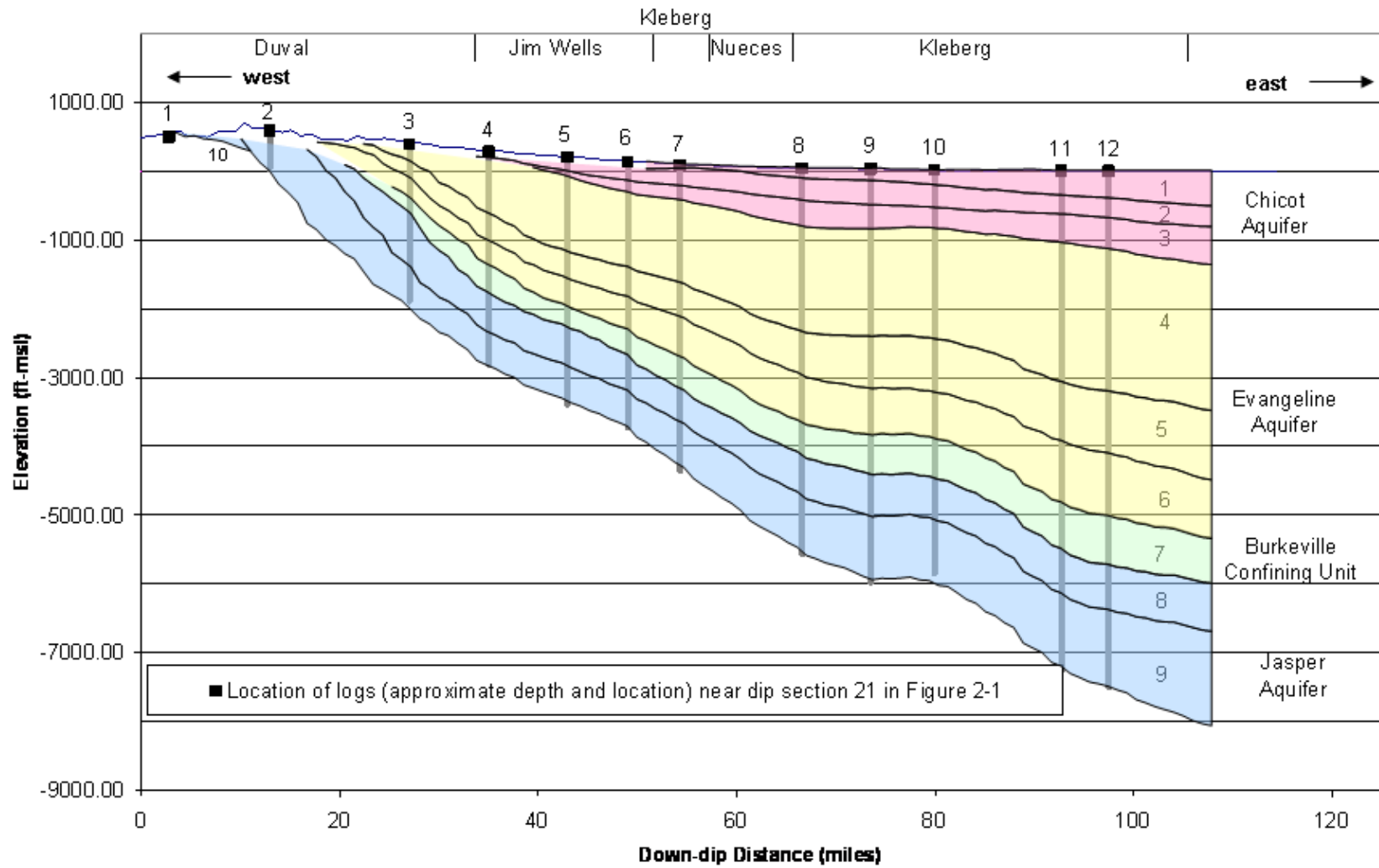


Figure 7-6. Vertical cross-section of the geological units near dip section 21 in Figure 2-1.

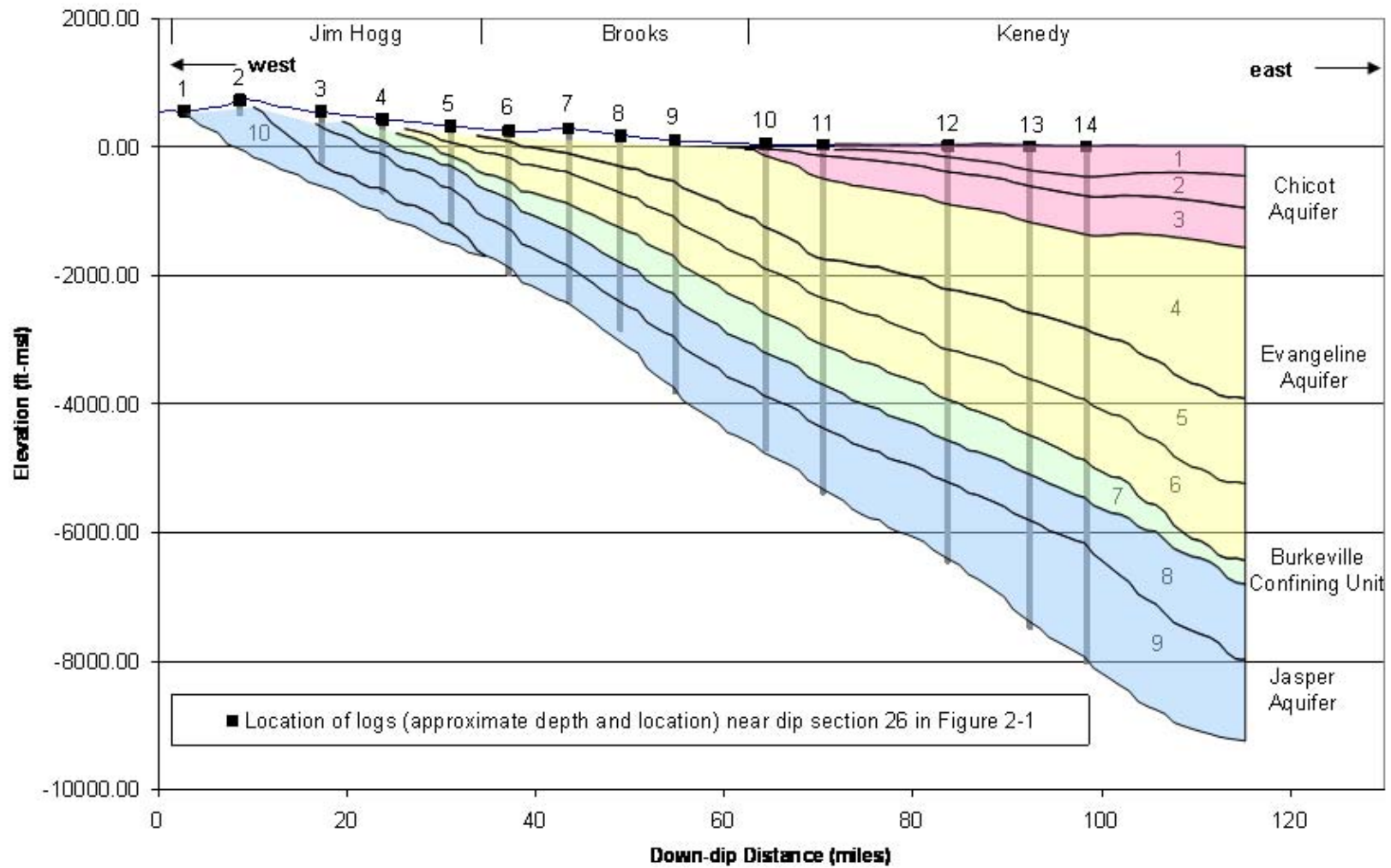


Figure 7-7. Vertical cross-section of the geological units near dip section 26 in Figure 2-1.

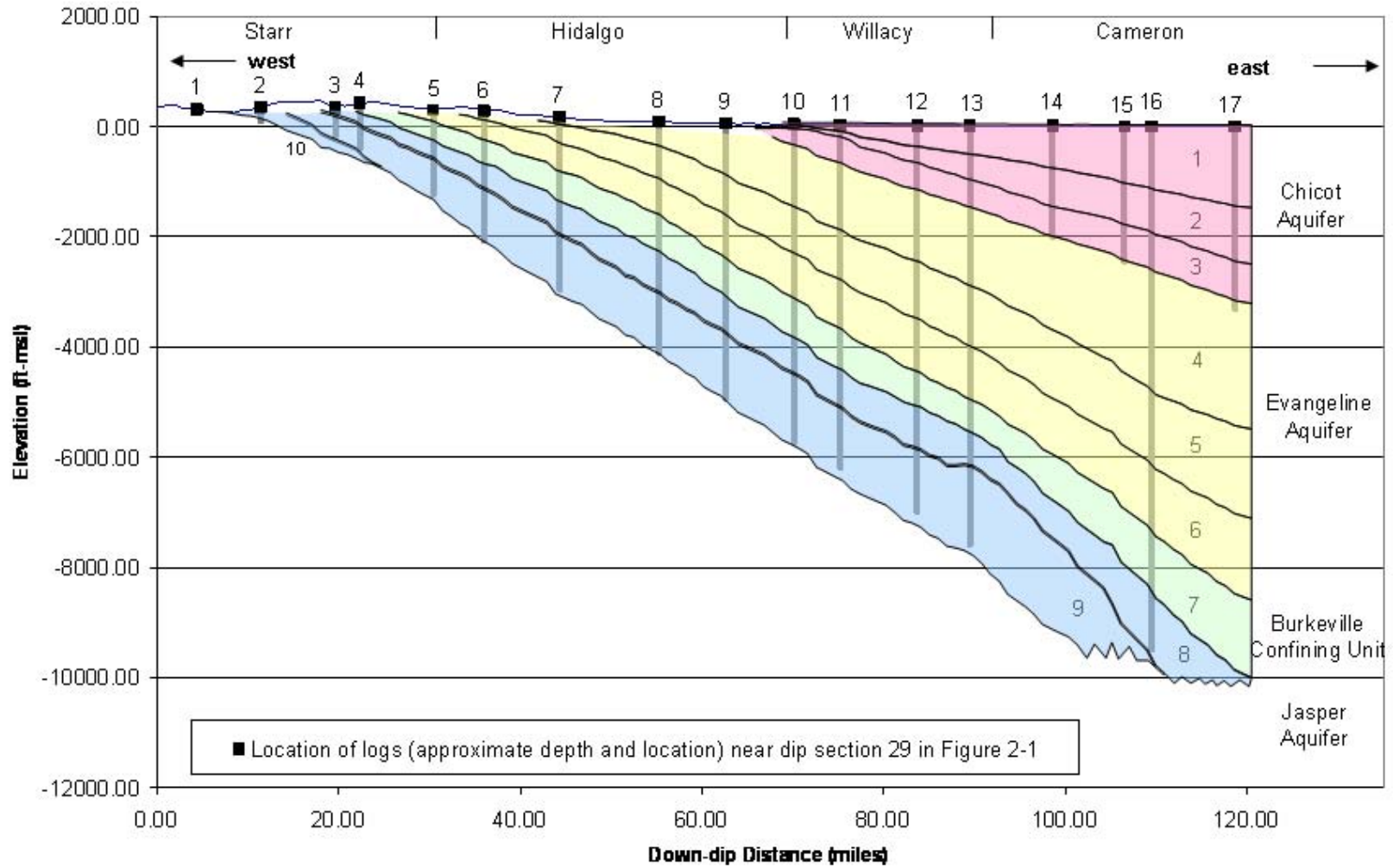


Figure 7-8. Vertical cross-section of the geological units near dip section 29 in Figure 2-1.

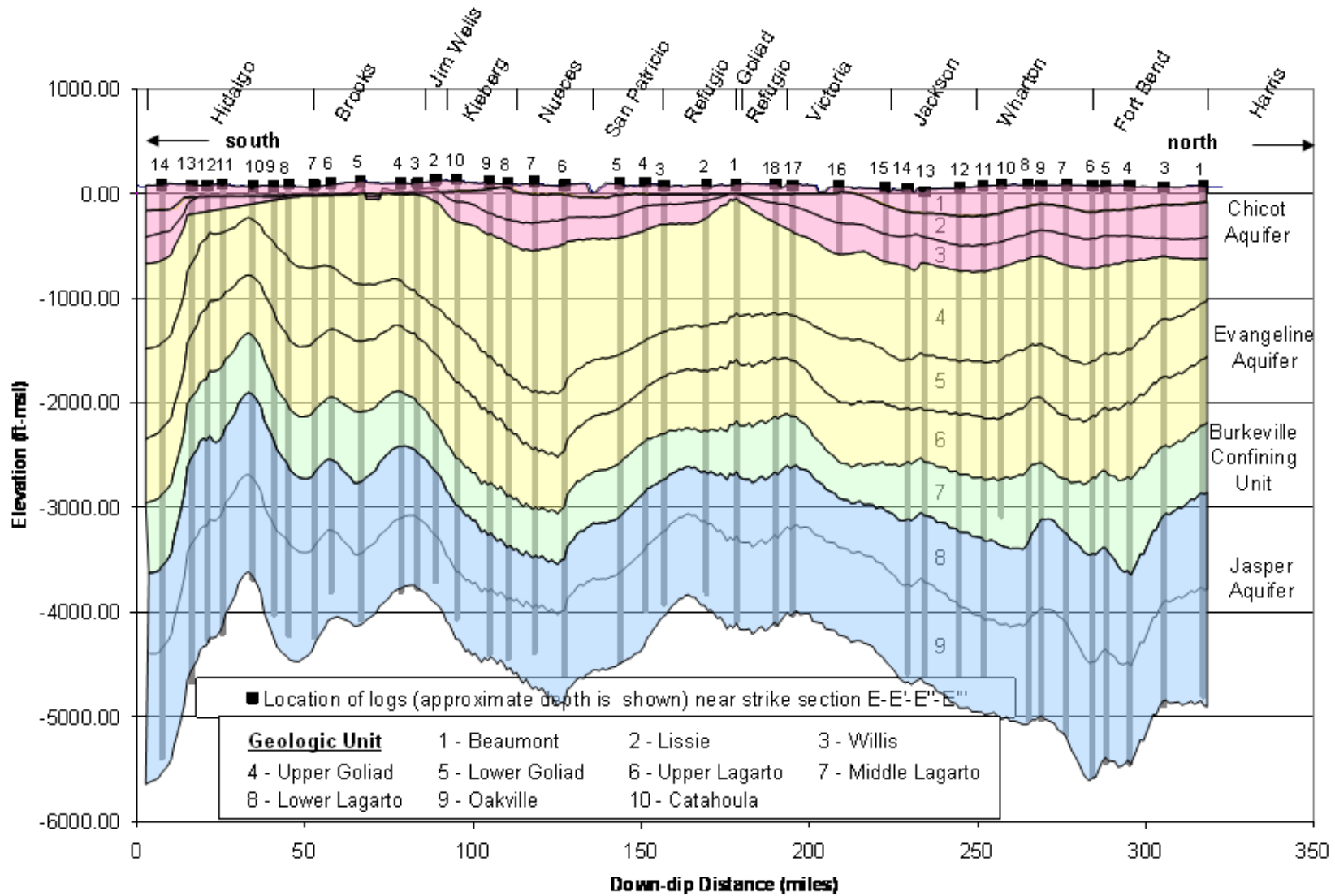


Figure 7-9. Vertical cross-section of the geological units near strike section E-E'-E''-E'''

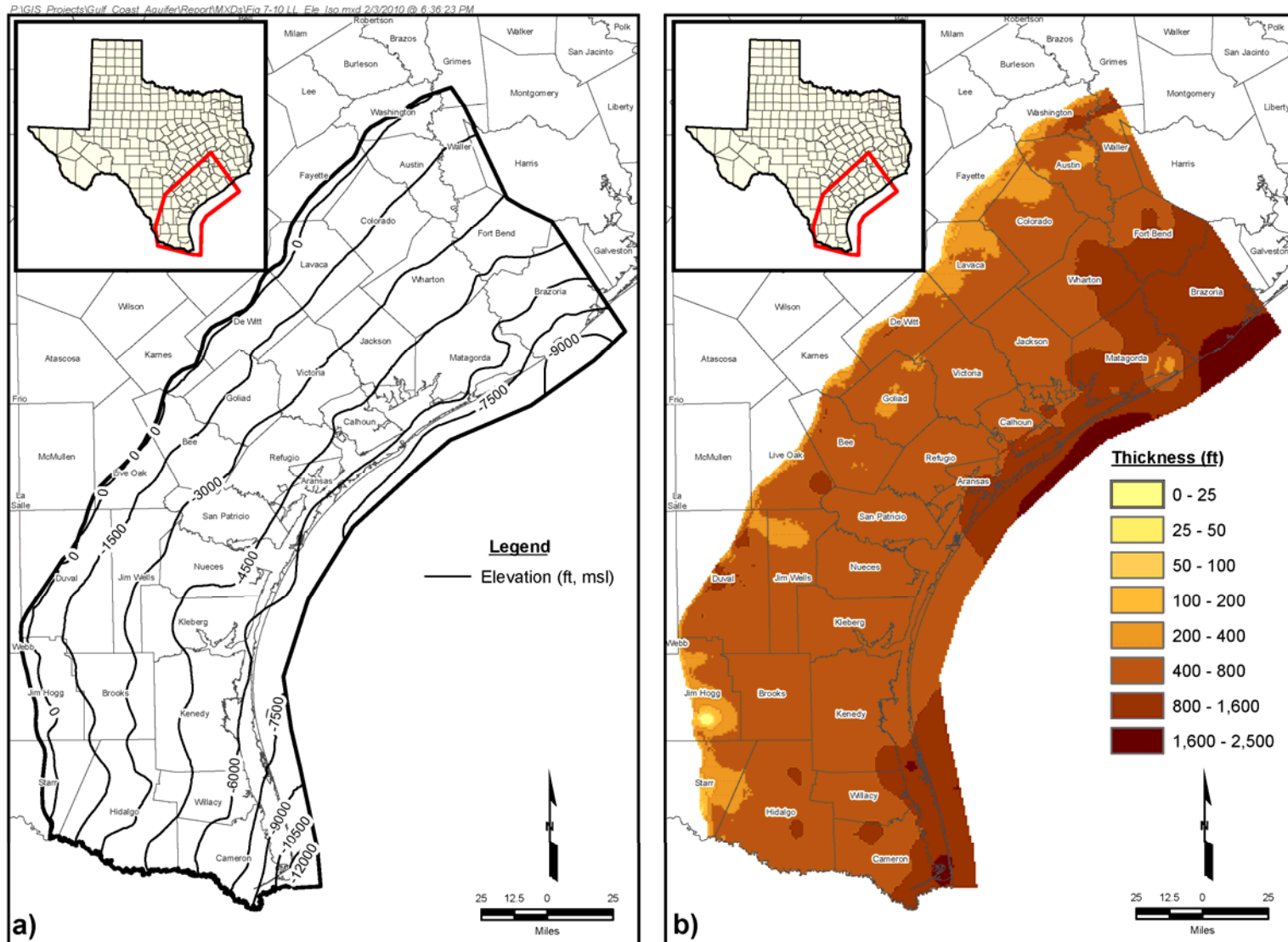


Figure 7-10. Contours for the upper Lagarto geologic unit showing: (a) base elevation and (b) thickness.

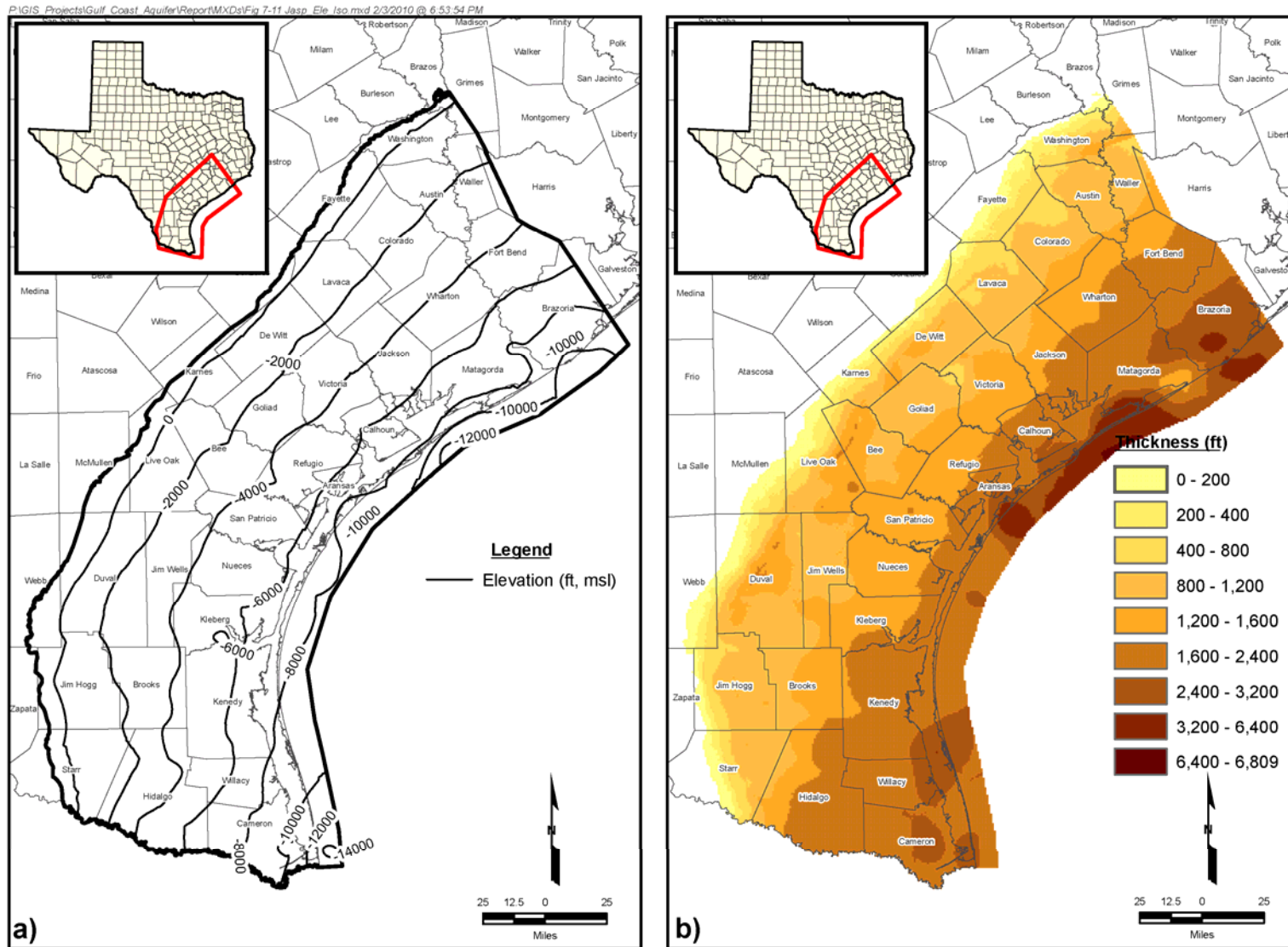


Figure 7-11. Contours for the Jasper Aquifer showing: (a) base elevation and (b) thickness.

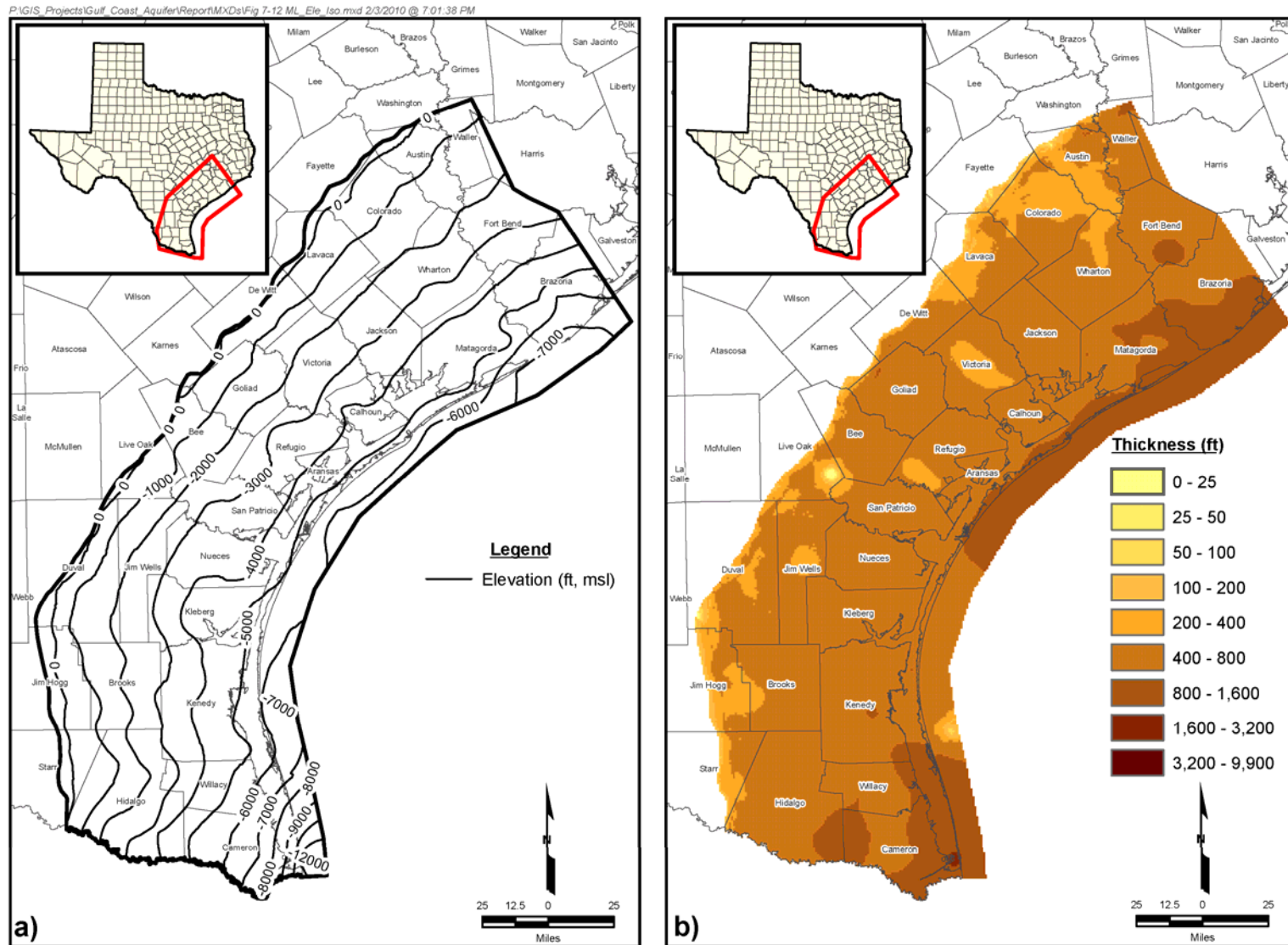


Figure 7-12. Contours for the Burkeville Confining Unit and the middle Lagarto Formation showing: (a) base elevation and (b) thickness.

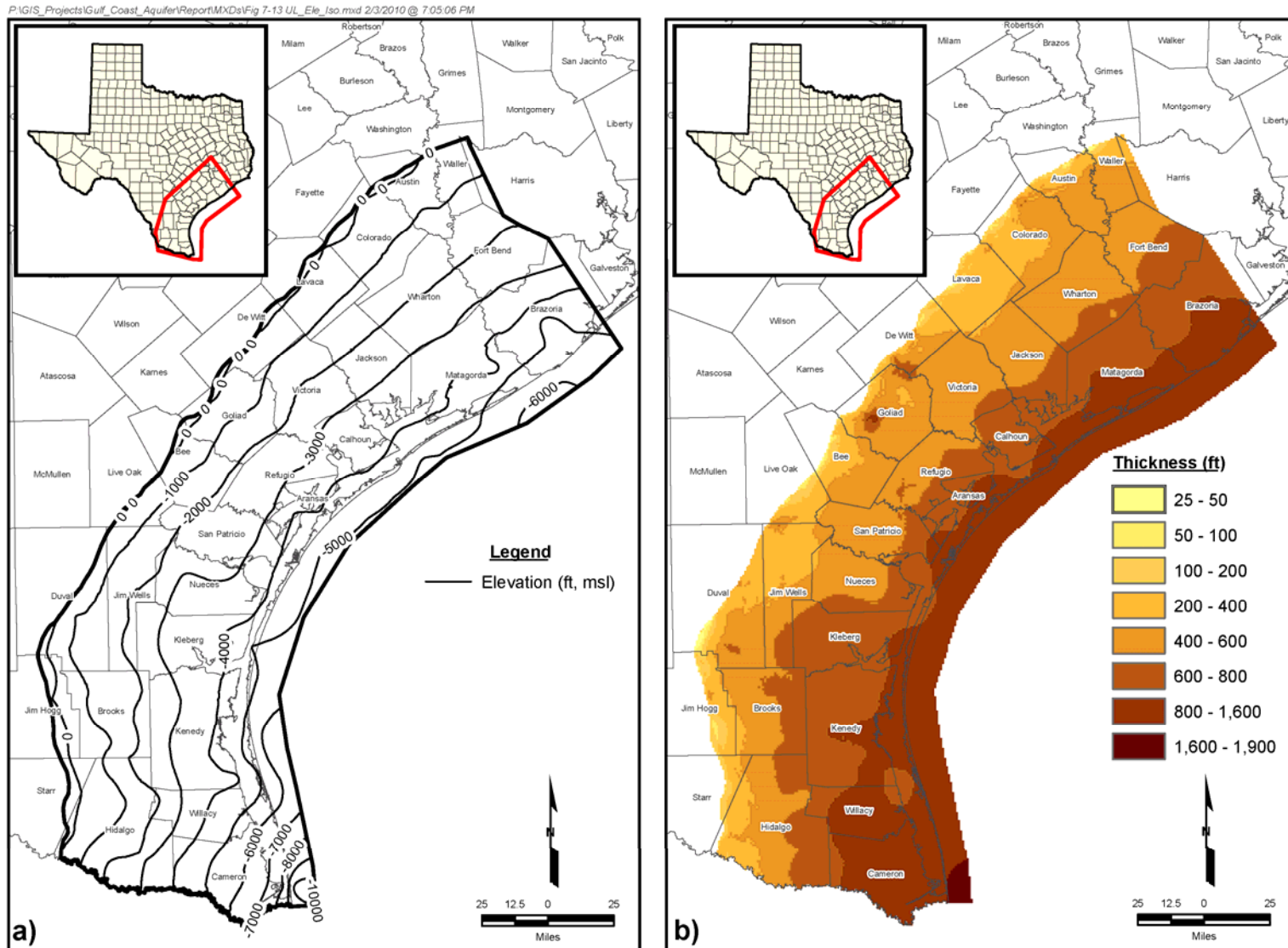


Figure 7-13. Contours for the upper Lagarto geologic unit showing: (a) base elevation and (b) thickness.

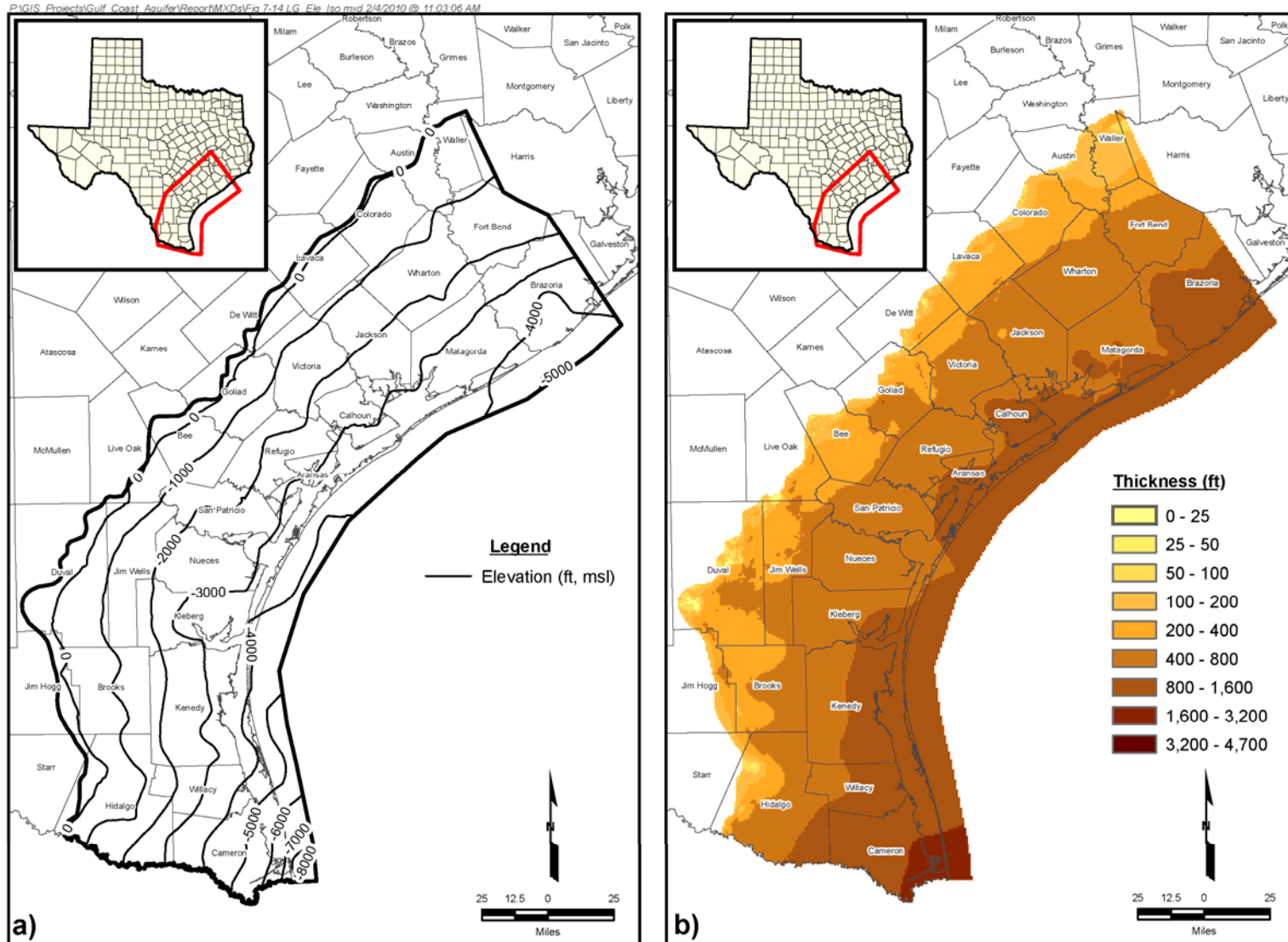


Figure 7-14. Contours for the lower Goliad geologic unit showing: (a) base elevation and (b) thickness.

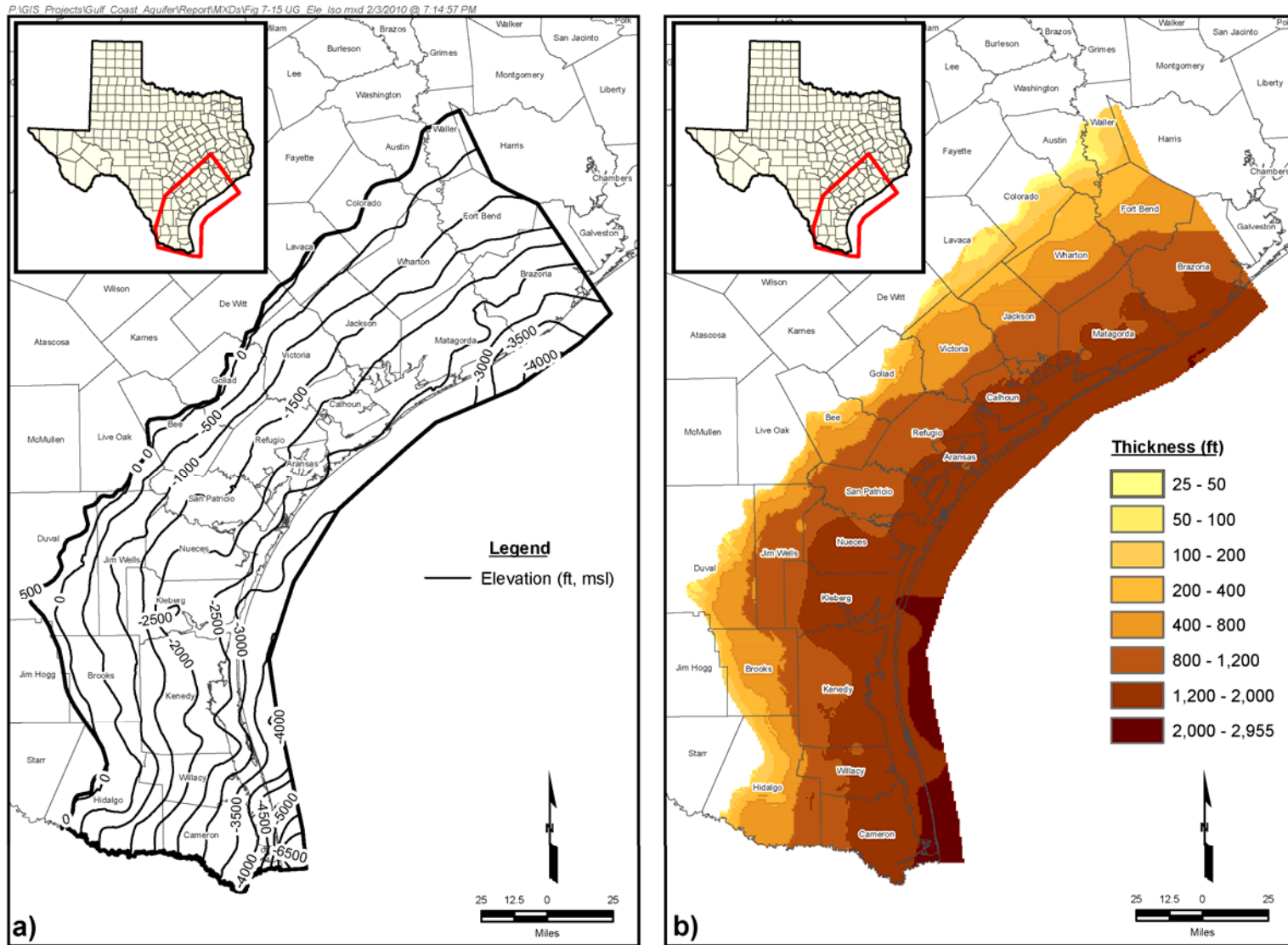


Figure 7-15. Contours for the upper Goliad geologic unit showing: (a) base elevation and (b) thickness.

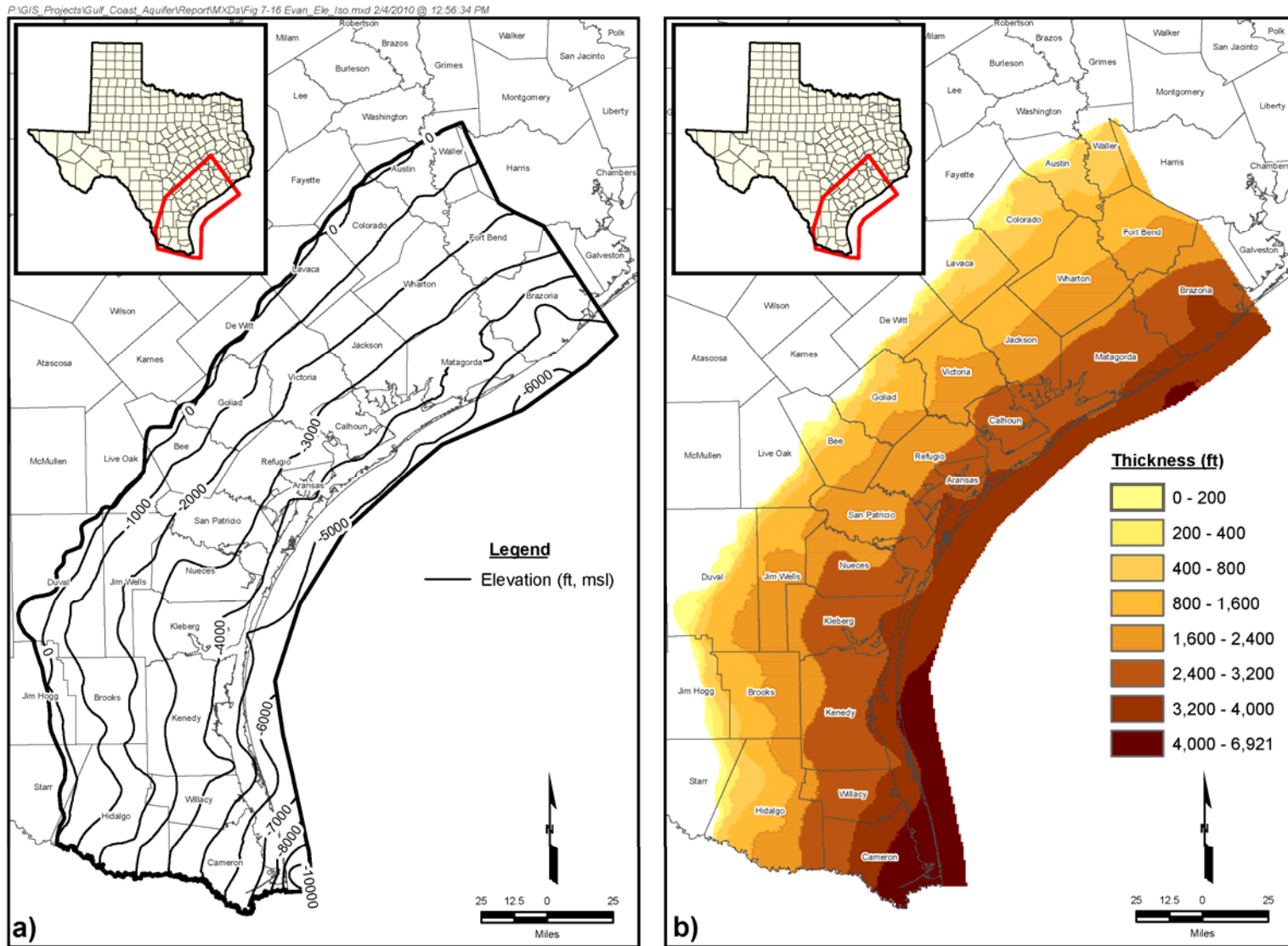


Figure 7-16. Contours for the Evangeline Aquifer showing: (a) base elevation and (b) thickness.

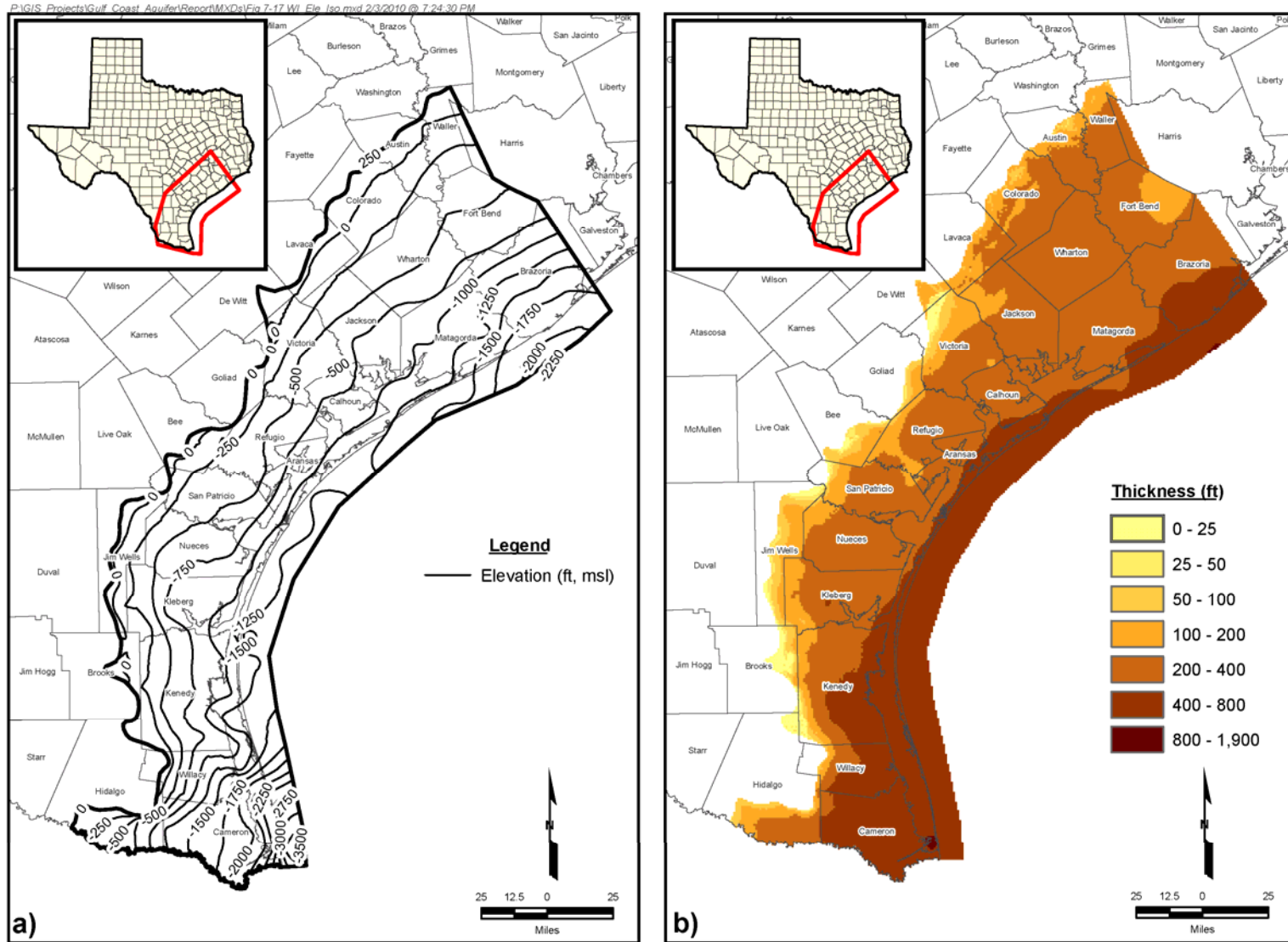


Figure 7-17. Contours for the Willis geologic unit showing: (a) base elevation and (b) thickness.

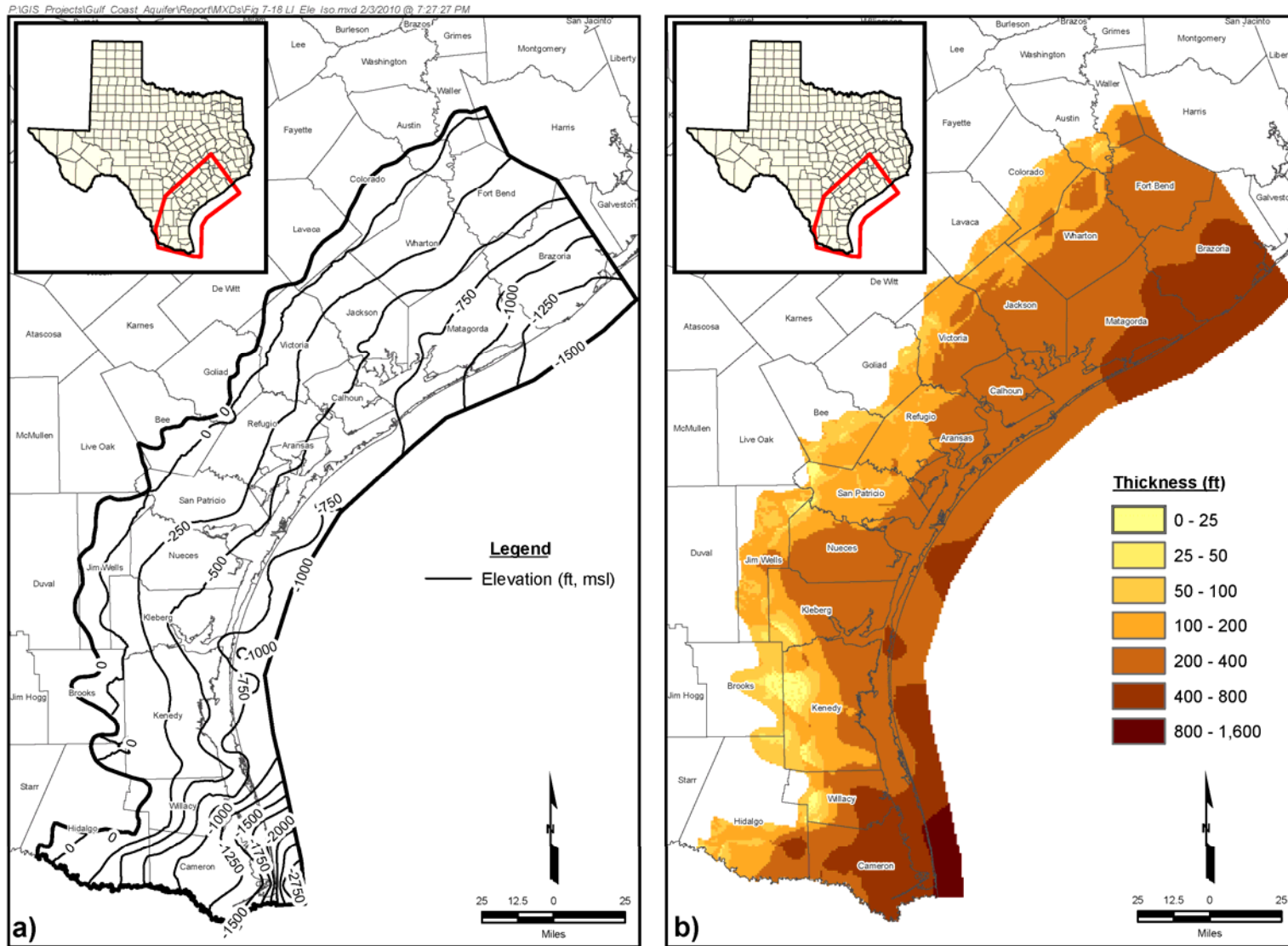


Figure 7-18. Contours for the Lissie geologic unit showing: (a) base elevation and (b) thickness.

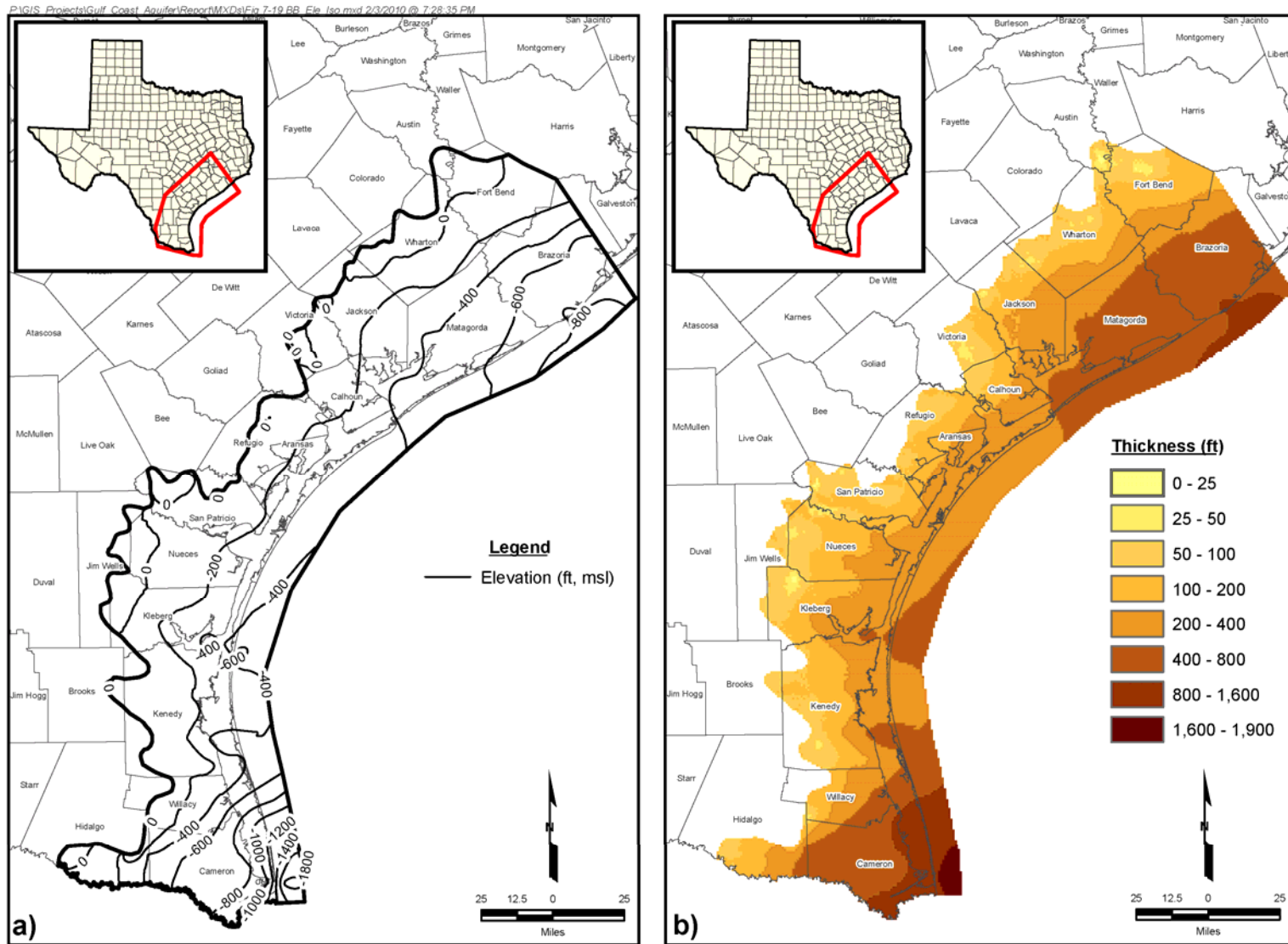


Figure 7-19. Contours for the Beaumont geologic unit showing: (a) base elevation and (b) thickness.

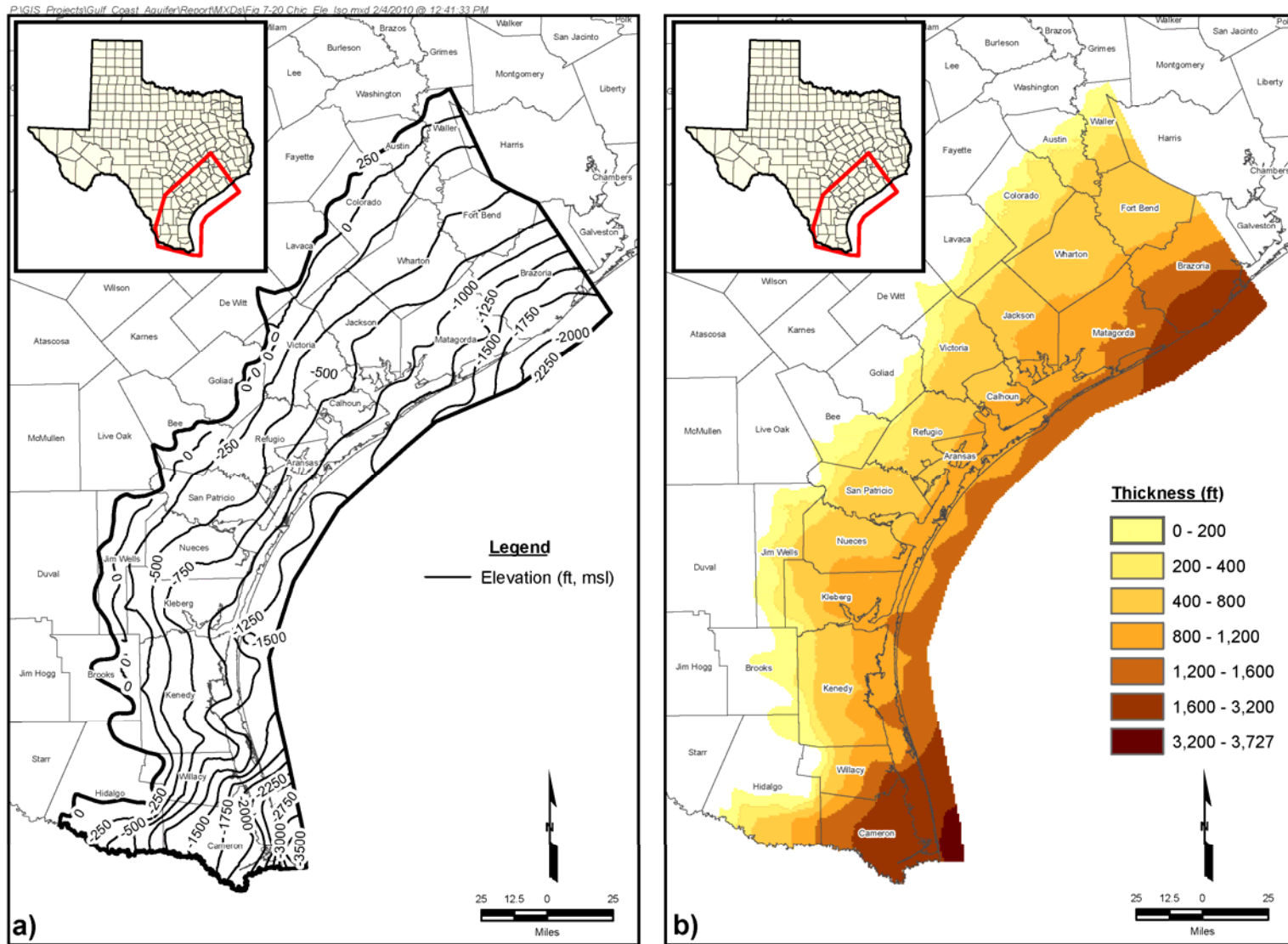


Figure 7-20. Contours for the Chicot Aquifer showing: (a) base elevation and (b) thickness.

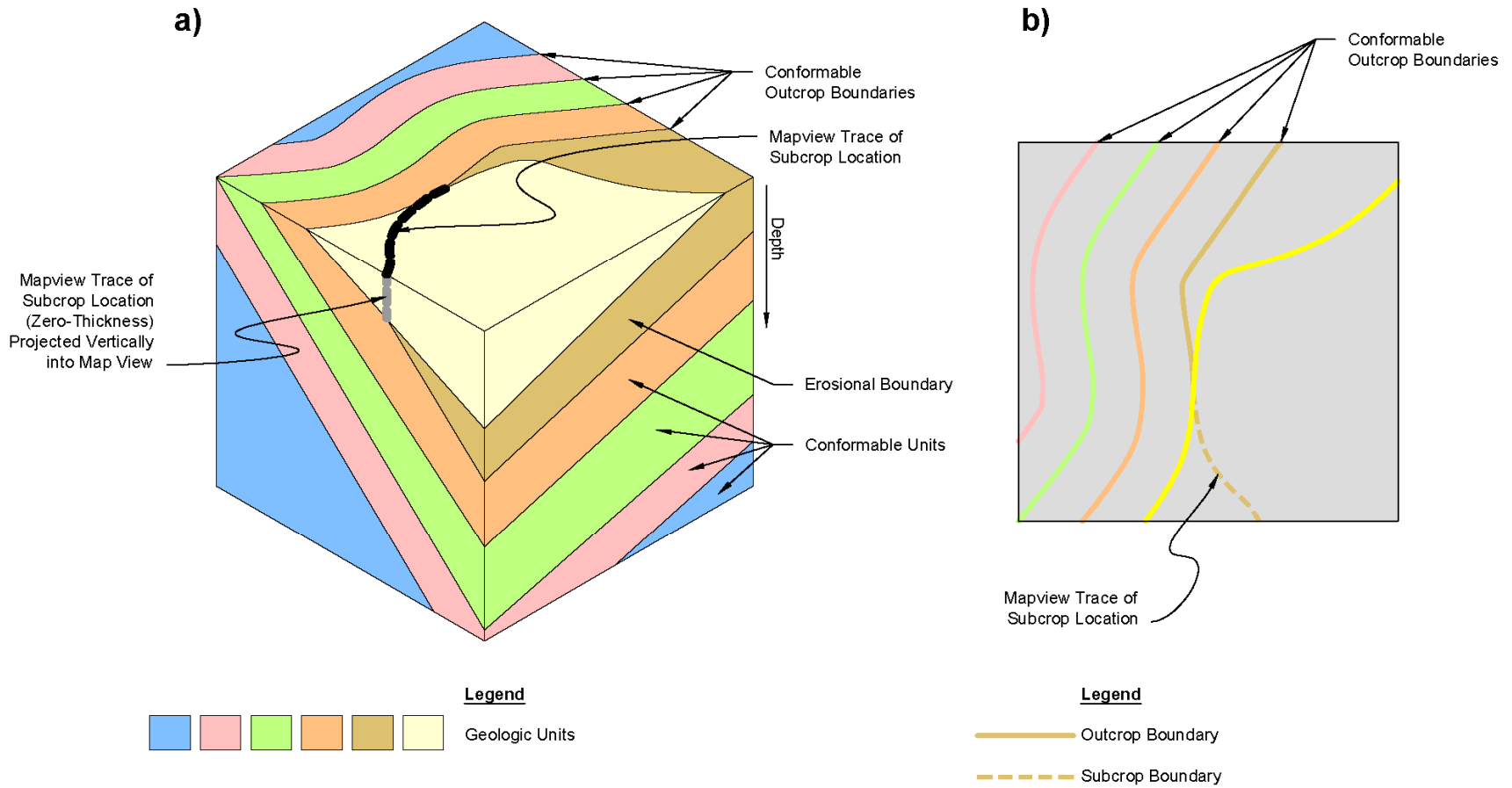


Figure 7-21. Schematic showing outcrop and subcrop locations of geologic units in a three-dimensional block (a) and in a map view (b).

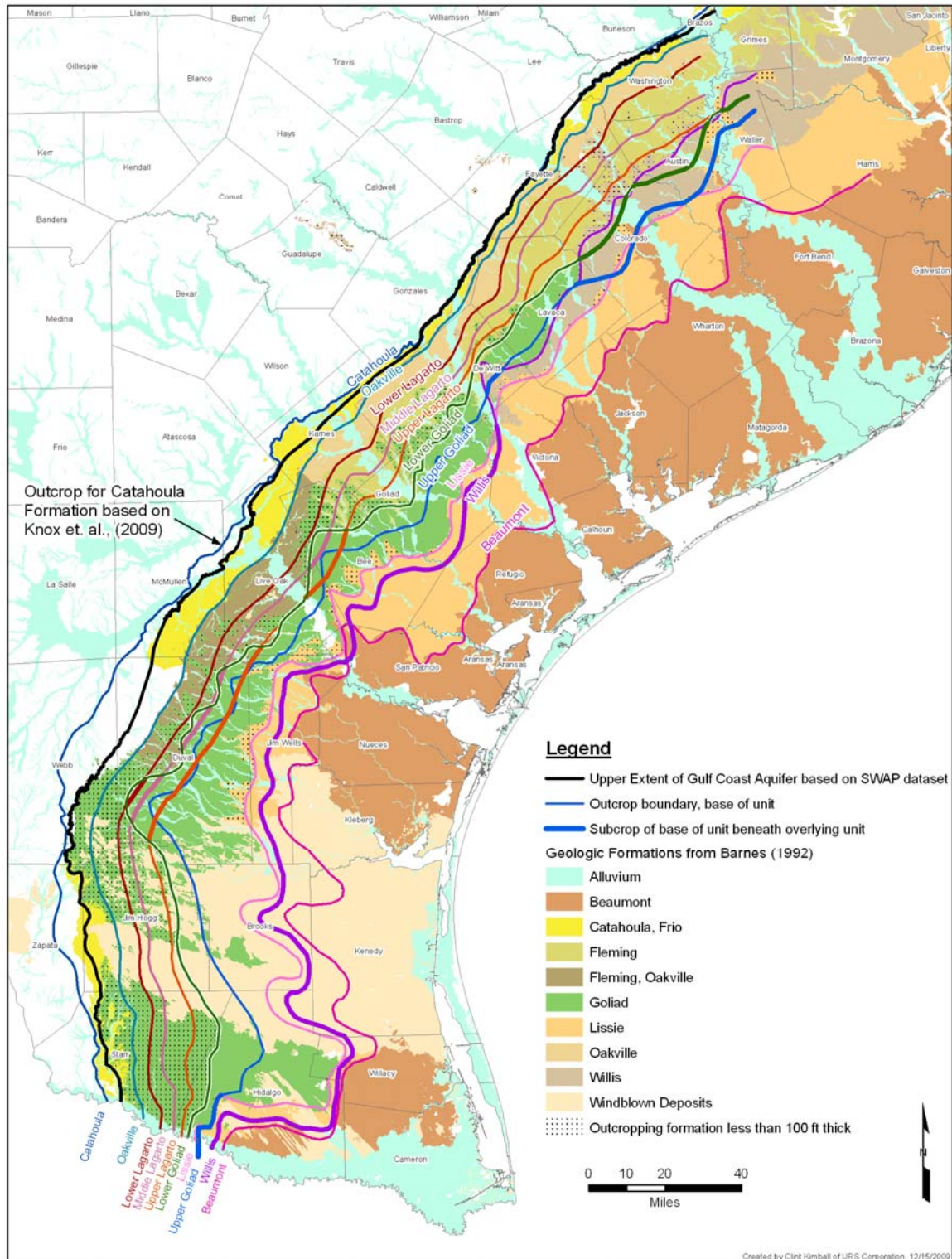


Figure 7-22. Surface geology map from Barnes (1992) showing the estimated locations of the subcrop of selected geologic units.

8 Approach for lithologic interpretation

This section explains the approaches used to classify the deposits into groups related to their sand percentages and their depositional environments. These approaches are important because they indirectly determine the type of analysis that can be used to estimate spatial distribution of aquifer properties.

8.1 Lithology classification

The geophysical logs were interpreted to develop a continuous lithology profile with depth. The traditional approach for this interpretation is to use a binary classification system. The "binary" system, namely aggregating or restricting the sediment beds (as shown on electric logs) into only two classes, either basically sand beds or clay beds, has been traditional through decades of Federal/State investigative studies of county or regional groundwater projects. Figure 8-1 provides an example using an SP log to determine lithology based on a binary system. The interpretation requires that a cutoff value (which is shown in Figure 8-1) be used to determine whether the deposit is classified as either a sand or a clay. For this project, Mr. Ernest Baker performed all of the lithologic interpretations visually.

Among the obstacles associated with interpreting a log for lithology is how to interpret relatively thin beds of sands and clays, which can be very time-consuming to track at a scale of less than a few feet. A common approach that Mr. Baker and many other log analysts have used is to ignore lithology changes that occur below a designated vertical distance. For this project, another approach was used, which involved using a four-class system. This system was first discussed by Young and Kelley (2006) and was used by Mr. Baker for the Gulf Coast Aquifer. The four-class system uses the four textural classes described in Table 8-1. Figure 8-2 compares the results from using the binary and four-class systems to interpret lithology from a log.

The reason for using the four-class system is to more precisely characterize the nature of the sand-clay relationship without having to expend the resources to define small-scale changes in the lithologic profile. With the commonly used approach of ignoring alternating sand and clay layers to implement the binary system, vertical intervals of intermixed sands and clays that extend more than 20 or 30 feet are represented as either a sand or a clay. With the four-class system, there is less chance of falsely indicating too much sand or clay, and a greater chance of more accurately representing the thicker beds of sands. The increased level of specificity with the four-class system provides a lithologic description that better supports characterizing the aquifers' permeability and storage properties. For instance, a sand bed consisting of primarily sands typically will be more permeable than an equally thick bed of a sand mixed with clays. Similarly, a clay bed consisting primarily of clay typically will have a lower vertical permeability than does an equally thick bed of clay mixture with appreciable amounts of sand.

Table 8-1. Description of the four textural classes used to characterize the lithology of the LSWP wells

Class	Description
Sand	A vertical interval of 20 feet or more, composed of 50% to 95% sand-size grains or gravel
Clay	A vertical interval of 20 feet or more, composed of less than 20% sand-size grains
Sand-with-clay	A vertical interval, composed of individual sand and clay beds less than 20 feet thick and composed of more sand than clay
Clay-with-sand	A vertical interval of 20 feet or more, composed of less than 20% sand-size grains

8.2 Depositional facies classification

Depositional facies can be viewed as how different environments arrange and pack sand beds. The basis for understanding deposition is that sediments are transported by well-understood processes that carry them from the hills from which they are eroded to a lower-energy resting place, such as the ocean or a floodplain. The environmental factors that govern the nature of the deposits include climate, ocean level, sediment sources, and chemistry. As these factors change over time, the composition of the deposits change, and cycles of repeating sequences of sand and clay occur. Based on a detailed study of depositional cycles from cores and geophysical logs, geologists have defined facies that characterize deposition in the fluvial and coastal environments of the Gulf Coast.

The depositional facies of aquifer layers provide information on factors that affect groundwater flow such as the sorting, arrangement, and sizes of the particles in a deposit and how the deposit is or is not interconnected to similar and different deposits. For this project, we have selected depositional facies based on the work of Galloway (2000) that were previously used by Young and Kelley (2006) to develop a model of the Gulf Coast Aquifer. These facies can be divided into fluvial facies, coastal facies, and shelf facies. Fluvial facies are associated with deposition in rivers and on the floodplains of rivers. Coastal facies are associated with depositions in coastal and shoreline environments. Shelf facies are associated with off-shore environments.

Galloway (2000) describes the deposition across a coastal plain of the Gulf Coast that was located updip of the shoreline during highstands of sea level and in an area between major axes of fluvial input, with the exception of the Corsair system of the Middle and Late Miocene. As modified from Young and Kelley (2006), the lithologies and depositional facies in this study included:

- Floodplain clays deposited during flooding of coastal streams and, less frequently, major rivers;
- Fluvial channel sands deposited within or immediately adjacent to coastal streams or major rivers;
- Coastal or deltaic bayfill clays, silts, and, rarely, sands deposited behind barrier islands, away from channels on alluvial aprons, or between deltaic distributary channels;
- Lower coastal plain fluvial or coastal sands deposited on alluvial aprons fed by streamplain systems or on delta plains of major extrabasinal rivers;

- Delta front sands, most likely deposited as narrow strike-elongated bodies of a wave-dominated delta;
- Coastal sands deposited as barrier bars, strandplains, or delta fronts where local fluvial input is minor and sand is transported and deposited primarily by along-shore currents; and
- Shallow marine shelf clays and minor silts and sands deposited seaward of the highstand shoreline, which may include interbedded muddy floodplain, bayfill, or lagoonal lowstand deposits..

Based on the information from Galloway et al. (2000), Mr. Paul Knox constructed the facies categories and descriptions listed in Table 8-2. Each facies in Table 8-2 has a different range of hydrologic flow characteristics as a consequence of varying grain size, sorting, mineralogy, sedimentary features, and the degree to which contrasting lithologies are intimately interbedded. Also because of the long time period and large area associated with the project, there may be a large range in the hydraulic properties among deposits with the same facies because of the differences in environmental conditions and sediments that formed them. The flow characteristics ascribed to the different facies in Table 8-2 are generalized estimations and should be used as a relative measure for comparison. They are not intended to be used as an absolute measure estimating hydraulic properties at a scale other than that of a typical bed deposit, which may be a foot to tens of feet. Flow characteristics of these deposits are ultimately controlled by their site-specific conditions and measurement scale.

Table 8-2. Depositional Facies Definition and Predicted Flow Characteristics [modified from Table 3.1.3 in Young and Kelley (2006)]

Code	Facies	Definition	Flow Character	Log Profile
FP	Floodplain	Clay-dominated interval of floodplain and overbank clay, mud, and silt, with rare interbedded fluvial channel, levee, or splay sands less than 20-ft thick.	Sand: relative Kh rating of 2 (1 being lowest K, 7 being highest), Kv rating of 2. <u>Kv/Kh ~ 0.3.</u> Clay: Kh rating of 1, Kv rating of 2. <u>Kv/Kh ~ 0.1.</u>	See Figures 8-3 and 8-4
F	Fluvial Meanderbelt	Sand-dominated interval containing fluvial channel (rarely levee and splay) sands. Bankfull fluvial channel depths or combinations of channel sand thickness and other facies exceed 30 ft in thickness. Interbedded clays can include channel abandonment and floodplain with potential for development of soil profiles or calichification of either clays or sands.	Sand: relative Kh rating of 7 (1 being lowest K, 7 being highest), Kv rating of 5. <u>Kv/Kh ~ 0.5.</u> Clay: Kh rating of 2, Kv rating of 3. <u>Kv/Kh ~ 0.05.</u>	
FD	Lower-Coastal Plain Fluvial and Coastal	Sand-dominated interval containing fluvial and, rarely, distributary channel, levee, splay, and coastal sands often exceeding 30 ft in thickness. Channel sands are	Sand: relative Kh rating of 4 (1 being lowest K, 7 being highest), Kv rating of 4. <u>Kv/Kh ~ 0.4.</u> Clay: Kh rating of 5, Kv rating of 5. <u>Kv/Kh ~ 0.1.</u>	

Code	Facies	Definition	Flow Character	Log Profile
		<p>commonly stacked. Coastal sands may include wave-networked terminal fluvial deposits, minor shorezone and tidal channel, and localized incised-valley deposits. Interbedded muds are most often silty floodplain, bayfill, or lagoonal deposits. Upward-coarsening silty profiles occur far more frequently than in F facies.</p>		
BF	Bayfill	<p>Mud-dominated interval containing interbedded bayfill, lagoonal, and coastal plain deposits. Sands are typically thin, spiky bayfill splay, overbank, or washover deposits.</p>	<p>Sand: relative Kh rating of 1 (1 being lowest K, 7 being highest), Kv rating of 1. <u>Kv/Kh ~ 0.5</u>. Clay: Kh rating of 3, Kv rating of 4. <u>Kv/Kh ~ 0.1</u>.</p>	
WD	Wave-Dominated Delta	<p>Sand-dominated intervals containing upward-coarsening to blocky mouth bar, delta front, strandplain, or barrier bar, and upward-fining distributary channel deposits where sand-component thicknesses of each deposit typically exceed 30 ft. Clays are prodelta, shelf, and bayfill / lagoonal deposits.</p>	<p>Sand: relative Kh rating of 6 (1 being lowest K, 7 being highest), Kv rating of 6. <u>Kv/Kh ~ 0.5</u>. Clay: Kh rating of 7, Kv rating of 6. <u>Kv/Kh ~ 0.1</u>.</p>	
SF	Shoreface / Barrier Bar / Delta Front / Shorezone Coastal	<p>Sand-dominated intervals with upward-coarsening to blocky (rarely upward-fining) sand bodies exceeding 30 ft in thickness. Clays are prodelta, shelf, or bayfill / lagoonal deposits.</p>	<p>Sand: relative Kh rating of 5 (1 being lowest K, 7 being highest), Kv rating of 7. <u>Kv/Kh ~ 0.7</u>. Clay: Kh rating of 6, Kv rating of 7. <u>Kv/Kh ~ 0.1</u>.</p>	
SH	Shelf / Lagoonal / Bayfill / Floodplain	<p>Mud-dominated intervals with rare sandy marine or non-marine scour or reworked deposits. Clays are commonly shelf deposits, with lowstand facies such as FP, BF, or lagoonal sediments.</p>	<p>Sand: relative Kh rating of 3 (1 being lowest K, 7 being highest), Kv rating of 2. <u>Kv/Kh ~ 0.2</u>. Clay: Kh rating of 4, Kv rating of 1. <u>Kv/Kh ~ 0.01</u>.</p>	

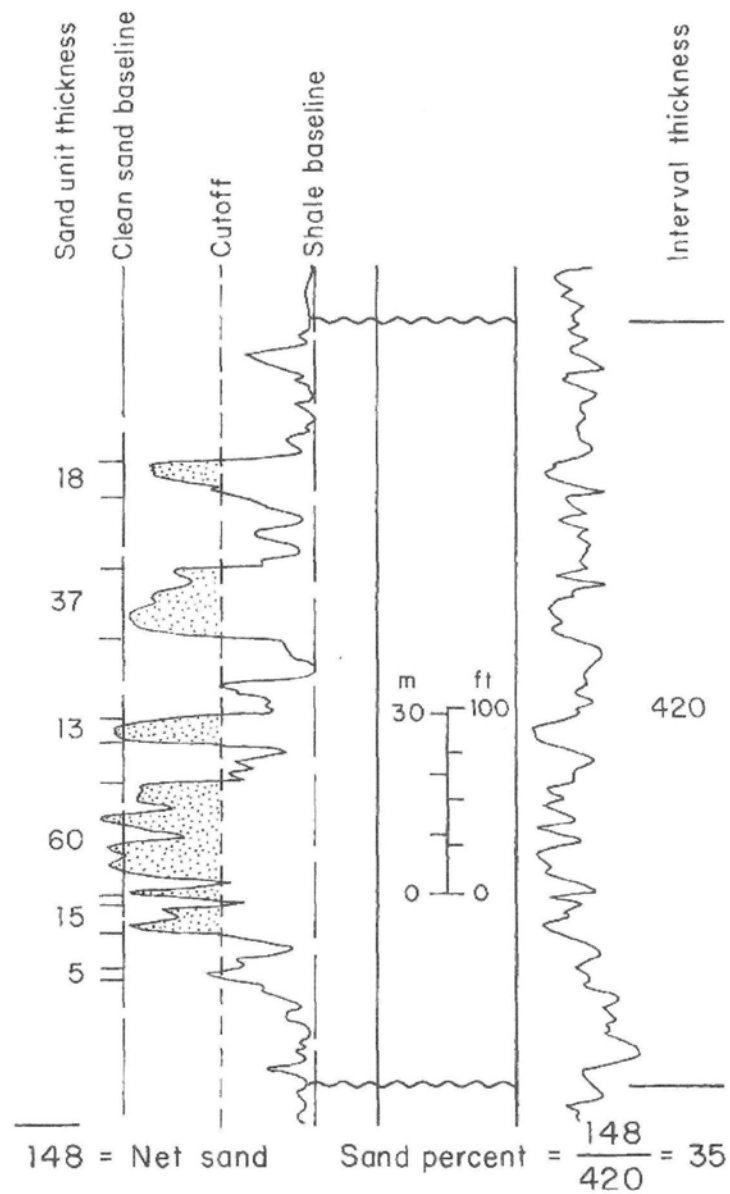


Figure 8-1. Example calculation of net and percent sand from a spontaneous potential (SP) log curve. First baselines are established for the end member lithologies, and then a cutoff is picked for measuring sand thickness and sand/mud ratio (sand percent). Source: Galloway and Hobday (1996).

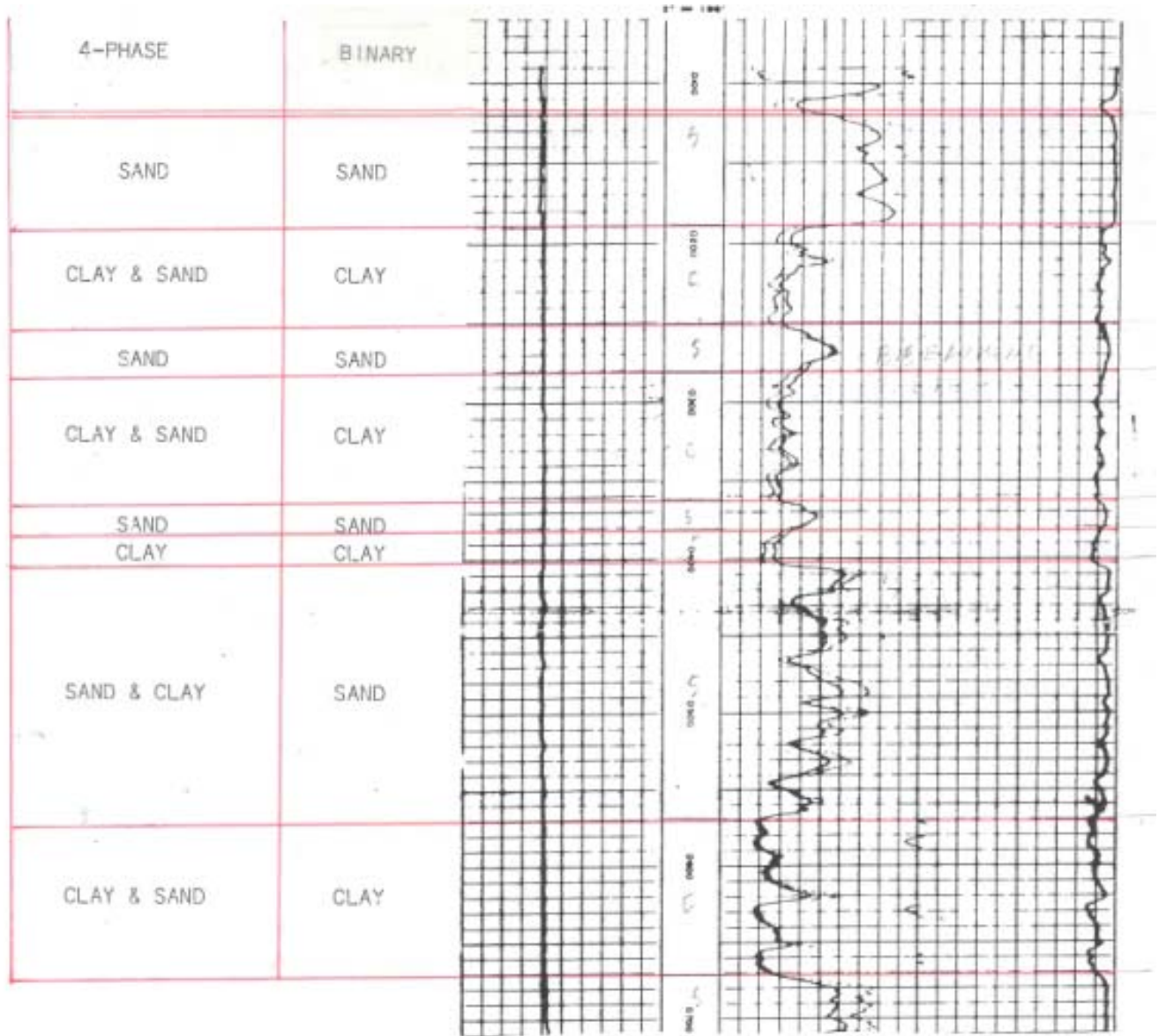
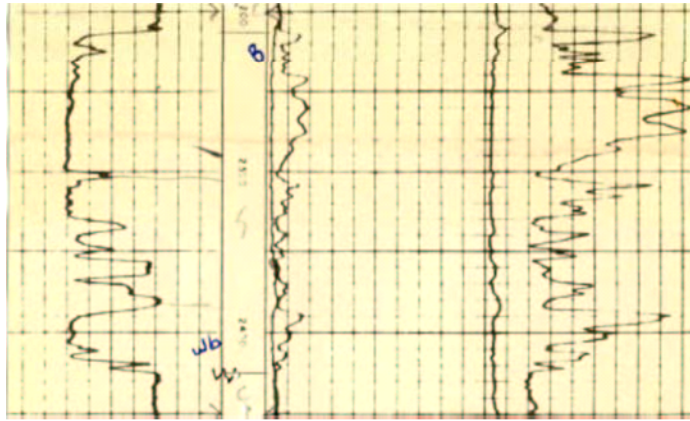
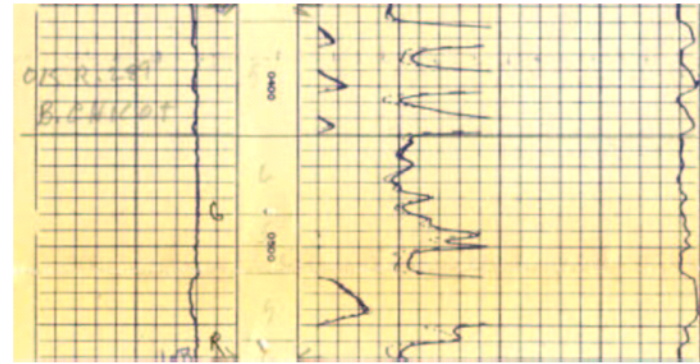


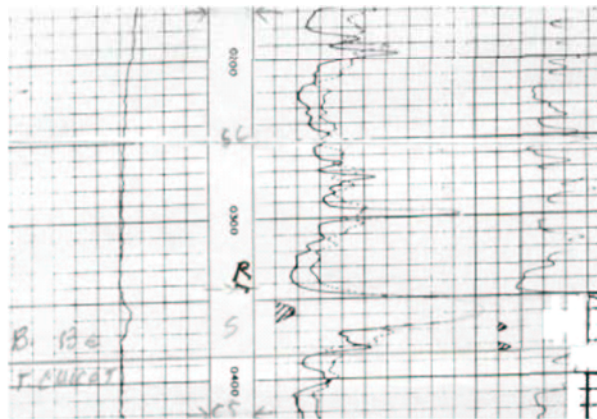
Figure 8-2. Example analysis of a geophysical log showing a binary and four-phase classification of lithology (taken from Young and Kelley, 2006).
 Resistivity log is on the right-hand side, and spontaneous potential log is on the left-hand side. Each grid block has a height of 1 foot.



Log profile example of shorezone facies (SF)



Log profile example of fluvial facies (F)

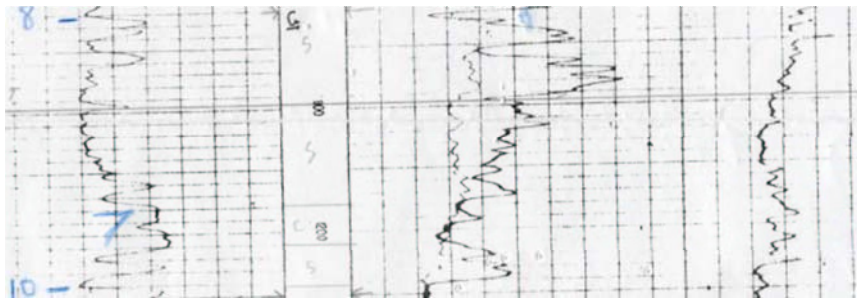


Log profile showing example of floodplain facies (FP)

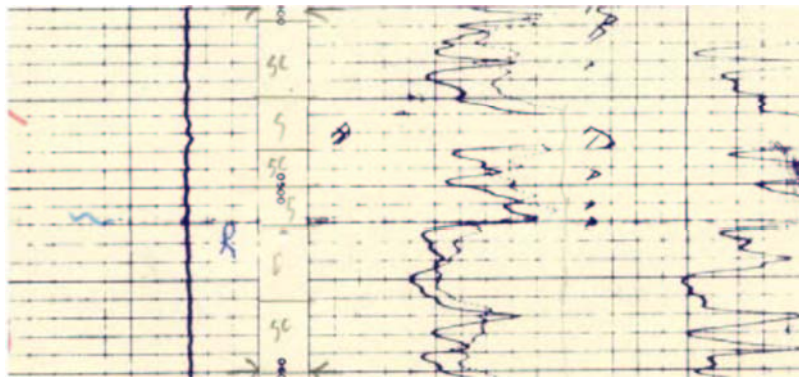


**Log profile showing example of shelf/lagoon/
coastal plain facies (SH)**

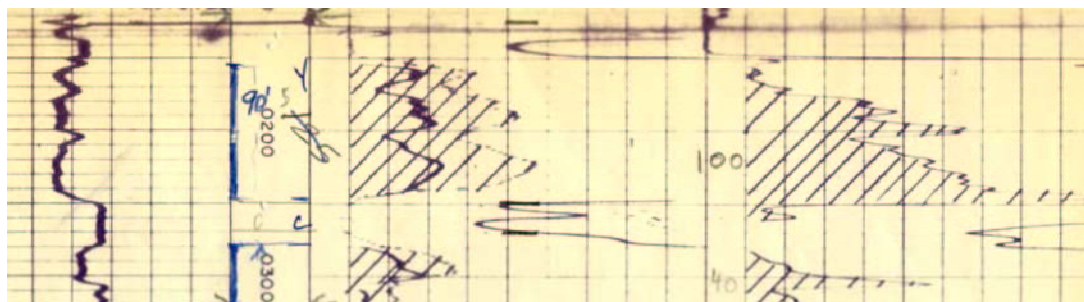
Figure 8-3. Example analysis of a geophysical log showing a binary and four-phase classification of lithology (taken from Young and Kelley, 2006). Resistivity log is on the right-hand side and spontaneous potential log is on the left-hand side.



Log profile showing example of wave-dominated delta facies (WD)



Log profile showing example of bayfill facies (BF)



Log profile showing example of lower coastal plain fluvial and coastal facies (FD)

Figure 8-4. Example analysis of a geophysical log showing a binary and four-phase classification of lithology (taken from Young and Kelley, 2006). Resistivity log is on the right-hand side and spontaneous potential log is on the left-hand side.

9 Gulf Coast Aquifer lithology

The Gulf Coast Aquifer system is a mixture of interbedded sands and clays of various physical properties, sizes, shapes, and dimensions. As a result of these variations, considerable spatial variability occurs in the hydraulic properties of the deposits. This section provides maps of sand fraction, total sand thickness, and distribution of facies type to identify differences among and within the geologic units that can contribute to differences in the transmissive properties of deposits.

9.1 Sand thickness and percent

The factors that govern the transmissivity of an aquifer include a wide range of physical characteristics of deposits that occur at a wide range of scale. These factors include different sizes and sorting of particles at the scale of less than 1 foot; the arrangement and orientation of beds at the scale of tens of feet, and the interconnection and distribution of different facies at the scale of hundreds of feet. Despite the complexities associated with these different factors, a simple approach commonly practiced in the groundwater industry is to estimate transmissivity based on sand fractions and total sand thickness.

Total sand thickness for each geologic unit was calculated by summing the total sand amount for each lithology interval characterized by Mr. Baker using the four-class system. In performing the calculation, the sand class was assigned a sand fraction of 1.0. The sand-with-clay class was assigned a sand fraction of 0.65. The clay-with-sand class was assigned a sand fraction of 0.35. The clay class was assigned a sand fraction of 0.0. Using these sand fraction distributions, the total sand thickness for each geologic unit of interest was calculated for each of the 706 geological logs shown in Figure 5-4. Appendix C lists these sand thickness values. The sand fraction for each geophysical log was calculated by dividing the total thickness by the total sand thickness of the sand.

A continuous distribution of sand fraction for each geologic unit was constructed from the point measurements taken at the geophysical log locations. Only logs with 70% coverage across the layer thickness was used in the calculations. These distributions then were mapped onto a raster grid using kriging algorithms provided in GSLIB (Deutsch and Journel, 1998). The raster grid had a resolution of 4,000 ft, and two-dimensional ordinary kriging was used for this process. These values were similar to those used in Young and Kelley (2006) for mapping deposits in the Gulf Coast. The continuous distribution for the sand thickness map was developed by multiplying the raster grid of total geologic unit thickness discussed in Section 7 by the raster grid for the sand fraction.

A recent study of the Chicot and Evangeline Aquifers in a 10-county area near Wharton County (Young and others, 2009; Young and Kelley, 2006) showed good correlations between sand fractions and hydraulic conductivity after different depositional environments have been considered. Based on these correlations, they were able to successfully calibrate a model using aquifer transmissivity values that were generated with relatively simple algorithms that relate transmissivity to sand fraction, total sand thickness, geologic unit, and facies type. An important component of these relationships is that they are sensitive to the unique conditions at

the scale of the geologic unit and to the facies type within a geologic unit. This sensitivity is attributed to the fact that the geologic unit and the facies type can be indicators of the general nature, distribution, and interconnectivity of the sand beds that comprise the total sand thickness.

Figures 9-1 through 9-21 provide sand fraction and sand thickness maps for the Chicot Aquifer, Evangeline Aquifer, Burkeville Confining Unit, Jasper Aquifer, and the geologic units that compose the three aquifers. These figures show a wide range of sand fractions and sand thicknesses across the study area that include significant differences among the geologic units that comprise the Gulf Coast Aquifer system.

9.1.1 Chicot Aquifer

Figure 9-1 shows the sand thickness distribution for the Chicot Aquifer. The sand thickness increases toward the coast and reaches thicknesses up to about 1,500 ft. Among the three geologic units that comprise the Chicot Aquifer, the units all have distinctly different distributions of sand fractions. In the Beaumont Formation (Figure 9-2), the highest sand fractions occur in the central and northern regions with the highest and lowest fractions occurring near Fort Bend and Kleberg Counties, respectively, and with the largest continuous area with sand fractions greater than 0.6 occurring near Aransas, Refugio, and Calhoun Counties. In the Lissie Formation (Figure 9-4), sand fractions greater than 0.6 are most common near the updip portion of the central and northern regions between San Patricio and Fort Bend Counties. As with the Beaumont, the Lissie's lowest sand fraction values are near Kleberg County. In the Willis Formation (Figure 9-6), the sand fraction distributions are greatest north of Victoria County with sand fractions typically greater than 0.6. South of Victoria County, the sand fractions typically are above 0.4 and occasionally above 0.8. Because the Beaumont, Lissie, and Willis Formations dip and thicken towards the coast, all of their maps for total sand thickness thicken toward the coast.

9.1.2 Evangeline Aquifer

Figure 9-8 shows the sand thickness distribution for the Evangeline Aquifer. The sand thickness increases toward the coast and approaches or exceeds a thickness of 3,200 feet near the coastline. In the upper Goliad (Figure 9-9), the sand fractions are generally the highest through about a 30-mile-wide strip that covers the updip region of the geologic unit. In this area, the sand fractions usually exceed 0.6. Across the two lower units that comprise the Evangeline Aquifer, the lower Goliad (Figure 9-11) and upper Lagarto (Figure 9-14), the sand fraction distributions are similar. In general, the sand fractions are the lowest in the central region with values usually less than 0.4 and with values greater than 0.6 occurring near the updip boundary of the geologic units and in the south in Hidalgo and Brooks Counties. The sand thickness maps for the upper Goliad, lower Goliad, and upper Lagarto suggest that the majority of the sands in the Evangeline Aquifer exist within the upper Goliad.

9.1.3 Burkeville Confining Unit

Figure 9-16 shows the sand thickness distribution for the Burkeville Confining Unit. Across most of the unit, the sand thickness varies between 50 and 200 feet and increases toward the

coast. The sand fraction distribution (Figure 9-15) shows that for most of the Burkeville Confining Unit, the sand fraction varies between 0.2 and 0.6, with localized regions where the sand fraction is less than 0.2 or greater than 0.8. Within the on-shore area, the sand fractions tend to decrease toward the coast.

9.1.4 Jasper Aquifer

Figure 9-17 shows the sand thickness distribution for the Jasper Aquifer. The sand thickness increases toward the coast and is greater than 1,600 feet along the coastline. In the lower Lagarto (Figure 9-18), the sand fractions are similar but slightly higher than those in the Burkeville Confining Unit. Across most of the unit, the sand fractions are between 0.2 and 0.6. A region of relatively low sand fraction values below 0.4 stretches from Duval County through San Patricio County to Refugio County. A region of higher sand fraction values above 0.6 stretches from Duval County through San Patricio County to Refugio County. In the Oakville Formation (Figure 9-20), the sand fractions are significantly higher than in the lower Lagarto. Across most of the unit, the sand fractions are greater than 0.4. The sand thickness maps for the lower Lagarto and Oakville suggest that the majority of the sands in the Jasper Aquifer occur in the Oakville.

9.2 Depositional facies

The hydrological properties of the Gulf Coast Aquifer system and its component hydrogeologic units are governed strongly by characteristics of the sediments imparted at the time of deposition. Sediment texture (grain size, sorting, etc.) and composition of framework grains and matrix material are dependent upon the influences of depositional energies, which vary with depositional setting. Sand body size, shape, orientation, and interconnection are similarly products of the depositional setting. Sediments and rocks deposited in a similar depositional setting can be grouped together as a "facies." Facies are in turn elements of a given "depositional system." Thus, sediments deposited in a fluvial depositional system can have relatively coarser grain size and good sorting when deposited in a high-energy river channel, and can be considered "fluvial" facies. In contrast, fine-grained, often less well sorted sediments also deposited as part of a fluvial depositional system are deposited in low-energy overbank and floodplain settings, and can be considered "floodplain facies." Sediments in a floodplain facies will have substantially poorer hydrologic properties as a result. Table 8-2 provides a summary of facies types and brief descriptions of each type.

9.2.1 Chicot Aquifer

Depositional facies within layers of the Chicot Aquifer are shown in Figures 9-2, 9-4, and 9-6. The depositional axes in the Willis Formation (Figure 9-6) can be separated, as in the underlying Goliad, into a southern set roughly coincident with the Realitos and Mathis axes, and a northern set roughly coincident with the Cuero and Eagle Lake axes. The northern axes provided the most sand-rich deposits during Willis time, prograding out to the current shoreline during highstand time. A dip-oriented sand thick near and south of Matagorda Bay likely carried sediment out to shelf-edge and slope systems mapped by Morton and others (1991). In the southern part of the area, purely fluvial facies extend farther into the study area, and closer to the

current shoreline. Lower coastal plain facies are isolated into distinct localized depocenters, and at least one deltaic assemblage in Kenedy County appears, from log signatures, to be strongly wave-dominated. Shorezone facies cover a broad area of San Patricio County, but this facies belt narrows as it extends northward, just landward of the current coastline. Shelf facies downdip of this shorezone belt, and downdip of lower coastal plain facies in South Texas, are interrupted by two broad dip-oriented areas of lower coastal plain facies. These include the area near and south of Matagorda Bay and another area from San Patricio to Kenedy Counties. Again, facies terminology used for the Willis, and other layers within the Chicot Aquifer, are simplified from those in Knox and others (2006) to reflect distinctions in hydraulic properties and simplify the association of highstand and lowstand facies.

Unlike the Willis Formation, fluvial facies in the Lissie Formation extend a substantial distance downdip into the study area (Figure 9-4), indicating significant progradation. The southern fluvial axis is substantially reduced in extent, with widespread sand-poor floodplain facies across Willacy, Kenedy, Kleburg, Brooks, and Jim Wells Counties. The northern axes, from Live Oak to Colorado and Fort Bend Counties, form a broad continuous belt of sand-rich facies reminiscent of an alluvial apron. The lower coastal plain facies region downdip of the fluvial axes is again a very sand-rich region, especially in San Patricio County. The lower coastal plain region contains only small areas of sand-poor bayfill facies and transitions into the shorezone system without decrease of sand percent. Shorezone facies lie just inland of the current shoreline in Brazoria and Matagorda Counties, becoming nearly coincident with it southward through Kleburg County. South of this, the trend turns slightly inland and gradually increases its distance inland from the modern shore as it continues south to the Rio Grande River. A broad area of lower coastal plain facies occur downdip of the shorezone system, and likely extend to near the shelf edge of the underlying Goliad Formation. Morton and others (1991) mapped deltaic and strandplain facies more than 30 miles offshore from the modern Colorado/Brazos River deltaic headland. Lowstand lower coastal plain facies in South Texas are not as uniformly widespread, and shelf facies dominate in areas of Kleburg, Willacy, and southern Cameron Counties.

Depositional patterns in the uppermost layer of the Chicot Aquifer, the Beaumont Formation, are similar in trend to the underlying Lissie Formation and strongly mimic the depositional systems seen at the surface. A broad belt of fluvial facies reach far downdip into the middle of coastal counties from Nueces County northward (Figure 9-2). From Nueces through west central Kenedy Counties, no evidence of significant fluvial facies is seen, and fluvial facies south of this are generally only moderate in sand percentage with the exception of southernmost Hidalgo and Cameron Counties. Lower coastal plain facies form a narrow sand-rich band between fluvial and shorezone facies. Shorezone facies in the Beaumont Formation are distributed similar to those in the underlying Lissie Formation in that they lie roughly coincident with or slightly inland of the current coast. Shorezone facies reach their greatest width in the central coast, from Nueces through Aransas Counties. Lower coastal plain facies are widespread, with the exception of Willacy and southern Kenedy Counties, and likely feed significant lowstand shelf-edge and slope facies similar to those mapped by Morton and others (1991) offshore of the upper Texas coast.

9.2.2 Evangeline Aquifer

Within the Evangeline Aquifer, depositional facies are increasingly dominated by fluvial and lower coastal plain settings when progressing from the upper Lagarto unit to the lower Goliad, and finally the upper Goliad units. Figure 9-13 shows the facies for the upper Lagarto unit. The overall pattern is similar to that of the middle Lagarto of the Burkeville system, with widespread sand-poor facies in the mid- to down-dip areas. To some extent, the sand-poor bayfill/lagoonal facies of the upper Lagarto reinforce the confining aspects of the Burkeville, and can even extend confinement over a larger area in regions where sandy areas of the Burkeville are overlain by sand-poor areas of the upper Lagarto.

Bayfill/lagoonal facies in the lower Goliad unit (Figure 9-11) extend farther landward than those of the underlying Lagarto units and, importantly, are more continuous in South Texas, where finer-grained Lagarto facies are breached by coarse clastic input from the Santa Cruz fluvial axis. Consequently, the lower Goliad can act to further reinforce the confinement reflected by the middle Lagarto (Burkeville) unit. Lower coastal plain facies in the updip part of the study area again represent highstand deposition, with fluvial/coastal or even incised valley deposits hydraulically linking them to downdip lower coastal plain facies. As in the underlying Lagarto and Oakville Formations, the southern fluvial axes of the lower Goliad, the Realitos and Mathis, which reach from Starr to Duval Counties, are bedload-dominated (Hoel, 1982). More northerly axes, the Cuero of Goliad County and the Eagle Lake of Lavaca and Colorado Counties, respectively, are mixed-load systems. Morton and others (1988) named the South Padre Strandplain System for the downdip equivalents of Realitos and Mathis axes while using the term South Brazos Delta System for the downdip deposits of the Cuero and Eagle Lake axes.

Upper Goliad facies (Figure 9-9) consist of a much higher percentage of lower coastal plain facies than the lower two layers of the Evangeline Aquifer. Fluvial facies are limited to the most updip parts of the study area but sandy lower coastal plain facies extend nearly unbroken to counties along the modern shoreline. A shorezone facies stretches northward from offshore Corpus Christi Bay, coming ashore in Aransas County and thence paralleling the coast through Matagorda and Brazoria Counties. Shelf facies lie basinward of this trend and include shelf muds, fluvial floodplain deposits, and possibly bayfill or lagoonal intervals deposited during transgression. Large areas of lower coastal plain facies extend past the shorezone and shelf facies along the coast to feed lowstand shelf-edge deltaic and strandplain systems mapped by Morton and others (1988). This interpretation of separate highstand and lowstand depocenters results in different facies terminology from Knox and others (2006), where highstand deltas were labeled as bayhead deltas, and dip oriented features extending offshore were labeled incised valleys. The simplified approach used here resulted from subsequent modeling of units characterized by Knox and others (2006). The greatest distinction found when comparing hydraulic conductivity values was between fluvial and deltaic/marine facies (Young and others, 2009).

9.2.3 Burkeville Confining System

Depositional facies within the Burkeville Confining System are shown in Figure 9-13, the facies map for the middle Lagarto unit. Facies for the middle Lagarto unit are similar to those in the

lower Lagarto unit, with the exception that fine-grained bayfill/lagoonal facies are more continuous and extensive in the mid-dip region than in the lower Lagarto unit. This pattern is readily apparent in logs and accounts for the designation of this unit as a confining layer. The bayfill/lagoonal facies trend is interrupted in South Texas by a broad area of lower coastal plain facies associated with the Santa Cruz and North Padre Systems, and by narrower breeches in the northern part of the study area by lower coastal plain facies that depositionally link highstand and lowstand parts of the Moulton/Point Blank and Matagorda Systems.

9.2.4 Jasper Aquifer

Depositional facies of the Jasper Aquifer include the sandy fluvial and floodplain facies of the Catahoula Formation discussed previously, the sandy deltaic and shorezone facies of the Frio Formation, sandy facies within the Oakville Formation (Figure 9-20), and facies within the lower Lagarto unit. Sandy facies in the Frio Formation include the Gueydan Fluvial System and Norias Delta System of South Texas, the Choke Canyon/Flatonía Streamplain and associated Greta/Carancahua Barrier/Strandplain Systems of the central coast, and the Chita/Corrigan Fluvial and associated Houston Delta systems from Jackson County northwards.

Figures 9-18 and 9-16 present the depositional systems of the Oakville and lower Lagarto Formations. In South Texas, an extrabasinal fluvial system delivers sandy and gravelly sediment to the bedload-dominated Santa Cruz Fluvial System (Galloway et al, 1986). Log intervals containing only sharp-based upward-fining patterns are limited to the most updip areas, and are mapped as purely fluvial facies. The bulk of this area includes some upward-coarsening sandy beds and spiky upward-coarsening silty intervals. It is here considered lower coastal plain fluvial and coastal facies. In the central and northern parts of the study area, purely fluvial facies only exist in the most updip fringe of the study area, and lower coastal plain facies extend across the northwestern (updip) half of the study area. Galloway and others (1986) named sediments in the same area to the Moulton/Point Blank Streamplain System.

Upward-coarsening log patterns become more predominant toward the coast. In the eastern parts of Willacy and Kenedy Counties, log signatures, especially in the Oakville Formation, are upward-coarsening to blocky, and less serrate, indicating a wave-dominated deltaic setting. Galloway and others (1986) named this the North Padre Delta System. Wave-dominated facies extend northward, covering half or more of the downdip part of the study area, which is coincident with the Matagorda Barrier/Strandplain System of Galloway and others (1986). Blocky log patterns are less common in Lagarto units and were not distinguished specifically as wave-dominated deltaic or shorezone deposits. In the lower Lagarto unit, this area was classified as lower coastal plain facies.

Sand-poor areas between lower coastal plain and wave-dominated facies, and within or downdip of wave-dominated facies, are labeled as "shelf" facies, and are expected to include a vertical succession of highstand shelf facies and lowstand floodplain, bayfill, and lagoonal facies. The areas within and adjacent to lower coastal plain facies are interpreted as bayfill deposits.

9.2.5 Catahoula Confining System

Facies within the Catahoula Confining System include the mud-dominated marine and nonmarine facies of the Frio Clay (the outcrop equivalent of the Vicksburg Formation of the subsurface) as well as sand-poor marine and nonmarine facies of the shallow subsurface extent of the Catahoula Formation and its deeper subsurface equivalent, the Frio Formation.

Most important to confinement, perhaps, are the broad floodplain muds of the Vicksburg Formation (Frio Clay) at outcrop and in the shallow subsurface. In south Texas, Coleman (1990) mapped broad regions of coastal plain deposits extending 15 to 20 miles downdip of the outcrop, and laterally interrupted by narrow (2 to 7 mile wide) fluvial axes. Farther downdip in South Texas are widespread deltaic and shorezone sands. The situation is similar in the northern half of this study area, with the exception that increasingly broad deltaic and shorezone sand belts exist closer to the updip truncation, being within 10 miles of the pinchout area across Lavaca, Colorado, and Austin Counties (Coleman, 1990). Galloway et al. (1986) indicated that Frio clay/Vicksburg deposits do not actually crop out north of the San Marcos arch.

In the overlying Catahoula Formation, bedload-dominated streamplains of the Gueydan Fluvial System in the south and mixed-load fluvial deposits of the Chita-Corrigan Fluvial System in the north transition downdip to delta and strandplain systems of the Frio Formation (Galloway, 1977). Confinement in these units is limited to less widespread floodplain muds than in the underlying Vicksburg Formation (Frio Clay).

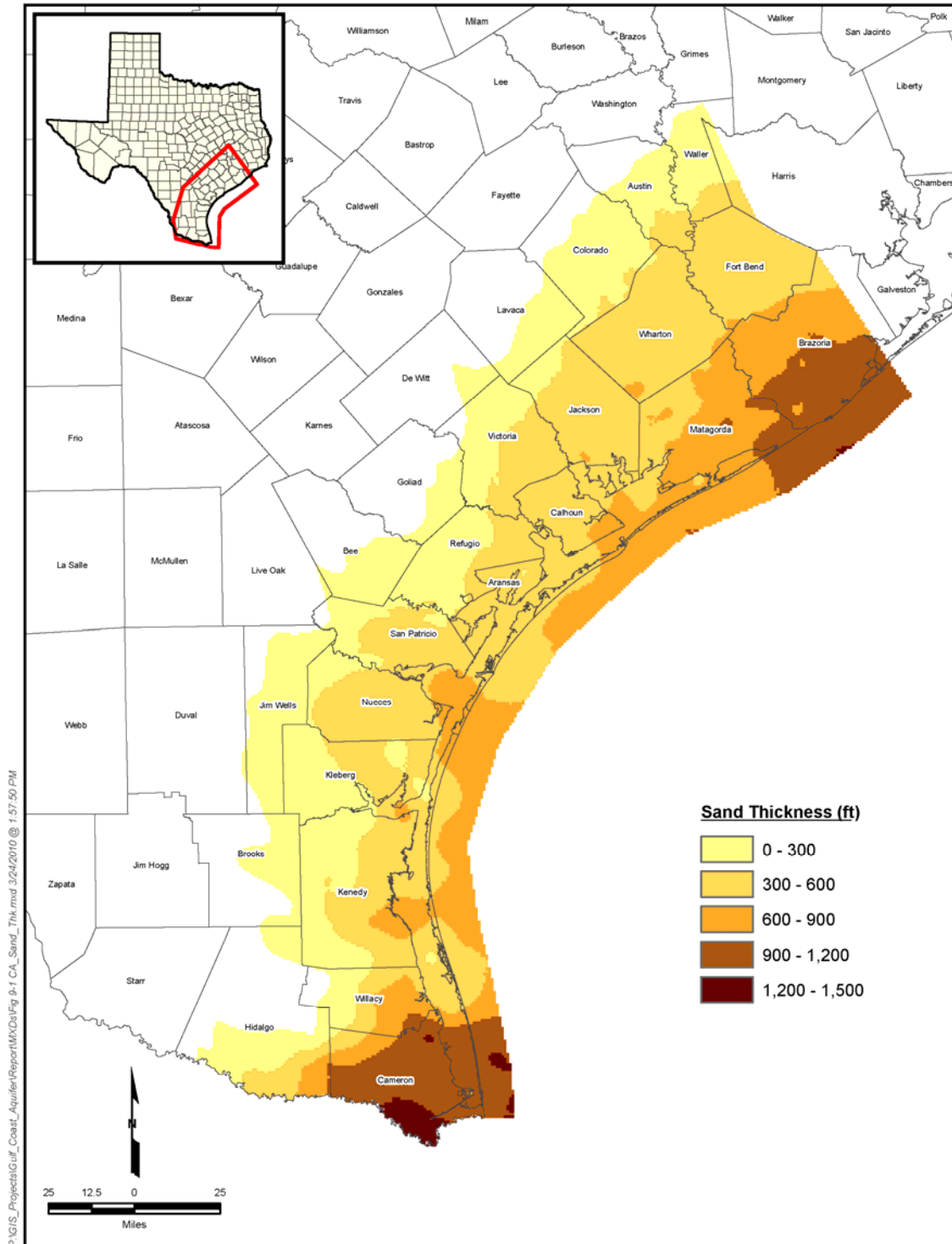


Figure 9-1. Map of the Chicot Aquifer showing total sand thickness.

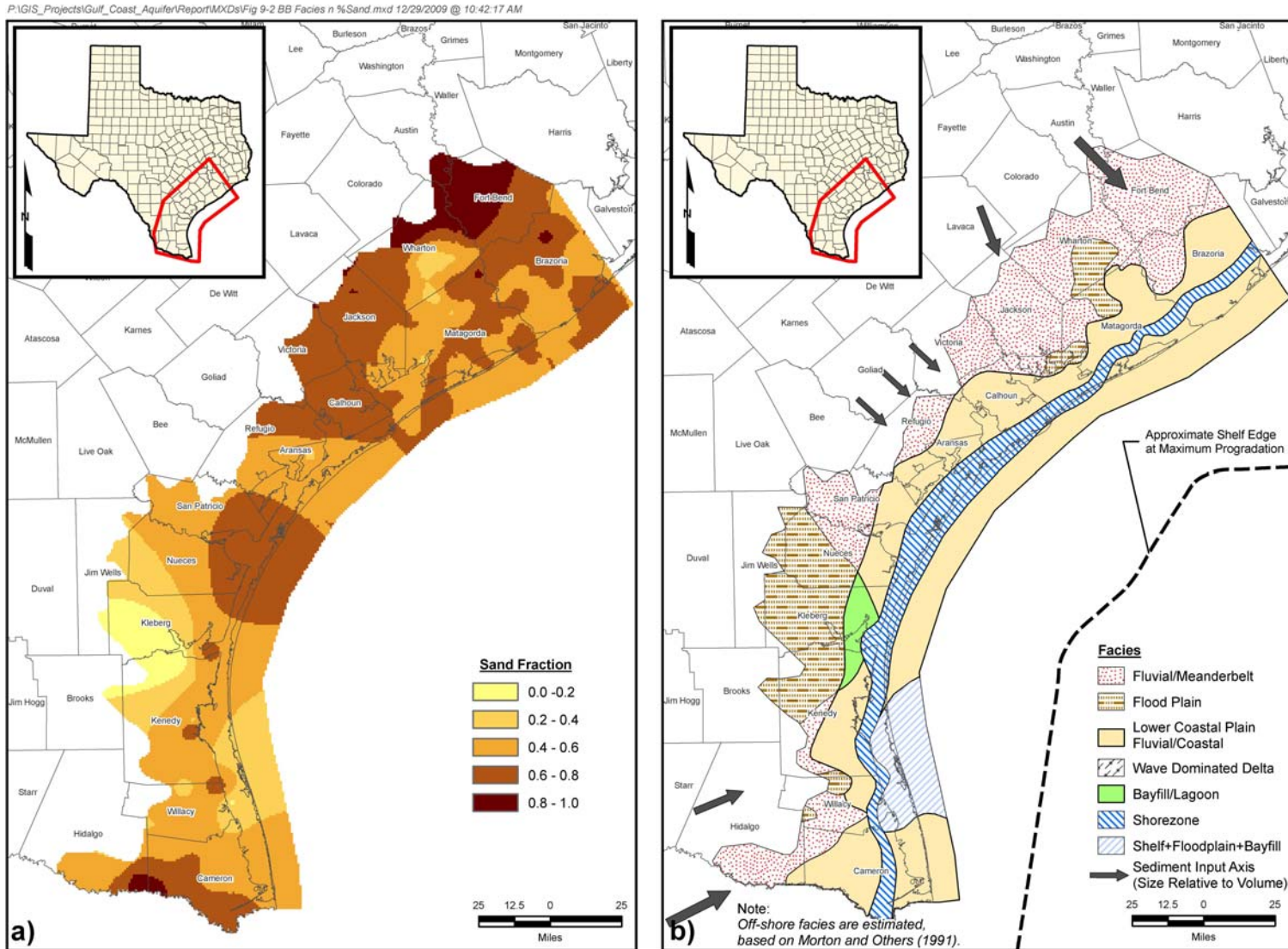


Figure 9-2. Map of the Beaumont geologic unit showing: (a) percentage sand coverage and (b) depositional facies.

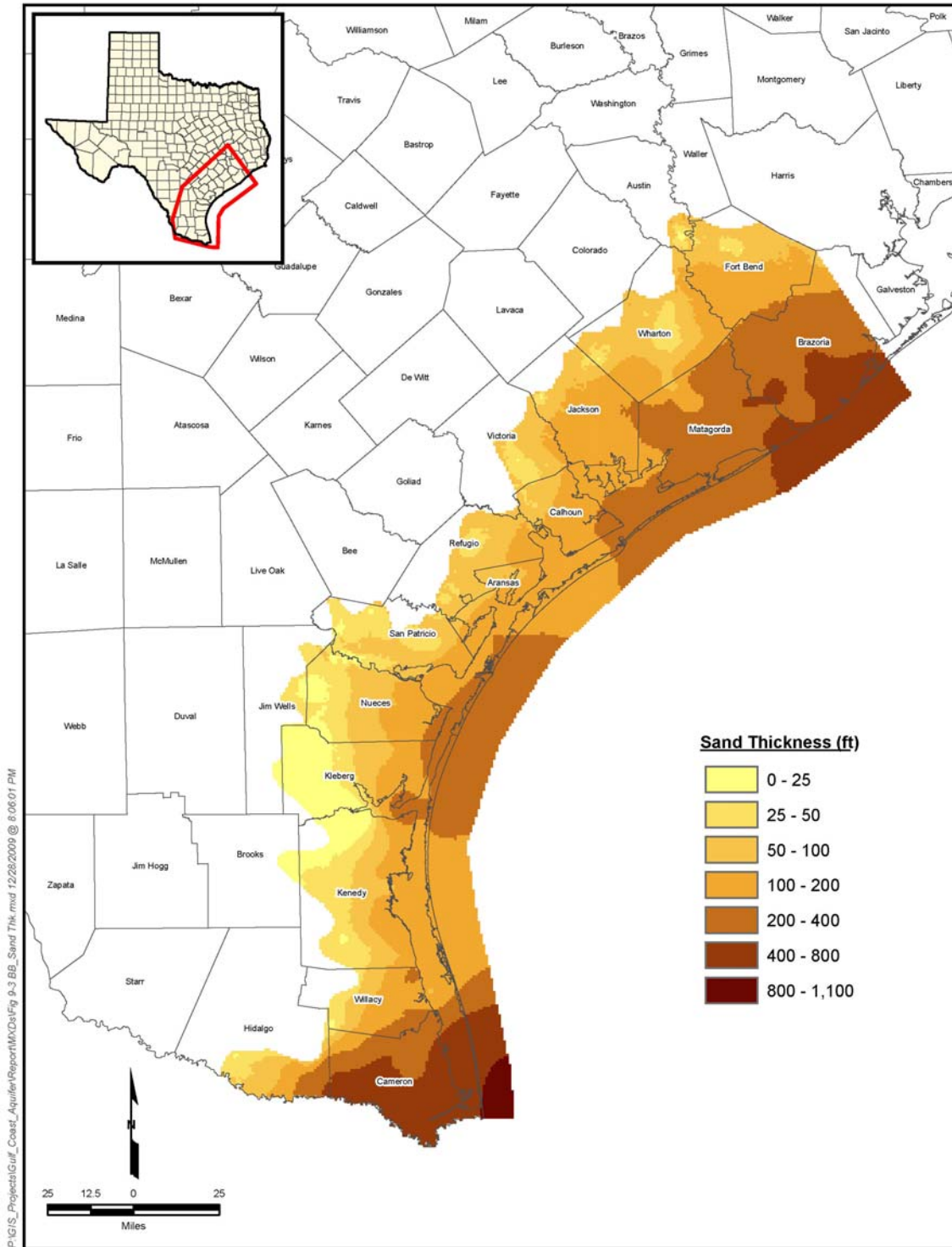


Figure 9-3. Map of the Beaumont geologic unit showing total sand thickness.

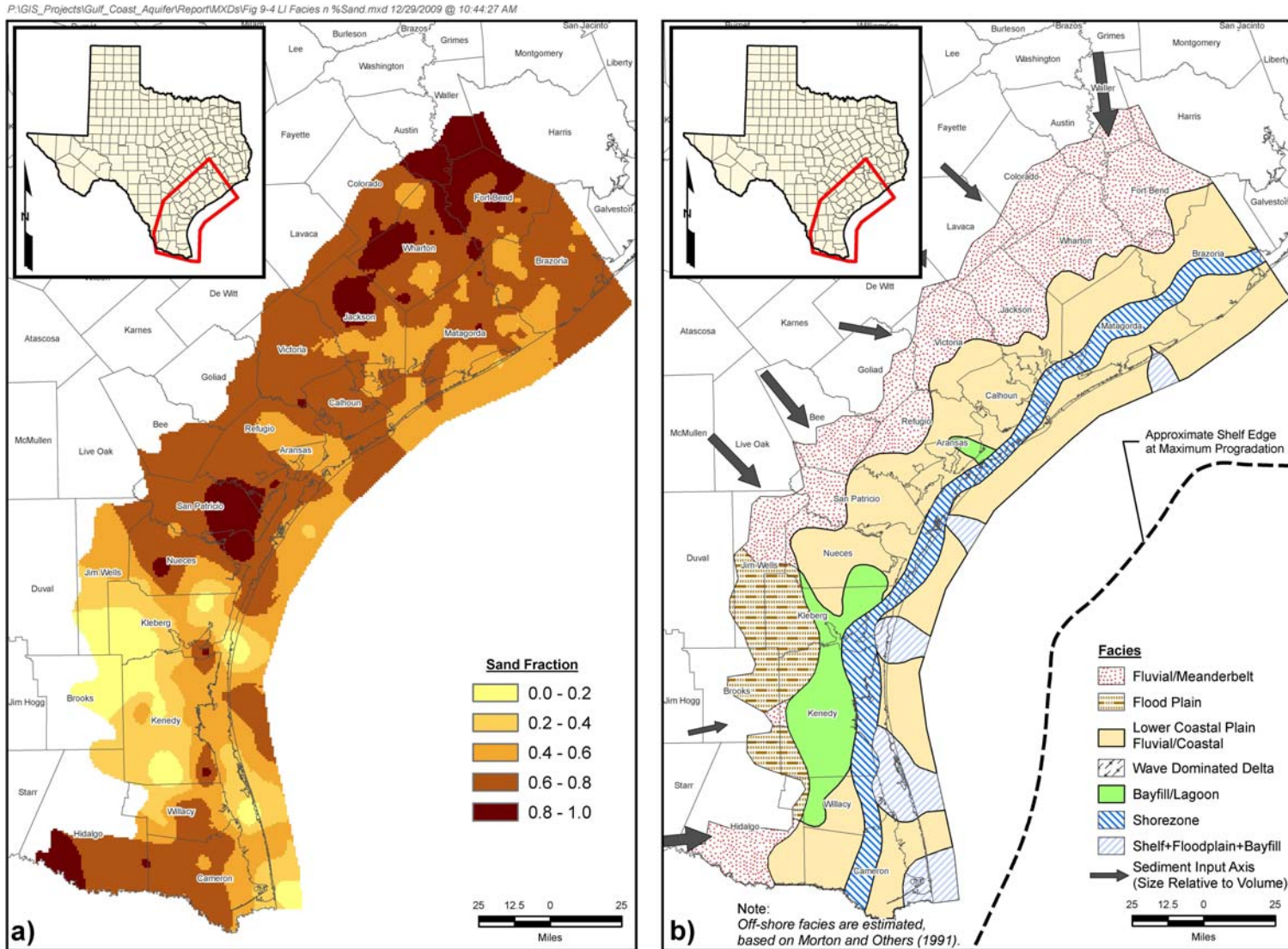


Figure 9-4. Map of the Lissie geologic unit showing: (a) percentage sand coverage and (b) depositional facies.

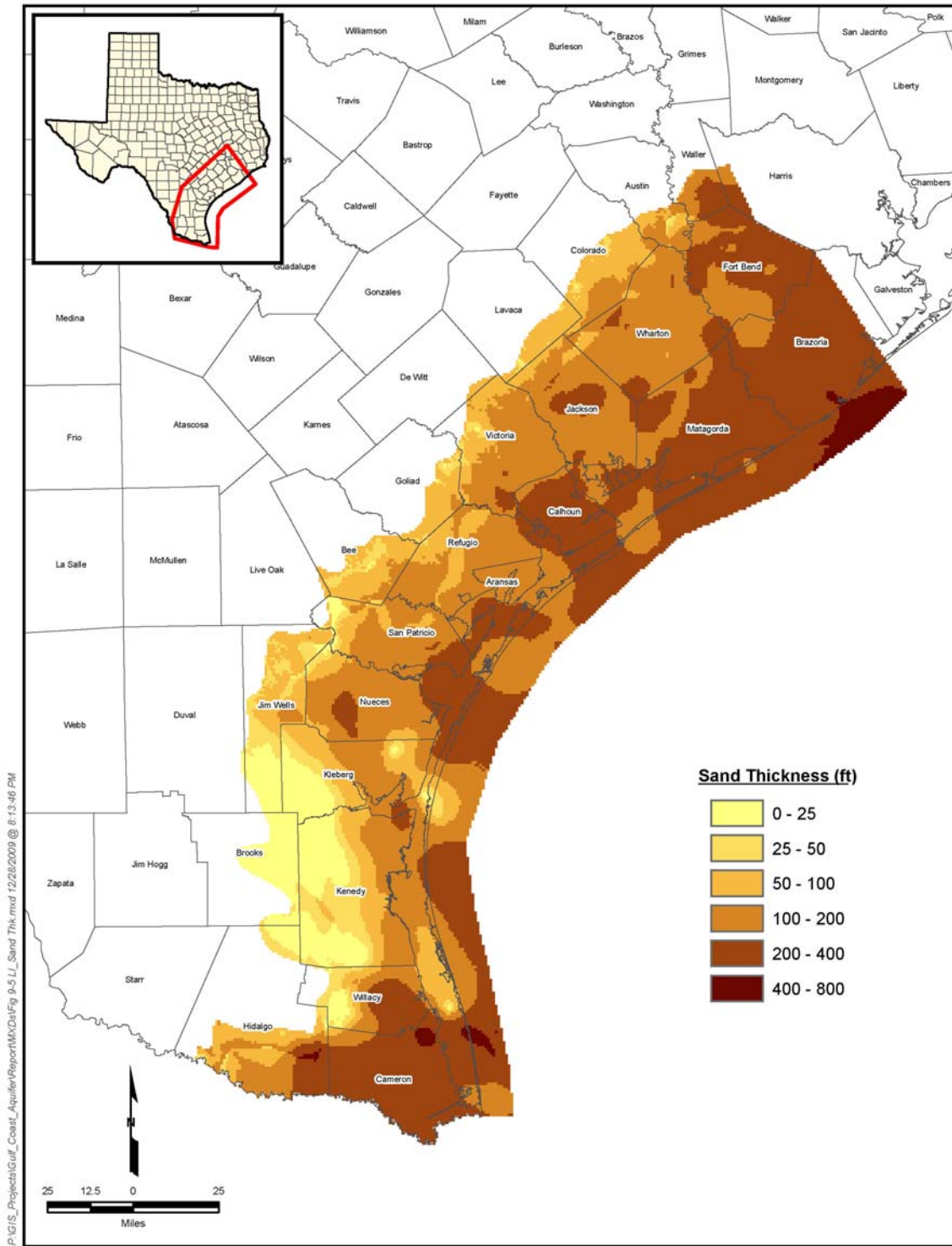


Figure 9-5. Map of the Lissie geologic unit showing total sand thickness.

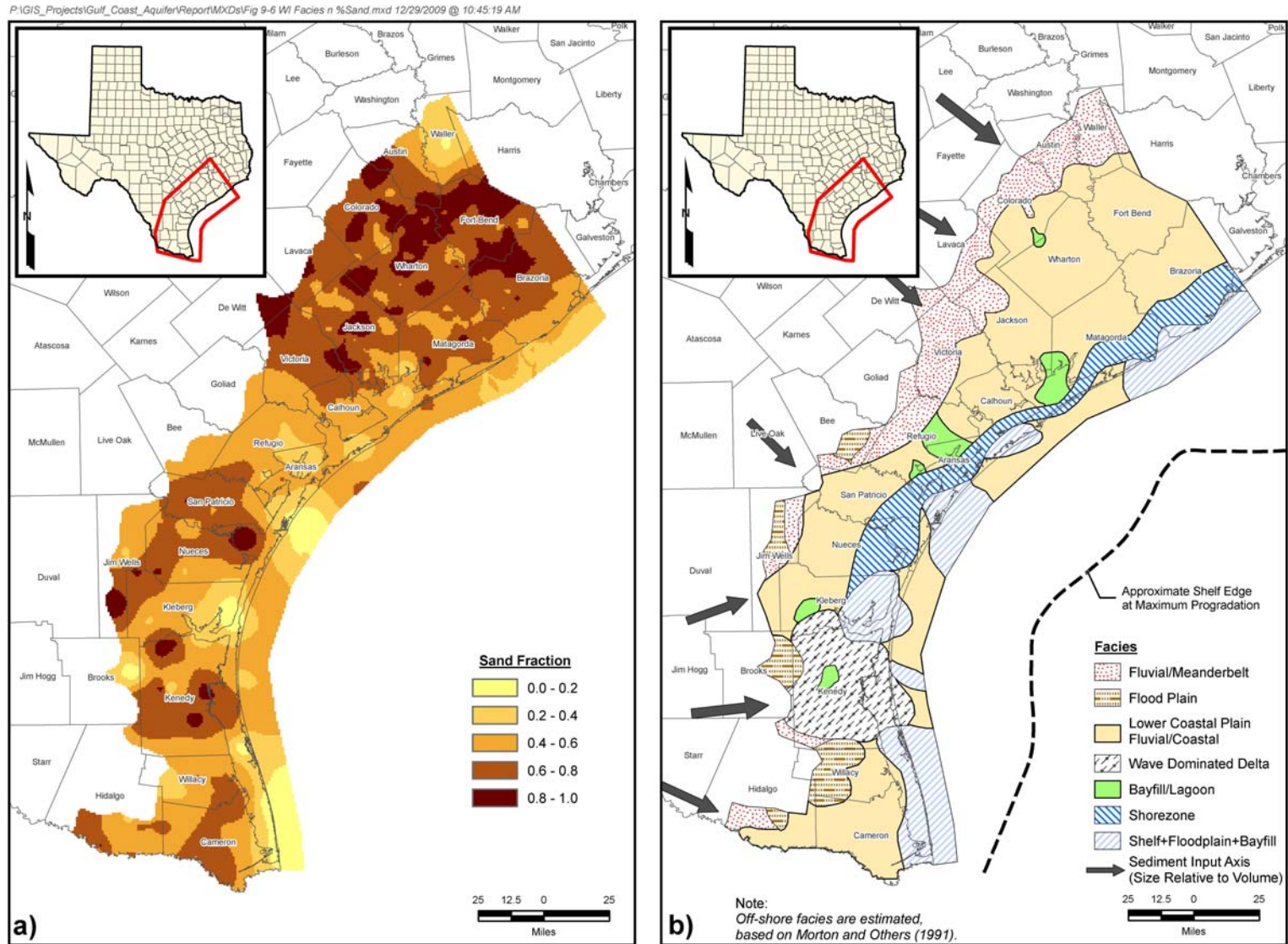


Figure 9-6. Map of the Willis geologic unit showing: (a) percentage sand coverage and (b) depositional facies.

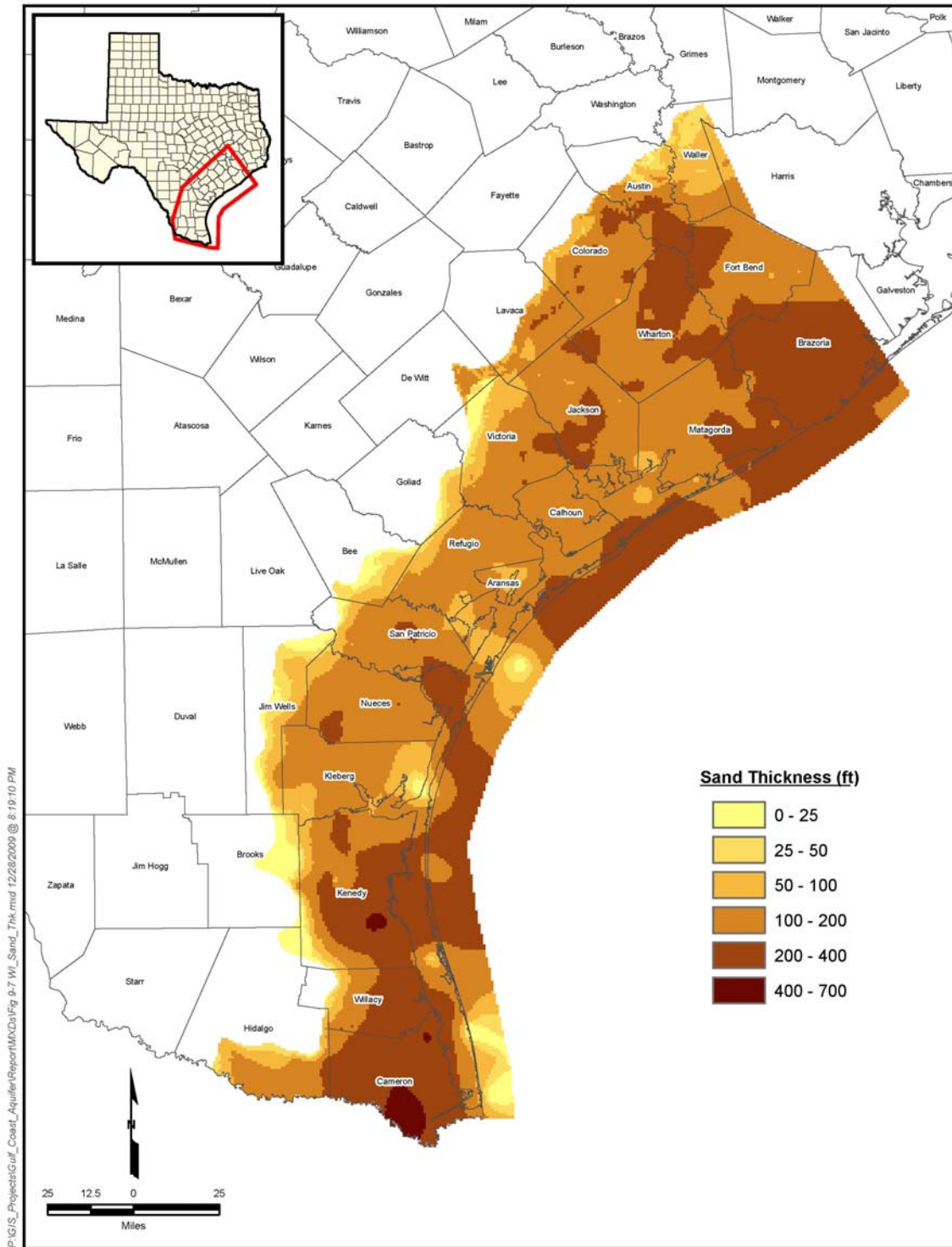


Figure 9-7. Map of the Willis geologic unit showing total sand thickness.

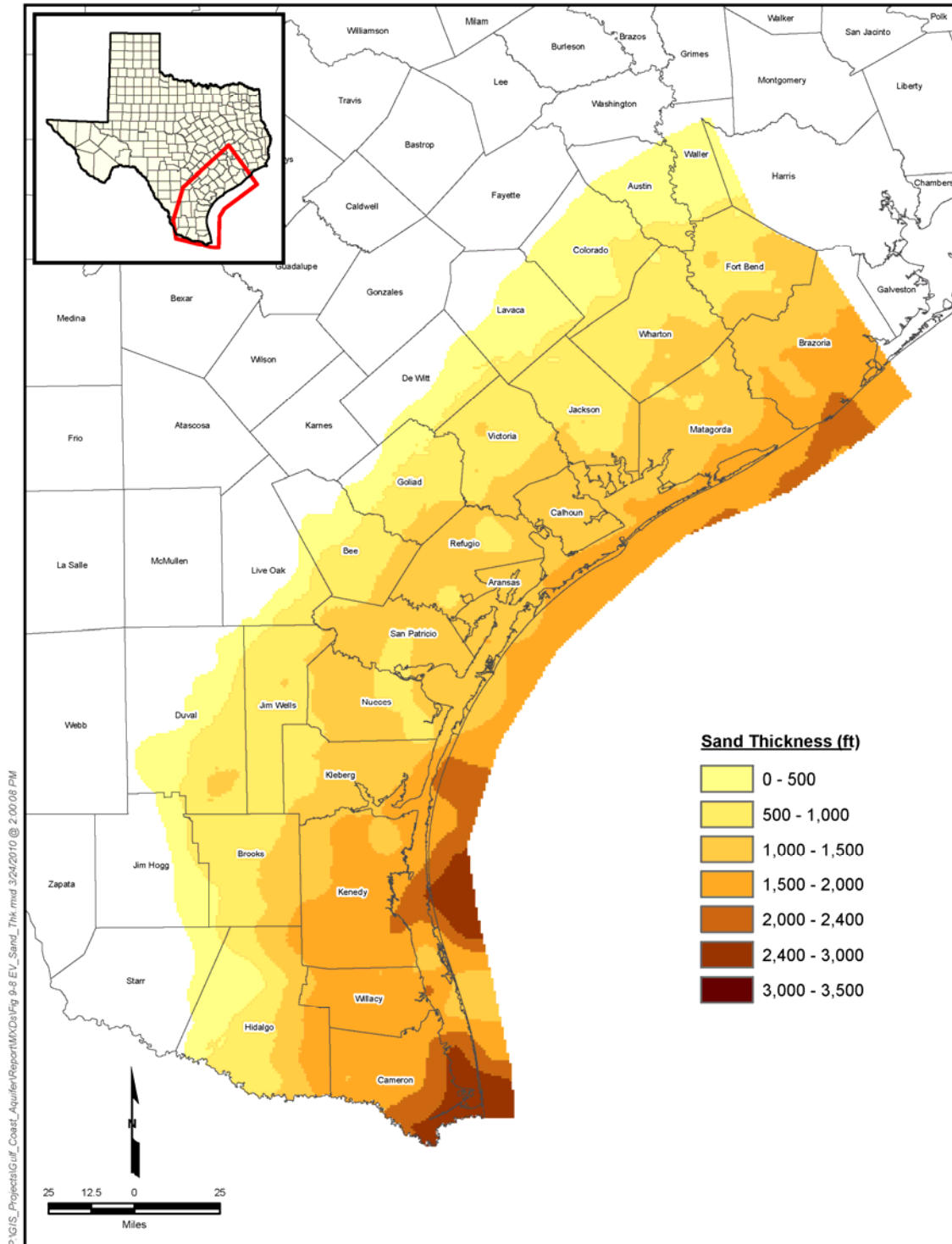


Figure 9-8. Map of the Evangeline Aquifer showing total sand thickness

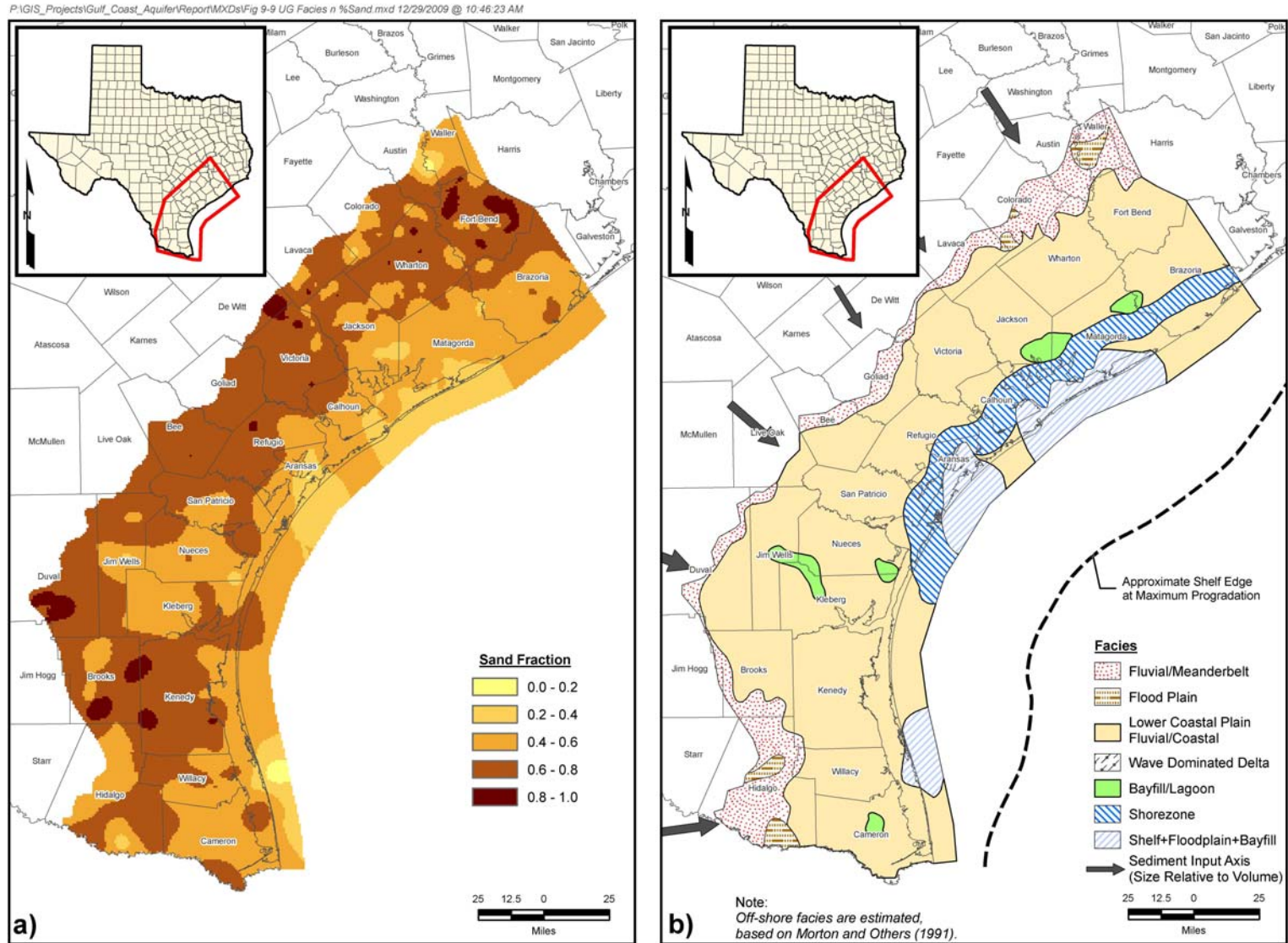


Figure 9-9. Map of the upper Goliad geologic unit showing: (a) percentage sand coverage and (b) depositional facies.

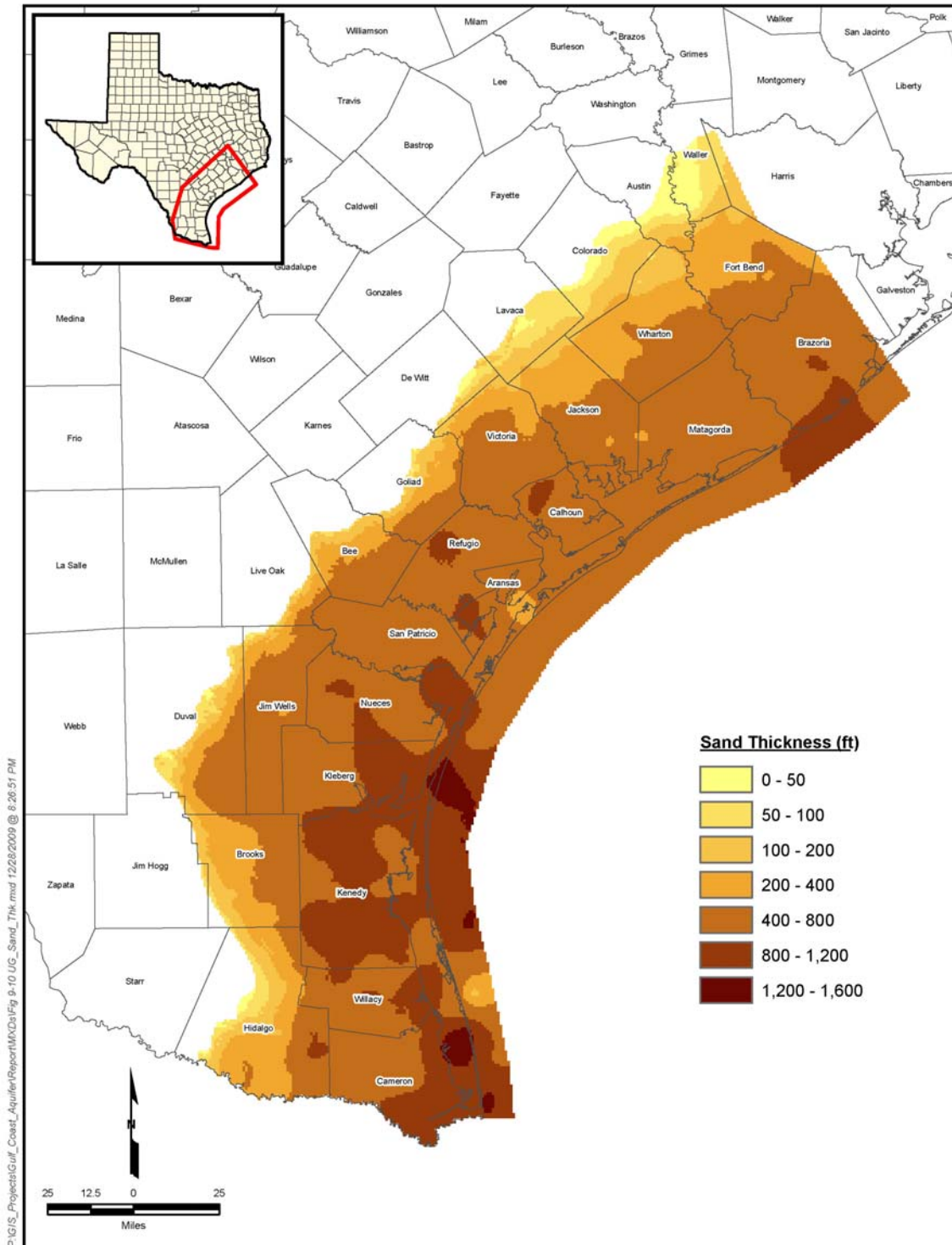


Figure 9-10. Map of the upper Goliad geologic unit showing total sand thickness.

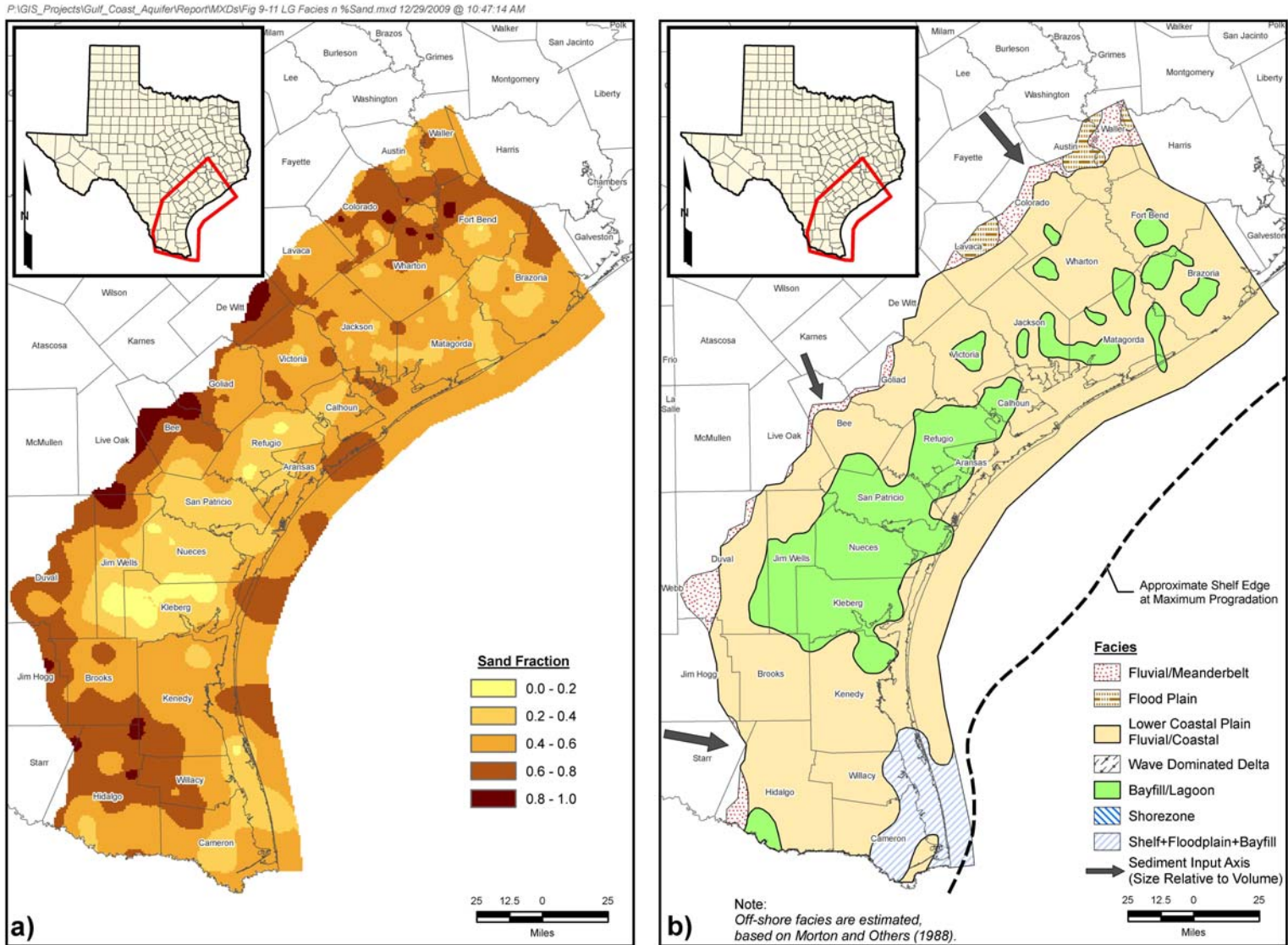


Figure 9-11. Map of the lower Goliad geologic unit showing: (a) percentage sand coverage and (b) depositional facies.

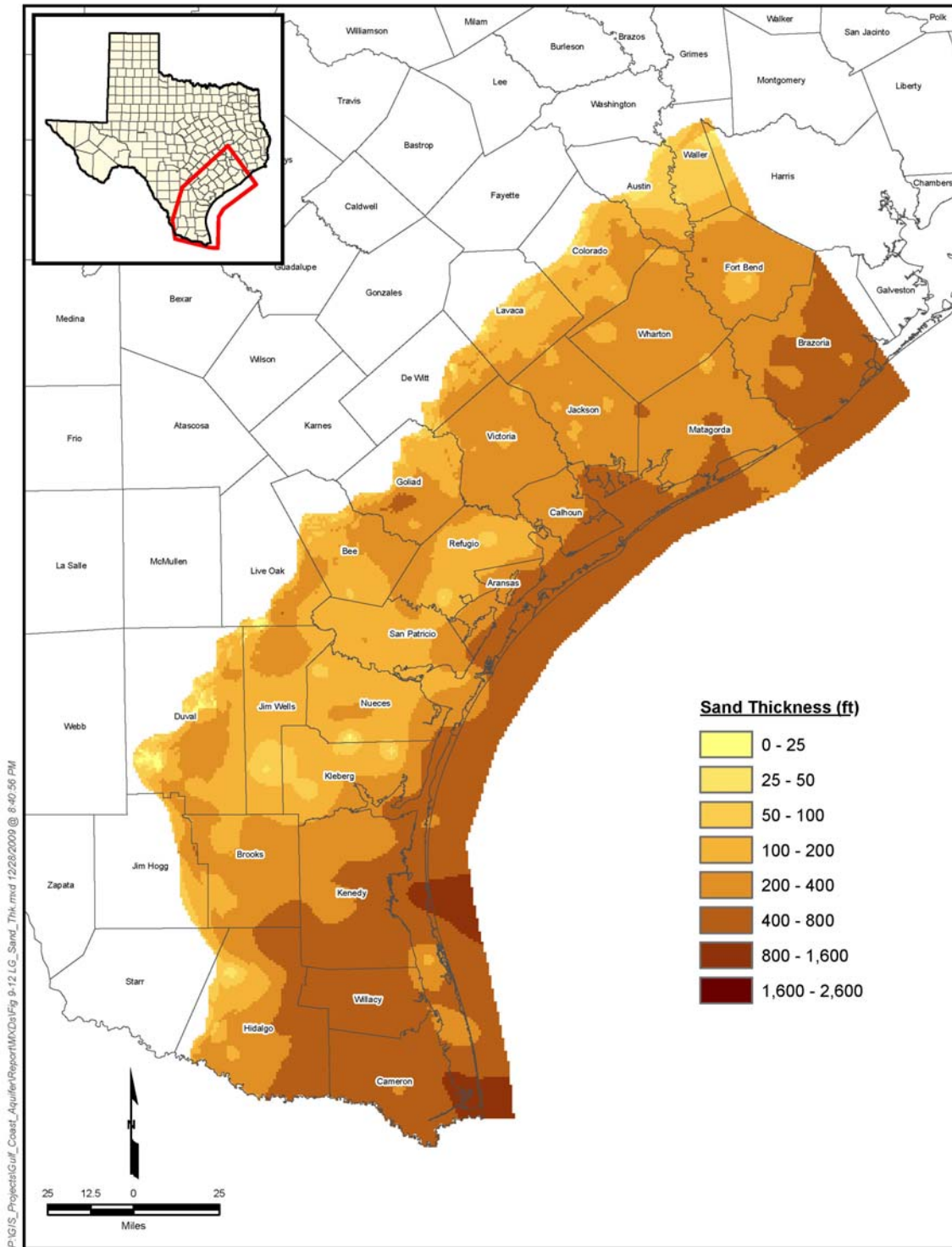


Figure 9-12. Map of the lower Goliad geologic unit showing total sand thickness.

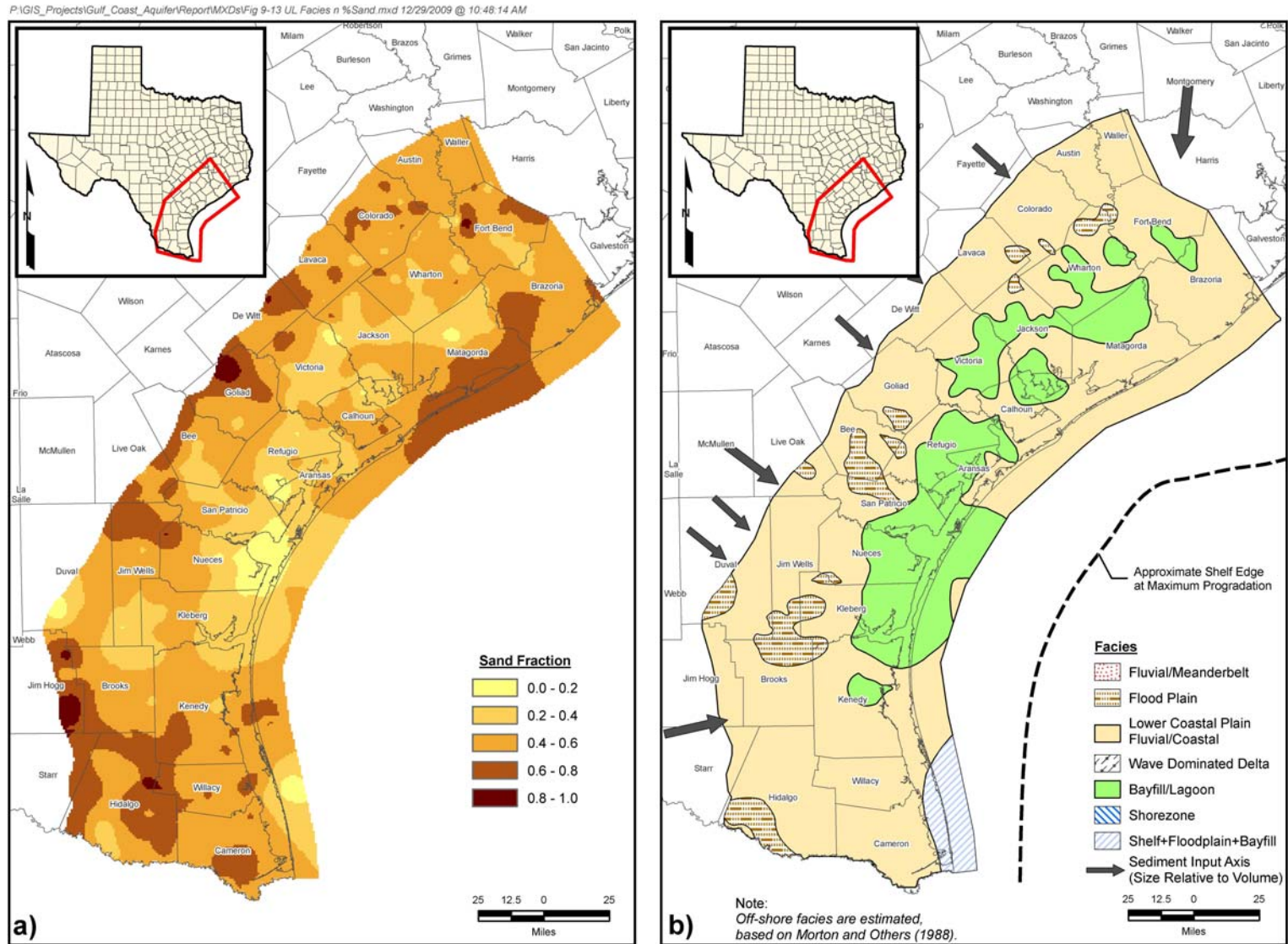


Figure 9-13. Map of the upper Lagarto geologic unit showing: (a) percentage sand coverage and (b) depositional facies.

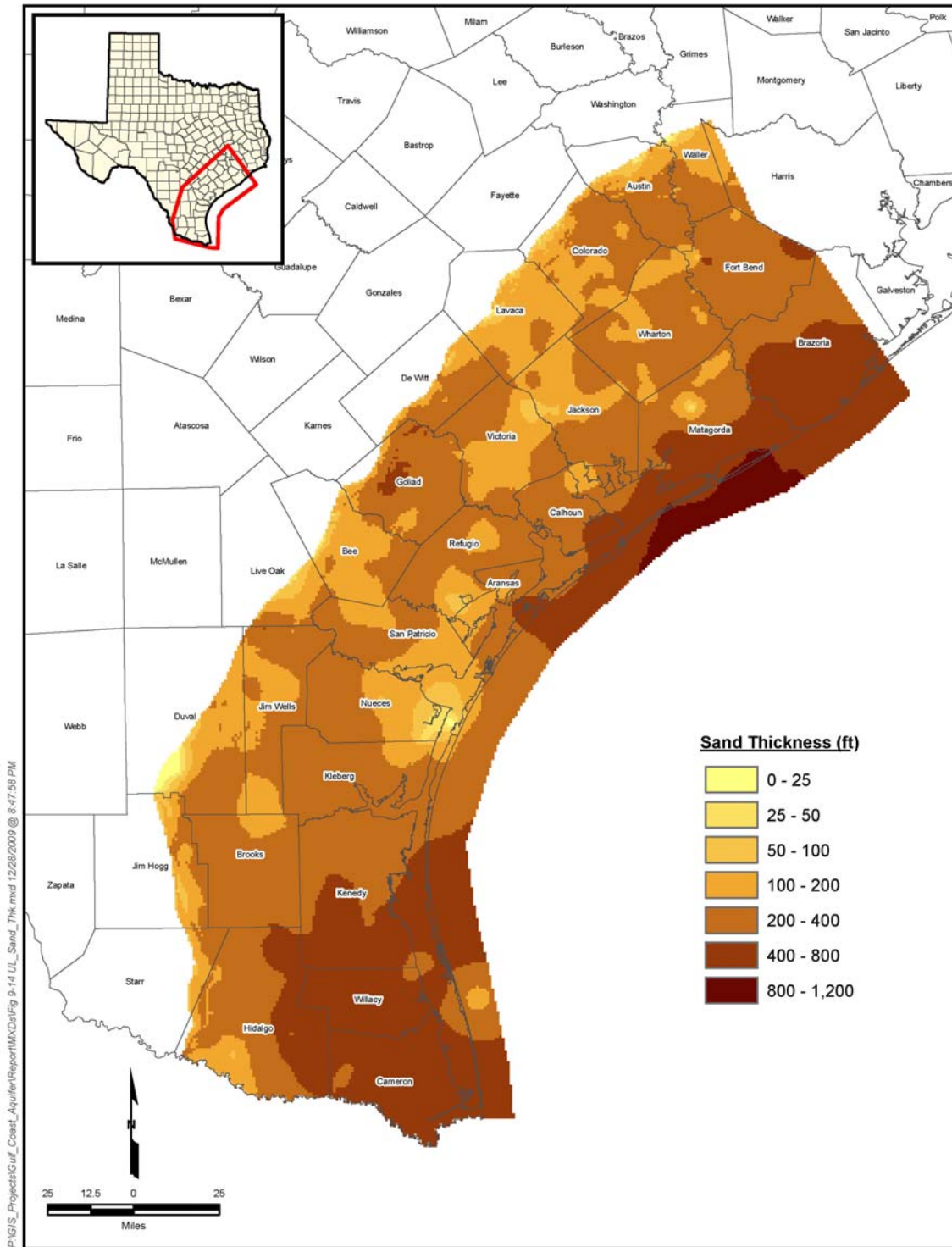


Figure 9-14. Map of the upper Lagarto geologic unit showing total sand thickness.

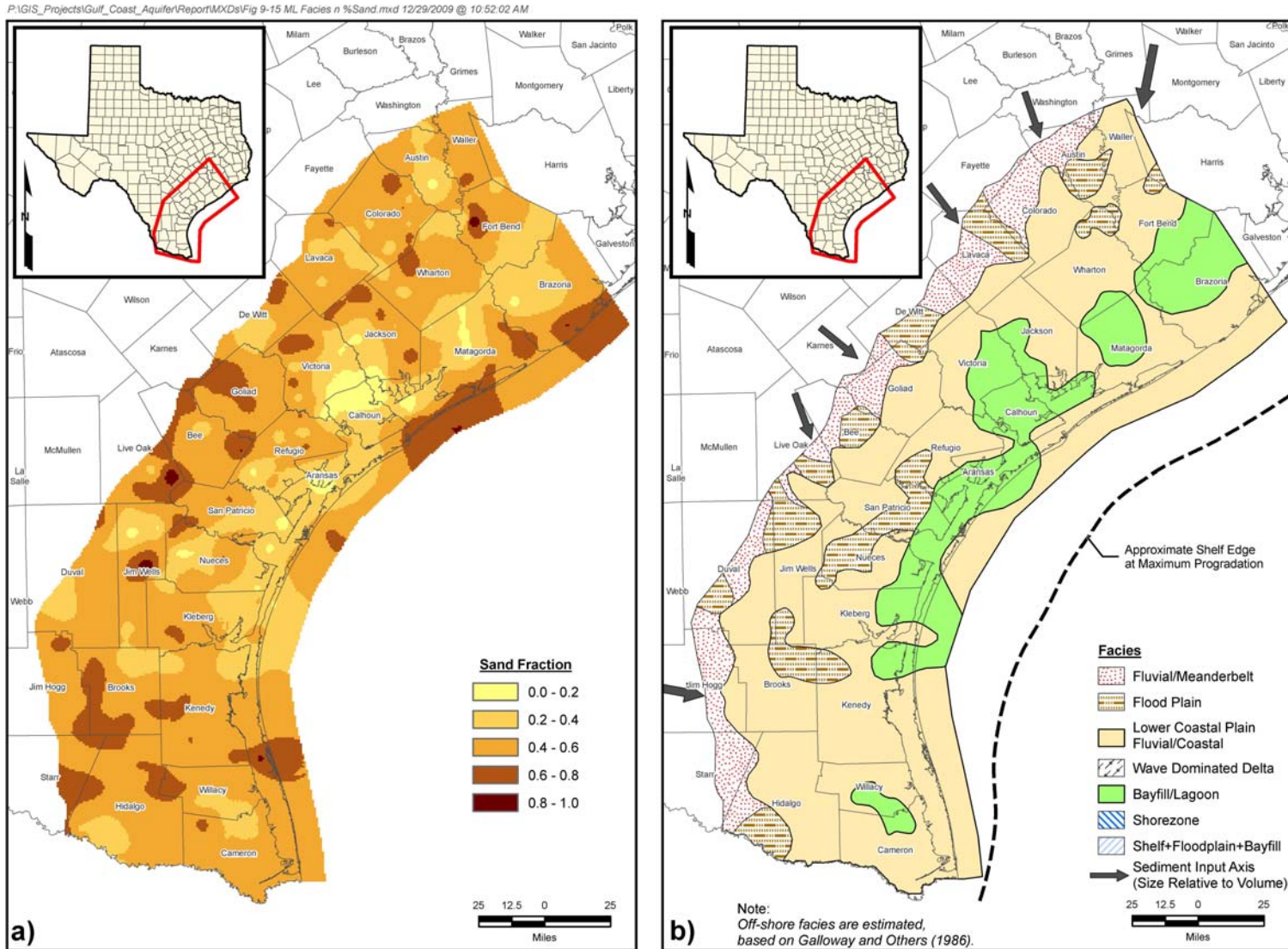


Figure 9-15. Map of the Burkeville Confining Unit (middle Lagarto geologic unit) showing: (a) percentage sand coverage and (b) depositional facies.

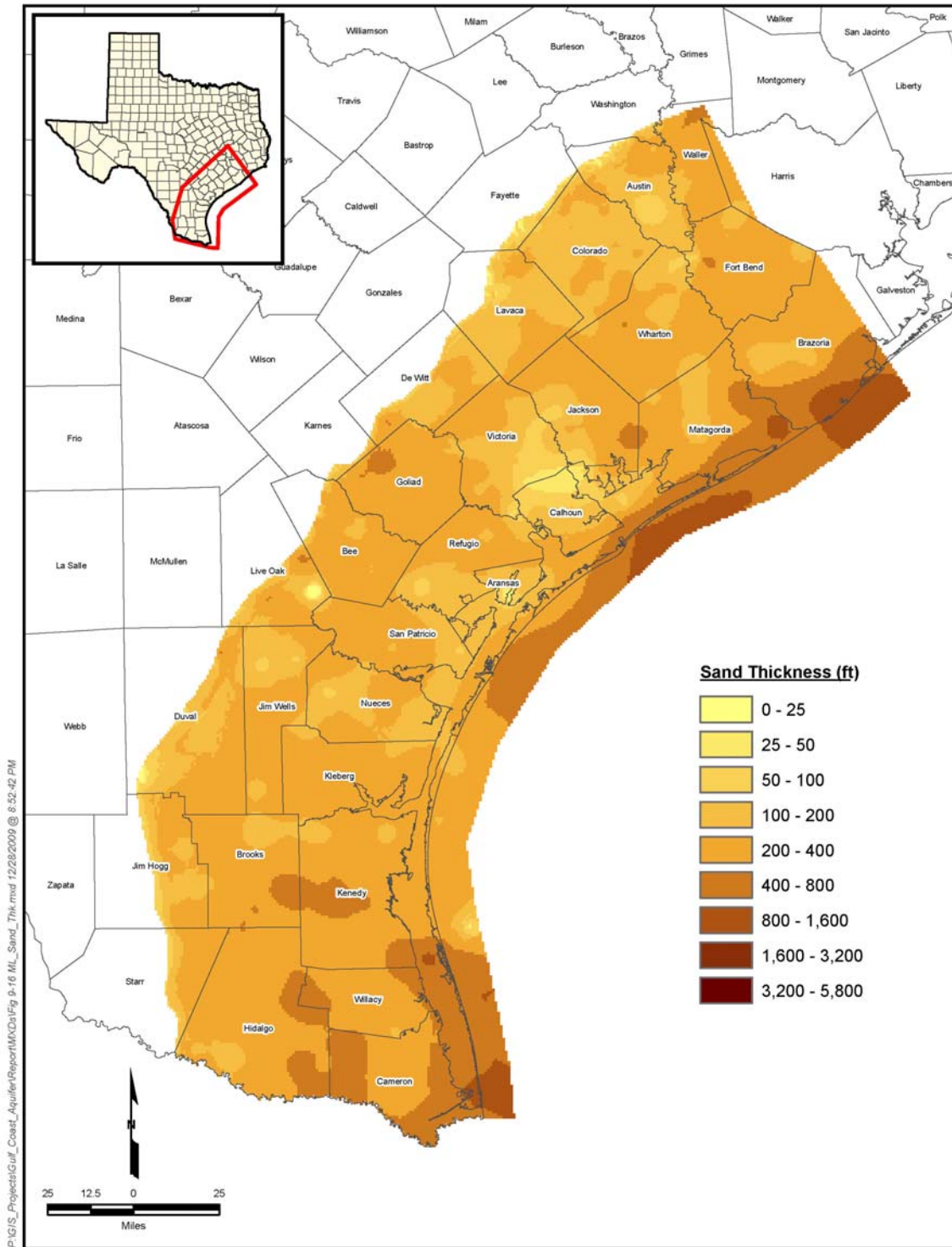


Figure 9-16. Map of the Burkeville Confining Unit (middle Lagarto geologic unit) showing total sand thickness.

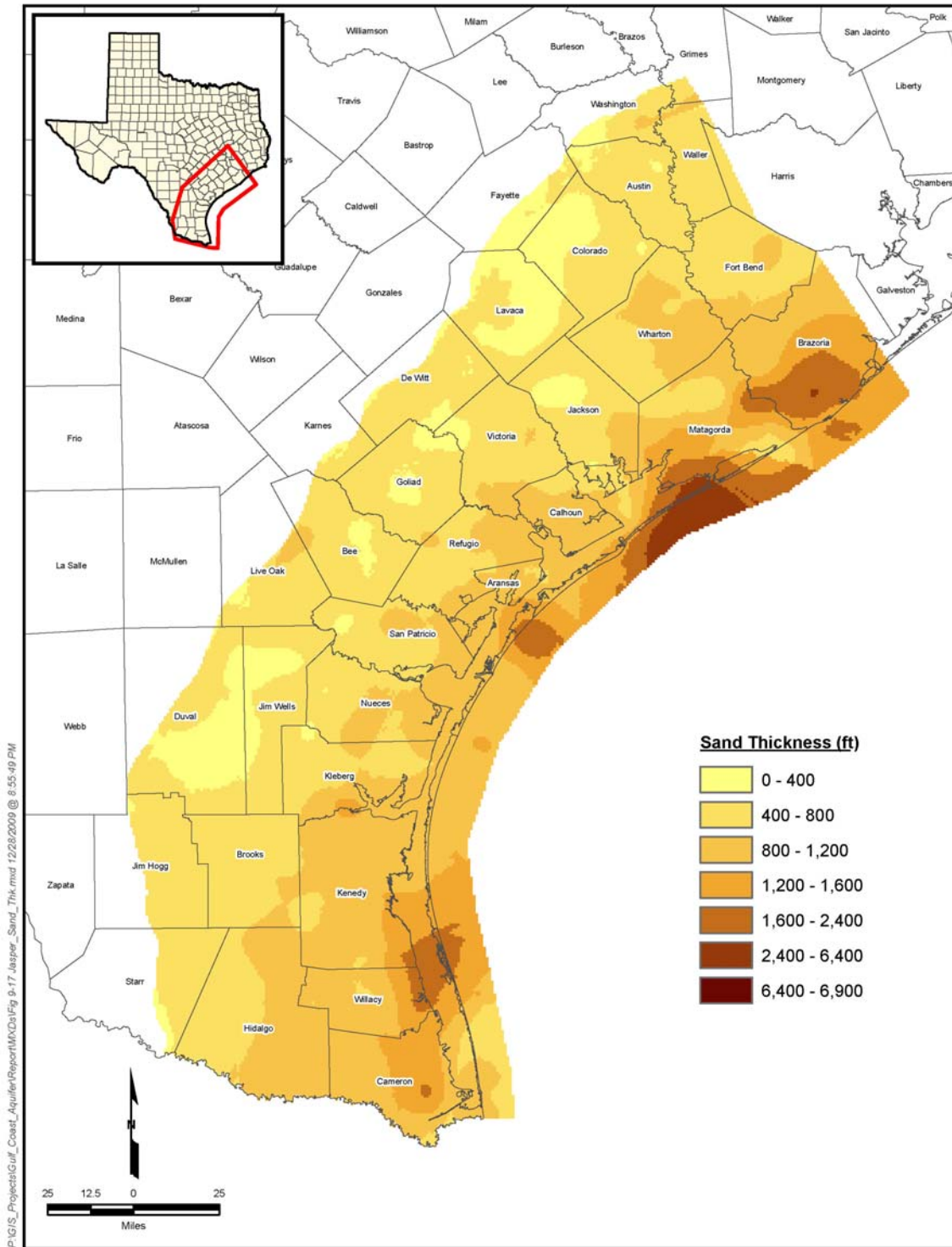


Figure 9-17. Map of the Jasper Aquifer showing total sand thickness.

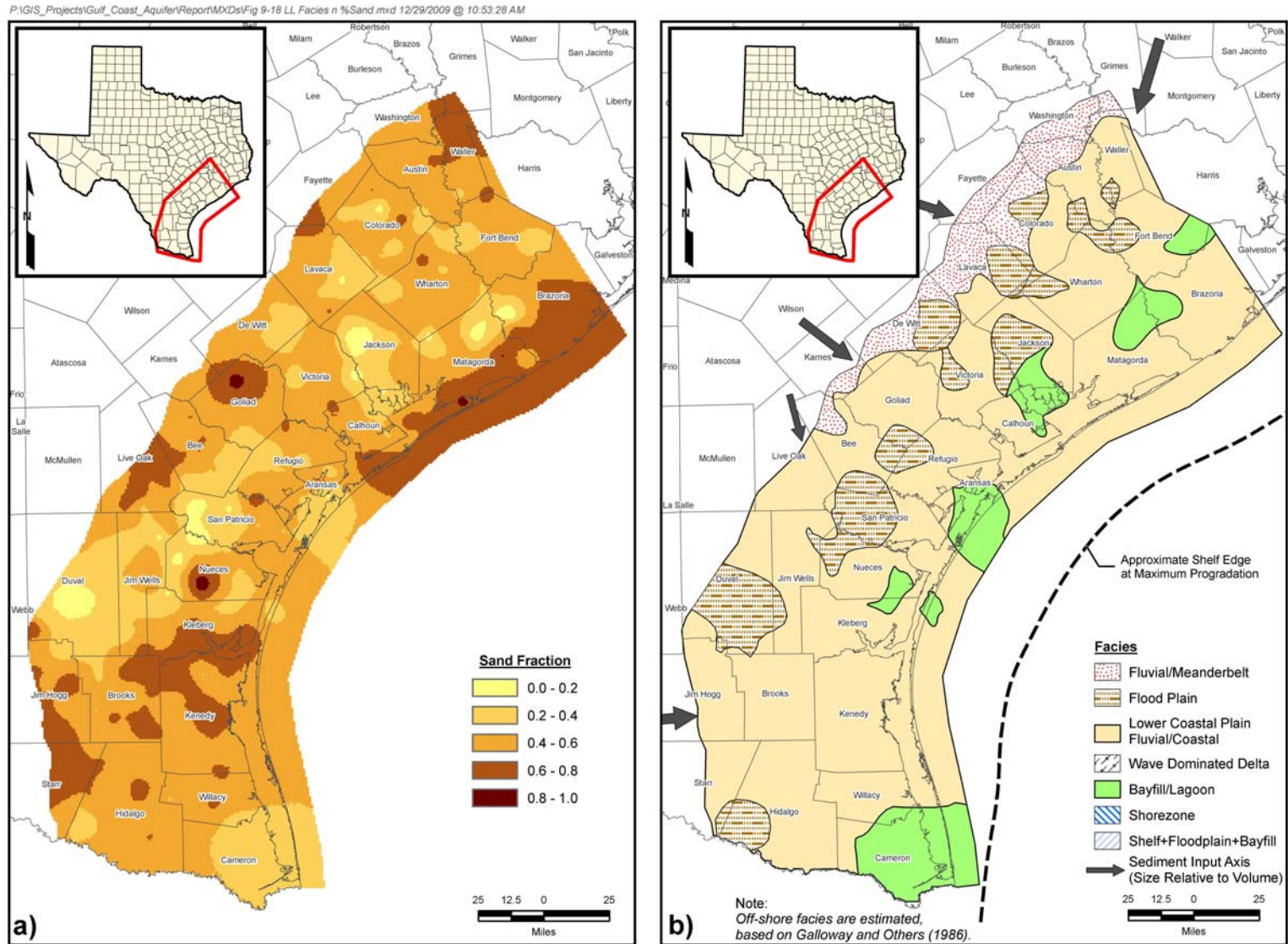


Figure 9-18. Map of the lower Lagarto geologic unit showing: (a) percentage sand coverage and (b) depositional facies.

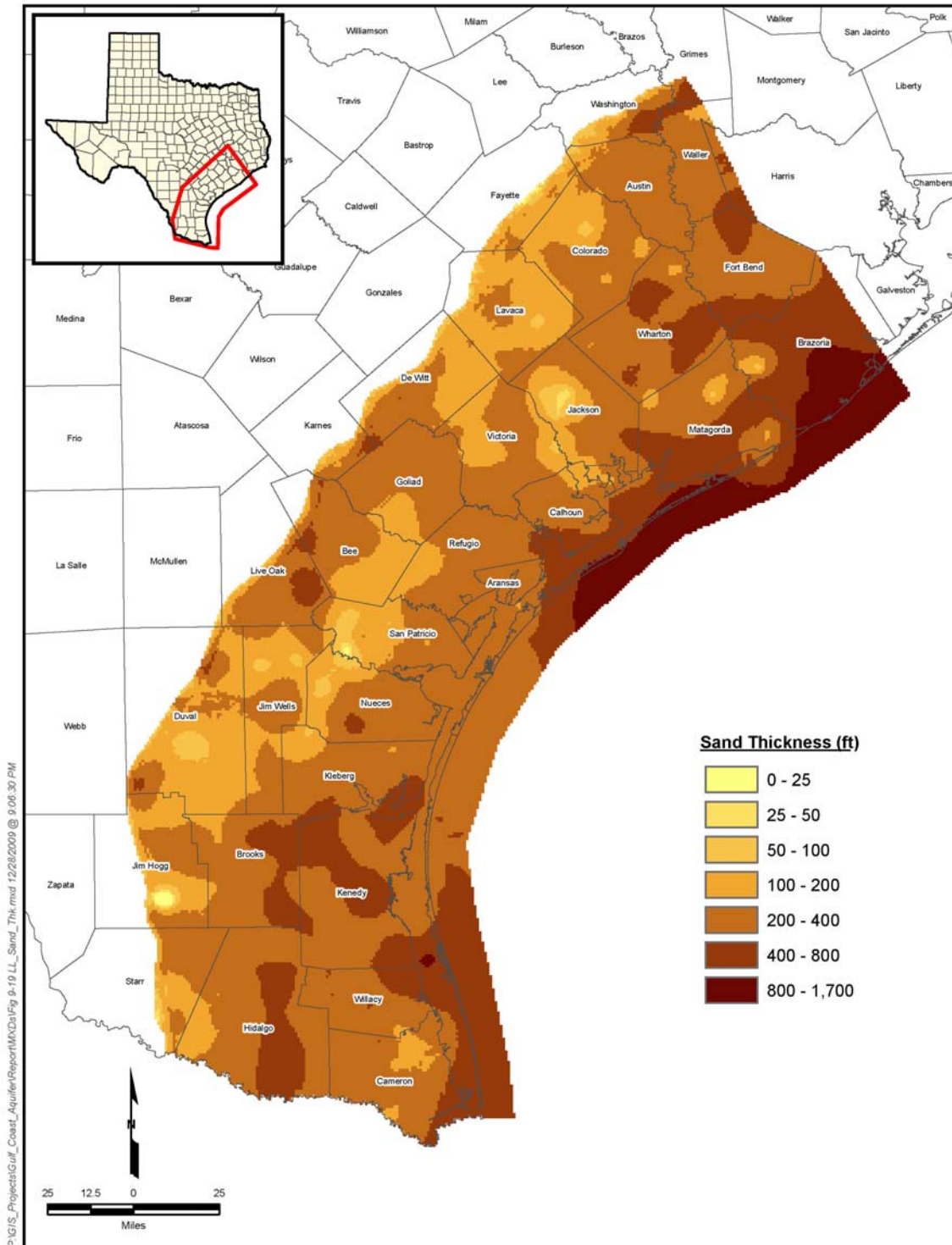


Figure 9-19. Map of the lower Lagarto showing total sand thickness.

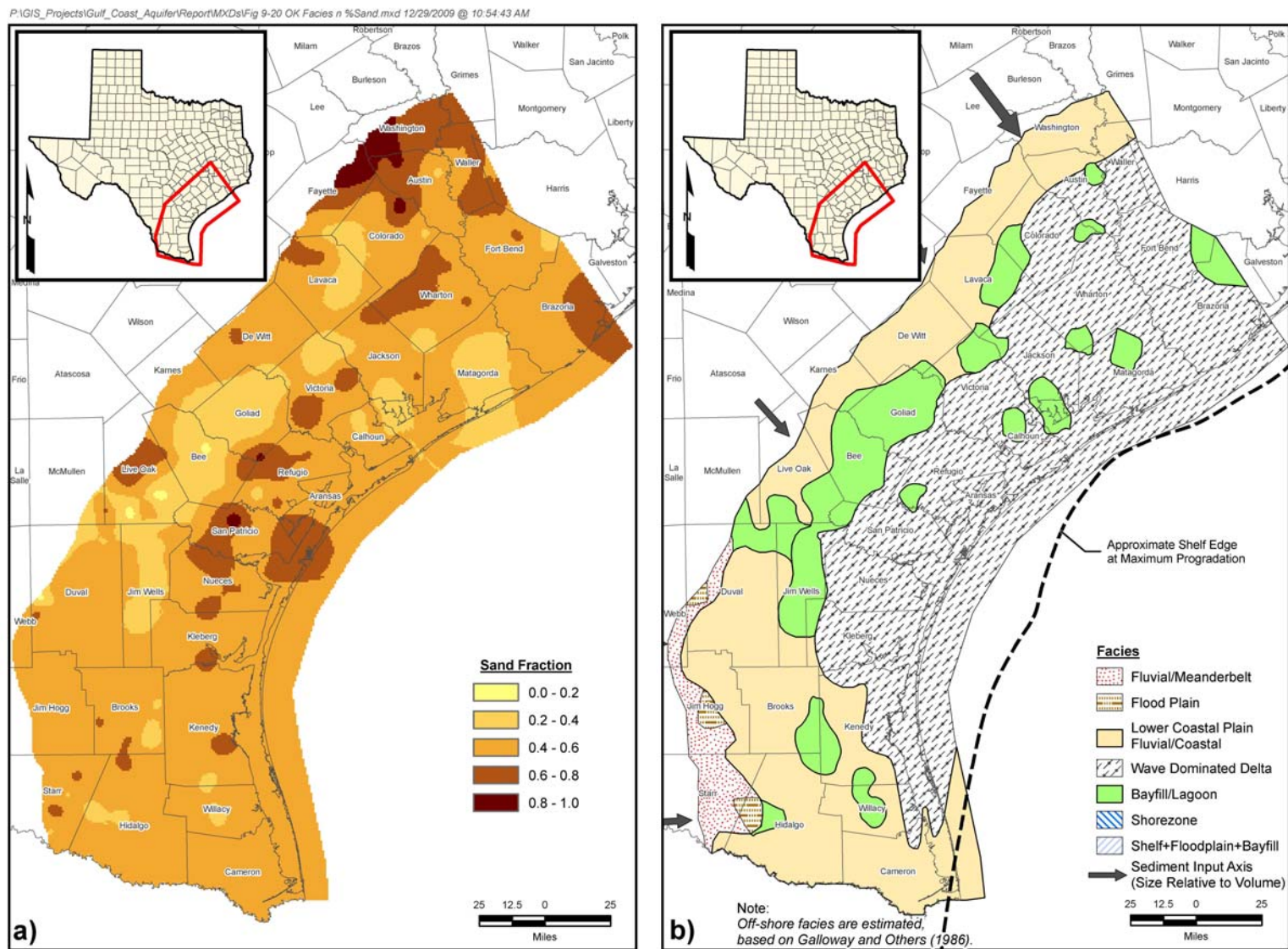


Figure 9-20. Map of the Oakville geologic unit showing: (a) percentage sand coverage and (b) depositional facies.

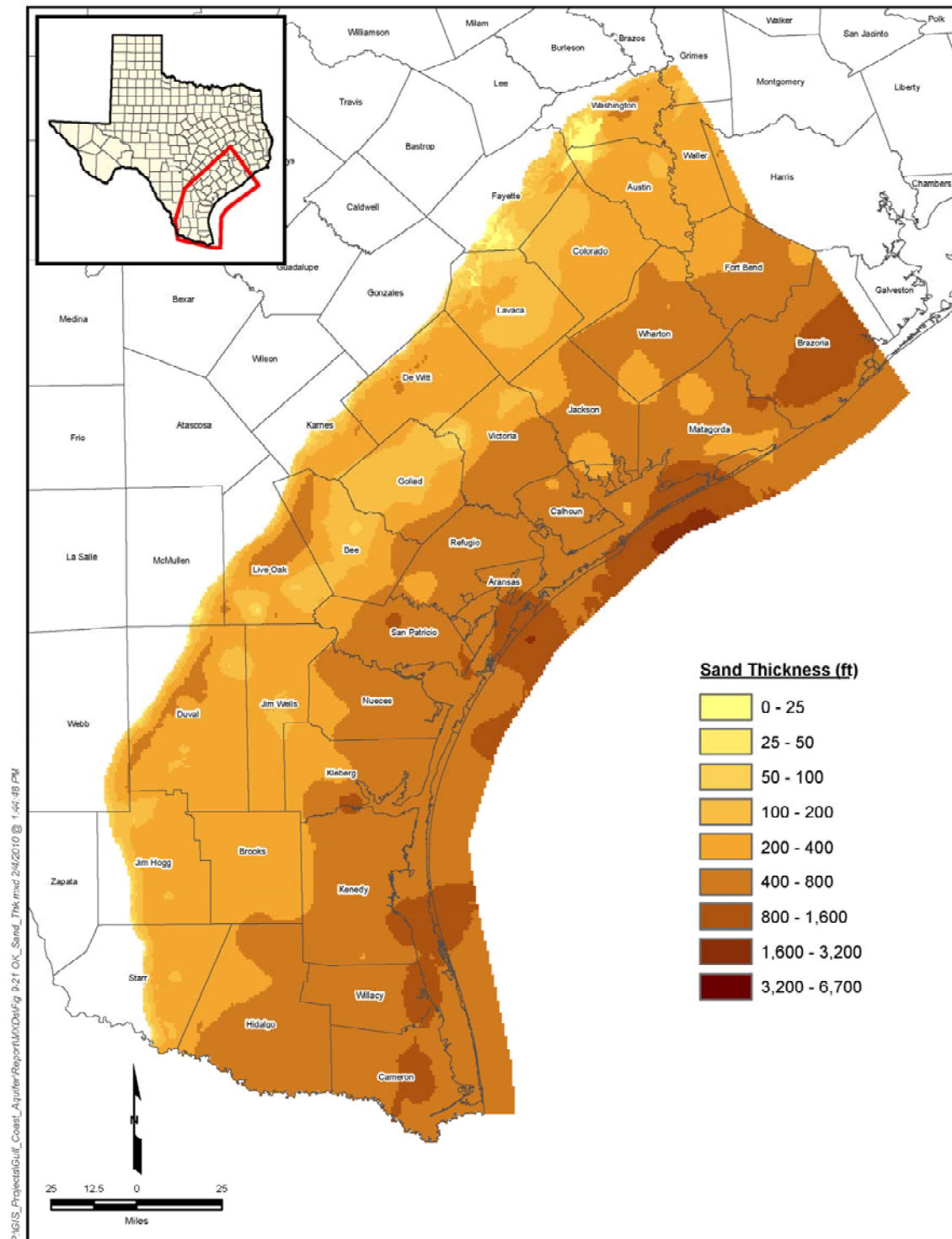


Figure 9-21. Map of the Oakville geologic unit showing total sand thickness.

10 Gulf Coast water quality

The quality of the groundwater in the Gulf Coast Aquifer System varies significantly. From the water supply perspective, a useful metric for measuring water quality is concentration of total dissolved solids (TDS). Groundwater is categorized as fresh water and as brackish water based on its measured TDS. In this section, estimates of fresh water are provided based on analysis of geophysical logs and water well data.

10.1 Terminology

10.1.1 Fresh and brackish groundwater

Total dissolved solids (TDS) is a measurement of all the dissolved solids in a specific water sample and is often used to classify groundwater based on water quality. Table 10-1 divides groundwater into five classes based on TDS. This project uses these five classes to characterize the groundwater of the Gulf Coast. LGB-Guyton and NRS Consulting (2003) have grouped the classes of slightly saline and moderately saline water under the general category of brackish groundwater. Thus, brackish groundwater by definition has a TDS between 1,000 ppm and 10,000 ppm, and fresh water has a TDS less than 1,000 ppm. Water with a TDS greater than 10,000 ppm is classified as being saline water (LGB-Guyton and NRS Consulting, 2003).

Table 10-1. Groundwater classifications based on TDS (from Collier, 1993).

Class	Total Dissolved Solids (mg/L)	Example of Use
Fresh water	0 to 1,000	Drinking and all other uses
Slightly saline water	More than 1,000 to 3,000	Drinking if fresh water is unavailable, irrigation, industrial, mineral extraction, oil and gas production
Moderately saline water	More than 3,000 to 10,000	Potential future drinking and limited livestock watering and irrigation if fresh or slightly saline water is unavailable; mineral extraction, oil and gas production
Very saline water	More than 10,000 to 100,000	Mineral extraction, oil and gas production
Brine water	More than 100,000	Mineral extraction, oil and gas production

10.1.2 Total dissolved solids and specific conductivity

In the groundwater industry and for this report, TDS is used interchangeably with dissolved solids even though there is a real difference between the two measurements. Dissolved solids refers to the sum of all the chemical constituents that were analyzed in a specific water sample. The practice of using TDS and dissolved solids interchangeably is generally acceptable as long as the water analysis has been designed and executed to account for 90% or more of the dissolved ions in solution. The major ions that comprise TDS for most groundwaters include silica, calcium, magnesium, sodium, chloride, bicarbonate, sulfate, and carbonate. Secondary

ions that should be considered as part of the TDS measurement include fluoride, nitrate, potassium, manganese, iron, and aluminum.

Measurements of TDS usually are reported as parts per million by weight (ppm) or milligrams per liter (mg/L). For fresh and brackish water, the terms can be used interchangeably even though the two terms can differ because the weight of 1 liter of water depends on the solute concentrations. Hem (1985) estimates that for a typical groundwater sample, the analytical method is within $\pm 5\%$ of the actual TDS value.

Specific conductivity is a measure of a water's ability to conduct electricity and therefore is a measure of a water's ionic activity. The standard unit of measure for specific conductance is microhms per centimeter ($\mu\text{mhos/cm}$) at 25°Celsius (77°Fahrenheit). The specific conductivity is affected by the nature and movement of the ions in solution. Thus, the specific conductivity is affected by the concentration of the ions, the activity of the ions, the electric charge on ions, and water temperature. When adjusting for temperature, a general rule of thumb stated in the literature is that specific conductivity increases about 2% per degree Celsius increase in temperature (Hem, 1982). Figure 10-1 illustrates how the relationships between concentration and specific conductivity can vary among different salts and is concentration dependent.

The reciprocal of electrical conductivity is electrical resistivity. The unit of measure for resistivity is the mirror inverse of the conductivity unit of mho, or ohm. The relationship between conductivity and resistivity is important to a log analyst because resistivity is one of the measurements that comprise most geophysical logs. The relationship between resistivity and conductivity is as follows:

$$\text{Resistivity (ohm-m)} = 10,000 / \text{Specific Conductivity}(\mu\text{mhos/cm})$$

10.2 Analysis of geophysical logs

10.2.1 Approach

Any approach for estimating TDS from the geophysical logs involves three general steps. The first step is to estimate the resistivity of the formation water from a geophysical log. The second step is to convert the resistivity value into a specific conductivity value. The third step is to convert the specific conductivity into a TDS value. Thus, a TDS concentration estimated from the analysis of a geophysical log is dependent on the accuracy of the log analyst's ability to estimate the resistivity of the formation water and the relationship between the specific conductivity and TDS for the specific conditions at the borelog.

To illustrate the relationship among TDS, specific conductivity, and resistivity, we have created Table 10-2. In developing Table 10-2, we skipped the key step of interpreting the geophysical log to estimate the resistivity of the formation water. The conversion from resistivity to specific conductivity is performed by applying the equation discussed above. To calculate the TDS from specific conductivity, we used general relationships developed and reported by Collier (1993) in Table 4-1 for groundwater measurements taken in the Chicot, Evangeline, and Jasper Aquifers. For this example, we have selected resistivity values of 0.7, 2.5, 7.1, 15.4, and 30.8 and have

calculated specific conductivities of 14000, 4000, 1400, 650, and 325 $\mu\text{mhos/cm}$., respectively, based on the above equation. For each of the five specific conductivities, Table 10-2 shows the TDS value calculated for the three aquifers using the relationships provided by Collier (1993) and shown in Table 10-2. The results in Table 10-2 show that the range in the calculated TDS values for the different aquifers increases with higher resistivity values because of the non-linearities in the TDS-specific conductivity relationships.

Table 10-2. Relationship among TDS, specific conductivity, and resistivity (from Collier, 1993).

Aquifer	Relationship between TDS (mg/L) and specific conductivity ($\mu\text{mhos/cm}$)	Specific conductivity of formation water ($\mu\text{mhos/cm}$)				
		14,000	4,000	1400	650	325
Chicot	TDS = 1.283*SC 0.922	8,530	2,687	1,021	503	266
Evangeline	TDS = 1.780*SC 0.994	10,312	2,969	1,046	488	245
Jasper	TDS = 0.751*SC 1.010	11,567	3,264	1,130	521	259
Average TDS (mg/L) for three aquifers		10,136	2,973	1,066	504	256
Percent variation in predicted TDS among aquifers		30%	19%	8%	7%	5%

The specific approach we used to estimate TDS from geophysical logs is similar to the general approach discussed above with the additional step of estimating the resistivity of the aquifer formation water from the geophysical log signatures. Mr. Baker performed all of the TDS interpretations for this project at the same time that he performed the lithologic interpretations. For every lithologic interval identified, Mr. Baker assigned a classification of fresh, slightly saline, or moderately saline water. Table 10-3 provides a description of the general criteria and assumptions used by Mr. Baker. Where appropriate, Mr. Baker deviated from the general criteria to accommodate site-specific conditions and adjusted his criteria as needed based on his 40 years of log analyst experience. Mr. Baker's approach is based on numerous references that include Schlumberger (1972), Keys and McCary (1971), Whitman (1965), and Alger (1966).

Table 10-3. General criteria used by Mr. Baker to estimate the TDS from the geophysical logs.

Classification	Resistivity (ohms-m) of aquifer formation	Assumptions
Freshwater (<1,000 ppm TDS)	> 18-20 ohms	Assume water has major calcium ions
Slightly saline (1,000-3,000 ppm TDS)	8-18 ohms	Calcium ions decreasing, sodium ions gaining
Moderately saline (3,000 -10,000 ppm TDS)	< 8 ohms	Sodium and chloride ions predominate

10.2.2 Results

For each of the major aquifers and the Burkeville Confining Unit, maps of the fraction of fresh water were calculated using a two-step process. The first step was to determine the fraction of fresh water at each of the geophysical log locations with the water quality information shown in

Figure 5-4. This was accomplished by summing the lithologic intervals associated with fresh water and dividing by the total thickness the geologic unit. The second step was to generate a continuous distribution of percent fraction of fresh water by interpolating between the point values of fraction of fresh values. The interpolation was performed using a kriging algorithm in ARCMAP 9.3 with a rectangular grid consisting of nodes spaced 4,000 feet apart.

Figures 10-2 through 10-5 show the fraction of fresh water for the Chicot Aquifer, the Evangeline Aquifer, the Burkeville Confining Unit, and the Jasper Aquifer, respectively. The maps represent results from a series of first-cut analyses performed at approximately 700 log locations. The maps primarily provide the overall picture regarding the relative differences in the water quality across each of the geologic units. Because of the numerous assumptions that were made in each analysis, the results should not be used without complementary information to determine the absolute water quality at a specific location. Using the data associated with each of these figures, maps of total thickness of fresh water were generated by multiplying the fresh-water fractions by the average porosity and by the corresponding values for the thickness of each of the respective units, which are shown in Section 7.

As shown in Figure 10-2, the majority of the fresh water in the Chicot Aquifer lies in the northern region east of Victoria County and is concentrated more in the fluvial than the coastal facies. In Matagorda, Fort Bend, and Brazoria Counties, several areas have a fresh water fraction below 0.2, which is attributed to the salt domes shown in Figure 3-3. In the central and southern part of the Chicot Aquifer, relatively little fresh water exists in the coastal facies but a fresh water percentage greater than 40% can be found in a few counties, including Brooks, Kenedy, Refugio, Bee, and Goliad.

As shown in Figure 10-3, the highest fractional values for fresh water in the Evangeline Aquifer lie in the northern region within about a 25-mile strip along the updip extent of the aquifer from Goliad to Waller. Within 25 miles of the Gulf of Mexico and south of Nueces County, there are no fresh water fractions that exceed 0.2, except in a small area covering Jim Hogg, Brooks, and Hidalgo Counties.

As shown in Figure 10-4, the Burkeville Confining Unit includes relatively little fresh water, except for a few areas in counties located near where the Burkeville Confining Unit outcrops. Where the fresh water fraction exceeds 0.8 in these few areas, a likely cause for the fresh water is recharge through a sandy portion of the outcrop of the Burkeville Confining Unit. As shown in Figure 10-5, the Jasper Aquifer only has fresh water fractions above 0.4 near the updip regions of the aquifers in counties within about 25 miles of the aquifer's updip boundary.

10.3 Analysis of water well measurements

10.3.1 Approach

In July 2009, the TWDB database for water quality (GWDB.mdb) was queried for at least one TDS measurement in wells with the aquifer codes in Table 10-3. The query produced 6,270 wells. For wells that had multiple TDS measurements, the measurements were averaged to produce a single measurement. For wells without screen information, we performed a regression

of screen midpoint versus total well depth to fill in the missing screen midpoints. This allowed each TDS measurement to be assigned a depth that corresponded to each well measurement.

Table 10-4. Aquifer codes used in Gulf Coast query

Aquifer Name
Alluvium and Evangeline Aquifer
Burkeville Aquiclude
Chicot and Evangeline Aquifers
Chicot Aquifer
Chicot Aquifer, Lower
Chicot Aquifer, Middle
Chicot Aquifer, Upper
Evangeline and Jasper Aquifers
Evangeline Aquifer
Evangeline Aquifer and Burkeville Aquiclude
Evangeline Aquifer and Upper Unit of Jasper Aquifer
Fleming Formation and Burkeville Aquiclude
Gulf Coast Aquifer
Jasper Aquifer
Jasper Aquifer and Burkeville Aquiclude
Jasper Aquifer and Catahoula Sandstone
Jasper Aquifer, Upper Unit

10.3.2 Results

Figure 10-6 shows which wells in the study area have TDS concentrations greater than and less than 1,000 ppm. From an overall perspective, the results in Figure 10-6 are very consistent and supportive of the results in Figure 10-5. This comparison indicates that the water quality picks by Mr. Baker are reasonable and confirm the general appropriateness of his approach.

In Figure 10-6, there are several areas where there is an intermixing of points showing TDS concentrations less than and greater than 1,000 ppm. This intermixing is attributed to nearby wells having different depths and well screen lengths, different sampling dates, concentration measurements only slightly above or below 1,000 ppm, and influences from surface contamination. Surface contamination includes oil and gas operations that used brined disposal into surface pits and wind-blown salts from the Gulf Coast.

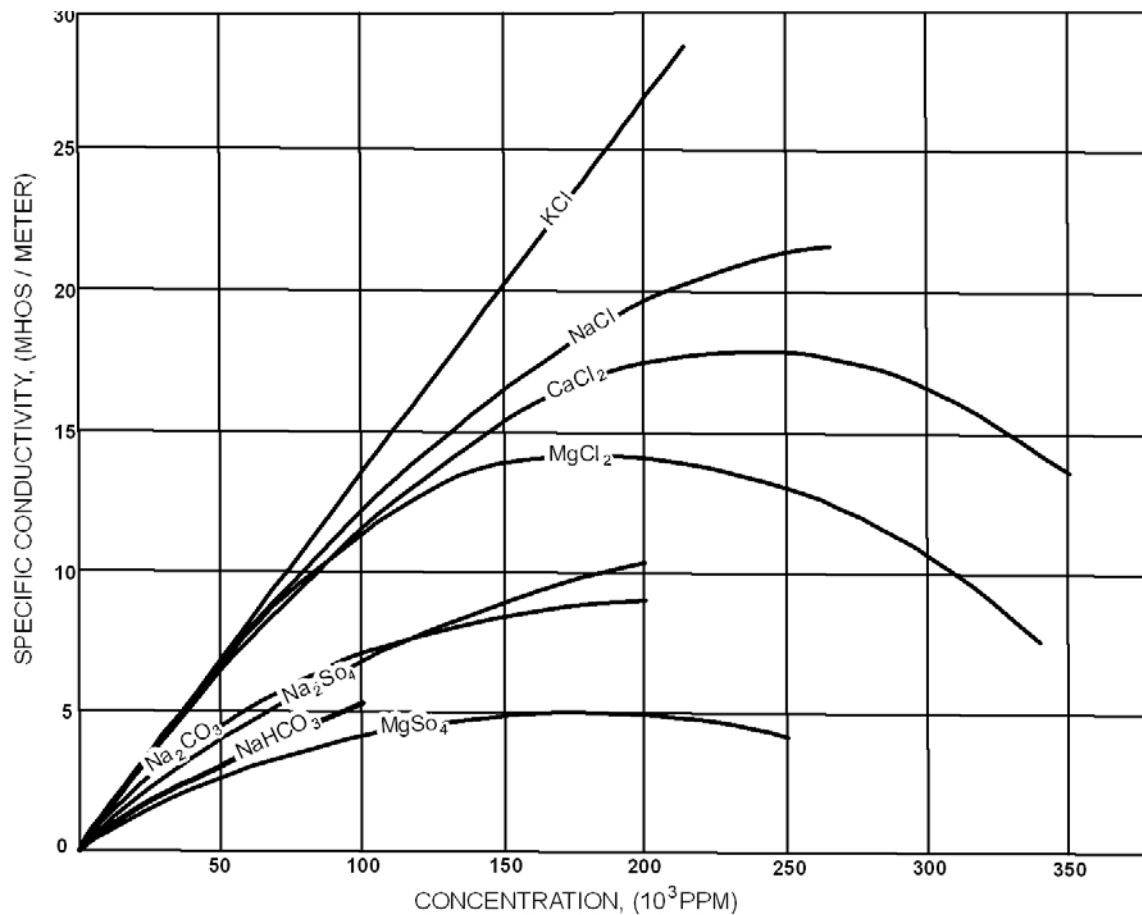


Figure 10-1. Specific conductivity of salt solutions (modified from Moore, 1966).

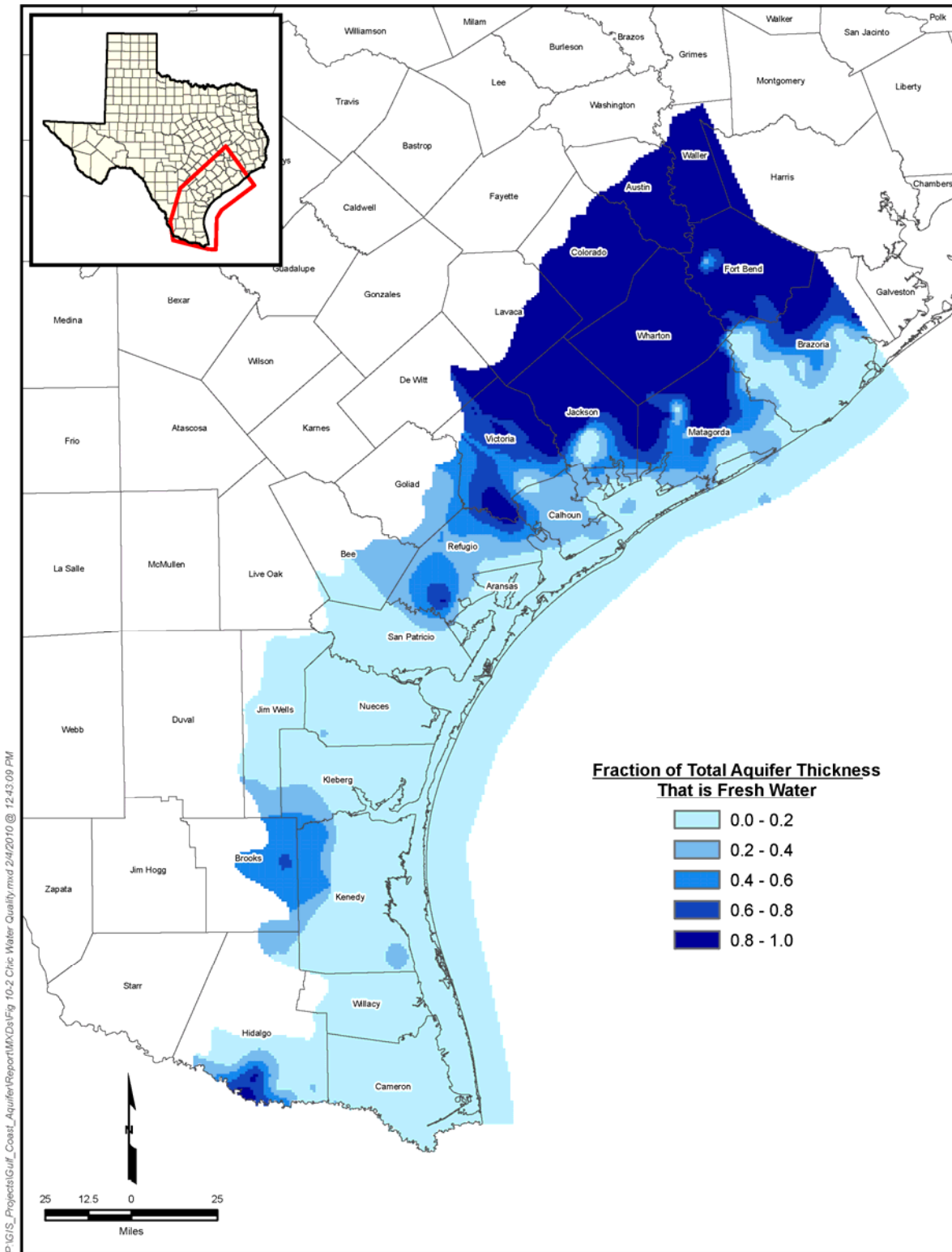


Figure 10-2. Fraction of the Chicot Aquifer estimated to be fresh water with a TDS concentration less than 1,000 ppm, as determined by the analysis of geophysical logs.

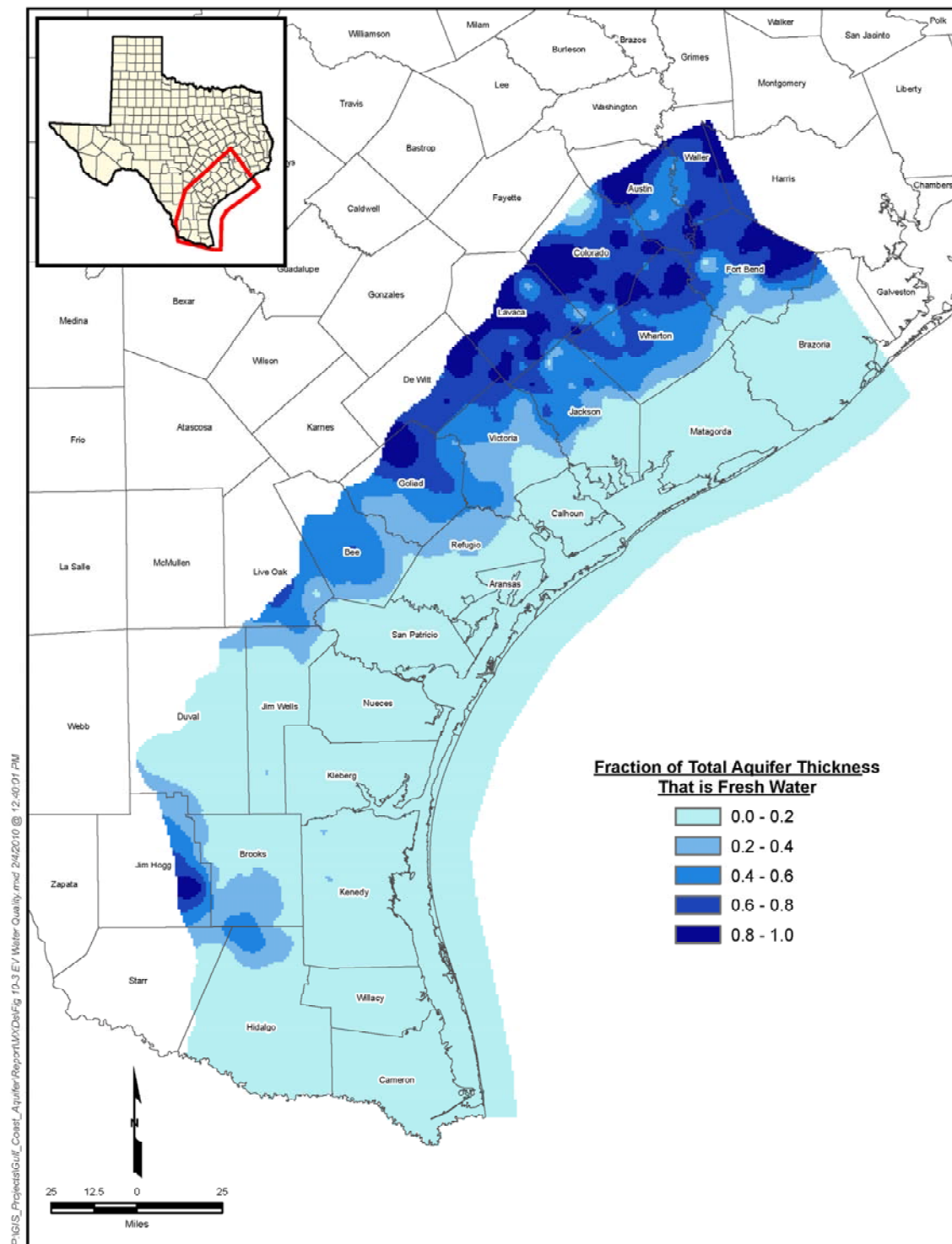


Figure 10-3. Fraction of the Evangeline Aquifer estimated to be fresh water with a TDS concentration less than 1,000 ppm, as determined by the analysis of geophysical logs.

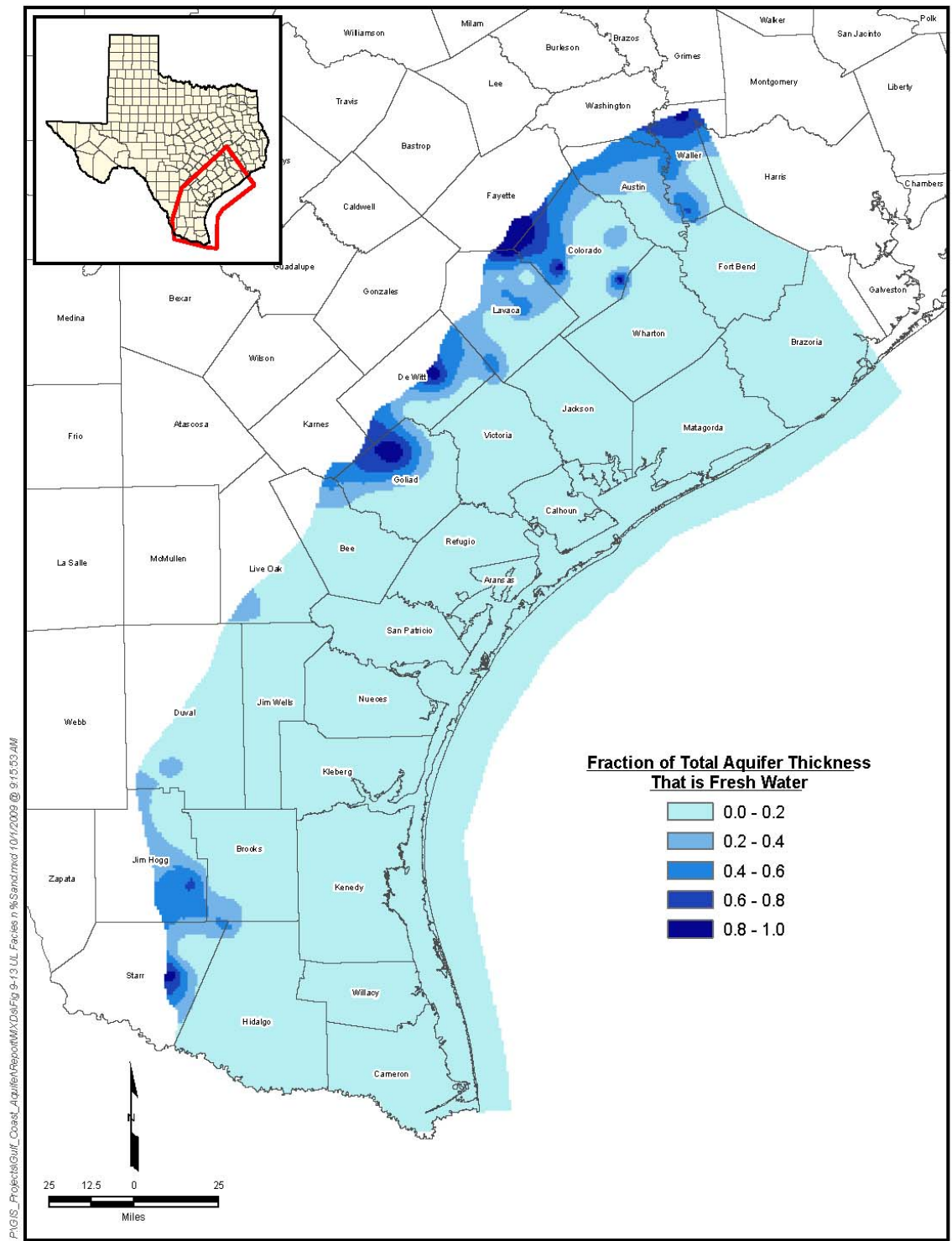


Figure 10-4. Fraction of the Burkeville Confining Unit estimated to be fresh water with a TDS concentration less than 1,000 ppm, as determined by the analysis of geophysical logs.

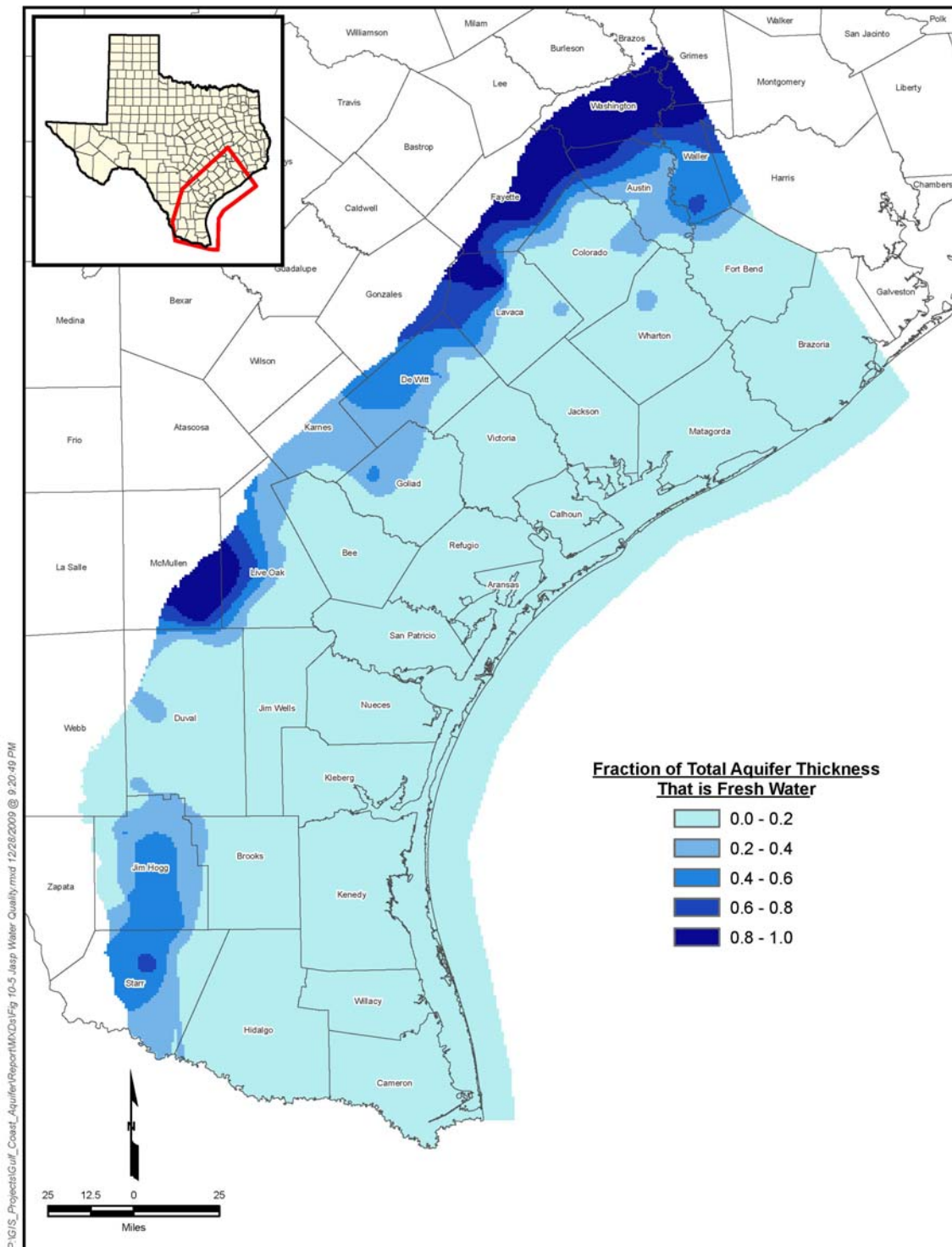


Figure 10-5. Fraction of the Jasper Aquifer estimated to be fresh water with a TDS concentration less than 1,000 ppm, as determined by the analysis of geophysical logs.

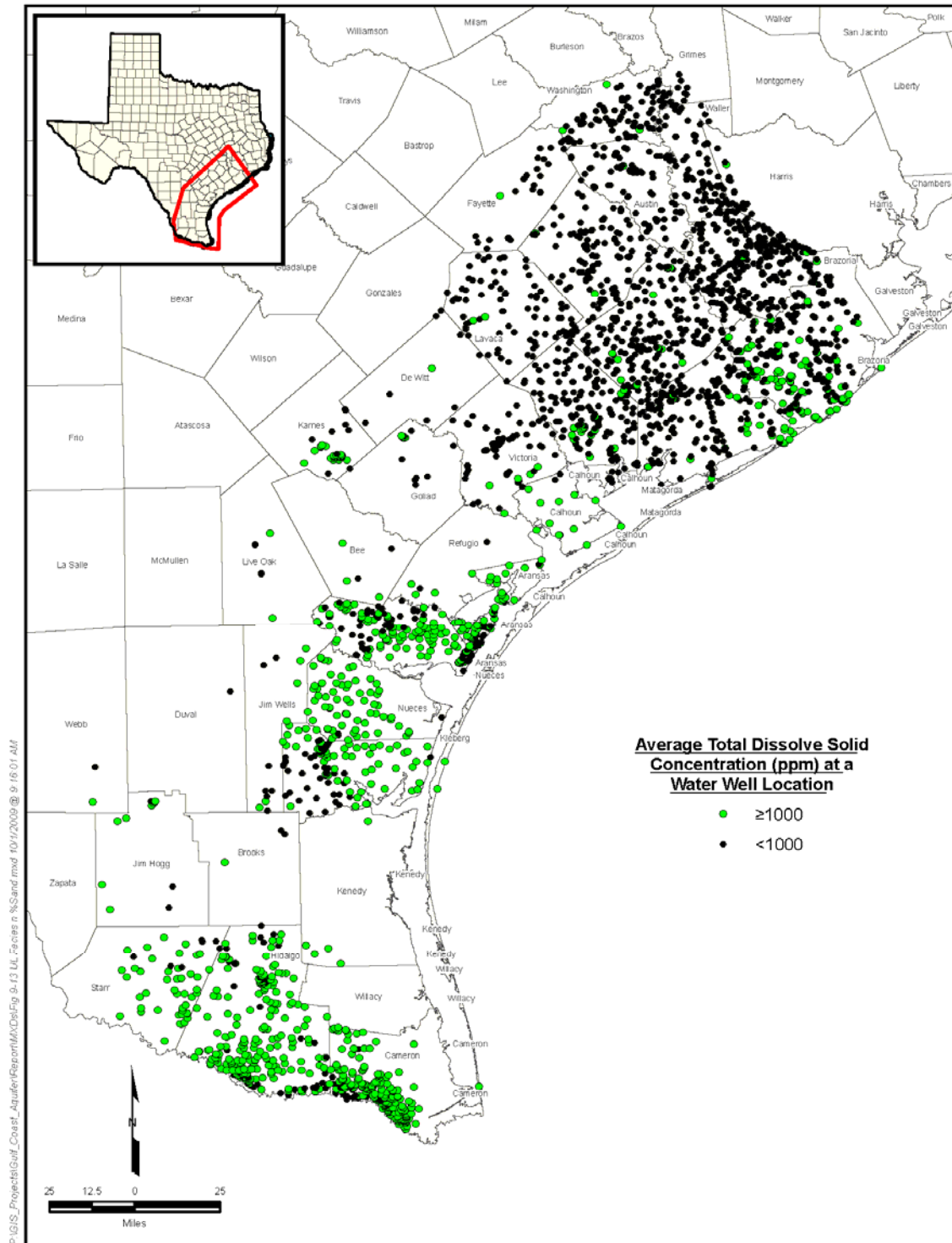


Figure 10-6. Map of water well locations with at least one measurement of TDS concentrations.

11 References

- Alger, R.P. 1966, Interpretation of electric logs in fresh water wells in unconsolidated formations, paper CC, in 7th Annual Symposium Transactions: Society of Professional Well Log Analysts, 25 p.
- Anders, R.B., and E.T. Baker, Jr., 1961, Ground-Water Geology of Live Oak County, Texas: Texas Board of Water Engineers Bulletin 6105, 93 p.
- Anderson, J.B., and R.H. Fillon, eds., 2004, Late Quaternary stratigraphic evolution of the northern Gulf of Mexico margin: SEPM Special Publication No. 79, 314 p.
- Applin, E.R., A.E. Ellisor, and H.T. Kniker, 1925, Subsurface stratigraphy of the Coastal Plain of Texas and Louisiana: American Association of Petroleum Geologists Bulletin, v. 9, p. 79–122.
- Aronow, S., and V.E. Barnes, 1968, Geologic atlas of Texas, Houston sheet: The University of Texas at Austin, Bureau of Economic Geology.
- Aronow, S., and V.E. Barnes, 1975, Geologic atlas of Texas, Corpus Christi sheet: The University of Texas at Austin, Bureau of Economic Geology.
- Aronow, S., T.E. Brown, J.L. Brewton, D.H. Eargle, and V.E. Barnes, 1975, Geologic atlas of Texas, Beeville-Bay City sheet: The University of Texas at Austin, Bureau of Economic Geology.
- Arroyo, J.A., Editor, 2004, The Future of Desalination in Texas: Texas Water Development Board Volume II Biennial Report on Seawater Desalination.
- Ashworth, J.B., and J. Hopkins, 1995, Aquifers of Texas: Texas Water Development Board Report 345, 69 p.
- Baker, E.T., Jr., 1961, Ground-Water Resources of the Lower Rio Grande Valley Area, Texas: Texas Board of Water Engineers Bulletin 6014 Volume II, 269 p.
- Baker, E.T., Jr., 1964, Geology and Ground-water resources of Hardin County, Texas: Texas Water Commission Bulletin 6406, 174 p.
- Baker, R.C., O.C. Dale, and G.H. Baum, 1965, Ground-Water Condition in Menard County, Texas: Texas Water Commission Bulletin 6519, 92 p.
- Baker, E.T., Jr., 1979, Stratigraphic and hydrogeologic framework of part of the coastal plain of Texas: Texas Department of Water Resources Report 236, 43 p.
- Baker, E.T., Jr., 1986, Hydrology of the Jasper Aquifer in the Southeast Texas Coastal Plain: Texas Water Development Board Report 295, 64 p.

- Barnes, V.E., 1992, Geologic map of Texas: The University of Texas at Austin, Bureau of Economic Geology, State Map No. 3.
- Barton, D.C., 1930, Surface geology of coastal southeast Texas: American Association of Petroleum Geologists Bulletin, v. 14, p. 1301–1320.
- Barton, D.C., C.H. Ritz, and M. Hickey, 1933, Gulf Coast geosyncline: American Association of Petroleum Geologists Bulletin, v. 17, p. 1446–1458.
- Bates, R.L., and Jackson, J.A., 1983, Dictionary of Geological Terms. Prepared by the American Geological Institute. Doubleday Publishers, New York. 570 pp.
- Berggren, W.A., D.V. Kent, C.C. Swisher, and M.P. Aubry, 1995, A revised Cenozoic geochronology and chronostratigraphy: Society of Sedimentary Geology (SEPM) Special Publication 54, p. 129–212.
- Bernard, H.A., and R.J. LeBlanc, 1965, Resume of the Quaternary geology of the northwestern Gulf of Mexico province, *in* H.E. Wright and D.G. Frey, eds., The Quaternary of the United States: Princeton University Press, Princetown, New Jersey, p. 137–185.
- Blum, M.D., and D.M. Price, 1998, Quaternary alluvial plain construction in response to glacio-eustatic and climatic controls, Texas Gulf Coastal Plain: Society of Sedimentary Geology (SEPM) Special Publication No. 59, p. 31–48.
- Bornhauser, M., 1947, Marine sedimentary cycles of Tertiary in Mississippi Embayment and central Gulf Coast area: American Association of Petroleum Geologists Bulletin, v. 31, p. 698–712.
- Bornhauser, M., 1958, Gulf coast tectonics: American Association of Petroleum Geologists Bulletin, v. 42, p. 339–370.
- Boyd, D.B., and B.F. Dyer, 1964, Frio barrier bar system of South Texas: Gulf Coast Association of Geological Societies Transactions, v. 14, p. 309–322.
- Brewton, J.L., F. Owen, S. Aronow, and V.E. Barnes, 1976a, Geologic atlas of Texas, Laredo sheet: The University of Texas at Austin, Bureau of Economic Geology.
- Brewton, J.L., F. Owen, S. Aronow, and V.E. Barnes, 1976b, Geologic atlas of Texas, McAllen-Brownsville sheet: The University of Texas at Austin, Bureau of Economic Geology.
- Brown, L.F., Jr., and others, 1976, Environmental geologic atlas of the Texas coastal zone—Corpus Christi area: The University of Texas at Austin, Bureau of Economic Geology, 123 p.

- Brown, L.F., Jr., and others, 1977, Environmental geologic atlas of the Texas coastal zone—Kingsville area: The University of Texas at Austin, Bureau of Economic Geology, 131 p.
- Brown, L.F., Jr., and others, 1980, Environmental geologic atlas of the Texas coastal zone—Brownsville-Harlingen area: The University of Texas at Austin, Bureau of Economic Geology, 140 p.
- Bryant, W.R., J. Lugo, C. Cordova, and A. Salvador, 1991, Physiography and bathymetry, *in* A. Salvador, ed., The geology of North America: the Gulf of Mexico basin, v. J: Boulder, Colorado, Geological Society of America, p. 13–30.
- Carr, J.E., W.R. Meyer, W.M. Sandeen, and I.R. McLane, 1985, Digital models for simulation of ground-water hydrology of the Chicot and Evangeline aquifers along the Gulf Coast of Texas: Texas Department of Water Resources, Report 289, 101 p.
- Catuneanu, O., and 27 others, 2009, Towards the standardization of sequence stratigraphy: Earth-Science Reviews, v. 92, p. 1–33.
- Chowdhury, A., S. Wade, R.E. Mace, and C. Ridgeway, 2004. *Groundwater Availability of the Central Gulf Coast Aquifer System: Numerical Simulations through 1999*. Texas Water Development Board, unpublished report.
- Chowdhury, A.H., and M.J. Turco, 2006, Geology of the Gulf Coast aquifer, Texas, *in* R.E. Mace and others, eds., Aquifers of the Gulf Coast of Texas: Texas Water Development Board Report 365, p. 23–50.
- Chowdhury, A., and R.E. Mace, 2007, Groundwater Resource Evaluation and Availability Model of the Gulf Coast Aquifer in the Lower Grande Valley of Texas, Texas Water Development Board Report 368, p. 120.
- Collier, H., 1993, Borehole Geophysical Techniques for Determining the Water Quality and Reservoir Parameters of Fresh and Saline Water Aquifers in Texas, Report 343, Texas Water Development Board, Austin, TX.
- Core Laboratories, Inc., 1972, A Survey of the Subsurface Saline Water of Texas, Volume II Chemical Analysis of Saline Water: Texas Water Development Board Report 157, 118 p.
- Core Laboratories, Inc., 1972, A Survey of the Subsurface Saline Water of Texas, Volume IV Geologic Well Data West Texas: Texas Water Development Board Report 157, 150 p.
- Dale, O.C., 1952, Ground-Water Resources of Starr County, Texas: Texas Board of Water Engineers Bulletin 5209, 47 p.
- Deussen, A., 1914, Geology and underground waters of the southeastern part of the Texas Coastal Plain: U.S. Geological Survey Water-Supply Paper 335, 365 p.

- Deussen, A., 1924, Geology of the coastal plain of Texas west of Brazos River: U.S. Geological Survey Professional 126, 145 p.
- Deutsch, C. V., and A. G. Journel, 1998. GSLIB Geostatistical Software Library and User's Guide, Oxford University Press, New York, 340 p.
- Dodge, M.M., and J.S. Posey, 1981, Structural cross sections, Tertiary formations, Texas Gulf Coast: University of Texas at Austin, Bureau of Economic Geology.
- Doering, J.A., 1935, Post-Fleming surface formations of southeast Texas and south Louisiana: American Association of Petroleum Geologists Bulletin, v. 19, 651–688.
- Doering, J.A., 1956, Review of Quaternary surface formations of the Gulf Coast region: American Association of Petroleum Geologists Bulletin, v. 40, 1816–1862.
- Doyle, J.D., 1979, Depositional patterns of Miocene facies, middle Texas Coastal Plain: The University of Texas at Austin, Bureau of Economic Geology Report of Investigations No. 99, 28 p.
- Driscoll, F.G., 1986. Groundwater and Wells, Johnson Filtration Systems, Inc., St. Paul, MN, 1079 p.
- Dubar, J.R., 1983, Miocene depositional systems and hydrocarbon resources: the Texas Coastal Plain: The University of Texas at Austin, Bureau of Economic Geology, report prepared for U.S. Geological Survey under contract no. 14-08-0001-G-707, 99 p.
- Dubar, J.R., T.E. Ewing, E.L. Lundelius, Jr., E.G. Otvos, and C.D. Winker, 1991, Quaternary Geology of the Gulf of Mexico Coastal Plain, *in* R. B. Morrison, ed., Quaternary Non-Glacial Geology of the Conterminous United States: Boulder, Colorado, The Geological Society of America, The Geology of North America, v. K-2, p. 583–610.
- Dutton, A.R., and B.C. Richter, 1990, Regional geohydrology of the Gulf Coast Aquifer in Matagorda and Wharton Counties: Development of a numerical model to estimate the impact of water-management strategies: Contract report prepared for Lower Colorado River Authority, Austin, Texas, under Contract IAC (88-89) 0910, 116 p.
- Ewing, T.E., 1990, Tectonic map of Texas: University of Texas at Austin, Bureau of Economic Geology, scale 1:750,000, 4 sheets.
- Ewing, T.E., 1991, Structural framework, *in* A. Salvador, ed., The geology of North America: the Gulf of Mexico basin, v. J: Boulder, Colorado, Geological Society of America, p. 31–52.
- Fillon, R.H., and P.N. Lawless, 2000, Lower Miocene-early Pliocene deposystems in the Gulf of Mexico: Regional sequence relationships: Gulf Coast Association of Geological Societies Transactions, v. 50, p. 411–428.

- Fisher, W.L., and J.H. McGowen, 1967, Depositional systems in the Wilcox Group of Texas and their relationship to occurrence of oil and gas: *Gulf Coast Association of Geological Societies Transactions*, v. 17, p. 105–125.
- Frazier, D.E., 1974, Depositional episodes; Their relationship to the Quaternary stratigraphic framework in the northwestern portion of the Gulf Basin: *The University of Texas at Austin, Bureau of Economic Geology Geological Circular 74-1*, 28 p.
- Galloway, W.E., C.W. Kreitler, and J.H. McGowen, 1979, Depositional and ground-water flow systems in the exploration for uranium: *The University of Texas at Austin, Bureau of Economic Geology*, 267 p.
- Galloway, W.E., 1981, Depositional architecture of Cenozoic Gulf Coastal Plain fluvial systems: *SEPM Special Publication No. 31*, p. 127–155.
- Galloway, W.E., C.D. Henry, and G.E. Smith, 1982, Depositional framework, hydrostratigraphy, and uranium mineralization of the Oakville Sandstone (Miocene), Texas Coastal Plain: *The University of Texas at Austin, Bureau of Economic Geology Report of Investigations No. 113*, 51 p.
- Galloway, W.E., L.A. Jirik, R.A. Morton, and J.R. DuBar, 1986, Lower Miocene (Fleming) depositional episode of the Texas Coastal Plain and continental shelf: *The University of Texas at Austin, Bureau of Economic Geology Report of Investigations No. 150*, 50 p.
- Galloway, W.E., 1989a, Genetic stratigraphic sequences in basin analysis I: Architecture and genesis of flooding-surface bounded depositional units: *American Association of Petroleum Geologists Bulletin*, v. 73, p. 125–142.
- Galloway, W.E., 1989b, Genetic stratigraphic sequences in basin analysis II: application to northeast Gulf of Mexico Cenozoic basin: *American Association of Petroleum Geologists Bulletin*, v. 73, p. 143–154.
- Galloway, W.E., D.G. Bebout, W.L. Fisher, R. Cabrera-Castro, J.E. Lugo-Rivera, and T.M. Scott, 1991, Cenozoic, in A. Salvador, ed., *The geology of North America: the Gulf of Mexico basin*, v. J: Boulder, Colorado, Geological Society of America, p. 245–324.
- Galloway, W.E., X. Liu, D. Travis-Neuberger, and L. Xue, 1994, Reference high-resolution correlation cross sections, Paleogene section, Texas Coastal Plain: *The University of Texas at Austin, Bureau of Economic Geology*.
- Galloway, W.E., and D.K. Hobday, 1996, *Terrigenous clastic depositional systems*: 2nd ed., New York, Springer-Verlag, 489.

- Galloway, W.E., P.E. Ganey-Curry, X. Li, and R.T. Buffler, 2000, Cenozoic depositional history of the Gulf of Mexico basin: American Association of Petroleum Geologists Bulletin, v. 84, p. 1743–1774.
- Galloway, W.E., 2005, Gulf of Mexico Basin depositional record of Cenozoic North American drainage basin evolution: International Association Sedimentologists Special Publication 35, p. 409–423.
- Guevara-Sanchez, E.H., 1974, Pleistocene facies in the subsurface of the southeast Texas Coastal Plain: Ph.D. dissertation, The University of Texas at Austin, 133 p.
- Hamlin, H.S., 2006, Salt domes in the Gulf Coast aquifer, *in* Mace, R. E., and others, eds., Aquifers of the Gulf Coast of Texas: Texas Water Development Board Report 365, p. 217–230.
- Hammond, W.W., Jr., 1969, Ground-Water Resources of Matagorda County, Texas: Texas Water Development Board Report 91, 163 p.
- Haq, B.U., J. Hardenbol, and P.R. Vail, 1987, Chronology of fluctuating sea levels since the Triassic: Science, v. 235, p. 1156–1167.
- Hem, J.D., 1982, Conductance, a collective measure of dissolve ions, in R. A. Minear and L. H. Keigh, editors, Water analysis, v. 1, Inorganice species, pt. 1: Academic Press, p. 137-161
- Hem, J.D., 1985, Study and interpretation of the chemical characteristics of natural water: U. S. Geological Survey Water Supply Paper 2254, 249 p.
- Hernandez-Mendoza, J.J., T.F. Hentz, M.V. DeAngelo, T.F. Wawrzyniec, S. Sakurai, S.C. Talukdar, and M.H. Holtz, 2008, Miocene chronostratigraphy, paleogeography, and play framework of the Burgos Basin, southern Gulf of Mexico: American Association of Petroleum Geologists Bulletin, v. 92, p. 1501–1535.
- Hoel, H.D., 1982, Goliad Formation of the south Texas Gulf Coastal Plain: regional genetic stratigraphy and uranium mineralization: Master's thesis, The University of Texas at Austin, 173 p.
- Kasmarek, M.C., and Robinson, 2004. *Hydrogeology and Simulation of Groundwater Flow and Land-Surface Subsidence in the Northern Part of the Gulf Coast Aquifer System, Texas*. Scientific Investigation Report 2004-5102. United States Geological Society.
- Keys, W.S., and L.M. MacCary, 1971, Application of borehole geophysics to water-resources investigations: U.S. Geological Survey Techniques of Water-Resources Investigations, Book 2, Chapter E1, 126 p.

- Knox, P.R., S.C. Young, W.E. Galloway, E.T. Baker, Jr., and T. Budge, 2006, A stratigraphic approach to Chicot and Evangeline aquifer boundaries, central Texas Gulf Coast: Gulf Coast Association of Geological Societies Transactions, v. 56, p. 371–393.
- Kreitler, C.W., E. Guevera, G. Granata, and D. McKalips, 1977, Hydrogeology of Gulf Coast aquifers, Houston-Galveston area, Texas: Gulf Coast Association of Geological Societies Transactions, v. 27, p. 72–89.
- Lang, J.W., A.G. Winslow, and W.N. White, 1950, Geology and ground-water resources of the Houston district, Texas: Texas Board of Water Engineers, Bulletin 5001, 37 p.
- Lawless, P.N., R.H. Fillon, and R.G. Lytton III, 1997, Gulf of Mexico Cenozoic biostratigraphic, lithostratigraphic, and sequence stratigraphic event chronology: Gulf Coast Association of Geological Societies Transactions, v. 47, p. 271–282.
- LBG-Guyton and Norris Consulting, 2003, Brackish Groundwater Manual for Texas Regional Water Planning Groups, Texas Water Development Board, Austin, Texas.
- Loskot, C.L., W.M. Sandeen, and C.R. Follett, 1982, Ground-Water Resources of Colorado, Lavaca, and Wharton Counties, Texas: Texas Department of Water Resources Report 270, 199 p.
- Lundelius, E.L., 1972, Fossil vertebrates from the late Pleistocene Ingleside fauna, San Patricia County, Texas: The University of Texas at Austin, Bureau of Economic Geology Report of Investigations No. 77, 74 p.
- Marvin, R.F., G.H. Shafer, and O.C. Dale, 1962, Ground-Water Resources of Victoria and Calhoun Counties, Texas: Texas Board of Water Engineers Bulletin 6202, 147 p.
- Mason, C.C., 1963, Ground-Water Resources of Refugio County, Texas: Texas Water Commission Bulletin 6312, 115 p.
- McCoy, T.W., 1990, Evaluation of Ground-Water Resources in the Lower Rio Grande Valley, Texas: Texas Water Development Board Report 316, 48 p.
- McGowen, J.H., and others, 1976a, Environmental geologic atlas of the Texas coastal zone—Bay City-Freepport area: The University of Texas at Austin, Bureau of Economic Geology, 98 p.
- McGowen, J.H., and others, 1976b, Environmental geologic atlas of the Texas coastal zone—Port Lavaca area: The University of Texas at Austin, Bureau of Economic Geology, 107 p.
- Miller, J.A., 1986, Hydrogeologic framework of the Floridian aquifer system in Florida and in parts of Georgia, Alabama, and South Carolina: U.S. Geological Survey Professional Paper 1403-B, 91 p.

- Moore, E.J., 1966, A graphical description of new methods of determining equivalent NaCl concentration of chemical analysis, in 7th annual symposium transactions: Society of Professional Well Log Analysts, Houston, TX, 34 p.
- Morton, R.A., and J.H. McGowen, 1980, Modern depositional environments of the Texas Coast: The University of Texas at Austin, Bureau of Economic Geology Guidebook 20, 167 p.
- Morton, R.A., L.A. Jirik, and R.Q. Foote, 1985, Structural cross sections, Miocene series, Texas continental shelf: University of Texas at Austin, Bureau of Economic Geology.
- Morton, R.A., L.A. Jirik, and W.E. Galloway, 1988, Middle-Upper Miocene depositional sequences of the Texas Coastal Plain and continental shelf: The University of Texas at Austin, Bureau of Economic Geology Report of Investigations No. 174, 40 p.
- Morton, R.A., and W.E. Galloway, 1991, Depositional, tectonic and eustatic controls on hydrocarbon distribution in divergent margin basins: Cenozoic Gulf of Mexico case history: *Marine Geology*, v. 102, p 239–263.
- Murray, G.E., 1961, Geology of the Atlantic and Gulf Coastal province of North America: New York, Harper and Brothers, 692 p.
- Myers, B.N., and O.C. Dale, 1966, Ground-Water Resources of Bee County, Texas: Texas Water Development Board Report 17, 101 p.
- Myers, B.N., and O.C. Dale, 1967, Ground-Water Resources of Brooks County, Texas: Texas Water Development Board Report 61, 87 p.
- Nehring, R., 1991, Chapter 15: oil and gas resources, in A. Salvador, ed., *The geology of North America: the Gulf of Mexico basin*, v. J: Boulder, Colorado, Geological Society of America, p. 445–494.
- Plummer, F.B., 1932, Cenozoic systems in Texas, in E.H. Sellards, W.S. Adkins, and F.B. Plummer, eds., *The geology of Texas*, v. 1, stratigraphy: The University of Texas at Austin, Bureau of Economic Geology Bulletin No. 3232, p. 519–818.
- Preston, R.D., 1983, Occurrence and Quality of Ground Water in the Vicinity of Brownsville, Texas: Texas Department of Water Resources Report 279, 98 p.
- Price, W.A., 1933, Role of diastrophism in topography of Corpus Christi area, south Texas: *American Association of Petroleum Geologists Bulletin*, v. 17, p. 907–962.
- Price, W.A., 1934, Lissie Formation and Beaumont Clay in south Texas: *American Association of Petroleum Geologists Bulletin*, v. 18, p. 948–959.
- Proctor, C.V., T.E. Brown, N.B. Waechter, S. Aronow, and V.E. Barnes, 1974, Geologic atlas of Texas, Seguin sheet: The University of Texas at Austin, Bureau of Economic Geology.

- Rainwater, E.H., 1964, Regional stratigraphy of the Gulf Coast Miocene: Gulf Coast Association of Geological Societies Transactions, v. 14, p. 81–124.
- Rawson, J., D.R. Reddy, and R.E. Smith, 1967, Low-Flow Studies Sabine and Old Rivers Near Orange, Texas, Quantity and Quality, April 12, October 31–November 4, 1966: Texas Water Development Board Report 66, 23 p.
- Reeves, R.D., 1967, Ground-Water Resources of Kendall County, Texas: Texas Water Development Board Report 60, 90 p.
- Rogers, L.T., 1967, Availability and Quality of Ground Water in Fayette County, Texas: Texas Water Development Board Report 56, 117 p.
- Rose, N.A., 1943, Progress report on the ground-water resources of the Texas City area, Texas: U.S. Geological Survey open-file report, 45 p.
- Ryder, P.D., and A.F. Ardis, 2002, Hydrology of Texas Gulf Coast aquifer systems: U.S. Geological Survey Professional Paper 1416-E, 77 p.
- Salvador, A., 1991, Introduction, *in* A. Salvador, ed., The geology of North America: the Gulf of Mexico basin, v. J: Boulder, Colorado, Geological Society of America, p. 1–12.
- Schlumberger, 1972. Log Interpretation Volume I, Principals. Schlumberger Wireline and Testing, Sugarland, TX 130 p.
- Schumm, S.A., 1977, The fluvial system: New York, John Wiley, 338 p.
- Seni, S.J., and M.P.A. Jackson, 1984, Sedimentary record of Cretaceous and Tertiary salt movement, East Texas basin—Times, rates, and volume of salt flow and their implications for nuclear waste isolation and petroleum exploration: The University of Texas at Austin, Bureau of Economic Geology Report of Investigations No. 139, 89 p.
- Shafer, G.H., 1965, Ground-Water Resources of Gonzales County, Texas: Texas Water Development Board Report 4, 89 p.
- Shafer, G.H., 1968, Ground-Water Resources of Nueces and San Patricio Counties, Texas: Texas Water Development Board Report 73, 129 p.
- Shafer, G.H., 1970, Ground-Water Resources of Aransas County, Texas: Texas Water Development Board Report 124, 81 p.
- Shafer, G.H., and E.T. Baker, Jr., 1973, Ground-Water Resources of Kleberg, Kenedy, and Southern Jim Wells Counties, Texas: Texas Water Development Board Report 173, 153 p.

- Shafer, G.H., 1974, Ground-Water Resources of Duval County, Texas: Texas Water Development Board Report 181, 117 p.
- Sharp, J.M., Jr., C.W. Kreitler, and J. Lesser, 1991, Ground water, *in* A. Salvador, ed., The geology of North America: the Gulf of Mexico basin, v. J: Boulder, Colorado, Geological Society of America, p. 529–543.
- Shelby, C.A., M.K. Pieper, S. Aronow, and V.E. Barnes, 1968, Geologic atlas of Texas, Beaumont sheet: The University of Texas at Austin, Bureau of Economic Geology.
- Spradlin, S.D., 1980, Miocene fluvial systems: southeast Texas: The University of Texas at Austin, Master's thesis, 139 p.
- Solis I., 1981, Upper Tertiary and Quaternary depositional systems, Central Coastal Plain, Texas, The University of Texas at Austin, Bureau of Economic Geology Report of Investigations No. 108, 89 p.
- Texas Water Commission, 1989, Ground-water quality of Texas—an overview of natural and man-affected conditions: Texas Water Commission Report 89–01, 197 p.
- Trowbridge, A.C., 1932, Tertiary and Quaternary geology of the Lower Rio Grande region, Texas: U.S. Geological Survey Bulletin 837, 260 p.
- Van Wagoner, J.C., R.M. Mitchum, K.M. Campion, and V.D. Rahmanian, 1990, Siliciclastic sequence stratigraphy in well logs, cores, and outcrops: concepts for high-resolution correlation of time and facies: American Association of Petroleum Geologists Methods in Exploration Series No. 7, 55 p.
- Weeks, A.W., 1933, Lissie, Reynosa, and upland terrace deposits of coastal plain of Texas between Brazos River and Rio Grande: American Association of Petroleum Geologists Bulletin, v. 17, p. 453–487.
- Weeks, A.W., 1945, Quaternary deposits of the Texas Coastal Plain between Brazos River and Rio Grande: American Association of Petroleum Geologists Bulletin, v. 29, p. 1693–1720.
- Wesselman, J.B., 1967, Ground-water resources of Jasper and Newton Counties, Texas: Texas Water Development Board Report 59, 167 p.
- Whitman, H.M, 1965, Estimating Water Quality From Electric Logs, Department of Conservation, Louisiana Geological Survey and Louisiana Department of Public Works in cooperation with the United States Geological Survey
- Williamson, J.D.M., 1959, Gulf Coast Cenozoic History: Gulf Coast Association of Geological Societies Transactions, v. 9, p. 15–29.

- Winker, C.D., 1979, Late Pleistocene fluvial-deltaic deposition Texas Coastal Plain and shelf: Master's thesis, The University of Texas at Austin, 187 p.
- Winker, C.D., 1982, Cenozoic shelf margins, northwestern Gulf of Mexico: Gulf Coast Association of Geological Societies Transactions, v. 32, p. 427–448.
- Winker, C.D., and M.B. Edwards, 1983, Unstable progradational clastic shelf margins, in D.J. Stanley and G.T. Moore, eds, The shelfbreak; Critical interface on continental margins: SEPM Special Publication 33, p. 139-157.
- Winker, C.D., and R.T. Buffler, 1988, Paleogeographic evolution of early deep-water Gulf of Mexico and margins, Jurassic to middle Cretaceous (Comanchean): American Association of Petroleum Geologists Bulletin, v. 72, p. 318–346.
- Wood, L.A., R.K. Gabrysch, and R. Marvin, 1963, Reconnaissance investigation of the ground-water resources of the Gulf Coast region, Texas: Texas Water Commission Bulletin 6305, 114 p.
- Young, S.C., and V. Kelley, eds., 2006, A site conceptual model to support the development of a detailed groundwater model for Colorado, Wharton, and Matagorda Counties: unpublished report prepared for the Lower Colorado River Authority, xxx p.
- Young, S.C., P.R. Knox, T. Budge, V. Kelley, N. Deeds, W.E. Galloway, and E.T. Baker, Jr., 2006a, Stratigraphy, lithology, and hydraulic properties of the Chicot and Evangeline aquifers in the LSWP study area, Central Texas Coast, *in* R.E. Mace and others, eds., Aquifers of the Gulf Coast of Texas: Texas Water Development Board Report 365, p. 129–138.

12 Appendix A Geophysical logs listing, including location and use

API number	NAD27 latitude	NAD27 longitude	Dip section/ position	Strike section/ position*	Company	Lease	County	Lithology and water qual data	Paleo data
424770023900	30.2602	-96.4029	8,1		Texas-Harvey Oil	Fred W Dallas	Washington		
424773062500	30.3299	-96.3944	8,2		Houston W S Oil & Ga	C G & H D	Washington		
424770029400	30.0950	-96.2708	8,3		Magnolia Petroleum C	Giddings Est	Washington		
NOAPI 18624	30.0465	-96.2013	8,4				Austin		
420150023000	30.0098	-96.1293	8,5		Humble Oil & Refg Co	Luther R Sherrod	Austin	X	
424730024300	29.9796	-96.0928	8,6		Humble Oil & Refinin	Hardy Rufus `B`	Waller		
424730031800	29.9054	-95.9314	8,7	D",1	Halbouty Michel T	John W Harris et al	Waller		
421570000100	29.7538	-95.8705	8,8		Humble Oil & Refinin	Albright F C	Fort Bend	X	
421570102600	29.6699	-95.8494	8,9		Mobil Oil Corporatio	Elizabeth McKennon	Fort Bend	X	
421573198300	29.5983	-95.8187	8,10		Petroleum Resource M	Foster Farms	Fort Bend	X	
421570089400	29.5853	-95.6728	8,11		Cockburn H C	Clayton Foundation	Fort Bend	X	
421570245900	29.4568	-95.6113	8,12	E",3	Humble Oil & Refinin	Lockwood H P	Fort Bend	X	
420390145200	29.3163	-95.4703	8,13		Group Oil Company Th	Grey J A-Second	Brazoria	X	
420390422400	29.2345	-95.4141	8,14		Humble Oil & Refinin	Moore Hiram	Brazoria		
420390427700	29.1295	-95.3051	8,15		Texas Company	General American	Brazoria	X	
420390429100	29.0239	-95.2919	8,16		Brazos Oil & Gas Com	Fletcher Trust Co	Brazoria	X	
427060002200	28.9094	-95.1847	8,17	G",1	Humble Oil & Refinin	St Tr 00278-L	Brazoria		
420150001700	30.0077	-96.4510	9,1		Dakamont Exploration	Weise #1	Austin		
420153053900	29.9172	-96.4099	9,2		Superior Oil Company	Woods Pet Gu 2	Austin		
420150066300	29.8287	-96.2879	9,3				Austin		
420150026200	29.7606	-96.2016	9,4	D",4	Magnum Producing LP	Hillboldt	Austin	X	
420150068300	29.6384	-96.1186	9,5				Austin		
420153073800	29.6167	-96.0497	9,6				Austin	X	
421573175200	29.5326	-96.0187	9,7		Thompson John R Oper	Oldag	Fort Bend		
421573180500	29.4631	-95.9521	9,8		Greenhill Petroleum	Patterson A E II	Fort Bend	X	
421570167400	29.3212	-95.8488	9,9	E",5	Howell H H & Cook Ce	Armstrong G W	Fort Bend		
420390271500	29.2703	-95.7585	9,10				Brazoria		
420390286500	29.1862	-95.7075	9,11		Pan American Petrole	Robertson W T	Brazoria	X	
NOAPI 18912	29.1379	-95.6458	9,12				Brazoria		
420390389800	29.0782	-95.6080	9,13	F",5	Pan American Petrole	Ida Hobbs	Brazoria		
420393035000	28.9813	-95.5783	9,14		Dow Chemical Company	John Bute	Brazoria		

TWDB Report ## Final – Hydrostratigraphy of the Gulf Coast Aquifer from the Brazos River to the Rio Grande

API number	NAD27 latitude	NAD27 longitude	Dip section/ position	Strike section/ position*	Company	Lease	County	Lithology and water qual data	Paleo data
420393211000	28.9779	-95.4655	9,15		Bhp Petroleum (Ameri	Beretta M A	Brazoria		
420390481100	28.8991	-95.3991	9,16	G",2	Humble Oil & Refinin	Freprt Sulphr A/C-1	Brazoria		
427064036000	28.5853	-95.1058	9,17		Seagull Energy E & P	Ocs-G-4567	Galveston		
421493208800	30.0748	-96.8488	10,1		G S I Incorporated	Schott-Rogers	Fayette		
421493132900	29.9842	-96.6822	10,2		Daleco Resources	Halamicek	Fayette	X	
420893153100	29.8066	-96.5792	10,3		Superior Production	Werland Albert	Colorado	X	
420890005700	29.7798	-96.5494	10,4		Quintana Petroleum C	Cullen et al	Colorado	X	
420890009000	29.7736	-96.4365	10,5		Paul W U	Reinhardt Henry	Colorado	X	
420893124600	29.6453	-96.3891	10,6	D",6	Ponexco Incorporated	Dixon Loma et al	Colorado	X	
NOAPI 18620	29.5740	-96.2899	10,7				Colorado		
424810121800	29.4747	-96.2802	10,8				Wharton	X	
424810120500	29.4738	-96.1920	10,9				Wharton	X	
424813403300	29.2858	-96.1627	10,10		Carrizo O&G Inc	McMillan	Wharton		
424813344200	29.3679	-96.1512	10,11				Wharton	X	
424813294400	29.2353	-96.0156	10,12	E",7	Ashland Expl Inc	Fields	Wharton	X	
424810256200	29.1560	-96.0105	10,13		Flaitz J M & Mitchel	H C Cockburn	Wharton		
NOAPI 18639	29.1034	-95.9051	10,14				Matagorda		
423210067000	29.0641	-95.7842	10,15		Brazos Oil & Gas Com	Findley Estate	Matagorda	X	
NOAPI 18891	28.9501	-95.7767	10,16	F",7			Matagorda		
423210082400	28.8138	-95.6907	10,17		Gulf Oil Corporation	Phillips Olivia E	Matagorda	X	
427043007300	28.7159	-95.5428	10,18	G",4	Corpus Christi Oil &	St Tr 00369-L	Brazos		
427043000500	28.4430	-95.5010	10,19		Forest Oil Corporati	Ocs G01721	Brazos		X
427040007100	28.5478	-95.4866	10,20		Sun Oil Company	Ocs G01715	Brazos		
427040007000	28.3688	-95.3998	10,21		Phillips Petroleum C	Ocs G01724	Brazos		X
427044002600	28.3638	-95.3552	10,22		Anr Production Compa	Ocs G03469	Brazos		
421493204900	29.7977	-96.8100	11,1		Billingsley-Gonzales	Cernosek Heirs	Fayette	X	
420893164500	29.7271	-96.7725	11,2		Txo Production Corpo	Wanjura	Colorado	X	
420893145600	29.6657	-96.7445	11,3		Quamagra Interests T	Weimar Gu	Colorado		
420893163900	29.6296	-96.6908	11,4		Mcrae-Fleming Entpr	Miller A L et al	Colorado		
420893173400	29.5423	-96.5854	11,5		Property Producing C	The Burkitt Foundati	Colorado		
420893215800	29.4341	-96.5178	11,6		Walter Oil & Gas Cor	Lehrer `A`	Colorado		
420893059200	29.5492	-96.5085	11,7	D",8	Napeco Incorporated	R E Miller	Colorado	X	
420890075900	29.4161	-96.4716	11,8		Hamill Claud B	Schiurring C R	Colorado		
424813369000	29.3246	-96.3965	11,9		Talon Development Co	Naiser	Wharton		

TWDB Report ## Final – Hydrostratigraphy of the Gulf Coast Aquifer from the Brazos River to the Rio Grande

API number	NAD27 latitude	NAD27 longitude	Dip section/ position	Strike section/ position*	Company	Lease	County	Lithology and water qual data	Paleo data
420893198100	29.3946	-96.3915	11,10		Talon Development Co	Wesselski	Colorado	X	
424813336100	29.2958	-96.3615	11,11				Wharton	X	
424813147700	29.1838	-96.2972	11,12		Texaco Incorporated	M S Swanson	Wharton	X	
424810357500	29.1611	-96.1883	11,13	E",8	Caribbean Oil	A Kluck	Wharton		
NOAPI_18827	29.0195	-96.1476	11,14				Matagorda		
NOAPI_18844	28.9397	-96.0505	11,15				Matagorda		
423210268900	28.8778	-96.0289	11,16		Continental Oil Comp	Fondren W W Jr	Matagorda		X
423210114700	28.8737	-95.9648	11,17	F",8	Michael J S Company	Vaughn et al Onella	Matagorda		
423210253900	28.7347	-95.9141	11,18		Parker R H	G Gottschalk	Matagorda	X	
426040001200	28.6146	-95.8580	11,19		Shell Oil Company	St Tr 00519-S	Brazos		
427040000700	28.5545	-95.8149	11,20	G",6	Shell Oil Company	St Tr 00440-L Nw/4	Brazos		
421490032700	29.6951	-97.0445	12,1		Bankline Oil Company	Novak John J	Fayette		
421493262000	29.6428	-96.9068	12,2		Pronghorn Oil & Gas	Miksches Daniel	Fayette	X	
NOAPI_18602	29.5634	-96.8414	12,3				Lavaca		
422853272900	29.4454	-96.7826	12,4		Mueller Exploration	Stanton M G U	Lavaca		
422853117200	29.4257	-96.7099	12,5		Osborn W B	Fougerousse	Lavaca		
422850032600	29.3769	-96.6851	12,6	D",10	Pure Oil Company	E E Kolar	Lavaca	X	
420893160400	29.2966	-96.6012	12,7		Louisiana Land & Exp	Cranz	Colorado	X	
NOAPI_18743	29.2070	-96.5321	12,8				Wharton		
424810169500	29.1517	-96.4980	12,9				Wharton		
424810177000	29.0662	-96.3844	12,10	E",11	Pure Oil Co The	W L Stewart	Wharton	X	
422393247200	28.9979	-96.3583	12,11		Smith Harry L	Kountze & Couch	Jackson		
423210217100	28.9451	-96.3059	12,12		Crown Central Petrol	Denman Kountz et al	Matagorda	X	
423210229500	28.8238	-96.2796	12,13		Union Producing Comp	Potthast	Matagorda	X	
423210267200	28.7983	-96.2201	12,14		Union Texas Petroleu	Sanders #1	Matagorda		
423213171600	28.7290	-96.1409	12,15		Sierra Minerals Inco	Solution	Matagorda		
423210251400	28.6420	-96.0380	12,16		Gulf Oil Corporation	Tex St Matgorda Bay	Matagorda	X	
426043004100	28.5746	-95.9899	12,17		Houston Oil & Minera	St Tr 00543-S	Brazos		
427043021000	28.5019	-95.9353	12,18	G",7	Superior Oil Company	St Tr 00446-L	Brazos		
427044023000	28.3725	-95.9034	12,19		Odeco Oil And Gas Co	Ocs-G-11277	Brazos		
427044030000	28.1710	-95.6854	12,20		Oryx Energy Company	Ocs-G-8120	Brazos		
422853026800	29.3941	-97.1922	13,1		Douglas L A	John H Petru	Lavaca	X	
422850035800	29.2793	-97.0484	13,2		Chavanne H J	Allen Carter	Lavaca		
422850050900	29.1815	-96.9818	13,3	D",13	Sterling Oil & Gas	Seekamp & Palmer	Lavaca		

TWDB Report ## Final – Hydrostratigraphy of the Gulf Coast Aquifer from the Brazos River to the Rio Grande

API number	NAD27 latitude	NAD27 longitude	Dip section/ position	Strike section/ position*	Company	Lease	County	Lithology and water qual data	Paleo data
422853176200	29.1267	-96.8621	13,4		La Campbell Energy C	Ploeger D B et al	Lavaca		
424693243200	28.9751	-96.8609	13,5		Miller W C	Allen Annie Bracken	Victoria	X	
422390004700	29.0104	-96.7845	13,6		Triad Oil & Gas Comp	C D Holzheuser	Jackson	X	
422390155600	28.9560	-96.7113	13,7		Texana Petroleum Com	Wes Rogers	Jackson		
422390192100	28.8625	-96.6758	13,8	E",14	Howell H H Frank Wil	Francis Koop et al	Jackson		
422390337800	28.7646	-96.5909	13,9		Socony Mobil Oil Com	West Ranch /A/	Jackson	X	
422390319800	28.7070	-96.5210	13,10		Superior Oil Company	W L Traylor	Jackson		
420570085200	28.6323	-96.4482	13,11	F",14	Humble Oil & Refinin	Elizabeth K Hardie	Calhoun	X	
420573090300	28.5293	-96.3816	13,12		Pennzoil Prod Co Sta		Calhoun	X	
NOAPI_18786	28.4688	-96.3600	13,13	D",5			Colorado		
427033000600	28.3680	-96.2364	13,14	G",10	Occidental Petroleum	St Tr 00522-L	Matagorda Isl.		X
421770042400	29.2352	-97.4553	14,1		Hunt H L	Robert Miller	Gonzales	X	
421230087000	29.0982	-97.4010	14,2		Gulf Oil Corporation	Mueller	De Witt		
421230029000	29.1009	-97.2635	14,3		Bridewell W F (Billy	John W Burns Est	De Witt	X	
421233187900	28.9945	-97.2320	14,4	D",15	Austin Resources Cor	Rath	De Witt	X	
424693155300	28.9470	-97.1499	14,5		Killam & Hurd Limite	Murphy Trust	Victoria	X	
424690093400	28.8691	-97.0858	14,6		Wiseman W M & White	Louise G Williams	Victoria		
NOAPI_993	28.8119	-97.0128	14,7		Crowell Water Well D	City of Victoria	Victoria		
424690162400	28.7560	-96.9600	14,8		Robinson P W	Welder Minnie S Est	Victoria	X	
NOAPI_990	28.6850	-96.9461	14,9	E",16	Layne Texas Co.	Deep Observation Wel	Victoria		
424693189700	28.6383	-96.8678	14,10		Maynard Oil Company	Diemer P O	Victoria	X	
420570132300	28.5220	-96.8165	14,11		Alcoa	M L K Bryan et al	Calhoun	X	X
420570122100	28.2925	-96.5861	14,12		Texaco Incorporated	Esp Snt Bay S T 186	Calhoun	X	
427033031900	28.1870	-96.4442	14,13	G",13	Sonat Exploration Co	Sl 80375	Matagorda Isl.	X	
427034001000	28.1102	-96.2426	14,14				Matagorda Isl.		
422550023600	29.1622	-97.7297	15,1		Frazier Jack W	O L Cochran	Karnes		
421230033700	29.0145	-97.6862	15,2		Geochemical Surveys	A F Tam Jr	De Witt	X	
421230036200	28.9285	-97.5382	15,3		Sohio Producing	1st Nat Bk Yorktown	De Witt		
421750043400	28.8485	-97.4546	15,4	D",17	Goldston W	Reitz Unit	Goliad		
421753010500	28.7668	-97.3455	15,5		Chevron U S A Incorp	Raymond G Jacobs	Goliad		
421753166400	28.7156	-97.2555	15,6		Dinero Oil Company	Swickheimer	Goliad		

TWDB Report ## Final – Hydrostratigraphy of the Gulf Coast Aquifer from the Brazos River to the Rio Grande

API number	NAD27 latitude	NAD27 longitude	Dip section/ position	Strike section/ position*	Company	Lease	County	Lithology and water qual data	Paleo data
421753171900	28.6396	-97.2365	15,7		Forney Bill Incorpor	Swickheimer	Goliad	X	
424690143800	28.6132	-97.1598	15,8		Hunt Hassie Trust	Emmit Fagan	Victoria		
423910002300	28.5072	-97.0778	15,9	E",17	Turnbull-Zoch-Franci	Mrs Jamie Hynes	Refugio	X	
423913146600	28.4547	-96.9826	15,10		Texas Oil & Gas Corp	Fagan /M/	Refugio	X	
423910008600	28.3491	-96.8660	15,11	F",17	Socony Mobil Oil Com	J W Galloway	Refugio	X	X
420570118500	28.2204	-96.7891	15,12		Western Natural Gas	State Tract 49	Calhoun	X	
427034014000	28.0412	-96.5861	15,13	G",14			Matagorda Isl.	X	
424930153600	29.0257	-98.0214	16,1		Texon Royalty Co.	Toczygamba #1	Wilson		
422550063400	28.9068	-97.8991	16,2		Texas Eastern Produc	Otis S Wuest	Karnes	X	
422553024600	28.8319	-97.7712	16,3		General Crude Oil Co	G C O Alexander	Karnes		
422553134600	28.7385	-97.6931	16,4		Turner M O	Robison Betty J	Karnes		
421750145600	28.6794	-97.6113	16,5	D',1	General Crude Oil Co	Pettus	Goliad	X	
421753335000	28.6388	-97.5197	16,6		Lightning Oil Compan	Lott J F	Goliad		
421753263600	28.5995	-97.4675	16,7		Bridge Oil (Usa) Inc	Oconnor Ranch Gu 1	Goliad	X	
421753216500	28.4883	-97.4112	16,8		Ginther N C Contract	Flowers Gas Unit	Goliad	X	
421753194500	28.4222	-97.3509	16,9	E',E",1,19	Mueller Engineering	Shay /D/	Goliad	X	
423913211800	28.4065	-97.2392	16,10		Bishop Petroleum Inc	Oconnor `A`	Refugio	X	
423913158800	28.3767	-97.1537	16,11		Quintana Petroleum C	Heard Clement	Refugio		
420070035400	28.2463	-97.0625	16,12		K & H Operating Comp	Tatton Ranch	Aransas	X	
420073066000	28.1284	-96.9119	16,13		Energy Development C	State Tract 3	Aransas	X	
427030000200	27.9667	-96.8676	16,14	G',G",1,15	Humble Oil & Refinin	St Tr 00692-L	Matagorda Isl.		
424930174700	28.9120	-98.2104	17,1		O.G. McClain	S.V. Houston #1	Wilson		
422970001100	28.7138	-98.0390	17,2		Hamman Oil & Refinin	Walter E Gaetze	Live Oak	X	
420253155700	28.6589	-97.8982	17,3		Luling O&G Co	Ashland #2	Bee	X	
420250030500	28.5936	-97.8484	17,4		Coastal States Gas T	Hall Imogene	Bee		
420253149300	28.5771	-97.7579	17,5	D',3	Texas O&G	Dirks Gu 2 #1	Bee	X	
420253258400	28.5101	-97.6166	17,6		1988 J V Indexgeo	Blackburn	Bee	X	
420253048700	28.3826	-97.5622	17,7		Millican Oil Company	M & M Murphy	Bee		
420250243000	28.3261	-97.4504	17,8	E',2	Horn L B Dassow D Et	E McCurdy /A/	Bee	X	
423913207400	28.2159	-97.3781	17,9		McLeod George L Inco	Rooke F B & Sons Ltd	Refugio		
423910365900	28.1617	-97.2705	17,10		Dennis L W	W A Boenig	Refugio	X	
423910372200	28.1408	-97.1926	17,11	F',F",1,19	Hunt Oil Company	Jack Robbins	Refugio	X	

TWDB Report ## Final – Hydrostratigraphy of the Gulf Coast Aquifer from the Brazos River to the Rio Grande

API number	NAD27 latitude	NAD27 longitude	Dip section/ position	Strike section/ position*	Company	Lease	County	Lithology and water qual data	Paleo data
420070033100	28.1223	-97.0805	17,12		Phillips Petroleum C	Copano	Aransas		
420070454000	28.0024	-97.0515	17,13		Amerada Petroleum Co	State-Tract 191	Aransas		
427033021500	27.8762	-96.9162	17,14	G',2	Oxy Petroleum Incorp	Sl M-76404	Matagorda Isl.	X	
422970004300	28.6330	-98.1838	18,1		Buzzini Drilling	W R Seale	Live Oak	X	
422970082400	28.4930	-98.1819	18,2		Seaboard Oil Company	Gibbens	Live Oak	X	
422970138700	28.4387	-98.0579	18,3		Kirkwood Drilling	Harry L Hinton	Live Oak	X	
422973327600	28.3491	-97.9516	18,4	D',6	American Shoreline I	Chandler-Nester Un	Live Oak	X	
420253181600	28.3400	-97.8242	18,5		Jennings Expl Co	Onell, Thomas #2	Bee	X	
420253191200	28.2386	-97.8011	18,6		Southern Royalty Inc	Wallek #1	Bee	X	
420250202600	28.1934	-97.7261	18,7		Orion Oil Company	Jack H Pickens	Bee	X	
424090034400	28.1197	-97.6294	18,8	E',4	Horn L B	Rozypal J	San Patricio		
424093225200	28.0604	-97.5235	18,9		Tri-C Resources Inco	Welder	San Patricio	X	
424093243800	28.0286	-97.4435	18,10		Averill W M Jr	Dycas Louna	San Patricio	X	
424090256200	27.9743	-97.3493	18,11		Warren B B et al	Locke J R	San Patricio		
424093228400	27.9098	-97.2364	18,12	F',3	Famcor Oil Incorpora	Sien A C	San Patricio		
420073080400	27.9063	-97.1365	18,13		North Central Oil Co	City of Aransas Pass	Aransas	X	
427023023300	27.8056	-96.9486	18,14	G',3	Bhp Petroleum (Ameri	St Tr 00722-L Se/4	Mustang Isl.		
423110117300	28.3248	-98.3842	19,1		Hickock & Reynolds	Shiner Ranch	McMullen	X	
422973265600	28.2550	-98.3294	19,2		Hawkins H L Jr	Riser E L	Live Oak	X	
422973033000	28.1729	-98.2742	19,3		Atlantic Richfield C	El Paso Natl G 300	Live Oak	X	
422970260400	28.1612	-98.1450	19,4	D',8	Blanco Oil Company &	F L Morris	Live Oak		
422973354100	28.1454	-98.0773	19,5		Arco Oil & Gas Corpo	New H M	Live Oak	X	
422973351100	28.1152	-97.9454	19,6		Shoreline Operating	Curlee Heirs #1	Live Oak		
422493198500	28.0443	-97.8945	19,7		Petroleum Management	Four L Ranch	Jim Wells		
424093171600	28.0363	-97.7723	19,8		Southern Royalty Inc	Timon Gas Unit	San Patricio	X	
424093188300	28.0015	-97.6592	19,9	E',5	Southern Royalty Inc	Luling Foundation	San Patricio	X	
423553024900	27.8395	-97.5464	19,10		Allen T M	W C Veters	Nueces		
423553127000	27.8001	-97.4250	19,11		Mobil Oil Corporatio	Charles B Weil et al	Nueces		
423550612200	27.7911	-97.2963	19,12	F',4	Atlantic Refining Co	State Tract 36	Nueces	X	X
426020004000	27.6635	-97.1399	19,13	G',4	Shell Oil Company	St Tr 00899-S	Mustang Isl.		
427020000300	27.6392	-97.0448	19,14		Gulf Oil Corporation	St Tr 00774-L	Mustang Isl.		
427024001200	27.5490	-96.8420	19,15		Marathon Oil Company	Ocs G03035	Mustang Isl.		X
423110183400	28.0650	-98.6506	20,1		Boysen Harold K	Walker	McMullen		

TWDB Report ## Final – Hydrostratigraphy of the Gulf Coast Aquifer from the Brazos River to the Rio Grande

API number	NAD27 latitude	NAD27 longitude	Dip section/ position	Strike section/ position*	Company	Lease	County	Lithology and water qual data	Paleo data
423113177900	28.0646	-98.5740	20,2		Inland Ocean Incorpo	Hagist	McMullen	X	
423113137300	28.1119	-98.4526	20,3		Arco Oil & Gas Corpo	Gouger Gas Un No 4	McMullen	X	
421313825400	27.9491	-98.3486	20,4	D',10	Clayton Williams Ene	Driscoll Foundation	Duval	X	
421310107500	27.9415	-98.2546	20,5		Argo Oil Company	Lopez Juan R	Duval		
422493172400	27.8845	-98.1422	20,6		M J G Incorporated	Jindra	Jim Wells	X	
422493019900	27.9011	-98.0402	20,7		McClain Oil & Gas	Rehmet /A/	Jim Wells	X	
422493145000	27.9145	-97.9727	20,8		Tx Petroleum Company	Goldapp	Jim Wells	X	
423553085900	27.8142	-97.9321	20,9		Cox Edwin L	Walker /A/	Nueces		
423550033900	27.7804	-97.8435	20,10		Union Producing Comp	T S Schroeder	Nueces		
423553266600	27.7744	-97.7478	20,11	E',6	Pennzoil Producing C	Eschberger	Nueces	X	
423550099200	27.6931	-97.6653	20,12		Southwestern Oil & R	Hawn Bros	Nueces	X	
423553130800	27.7121	-97.5014	20,13		Adobe Oil & Gas Corp	Fordyce Unit	Nueces		
423550318200	27.5612	-97.3737	20,14	F',6	Humble Oil & Refinin	King Ranch East Laur	Nueces	X	
423553170400	27.5959	-97.2935	20,15		Exxon Corporation	Pita Island Field Ga	Nueces		
427020001500	27.5510	-97.1411	20,16		Cities Service Oil C	St Tr 00796-L	Mustang Isl.	X	
421310545000	27.8920	-98.7101	21,1		Magnolia Petroleum C	Duval Co Ranch Sec 7	Duval		
421310350100	27.8282	-98.5617	21,2		Shell Oil Company	Penwell L H	Duval	X	
421313760200	27.8240	-98.3117	21,3		Harvey Brothers Oil	Lillian	Duval		
422493205300	27.7815	-98.1949	21,4		Hurd Enterprises Lim	Yorba Oil Co Gu	Jim Wells		
422493192300	27.6550	-98.1124	21,5		Glacier Energy Incor	Cable H F	Jim Wells		
422730000300	27.6342	-98.0159	21,6		Humble Oil & Refinin	King Ranch Morgan	Kleberg	X	
422730031600	27.5779	-97.9197	21,7	E',8	Humble Oil & Refinin	King Ranch Stratton	Kleberg		
423550408200	27.5838	-97.7290	21,8		Coastal Trend Oil &	Alfred Fuchs	Nueces	X	
422730053700	27.5167	-97.6348	21,9		Humble Oil & Refinin	King Ranch Chiltipin	Kleberg		
422730054200	27.5157	-97.5270	21,10	F',7	Humble Oil & Refinin	King Ranch Lobo	Kleberg	X	
422730200100	27.3858	-97.3609	21,11	G',7	Humble Oil & Refinin	Laguna Madre St Tr 1	Kleberg		X
426020006500	27.3466	-97.2948	21,12		King Resources	St Tr 00978-S	Mustang Isl.		
427024026400	27.3482	-97.0960	21,13		Houston Exploration	Ocs G12421	Mustang Isl.		
424790108500	27.6374	-98.8348	22,1		Atlantic Refining Co	Billings Ranch	Webb		
421313619300	27.6455	-98.7124	22,2		Arco Oil & Gas Corpo	Frost Bnk-Peters Lc	Duval		
421313519700	27.6185	-98.6010	22,3	D',13	Esenjay Petroleum Co	Driscoll Estate	Duval		
421310782600	27.5744	-98.5129	22,4		A M & R Company	Oliveira Jesus	Duval	X	
421313726100	27.5652	-98.4271	22,5		Hawk Exploration & P	West M R	Duval	X	
421313234100	27.5074	-98.2929	22,6		North American Produ	F Vela	Duval		

TWDB Report ## Final – Hydrostratigraphy of the Gulf Coast Aquifer from the Brazos River to the Rio Grande

API number	NAD27 latitude	NAD27 longitude	Dip section/ position	Strike section/ position*	Company	Lease	County	Lithology and water qual data	Paleo data
422493086800	27.5329	-98.1208	22,7		Huisache Operating C	Driscoll /C/	Jim Wells	X	
422733233600	27.4212	-97.9641	22,8		Exxonmobil Corporati	King Ranch Borregos	Kleberg	X	
422730108500	27.3758	-97.8022	22,9		Southern Minerals Co	Brookshire T M	Kleberg		
422730088100	27.2968	-97.6390	22,10		Continental Oil Comp	State of Texas	Kleberg		
422730088300	27.2707	-97.5090	22,11	F,8	Humble Oil & Refinin	State Tract 25	Kleberg	X	
426010000200	27.2222	-97.3278	22,12	G,G',1,9	Mobil Oil Corporatio	St Tr 01006-S	North Padre Isl.	X	
424793381200	27.4695	-98.9707	23,1		Sun Expl & Prod Co	Montoya, Santos	Webb	X	
424793451300	27.4653	-98.8670	23,2		Killam Oil Co	Benavides, Rosa V.,	Webb	X	
421311018900	27.4067	-98.7600	23,3	D,2	Killam & Hurd Limite	Benavides Juan	Duval	X	
421310996700	27.3642	-98.6148	23,4		Lone Star Producing	Miller E J	Duval		
422473177300	27.3309	-98.5440	23,5		Hughes Texas Petrole	Canales E G	Jim Hogg		
421313634000	27.3904	-98.4785	23,6		Rio Exploration Comp	Bahr John	Duval		
421310980400	27.3254	-98.4102	23,7		Standard Oil Company	Jack Casey	Duval		
422490337500	27.2850	-98.2173	23,8		Socony Mobil Oil Com	Caldwell J R	Jim Wells		
422490351400	27.3051	-98.1002	23,9	E,2	Humble Oil & Refinin	King Ranch	Jim Wells	X	
422730124200	27.2747	-97.9406	23,10		Humble Oil & Refinin	King Ranch Canelo	Kleberg		
422610014200	27.1846	-97.8711	23,11		Sunray Oil Corporati	J C McGill Jr et al	Kenedy		
422610035300	27.1435	-97.7136	23,12		Humble Oil & Refinin	East Mrs S K /G/	Kenedy	X	X
422610010000	27.1601	-97.5842	23,13	F,F',1,9	Humble Oil & Refinin	John G Kenedy Jr	Kenedy	X	
422610018700	27.1022	-97.4240	23,14	G,2	Humble Oil & Refinin	Laguna Madre St 249	Kenedy		X
427010000200	27.0921	-97.2827	23,15	G,3	Shell Oil Company	St Tr 00920-L	North Padre Isl.	X	
424793526800	27.3746	-98.9953	24,1		Herschap Bros	Wheatley	Webb	X	
424793868300	27.3404	-98.8724	24,2		Killam Oil Company L	Killam-Hurd-Bruni 77	Webb		
422470014000	27.3018	-98.7963	24,3		British American Oil	Adams L M	Jim Hogg		
422470035400	27.2420	-98.6855	24,4	D,3	Marsh & Coates Produ	Marsh Don H	Jim Hogg		
422473156500	27.2883	-98.5916	24,5		L Texas Petroleum	Mestena O&G Co	Jim Hogg	X	
422470031300	27.2123	-98.5182	24,6		Sun Oil Company	Eshleman A J	Jim Hogg	X	
420470043500	27.1478	-98.3570	24,7		Pronto Drilling Comp	Elbert Louis Maup	Brooks	X	
420470011700	27.1580	-98.2049	24,8		Magnolia Petroleum C	T S Proctor	Brooks	X	
420470023000	27.1522	-98.0393	24,9	E,4	Humble Oil & Refinin	D J Sullivan	Brooks		
422610016800	27.0002	-97.8898	24,10		Humble Oil & Refinin	East Mrs S K	Kenedy		
422610017800	27.0993	-97.7777	24,11		Humble Oil & Refinin	John G Kenedy Jr	Kenedy		

TWDB Report ## Final – Hydrostratigraphy of the Gulf Coast Aquifer from the Brazos River to the Rio Grande

API number	NAD27 latitude	NAD27 longitude	Dip section/ position	Strike section/ position*	Company	Lease	County	Lithology and water qual data	Paleo data
422610037300	27.0169	-97.7200	24,12		Humble Oil & Refinin	East Mrs S K	Kenedy		
422613017400	26.9998	-97.6039	24,13	F,2	Exxon Company U S A	East Mrs S K	Kenedy	X	
422613112700	26.9839	-97.5038	24,14		Exxon Corporation	East Mrs S K Est /B/	Kenedy	X	
422610020100	26.9108	-97.4387	24,15		Humble Oil & Refinin	St Tr 326	Kenedy	X	
427010000100	26.9029	-97.3007	24,16	G,5	Mobil Oil Corporatio	St Tr 00961-L	North Padre Isl.		X
427013003300	26.8999	-97.2645	24,17		Atlantic Richfield C	Sl 81921 Blk 960-L S	North Padre Isl.		
427014003000	26.8421	-96.9800	24,18		Shell Offshore, Inc.	Ocs-G-5953	North Padre Isl.		
425053098400	27.2520	-99.0616	25,1		Killam & Hurd Ltd	Bruni Mineral Trust	Zapata		
422473194000	27.2004	-98.9208	25,2		South Texas Operatin	Chapa Maria Eva	Jim Hogg	X	
422473169500	27.2006	-98.8231	25,3		Hughes Texas Petrole	Martinez H T et al	Jim Hogg	X	
422473187800	27.1769	-98.7357	25,4		Newman Operating Com	Mestina	Jim Hogg	X	
422473174900	27.1273	-98.6939	25,5	D,4	Alta Vista Explorati	Loma	Jim Hogg	X	
422473199500	27.1272	-98.6231	25,6		Corpus Christi Lease	Cacahuete	Jim Hogg		
422473225400	27.1109	-98.5663	25,7		Mestena Operating Li	Perro Grande	Jim Hogg	X	
422470261000	27.1219	-98.5266	25,8		Shell Oil Company	Mestena O&G	Jim Hogg	X	
420473155200	27.0896	-98.4299	25,9		Hunter & Hedrick Pro	Alexander 400 Ac	Brooks		
420473206500	27.0209	-98.3295	25,10		Mestena Operating Li	Tres Puertas	Brooks	X	
420470069400	26.9899	-98.2795	25,11		Humble Oil & Refinin	Scott & Hopper	Brooks		
420473001700	27.0430	-98.1916	25,12		Forest Oil Corporati	Ed Rachal Foundatn	Brooks	X	X
420470124900	26.9794	-98.0870	25,13	E,5	Humble Oil & Refinin	R J Kleberg Jr et al	Brooks	X	
420470126700	26.9481	-98.0032	25,14		Humble Oil & Refinin	R Kleberg Jr et al	Brooks		
422610022300	26.9015	-97.8232	25,15		Humble Oil & Refinin	Armstrong Charles M	Kenedy		
422610021900	26.8670	-97.6595	25,16		Humble Oil & Refinin	Armstrong Charles M	Kenedy		
422610034000	26.8996	-97.5938	25,17	F,3	Humble Oil & Refinin	J G Kenedy Jr	Kenedy	X	
427013000100	26.7638	-97.1927	25,18	G,6	Mobil Oil Corporatio	Sl 69027	North Padre Isl.	X	
422473148400	27.0467	-98.9257	26,1		Zachry H B Company	Zachry H B Fee	Jim Hogg	X	
422470152900	27.0556	-98.8285	26,2		Allen T M & Bemis J	D O Gallagher	Jim Hogg		
422473139400	26.9658	-98.7056	26,3	D,5	Texaco Incorporated	East A K Fee	Jim Hogg		
422470237100	26.9772	-98.5951	26,4		Sun Oil Company	Jones A C	Jim Hogg	X	
422470245900	26.9526	-98.4818	26,5		Humble Oil & Refinin	Sweeney Mrs Ophia F	Jim Hogg	X	

TWDB Report ## Final – Hydrostratigraphy of the Gulf Coast Aquifer from the Brazos River to the Rio Grande

API number	NAD27 latitude	NAD27 longitude	Dip section/ position	Strike section/ position*	Company	Lease	County	Lithology and water qual data	Paleo data
420473204100	26.9522	-98.3789	26,6		Mestena Operating Li	Bonita	Brooks	X	
420473163400	26.9160	-98.2824	26,7		Cometra Oil & Gas	Garcia 1	Brooks	X	
420473163900	26.8644	-98.2054	26,8		Shell Western E & P	Lips Barbara Gas Un	Brooks	X	
420473066200	26.8533	-98.1110	26,9	E,6	Exxon Corporation	Santa Fe Ranch	Brooks	X	
422610024800	26.7997	-97.9631	26,10		Humble Oil & Refinin	Santa Fe Ranch Julia	Kenedy	X	
422610025000	26.8417	-97.8537	26,11		Humble Oil & Refinin	Armstrong Charles M	Kenedy	X	
422610021000	26.7887	-97.6485	26,12	F,4	Humble Oil & Refinin	King Ranch Saltillo	Kenedy	X	X
422610026400	26.7829	-97.5074	26,13		Sinclair	M F Garcia	Kenedy		
422610029100	26.7391	-97.4190	26,14		Continental Oil Comp	St Tr 393	Kenedy	X	
425050228800	26.9172	-99.0413	27,1		Gulf Resources Inc.	Security Natinal Ban	Zapata	X	
425050274200	26.8541	-98.9567	27,2		Humble Oil & Refinin	Anastasio Garcia #1	Zapata		
422470225800	26.8656	-98.8407	27,3		Humble Oil & Refinin	Atwood E B	Jim Hogg		
422473227500	26.8245	-98.6818	27,4	D,7	Mestena Operating Li	Charco Nuevo	Jim Hogg	X	
422470237600	26.8010	-98.5677	27,5		Chizum Rhodes Hicks	Yzaguirra Eduardo	Jim Hogg	X	
422470249800	26.8049	-98.4269	27,6		Humble Oil & Refinin	Bass A M K	Jim Hogg	X	
422150000200	26.7568	-98.3245	27,7		Humble Oil & Refinin	McGill Bros	Hidalgo	X	
422150005400	26.7107	-98.2304	27,8		Union Oil Company Of	Lips C S	Hidalgo	X	
422150181400	26.6709	-98.1132	27,9	E,8	Humble Oil & Refinin	Santa Fe Ranch	Hidalgo	X	
422613004700	26.6819	-97.9627	27,10		Humble Oil & Refinin	Santa Fe Ranch Mula	Kenedy		
422610036100	26.7308	-97.7909	27,11		Humble Oil & Refinin	King Ranch Loma Prie	Kenedy	X	
422610027200	26.6378	-97.6948	27,12		Texas Company	Yturria Ld & Cattle	Kenedy	X	
422610027800	26.6836	-97.6205	27,13	F,5	Humble Oil & Refinin	King Ranch Tio Moya	Kenedy		X
422610027700	26.6509	-97.5278	27,14		Humble Oil & Refinin	King Ranch Tio Moya	Kenedy	X	X
422610028900	26.6629	-97.4725	27,15		Humble Oil & Refinin	King Ranch et al	Kenedy		
422610029400	26.6350	-97.3818	27,16		Gulf Oil Corporation	St Lse 48951	Kenedy	X	
427004000100	26.5071	-96.9304	27,17		Superior Oil Company	Ocs G02979	South Padre Isl.		
425050297300	26.7306	-99.1234	28,1		Jonnell Gas Company	Lopez (Heirs) #1	Zapata		
424270185900	26.7053	-98.8957	28,2		Clark Fuel Producing	Salinas Jose R	Starr		
424273084000	26.6219	-98.7722	28,3		Forest Oil Corporati	George Coates Est	Starr	X	
424270165700	26.6351	-98.6844	28,4	D,8	Clark Fuel Producing	Guerra Est V C	Starr	X	
424270103600	26.6583	-98.5370	28,5		Humble Oil & Refinin	Saenz Vicente	Starr	X	
422150021800	26.6047	-98.3036	28,6		Shell Oil Company	A. A. McAllen et al	Hidalgo		
422153142400	26.6030	-98.2356	28,7		Shell Western E & P	Beaurline A W	Hidalgo	X	

TWDB Report ## Final – Hydrostratigraphy of the Gulf Coast Aquifer from the Brazos River to the Rio Grande

API number	NAD27 latitude	NAD27 longitude	Dip section/ position	Strike section/ position*	Company	Lease	County	Lithology and water qual data	Paleo data
422150008100	26.5453	-98.1561	28,8		Shell Oil Company	A K Polis	Hidalgo		
422150010100	26.5148	-98.0662	28,9	E,10	Humble Oil & Refinin	W K Shepperd	Hidalgo	X	
422150194900	26.5389	-97.9926	28,10		Louisiana Land & Exp	A A McAllen et al	Hidalgo	X	X
424893061000	26.5491	-97.9370	28,11		Amoco Production Com	Corbett C M /B/	Willacy		
424890049800	26.4895	-97.8366	28,12		Abercrombie J S Comp	Garrett Gustin	Willacy	X	
424890046900	26.4801	-97.7614	28,13		Hunt H L	Wertz C E	Willacy		
424890005900	26.5098	-97.6418	28,14				Willacy		
424890066100	26.4309	-97.5464	28,15	F,7	Humble Oil & Refinin	Willamar Field Est	Willacy	X	X
424890008500	26.4428	-97.4372	28,16				Willacy		
424890064100	26.4115	-97.2945	28,17	G,8	Pan American Petrole	State Tract 569	Willacy	X	X
427003006000	26.4266	-97.0648	28,18		Genesis Petroleum Co	St Tr 01069-L Ne/4	South Padre Isl.		
424273128800	26.5460	-98.8891	29,1		Hawn Brothers Compan	Carmen G Garza et al	Starr	X	
424273165300	26.5358	-98.7763	29,2		Sun Exploration & Pr	Caffarelli	Starr		
424273178300	26.4699	-98.6558	29,3	D,9	Hilty Interests Inco	Burton et al	Starr	X	
424270471700	26.5064	-98.6047	29,4		Continental Oil Comp	Slick T B Est /B/	Starr		
422150067500	26.4189	-98.4877	29,5		C. G. Glasscock Oil	Daskam Oscar	Hidalgo	X	
422150080200	26.4310	-98.3931	29,6		Humble Oil & Refinin	Texan Development	Hidalgo		X
422150073600	26.4389	-98.2580	29,7		Hamman Oil & Refinin	Hamman John & Geo	Hidalgo	X	
422153117400	26.3807	-98.0929	29,8	E,11	Coloma Petroleum Inc	Hidalgo-Willacy Oil	Hidalgo	X	
422150109200	26.3862	-97.9682	29,9		Western Natural Gas	Patrick Emma	Hidalgo		
424890054800	26.3639	-97.8532	29,10				Willacy		
424890053800	26.4025	-97.7617	29,11		Stanolind Oil & Gas	Boden Mrs Lena	Willacy	X	
424890063800	26.3614	-97.6294	29,12		Kirkwood & Morgan In	Armendaiz	Willacy		
424890004900	26.3257	-97.5436	29,13	F,8	Texaco Incorporated	Yturria Land & Lives	Willacy	X	
420610001700	26.3016	-97.3978	29,14		Shell Oil Company	Continental Fee	Cameron	X	
420610002200	26.2785	-97.2736	29,15		Humble Oil And Refin	Laguna Madre St. Tr.	Cameron		
420610002900	26.3219	-97.2163	29,16	G,9	Gulf Oil Corporation	Gilbert Kerlin	Cameron		
427003001000	26.2005	-97.0906	29,17	G,10	Cities Service	Sl 70411	South Padre Isl.	X	
424273296400	26.3002	-98.7491	30,1		Neuhaus V F et al	Irene Sheerin-Texas	Starr		
424273268600	26.2751	-98.6703	30,2		Transtexas Gas Corpo	Garcia Heirs Gas Uni	Starr		
424273267200	26.3151	-98.6072	30,3	D,11	Southwest Oil & Land	Mckim-Alvarez	Starr		
422153002800	26.2524	-98.5391	30,4		Pioneer Corporation	Garcia L&L	Hidalgo		

TWDB Report ## Final – Hydrostratigraphy of the Gulf Coast Aquifer from the Brazos River to the Rio Grande

API number	NAD27 latitude	NAD27 longitude	Dip section/ position	Strike section/ position*	Company	Lease	County	Lithology and water qual data	Paleo data
422153105900	26.2399	-98.4774	30,5		Esenjay Petroleum Co	King Ralph et al	Hidalgo	X	
422150158100	26.2468	-98.3065	30,6		Continental Oil Comp	Talbot M L	Hidalgo	X	X
422150186000	26.1785	-98.2048	30,7		Tenneco Oil Company	McAllen Fieldwide	Hidalgo	X	
422153090100	26.1245	-98.1073	30,8	E,14	Atlantic Richfield C	Buchanan Gas Unit	Hidalgo	X	
422150119900	26.2083	-98.0139	30,9		Continental Oil Comp	De Los Thompson	Hidalgo	X	
422150117000	26.1297	-97.9401	30,10		Bettis & Shepherd	Baingo J F Unit	Hidalgo	X	
422150116100	26.2022	-97.8723	30,11		Magnolia Petroleum C	D. J. Schwarz	Hidalgo	X	
420610009700	26.1332	-97.7762	30,12		Pan American Petrole	Wentz Milton E	Cameron	X	
NOAPI 974	26.1831	-97.6897	30,13		A. & T. Drilling Com	Sw Packing Co. Water	Cameron		
420610009400	26.1455	-97.6384	30,14		Superior Oil Company	San Benito Unit 11	Cameron		
420613001600	26.1969	-97.5758	30,15	F,9	California Company T	Jose Rodriguez	Cameron	X	X
420613046300	26.1591	-97.4748	30,16		London Petroleum Cor	Gibbons	Cameron	X	
420613004000	26.0650	-97.4039	30,17		Dow Chemical Company	Conoco Fee	Cameron		
420613050000	26.1359	-97.2926	30,18		Texas Fuel Company	State Tract 726	Cameron	X	
420613046400	26.0547	-97.1994	30,19		Adobe Oil & Gas Corp	St Tr 667	Cameron	X	
426000000200	26.0467	-97.1082	30,20	G,11			South Padre Isl.	X	X
422470237200	26.8998	-98.6200		D,6	Sun Oil Company	A C Jones	Jim Hogg		
424273232200	26.3974	-98.6442		D,10	Harper Hefte Incorpo	La Brisa L & C Co	Starr		
421750192800	28.6276	-97.7006		D',2	Viking Drilling Comp	J W Ray Estate	Goliad	X	
420253003100	28.4987	-97.7918		D',4	Atlantic Richfield C	J R Dougherty Est	Bee		
420250166500	28.4902	-97.8730		D',5	Mim Oil Co	Holzmark C #C4	Bee	X	
422970216900	28.2334	-98.0050		D',7	Oil & Gas Reserves I	C N Freeman	Live Oak	X	
422973268100	28.1145	-98.1712		D',9	Sanchez-Obrien Oil &	Jones B M	Live Oak	X	
421313789500	27.8874	-98.4401		D',11	Hanson Production Co	Welder Heirs	Duval	X	
421313772000	27.7494	-98.5493		D',12	Beach Exploration In	Hoffman	Duval	X	
421313398000	27.5583	-98.6335		D',14	Blocker Exploration	Rob Driscoll et al	Duval	X	
424733043100	29.7969	-96.0035		D",2	Irvine Oil	Holzaepfel Chris Car	Waller		
420153023100	29.7633	-96.0963		D",3	Edwards O&G Co	Frank Hubenak Unit	Austin		
NOAPI 18752	29.6049	-96.4677		D",7			Colorado		
420890057200	29.4590	-96.5904		D",9			Colorado		
422850030800	29.3173	-96.7854		D",11	Hawkins H L Jr	E P Zock	Lavaca	X	
422853146400	29.2514	-96.9097		D",12	Petrosil Exploration	Cornelius	Lavaca	X	
421233162200	29.0698	-97.0837		D",14	Bhp Petroleum (Ameri	Pridgen J E	De Witt	X	

TWDB Report ## Final – Hydrostratigraphy of the Gulf Coast Aquifer from the Brazos River to the Rio Grande

API number	NAD27 latitude	NAD27 longitude	Dip section/ position	Strike section/ position*	Company	Lease	County	Lithology and water qual data	Paleo data
421230082400	28.9560	-97.3879		D",16	Brazos Oil & Gas Com	L C Sievers et al	De Witt	X	
421753159300	28.7773	-97.4671		D",18	Cline Walter D Jr	Meyer Lillie	Goliad	X	
421770028700	28.7576	-97.5928		D",19	Amerada Petroleum Co	Morgan & Kunetka	Gonzales	X	
421313586900	27.5097	-98.7137		D,D',1,15	H-M Oil Company	Dinn Elva L	Duval	X	
420473167100	27.2243	-98.0545		E,3	Cross Timbers Operat	Noll Marvin R	Brooks	X	
422150007700	26.7806	-98.1235		E,7	Socony Mobil Oil Com	Doughty Grace	Hidalgo	X	X
422150008300	26.6068	-98.1134		E,9	Argo Oil Company	Guerra D V	Hidalgo	X	
422150102400	26.3201	-98.0818		E,12	Union Producing Comp	Aderhold Unit	Hidalgo		
422150104100	26.2533	-98.0561		E,13	Union Producing Comp	P Anderson	Hidalgo	X	
422150203900	26.0440	-98.0411		E,15	Shell Oil Company	W H Drawe	Hidalgo	X	
420253002700	28.1686	-97.5554		E',3	Varn Petroleum Compa	Willie Murphy	Bee		
423553269800	27.7001	-97.8956		E',7	Union Pacific Resour	Elliff J S et al	Nueces		
422730050000	27.5098	-97.9708		E',9	Humble Oil & Refinin	King Ranch Borregos	Kleberg	X	X
421573151300	29.5720	-95.4666		E",1	American Hunter Expl	Tennant J A	Fort Bend	X	
420390001500	29.5420	-95.3598		E",2	Humble Oil & Refg Co	Massey C W Et Ux	Brazoria	X	
421573191300	29.3655	-95.7446		E",4	Amax Oil & Gas Incor	Landgrant	Fort Bend	X	
424813335000	29.3135	-95.9247		E",6	Keck, W. M. II	Gallia, A. A.	Wharton		
424810280200	29.1361	-96.0908		E",9	Brazos Oil & Gas Co	John Britton	Wharton	X	
424810189100	29.1118	-96.3115		E",10	Humble Oil & Refg Co	Greenebaum R	Wharton	X	
422390081600	28.9980	-96.4703		E",12	Tex-Star Oil & Gas C	Copsey Bertha	Jackson	X	
422390193600	28.8879	-96.5873		E",13	Howell H H	Lon R Drushel	Jackson	X	
NOAPI 992	28.8203	-96.7733		E",15	Crowell Drilling	Rovi Farms	Victoria		
423913025600	28.5020	-97.1724		E",18	Shenandoah Oil Corpo	Mary A Shay	Refugio		
422490282400	27.4066	-98.0751		E,E',1,10	Magnolia Petroleum C	Seeligson Unit	Jim Wells		
424890006300	26.5815	-97.6194		F,6	Humble Oil & Refinin	Sauz Ranch-Jardin	Willacy	X	
420610012400	26.0845	-97.5350		F,10	Humble Oil & Refinin	Cameron Co Wtr	Cameron	X	X
420610012500	25.9527	-97.5331		F,11	The Texas Company	P. J. Davis	Cameron	X	
424090395200	28.0284	-97.2785		F',2	Socony Mobil Oil Com	Bren Agnes E	San Patricio		X
423550629100	27.7058	-97.4283		F',5	Pan American Petrole	U S A	Nueces		
420390448100	29.2339	-95.1528		F",1	Midwest Oil	Houston Farms Dev	Brazoria	X	
420390426500	29.2289	-95.3178		F",2	Humble Oil & Refinin	R W Vieman	Brazoria		X
420390446700	29.1078	-95.4548		F",3	Humble Oil & Refinin	Retrieve State Fa	Brazoria	X	
420390388800	29.0863	-95.5566		F",4	Humble Oil & Refinin	Byers Ward et al	Brazoria		
420390406900	29.0140	-95.7016		F",6	Pan American Petrole	B R L D	Brazoria	X	

TWDB Report ## Final – Hydrostratigraphy of the Gulf Coast Aquifer from the Brazos River to the Rio Grande

API number	NAD27 latitude	NAD27 longitude	Dip section/ position	Strike section/ position*	Company	Lease	County	Lithology and water qual data	Paleo data
423210112000	28.8698	-95.9043		F",9	Magnolia Petroleum C	Ethel Cornelius	Matagorda	X	
423210211900	28.8648	-96.0674		F",10	Humble Oil & Refinin	J C Lewis	Matagorda	X	
423210204300	28.8270	-96.1295		F",11	Humble Oil & Refinin	S El Maton Gas Un 1	Matagorda	X	
423213099600	28.7114	-96.2525		F",12	Crest Resources & Ex	Palacios Ind St Un2	Matagorda	X	
423210237100	28.6474	-96.2965		F",13	Skelly Oil Company	Gulf D	Matagorda		
420570087200	28.5766	-96.4785		F",15	Humble Oil & Refinin	Elizabeth K Hardie	Calhoun	X	
420573087600	28.4433	-96.5187		F",16	Energy Development C	Powderhorn Ranch	Calhoun	X	
420070000600	28.2702	-97.0353		F",18			Aransas		X
426013011700	27.0151	-97.3449		G,4	Amoco Production Com	Sl 80477 Pn 1045-S	North Padre Isl.	X	
427003000400	26.4808	-97.1727		G,7	Mobil Oil Corporatio	Sl 68114	South Padre Isl.	X	
423550657700	27.6198	-97.2303		G',5	Cherryville Corp	Burton Dunn et al	Nueces		X
422730056500	27.5237	-97.3048		G',6	American Petrofina I	St Tr 168	Kleberg		X
422730177800	27.3221	-97.3871		G',8	Shell Oil Company	State Tr 206	Kleberg	X	X
422610006000	27.2025	-97.3909		G',10	Sun Oil Company	St Tr 228	Kenedy		
426043002400	28.8006	-95.4407		G",3	Union Texas Petroleu	Sl 68919	Brazos		
426040000600	28.6982	-95.7245		G",5	Gulf Oil Corporation	St Tr 00475-S	Brazos		
427043019500	28.4418	-96.0077		G",8	Cities Service	Sl 77337	Brazos		
427033020800	28.3999	-96.0869		G",9	Pennzoil Exploration	St Tr 00486-L Se/4	Matagorda Isl.		
427033031200	28.3665	-96.1307		G",11	Amoco Production Com	Sl 79414	Matagorda Isl.		
427033023100	28.2720	-96.2944		G",12	Mesa Petroleum Compa	St Tr 00559-L Se/4	Matagorda Isl.		
424810138700	29.3160	-96.4977			Sunray D-X Oil Co.	Maude Wallace	Wharton	X	
424810140100	29.2068	-96.5319			Harry Todd	G.G. Kelly Est.	Wharton	X	
424810114000	29.3538	-96.1807			Trice Production Co.	J.H.H. Dennis	Wharton	X	
424810067100	29.2567	-95.8896			Texas Gulf Sulfur Co	W.T. Taylor	Wharton	X	
	29.2955	-95.9811			Smith Bros.	L.N. Eldridge	Wharton	X	
	29.4275	-95.9993					Wharton	X	
420890023700	29.5106	-96.4336			Shell Oil Co.	Kyle Est.	Colorado	X	
420890035400	29.6857	-96.5991			Warren Oil Corp.	Joe Honak	Colorado	X	
420890044800	29.4578	-96.4095			Chicago Corp. & Skel	Dennis	Colorado	X	

TWDB Report ## Final – Hydrostratigraphy of the Gulf Coast Aquifer from the Brazos River to the Rio Grande

API number	NAD27 latitude	NAD27 longitude	Dip section/ position	Strike section/ position*	Company	Lease	County	Lithology and water qual data	Paleo data
420890044800	29.5575	-96.5895			Sinclair Oil & Gas C	A-1 H.R. Houck	Colorado	X	
420890001500	29.8358	-96.5197			Sinclair Prarie Oil	Tulane Gordon	Colorado	X	
420890044000	29.5643	-96.6001			Delhi-Taylor Oil Cor	L.B.Jenkins	Colorado	X	
	29.8420	-96.3035			Kirby Petroleum	Herring	Austin	X	
	29.9323	-96.4057			Cockburn-Hargrove &	Huebner	Austin	X	
	29.9682	-96.1809			Deering & Kayser	Clinton	Austin	X	
420150062400	29.9725	-96.3528			Sun Oil Co. & The Te	Mikeska	Austin	X	
	30.0601	-96.4716			Phillips Pet. Co.	Shul	Austin	X	
	29.6409	-96.1199			Southern Natural Gas	Frank Uhyrek	Austin	X	
	29.8321	-96.2877			The Texas Company	Kollatschny	Austin	X	
	30.0254	-96.4333			Pure Oil Co.	Stepan	Austin	X	
	29.8923	-96.4283			Magnolia Pet. Co.	Amelia Wrangler	Austin	X	
422390109000	28.9451	-96.4529			Dorfman Production &	A.A. Egg	Jackson	X	
422390313800	28.7246	-96.5577			Humble Oil & Refinin	Lig Baue	Jackson	X	
422393073600	28.7086	-96.5060			Superior Oil Co.	W.L. Traylor	Jackson	X	
422390191700	28.8782	-96.6189			Howell & Mayfair Min	Frances Koop "B"	Jackson	X	
	29.0207	-96.6904			H.H. Howell, Cox & R	Ben N. Good	Jackson	X	
422390001400	29.0841	-96.8743			Sun Oil Company	McDaniel	Jackson	X	
422390009800	29.1597	-96.6976			J.A. Gray	Flourney	Jackson	X	
422390051500	29.0439	-96.5547			H.H.Howell & Rudman,	Jackson Estate	Jackson	X	
422390051500	29.0594	-96.5803			Humble Oil & Refinin	R.F. Kubeka	Jackson	X	
422390142700	28.8323	-96.3620			Sun Oil Company	Kuppinger	Jackson	X	
422390199200	28.8515	-96.5677			K&H Operating Co.	Mitchell	Jackson	X	
422390195500	28.8664	-96.5913			Carthy Land & Miller	Simons	Jackson	X	
422390191000	28.8661	-96.6513			H.H. Howell, et al.	Koop Brothers	Jackson	X	
422390192500	28.8579	-96.6559			Lively & Fountain	Shutt	Jackson	X	
	28.8593	-96.6776			Howell & Wilson, Et	Francis Koop	Jackson	X	
422390190600	28.8721	-96.6884			Howell & Rudman	Pure Oil Company	Jackson	X	
	28.9732	-96.4020			Seaport Oil	Mauritz	Jackson	X	
422390045700	29.0224	-96.6453			John F. Camp	Wofford & Gayle	Jackson	X	
422390023300	29.0542	-96.6321			Cecil B. Burton, Et	F.L. Swanson	Jackson	X	
	28.9269	-96.6945			H.H. Howell	Drushel	Jackson	X	
	28.8809	-96.6441			D.C. Arnold, Trustee	Drushel	Jackson	X	
422390191500	28.8780	-96.6545			Hammonds & Logue-Pat	Arnold Koop	Jackson	X	

TWDB Report ## Final – Hydrostratigraphy of the Gulf Coast Aquifer from the Brazos River to the Rio Grande

API number	NAD27 latitude	NAD27 longitude	Dip section/ position	Strike section/ position*	Company	Lease	County	Lithology and water qual data	Paleo data
422390155400	28.9476	-96.7467			Arnold, Sinclair & Z	Dinkans	Jackson	X	
422390195200	28.8750	-96.5941			Texkan Oil Co.	Willie Clay Simons	Jackson	X	
422390322200	28.7117	-96.4377			Alcoa Mining Co.	W.F. Weed	Jackson	X	
422390322800	28.7398	-96.4024			Alcoa Mining Co.	Parfit	Jackson	X	
422390009200	29.1808	-96.7012			Gus Glasscock, Inc.	O.B. Fenner Unit # 1	Jackson	X	
	29.1790	-96.7014			Magnolia Petroleum C	O.B. Fenner	Jackson	X	
422390006200	29.1988	-96.6660			Skelly Oil Co.	J.H. Fenner	Jackson	X	
422390009400	29.1594	-96.7383			H.L. Brown	Helen Stafford	Jackson	X	
422390012000	29.1421	-96.5859			H.J. Porter	Wearden	Jackson	X	
422390001600	29.0586	-96.8954			Magnolia Pet. Co.	Aaron Kolle	Jackson	X	
	29.0609	-96.8244			Magnolia Pet. Co.	Robinson	Jackson	X	
422390004200	29.0466	-96.8064			Russell Maguine	J.H. Robinson Ranch	Jackson	X	
422390001700	29.0561	-96.8386			G.S. Hammonds	Robinson	Jackson	X	
422390003300	29.0990	-96.7837			Salem Oil Corp.	Henderson	Jackson	X	
422390030900	29.1316	-96.6861			H.R. Smith	L.R. Hollingsworth	Jackson	X	
422390152000	28.7928	-96.4531			Garrett & Wilder	L. Ranch	Jackson	X	
	29.1755	-96.7669			Magnolia Petroleum C	Annie Vaughn	Jackson	X	
	28.9572	-96.7110			Texana Petroleum Cor	Wes Rogers	Jackson	X	
422390331000	29.1565	-96.7656			Magnolia Petroleum C	C. Holzheuser	Jackson	X	
423210254700	28.7491	-95.8769			The Texas Company	Baer Estate	Matagorda	X	
423210098800	28.9942	-96.0210			Sun Oil Company	Braman	Matagorda	X	
423210208800	28.8985	-96.1361			Sun Oil Co.	Clara Juneke	Matagorda	X	
423210216200	28.7565	-96.0259			Magnolia Petroleum C	W.W. Rugeley	Matagorda	X	X
	28.4470	-96.1929			Western Natural Gas	State Tract 608	Matagorda	X	
423210107500	28.8707	-95.7813			Gulf Oil Co.	H.B. Hawkins, et al.	Matagorda	X	
423210278600	28.4685	-96.3598			Shell Oil Co.	State Tract 143	Matagorda	X	
423210130600	28.9806	-96.1599			Magnolia Petroleum C	Kountze	Matagorda	X	
423210000300	29.0121	-96.1608					Matagorda	X	
	28.6481	-96.2814					Matagorda	X	
423010250700	28.6372	-96.0751			The Texas Company	Pierce Estate	Matagorda	X	
	29.1147	-95.9761			Stanolind Oil & Gas	Pierce Estate	Matagorda	X	
	28.7735	-95.8359			Magnolia Pet. Co. &	Le Tulle	Matagorda	X	
423210083800	28.9823	-95.7929			Humble Oil & Refinin	First City Nat. Bank	Matagorda	X	
422850001000	29.5457	-96.9829			Seaboard Oil Co.	Emma Sebastian	Lavaca	X	

TWDB Report ## Final – Hydrostratigraphy of the Gulf Coast Aquifer from the Brazos River to the Rio Grande

API number	NAD27 latitude	NAD27 longitude	Dip section/ position	Strike section/ position*	Company	Lease	County	Lithology and water qual data	Paleo data
422850002900	29.5229	-96.7987			George Strake	Wolfsdorff	Lavaca	X	
422850003000	29.5005	-96.7342			Tidewater Oil Co.	Baum	Lavaca	X	
422850019100	29.4860	-96.8314			Horrigan & Fohs	Martisak	Lavaca	X	
	29.3394	-96.9246			Magnolia Petroleum C	Theo Long	Lavaca	X	
	29.1816	-96.9826			Sterling Oil & Refin	Seekamp	Lavaca	X	
	29.1861	-96.9574			Sterling Oil & Refin	Goodrich	Lavaca	X	
422850047500	29.1891	-96.8824			Shell Oil Co.	D.E. Kessler	Lavaca	X	
422850001000	29.5457	-96.9829			Union Producing Co.	W. Borchers	Lavaca	X	
422850043100	29.1841	-96.8272			Shell Oil Company	William Borchers	Lavaca	X	
422850044600	29.1627	-96.8655			Pure Oil Company	O.A. Pohl	Lavaca	X	
420893042700	29.3837	-96.4307			Prairie Producing Co	Stovall, et al.	Colorado	X	
420890071800	29.4924	-96.4298			Shell Oil Co.	Hurd	Colorado	X	
420890027000	29.5738	-96.2896			Shell Oil Co.	Martin	Colorado	X	
420890034500	29.7101	-96.5260			Sinclair O&G Co.	Gegenworth	Colorado	X	
420890052700	29.4777	-96.5822			Standard O&G Co.	Hoemeyer	Colorado	X	
420893059400	29.6862	-96.3142			Apexco Inc.	Meir	Colorado	X	
420893057000	29.6047	-96.4675			Buttes Resources Co.	Tate Gas Unit	Colorado	X	
420890097000	29.6121	-96.3701			Cico O&G Co.	Winterman	Colorado	X	
420893102900	29.5546	-96.3586			Florida Gas	Monahan	Colorado	X	
420893122100	29.5755	-96.6782			K B Explor. Co.	Fondren Est.	Colorado	X	
420893151000	29.6217	-96.8445			Getty Oil	Berger	Colorado	X	
420893134800	29.4117	-96.6144			Forney	Frapart	Colorado	X	
420893193400	29.5069	-96.4673			Padon Oil Operations	Wright	Colorado	X	
420893137600	29.6296	-96.2629			Energetics, Inc.	Willis	Colorado	X	
420893107600	29.6389	-96.2126			Dow Chemical Co.	Kaechele	Colorado	X	
420890008800	29.8041	-96.3885			Huddle & Rock Hill O	Tipp	Colorado	X	
420890072400	29.4955	-96.3507			Brazos Oil & Gas Co.	Gracey	Colorado	X	
424810002000	29.5434	-96.2491			Magnolia Pet. Co.	Lee	Wharton	X	
424810094300	29.4387	-96.1380			Texas Gulf Sulphur	Northington	Wharton	X	
424813384400	29.3938	-96.0186			Chevron Usa, Inc.	Chevron-Winston Et A	Wharton	X	
424813326000	29.3588	-96.2301			Dan A. Hughes Co.	Koonce Unit	Wharton	X	
424813376900	29.3473	-96.3115			Amerada Hess Corp.	Schumaker	Wharton	X	
424810147800	29.1984	-96.3991			Anderson & Cooke	Bergstrom	Wharton	X	
424810227200	29.1455	-96.1908			Cherosage	Danielson	Wharton	X	

TWDB Report ## Final – Hydrostratigraphy of the Gulf Coast Aquifer from the Brazos River to the Rio Grande

API number	NAD27 latitude	NAD27 longitude	Dip section/ position	Strike section/ position*	Company	Lease	County	Lithology and water qual data	Paleo data
424813252100	29.2746	-95.9333			Sisco Oil Producers,	Hawes	Wharton	X	
423210034100	29.1031	-95.9048			Union Oil of Califor	Armour	Matagorda	X	
423210011600	29.0807	-96.0384			Arkansas Fuel Oil Co	Crouch	Matagorda	X	
423210061200	29.1612	-95.8481			Humble O&R Co.	Armour Or Pierce	Matagorda	X	
423210196700	28.7581	-96.1562			The Ohio Oil Co	Kubela	Matagorda	X	
423213115900	28.9395	-96.0503			Natomas North Americ	O'connor Estate	Matagorda	X	
423210102600	28.9845	-95.9488			Stanolind Oil & Gas	Thompson Unit	Matagorda	X	
423210262100	28.9215	-95.8927			Humble O&R Co.	Huebner	Matagorda	X	
423210256600	28.7346	-95.8853			Texas Gulf Sulfur Co	Fee Davis & Cooken 8	Matagorda	X	
423210067100	29.0604	-95.8302			Humble O&R Co.	Truitt & Gravier	Matagorda	X	
423213082100	28.9513	-95.6917			Hawkins	Kee	Matagorda	X	
423210013200	29.0387	-96.0144			The Ohio Oil Co	Ohio-Sun Swd Well	Matagorda	X	
423210083600	28.9498	-95.7765			British-American Oil	M. B. Guess	Matagorda	X	
423210082800	28.8570	-95.6663			Guilf Oil Corporatio	Sanborn	Matagorda	X	
420890075500	29.4186	-96.4794			Shell Oil Co, Inc.	Schulering	Colorado	X	
420893022900	29.7491	-96.3764			Julian Evans	Truchard	Colorado	X	
420893027400	29.5543	-96.7358			Zoller & Dannenberg,	Tagge, et al	Colorado	X	
420893024500	29.3068	-96.5304			Hll Production Co.	Harfst	Colorado	X	
420890067400	29.3567	-96.5467			Crescent O&G Corp.	Kallina	Colorado	X	
420890048400	29.4907	-96.6833					Colorado	X	
420890043600	29.5928	-96.5857			Sinclair Prairie Oil	Glasscock	Colorado	X	
424810067200	29.2568	-95.8807			Texas Gulf Sulphur C	Bassett	Wharton	X	
424810128800	29.2607	-96.2604			Daubert & Hiawatha	Dorotik	Wharton	X	
424813307900	29.3446	-96.2685			Hughes Texas Pet	Miller	Wharton	X	
424813010500	29.5162	-96.1259			Getty Oil Co.	Leveridge	Wharton	X	
424810136700	29.2641	-96.4172			Cherosage	Wendel	Wharton	X	
424813058100	29.2893	-96.5298			McCormick Dig & Sola	Hancock	Wharton	X	
424810098900	29.4378	-96.0744			Gray Oil Co.	Hungerford Unit 1	Wharton	X	
424810354400	29.0308	-96.3747			Weltman & Peterek	Seeley	Wharton	X	
424810140900	29.1582	-96.5309			West Pet. Corp., Et.	Blaylock	Wharton	X	
424810355000	29.2031	-96.4661			Texas O&G Corp.	Hensley	Wharton	X	
424813162200	29.4963	-96.0361			Total Petroleum, Inc	Means	Wharton	X	
424810170200	29.1411	-96.4616			Garvey	Meneffe	Wharton	X	
424813336500	29.2223	-96.0182			Arkla Exploration Co	Fields	Wharton	X	

TWDB Report ## Final – Hydrostratigraphy of the Gulf Coast Aquifer from the Brazos River to the Rio Grande

API number	NAD27 latitude	NAD27 longitude	Dip section/ position	Strike section/ position*	Company	Lease	County	Lithology and water qual data	Paleo data
424813337700	29.4113	-96.1361			Greenhill Pet. Corp.	Meriwether(Edna Maye	Wharton	X	
424813127300	29.2207	-96.1851			Rio Bravo Oil Co.	Pierce Estate	Wharton	X	
424813169200	29.5876	-96.2234			Cico O&G Co.	Adkins Unit	Wharton	X	
423210257700	28.6903	-95.7994			Union Producing	State Tract 100	Matagorda	X	
423210214800	28.8233	-96.0383			Phillies Pet Co.	Pierce Estate	Matagorda	X	
423210077400	28.9039	-95.6453			Cockrell	Craig	Matagorda	X	
423210257800	28.7264	-95.7642			Union Producing	State Tract 77	Matagorda	X	
423213017100	28.7658	-95.8356			Dow Chemical	Letville Est.	Matagorda	X	
423213098000	28.5711	-96.2903			Pennzoil Producing C	State Tract 195	Matagorda	X	
423210262600	28.9190	-96.1599			Coastal States	Ferguson	Matagorda	X	
423210214700	28.8394	-96.0703			Halbouty	Pierce Est.	Matagorda	X	
423210171200	28.9914	-96.2483			Barnsdall Oil Co.	Duffy	Matagorda	X	
423210030800	29.1443	-95.8759			Pan American	Runnells, Jr.	Matagorda	X	
423210251700	28.5100	-96.1784			The Texas Company	Nuebner	Matagorda	X	
423210257600	28.6889	-95.8084			Union Producing Co.	State Tract 118	Matagorda	X	
423210111400	28.8743	-95.9201			Magnolia Pet. Co.	Sabage	Matagorda	X	
423213040500	29.3445	-96.2673			Davis Oil Co.	Wilkinson	Matagorda	X	
423213127300	28.6785	-96.1672			Exxon Co., Usa	Le Tulle Green	Matagorda	X	
423210277300	28.6355	-96.0546			Union Oil Co. of Cal	State Tract 28	Matagorda	X	
	29.3743	-95.7214					Fort Bend	X	
421570137400	29.4338	-96.0091			Knight & Croom	Allen	Fort Bend	X	
421570094000	29.6984	-95.7142			Standard Oil of Texa	Wing et al	Fort Bend	X	
421570135000	29.7259	-95.9832			Halbouty	Frost	Fort Bend	X	
	29.5724	-95.9856			Sterling Oil & Reini	Dusek	Fort Bend	X	
421573038600	29.6204	-95.7062			Hunt Oil Co.	Harlem State Prison	Fort Bend	X	
421570134900	29.7185	-95.9857			Humphreys Oil & Gas	Cooper	Fort Bend	X	
421570099600	29.7466	-95.8044			Union Producing Co	Reed	Fort Bend	X	
421570188700	29.4755	-95.7458			Gulf Oil Corp.	Davis	Fort Bend	X	
421570197400	29.4962	-95.6470			Humble O&R Co.	George	Fort Bend	X	
420390191000	29.2581	-95.5375			Tidewater	Ramsey Prison Farm	Brazoria	X	
420390387800	29.1203	-95.5998			Glenn McCarthy	Marmion	Brazoria	X	
	29.0364	-95.7416			Abercrombie Co	B.R.L.D.	Brazoria	X	
420390103200	29.2820	-95.1928			Phillips Pet. Co.	Houston "X"	Brazoria	X	

TWDB Report ## Final – Hydrostratigraphy of the Gulf Coast Aquifer from the Brazos River to the Rio Grande

API number	NAD27 latitude	NAD27 longitude	Dip section/ position	Strike section/ position*	Company	Lease	County	Lithology and water qual data	Paleo data
420390090300	29.3426	-95.2210			Phillips Pet. Co.	Bernadine	Brazoria	X	
420390387800	29.1203	-95.5998			McCarthy	Andru	Brazoria	X	
420390096500	29.3296	-95.2384			Phillips	Houston Farms	Brazoria	X	
	29.2724	-95.7549			Progress Pet. Co, Of	Gulf Fee	Brazoria	X	
	28.9136	-95.1769			Humble O&R Co.	State Lease	Brazoria	X	
	29.1377	-95.6456			Texas Water Wells	Water Well (West Col	Brazoria	X	
420390098400	29.3188	-95.2431			Phillips Pet. Co	Houston "M"	Brazoria	X	
420390392700	29.0917	-95.7177			Hessie Hunt Trust	Stone	Brazoria	X	
	28.9684	-95.3888			Dow Chemical Co.	Freeport Mineral Co.	Brazoria	X	
424810188500	29.1113	-96.2928			Humble O&R Co.	Nicoles	Wharton	X	
424810138700	29.3158	-96.4975			Sunray D-X Oil Co.	Wallace	Wharton	X	
	29.0538	-96.3917			Chambers & Kennedy,	Lancaster	Wharton	X	
	29.4122	-96.2530			Acco O&G Co.	Sand Ridge Baptist C	Wharton	X	
	29.1594	-96.1606			Texaco Inc.	E. M. Redwine 'B'	Wharton	X	
	28.8991	-95.7583			Stanglind-Skelly-Fla	Fall	Matagorda	X	
423210033700	29.0781	-95.9101			F. William Carr	Tyree	Matagorda	X	
423210168300	28.9444	-96.1297			Placid Oil Co.	Louis Le Tulle	Matagorda	X	
	28.9719	-96.0082			H&S Water Well Servi	Lera	Matagorda	X	
	29.0193	-96.1474			H. H. Johnson	H. H. Johnson Water	Matagorda	X	
	28.9791	-95.5600			A.T.Grabowski & L.W.	D.I.Lows	Brazoria	X	
	28.9943	-95.4733			Socony-Mobil Oil Co.	Dingle	Brazoria	X	
420153071600	30.0317	-96.4209			Rme Petroleum Co.	Ellers Unit	Austin	X	
420393256500	29.0636	-95.3490			Seminole Pipeline Co	Amoco Chem. Co.	Brazoria	X	
	29.5077	-95.2501			Amoco Production Com	West Hastings Unit	Brazoria	X	
420393189100	28.9178	-95.5368			Terry Oil Corp.	Poole	Brazoria	X	
420393240800	29.1429	-95.2291					Brazoria	X	
	29.4199	-95.4471			Cenergy Exploration	I.P. Farms - A	Brazoria	X	
	29.4199	-95.4471			Cenergy Exploration	I.P. Farms - B	Brazoria	X	
420390426300	29.2418	-95.3301			Humble O&R Co.	South Texas Dev. Co.	Brazoria	X	
420393229400	29.1066	-95.3112			Ultramar O&G LIP.	Sharp Corp.	Brazoria	X	
420893112000	29.4467	-96.5592			American Energy Capi	Hildebrand	Colorado	X	
420893161100	29.6871	-96.7889			Columbia Gas Develop	Dahse Unit	Colorado	X	
420893128700	29.5531	-96.6382			Tdc Exploration, Inc	Pargac	Colorado	X	
420893100100	29.4904	-96.6369			Shell Oil Company	Sheridan Unit	Colorado	X	

TWDB Report ## Final – Hydrostratigraphy of the Gulf Coast Aquifer from the Brazos River to the Rio Grande

API number	NAD27 latitude	NAD27 longitude	Dip section/ position	Strike section/ position*	Company	Lease	County	Lithology and water qual data	Paleo data
420893193200	29.5550	-96.7483			Dynamic Production,	Scott	Colorado	X	
420893181000	29.7587	-96.5684			Oxy U.S.A. Inc.	Columbus Field Unit	Colorado	X	
421573196100	29.7537	-95.8068			Western Gas Resource	Katy	Fort Bend	X	
421573200200	29.4494	-95.5653			Exxon	Lockwood	Fort Bend	X	
421573116500	29.5129	-95.6921			Arco O&G	George Foundation	Fort Bend	X	
421573173200	29.5644	-95.9702			Chevron U.S.A., Inc.	Moore	Fort Bend	X	
421573169500	29.6274	-95.9783			Southeastern Pipe Li	Talley	Fort Bend	X	
421573181500	29.2925	-95.8593			Union Exploration Pa	Giese	Fort Bend	X	
422853177700	29.5632	-96.8412			Arco Exploration Co.	Williams	Lavaca	X	
422853169100	29.1218	-96.9721			Union Texas Pet. Co.	Lampley	Lavaca	X	
422853195700	29.6211	-96.8903			Gat Oil U.S.A., Inc.	West Dubina Gas Unit	Lavaca	X	
422853135900	29.4542	-96.9284			Howell Drilling, Inc	Leopold	Lavaca	X	
422853208000	29.2370	-96.7653			C.J. Crawford	Cullen Unit	Lavaca	X	
	30.1988	-96.0914			Shell Oil Co.	Chapmon	Waller	X	
424733043200	30.1787	-96.0143			Conoco	Wiggins Gas Unit	Waller	X	
424733058700	29.7793	-96.0099			Prime Natural Resour	High Rabedian Unit	Waller	X	
424813307900	29.3444	-96.2682			Hughes Texas Petrole	Lise Et. Sl.	Wharton	X	
424813327400	29.3302	-96.2922			Dan A. Hughes Co.	L.B. Outlar	Wharton	X	
424813211700	29.3025	-95.8959			Willco Oil Co.	Frank Sitta	Wharton	X	
424813352200	29.3143	-95.9366			Tuscar (Texas) Inc.	Arco Fee	Wharton	X	
422390300000	28.7842	-96.6876			Ken Petroleum Corp.	Bennett	Jackson	X	
	29.2074	-95.6125			Quintana Pet. Corp.	White ET. AL.	Brazoria	X	
	29.0242	-95.6530					Brazoria	X	
420393012200	29.1030	-95.5210			Mobil Oil Corp.	Smith ET. AL.	Brazoria	X	
421570113700	29.5664	-95.9937			Sterling Oil & Refin	Dusek	Fort Bend	X	
	29.6654	-95.8516			Magnolia Petroleum &	McKennon	Fort Bend	X	
	29.4082	-95.7807			Apache Corp.	Annie Zich	Fort Bend	X	
	29.5629	-95.8046			Katy Drilling Co.	City of Rosenberg	Fort Bend	X	
	29.4217	-95.6125			Quintana Pet. Co.	George	Fort Bend	X	
	29.3265	-95.7450			Texaco, Inc.	Batchelor	Fort Bend	X	
	29.4993	-95.9247			Layne Texas Co., Inc		Fort Bend	X	
	29.5001	-95.6472			Humble Oil & Refinin	A.P. George	Fort Bend	X	
	28.8207	-96.0303			Phillips Pet. Co.	Pierce Estate	Matagorda	X	
	28.7066	-96.2167			Layne-Texas, Inc.	City of Palacios Wat	Matagorda	X	

TWDB Report ## Final – Hydrostratigraphy of the Gulf Coast Aquifer from the Brazos River to the Rio Grande

API number	NAD27 latitude	NAD27 longitude	Dip section/ position	Strike section/ position*	Company	Lease	County	Lithology and water qual data	Paleo data
423210260000	28.8394	-95.7079			Shell Oil Co.	Thome	Matagorda	X	
423210083600	28.9492	-95.7781			The British-American	Guess	Matagorda	X	
	29.4909	-96.6740			Katy Drilling Compan	Sheridan Water Well	Colorado	X	
	29.6839	-96.3564			Pan American Prod. C	Williams	Colorado	X	
	29.4599	-96.5915			Lone Star Prodn. Co.	Rutta	Colorado	X	
	29.6054	-96.2778			Shell Oil Co.	Mazac	Colorado	X	
	29.5677	-96.2507			Phillips Pet. Co.	Armit Fee	Wharton	X	
30138	30.0462	-96.2011					Austin	X	
	29.9804	-96.0871					Waller	X	
	29.8196	-96.0787			Petroleum Service Co	Mrs. Irene Allen Dav	Waller	X	
420393216000	29.2245	-95.4793			Zinn Petroleum	Heim	Brazoria	X	
	29.7951	-96.0371			Humble Oil And Refin	Rufus Hardy	Waller	X	
421670105400	29.2805	-95.1174			Strake Petroleum Co.	Griffith	Brazoria	X	
	29.0856	-95.5568			Humble Oil And Refin	Ward-Byers	Brazoria	X	
	29.0782	-95.6081			Pan Merican Petroleu	Ida Hobbs	Brazoria	X	
	28.8703	-95.9704			Joshua D. Ward A.K.	Onella Vaughn, Et. A	Matagorda	X	
	28.6512	-96.5993			Lone Star Producing		Calhoun	X	
	29.3210	-95.8490			H.H. Howell And Ceci	Armstrong Estate	Fort Bend	X	
	28.9584	-96.5334			Bobby Burns	Hasdorff	Jackson	X	
	28.9584	-96.5334			Bobby Burns	Hasdorff	Jackson	X	
	28.9326	-96.5732			H.H. Howell	Rosa Baker Estate	Jackson	X	
422853135900	29.4542	-96.9284			Howell Drilling, Inc		Lavaca	X	
	28.7688	-96.5899			Mobil Oil Company	West Ranch "A"	Jackson	X	
	28.7688	-96.5899			Magnolia Petroleum C	West Ranch	Jackson	X	
	28.7246	-96.5577			Humble Oil And Refg.	La Bauve	Jackson	X	
	28.6394	-96.4452			Humble Oil And Refin	Elizabeth Hardy	Calhoun	X	
	28.5634	-96.4445			Sun Oil Company	State Tract 71	Calhoun	X	
	29.7588	-96.1140			Edwards Oil And Gas	Frank Hubanek	Austin	X	
	29.8522	-95.8638			Humble Oil And Refin	R.F. Woods	Waller	X	
	29.9415	-95.9662			Humble Oil And Refin	J.W. Harris	Waller	X	
	29.4921	-95.5165			Humble Oil And Refin	Scanlon	Fort Bend	X	
	28.8281	-95.4986			Brazos Oil And Gas C	Ducroz	Brazoria	X	
	29.0322	-96.3089			Armour Properties	Davis-Applying Gas Un	Wharton	X	
	29.4524	-97.1038			Eastern Gas Systems	Darilek	Lavaca	X	

TWDB Report ## Final – Hydrostratigraphy of the Gulf Coast Aquifer from the Brazos River to the Rio Grande

API number	NAD27 latitude	NAD27 longitude	Dip section/ position	Strike section/ position*	Company	Lease	County	Lithology and water qual data	Paleo data
	29.3707	-96.8299			Lytle Creek Operatin	Steffek Unit	Lavaca	X	
420970126700					Humble Oil And Refin	Robt. Kleberg	Brooks	X	
420470011300	27.1593	-98.2039			Magnolia Petroleum C	Church Brethren Unit	Brooks	X	
420250151100	28.2803	-97.6178			Union Producing	Driscoll Estate	Bee	X	
420250150900	28.2607	-97.6344			W.B. Clearly, Inc. A	E-1 Driscoll Estate	Bee	X	
422493208600	27.8023	-98.0356			Golian Operating	Dunn	Jim Wells	X	
					Hurd Enterprises	Yorba Oil Co. F.As U	Jim Wells	X	
422473168700	27.1550	-98.8964			Edwin & Berry Cox	Dena	Jim Hogg	X	
422470020700	27.3363	-98.7565			Killam & Hurd Inc.	Kellen	Jim Hogg	X	
422150010000	26.5199	-98.0769			Humble O&G	Sheppard	Hidalgo	X	
421313776900	27.5679	-98.7606			Exxon Corp.	Kohler "A"	Duval	X	
420473160600	26.9122	-98.2791			Cometra O&G Garcia		Brooks	X	
					Hunter & Nedwick	Alexander 400 Ac.	Brooks	X	
420610002800					Gulf Oil Corp.	Kerlin	Cameron	X	
422610039400	26.9768	-97.8345			Humble O&R Co.	Charles M. Armstrong	Kenedy	X	X
422610017900	27.0920	-97.7914			Humble O&R Co.	John G. Kenedy, Jr.	Kenedy	X	
422610015500	27.2294	-97.9491			Atlantic Refining Co	McGill	Kenedy	X	
422610013500	27.2256	-97.7659					Kenedy	X	
422150096500	26.3009	-98.2007			Sinclair Prairie	Grade Callaway	Hidalgo	X	
422150100700	26.3300	-98.0293			Allen Hugo H.R. Smit	Stiegel Community B.	Hidalgo	X	
420573148000	28.2470	-96.6674			Pelto Oil Co	State Tract 160	Calhoun	X	
420573090500	28.6350	-96.6449			Republic Nat. Gas	Canion	Calhoun	X	X
420570124800	28.6220	-96.7300			Sutton Prod. Co. Bre		Calhoun	X	
420610004300	26.2423	-97.2833			Humble O&R Co	Laguna Madre State T	Cameron	X	
420610017600	26.1984	-97.5831			Shell Oil Co.	Hulsey	Cameron	X	
420610018900	26.2819	-97.7368			Gulf Oil Corp	McDaniel	Cameron	X	X
421313755200	27.9533	-98.7487			McGowan Working Part	Duval Ranch Sec 288	Duval	X	
421753328100	28.5663	-97.3892			Texaco	O'Connor	Goliad	X	
422150009200	26.7785	-98.1255			Shar-Alan Oil Co.	Guerra	Hidalgo	X	
							Cameron	X	
424273277600	26.7547	-98.8680					Starr	X	
					Humble O&R	Lagona Madre Sate Tr	Kenedy	X	
422473132100	26.9640	-98.8878					Jim Hogg	X	
422150167300	26.1030	-98.2544			The Texas Co.	El Texano Gas Unit #	Hidalgo	X	

TWDB Report ## Final – Hydrostratigraphy of the Gulf Coast Aquifer from the Brazos River to the Rio Grande

API number	NAD27 latitude	NAD27 longitude	Dip section/ position	Strike section/ position*	Company	Lease	County	Lithology and water qual data	Paleo data
422150074700	26.2503	-98.4827			Martin & Rock Hill	Tabasco Indep. Schoo	Hidalgo	X	
422490256200	27.4392	-98.1335			Magnolia	Seeligson	Jim Wells	X	
422490008100	28.0528	-97.9517			Glen Martin & Sun Ra	Rozypal	Jim Wells	X	
422616014200					Sunray	McGill Jr. et al	Kenedy	X	
422736053700					Humble O&R King Ranc		Kleberg	X	
423550594100	27.6342	-97.7054			H.H. Howell et al	Schubert	Nueces	X	
422150187000	26.3489	-97.9424			Standard Oil of Texa	Rio Farms	Hidalgo	X	X
422150155500	26.0915	-98.2649			Delhi - Taylor & May	Young	Hidalgo	X	
422150125500	26.0457	-98.0501			G.F. Shepherd et al	J.S. McManus Unit	Hidalgo	X	
422150063500	26.4878	-98.4255			Shell Oil	Boston - Texas Land	Hidalgo	X	
422150016800	26.6761	-98.3532			Humble Oil & Refinin	Barrera	Hidalgo	X	
					Humble O&R	State Tract 692	Aransas	X	
420253304200	28.6538	-98.0724			Chenier Energy	Kennedy	Bee	X	
					Magnolia Pet. Co.	Seeligson	Jim Wells	X	
					Argo Oil Corp	Lopez	Duval	X	
					Sun Oil Co	Jones	Jim Hogg	X	
					Texaco	A.K. East	Jim Hogg	X	
					Magnolia Petroleum	Derc	Duval	X	
					Mobil Oil	Weil Gas Unit	Nueces	X	
422973030100	28.0963	-98.0912			Humble O&R	McCaslin	Live Oak	X	
422550084200	28.8033	-98.0128			Seaboard Oil Co.	Treadwell	Karnes	X	
420250160200	28.4916	-97.8061			Mokeen Oil Co.	Brown	Bee	X	
					Jack Frazier	Cochran	Karnes	X	
420250047400	28.6090	-97.9973			Shell Oil Co.	O'Neal	Bee	X	
422973251900	28.2025	-97.8939			Dynamic Prod. Inc.	Boothe	Live Oak	X	
422970115400	28.3069	-98.1860			Humble O&R	Geo. West Gas Unit #	Live Oak	X	
421313173200	27.9972	-98.6902			Duval County Ranch C	Duval State Section	Duval	X	
421313494700	27.9898	-98.5001			Arco O&G Co.	Gas Unit	Duval	X	
422493228800	28.0216	-98.1525			Slawson Exploration	Freebzin-Floyd	Jim Wells	X	
421770029800	29.3028	-97.3742			Hunt Oil Co.	Emil Stoeltue	Gonzales	X	
424693311400	28.8487	-96.9489			Superior O&G Investm	Buhler - Telferner	Victoria	X	
422470221500	26.9213	-98.8141			Allen & Bemis	Gallagher	Jim Hogg	X	
421313695800	27.7055	-98.6547			Exxon Core Loma Novi		Duval	X	
					Humble O&R Co. Sulli		Brooks	X	

TWDB Report ## Final – Hydrostratigraphy of the Gulf Coast Aquifer from the Brazos River to the Rio Grande

API number	NAD27 latitude	NAD27 longitude	Dip section/ position	Strike section/ position*	Company	Lease	County	Lithology and water qual data	Paleo data
422470221500	26.9213	-98.8141			Humble O&R	Alice East	Jim Hogg	X	
421313166700	28.0219	-98.5945			Atlantic Richfield	Foster	Duval	X	
					Weeler Estate	Rives	McMullen	X	
422973360000	28.1305	-98.3226			Rutherford Oil	Baker Trust	Live Oak	X	
424273148900	26.6605	-98.8705			Sparkman Prod. Co.	Salinas	Starr	X	
424270043300					Sun Explor. & Prod.	Caggarelli	Starr	X	
421310991700	27.4559	-98.5510			Hillcrest Oil Co.	Shaffer	Duval	X	
					Atlantic Refining Co	Billings	Webb	X	
424273278100	26.3634	-98.6925			Trans Texas Gas Corp	Roos	Starr	X	
424790300400	27.3453	-98.8814			Killam-Blanco & Buck	McLean	Webb	X	
					Southern Royalty	Winsaver	San Patricio	X	
420473173000	26.9748	-98.2161			Union Pacific Resour	Scott & Hopper	Brooks	X	
420470030900	27.0599	-98.0256			Humble O&G	Sullivan	Brooks	X	
421313712800	27.4092	-98.4164			Esenjay Petroleum Co	Tilton	Duval	X	
421313499300	27.2710	-98.3817			C.J. Woffard	Glasscock	Duval	X	
421233002000	29.0613	-97.4657			Shell Oil Co.	Cora S. Brown	Dewitt	X	
423230036200					Sohio Producing Co.	First Nat. Bank York	Dewitt	X	
422973443400	28.0801	-98.0736			First Rock	Rollins Ranch	Live Oak	X	
420253243300	28.3729	-97.6915			Natural Resource Mgt	Brawer	Bee	X	
					Atlantic Richfield C	Dougherty Estate	Bee	X	
420253227800	28.4555	-97.6832			Exxon	Diebel	Bee	X	
421750072200	28.8267	-97.2159			Sun Oil Co & Geo. Co	Eliot	Goliad	X	
423913207000					George McLeod	Rooke & Sons	Refugio	X	
420250286000	28.3328	-97.6137			Logue & Patterson	Neard	Bee	X	
424693256400	28.5892	-97.0249			Victoria Operating,	C.K. McCan, Jr. Et.	Victoria	X	
422730003600	27.5611	-98.0561			Humble O&R	King Ranch Borrelos	Kleberg	X	
423553161000	27.6791	-97.7718			Egan-Wilson Pet. Co.	Balzar	Nueces	X	
422493087700	27.9612	-97.8914			Tepco Engineering	Hinze	Jim Wells	X	
422490271000	27.3644	-98.1705			Eddy & Messer	Henderson	Jim Wells	X	
424693342100	28.8914	-97.1552			Dewbre Pet. Corp.	Nickel	Victoria	X	
424693291200	28.5079	-96.9334			Coastline Expl. Inc.	Fagan et al	Victoria	X	
420076033100					Phillips Pet. Co.	Copano	Aransas	X	
423413025600					Orion, Howell & Huis	Shay	Refugio	X	
420073077800	27.9742	-97.0933			Fort Worth O&G Inc	Hullan Oil Unit	Aransas	X	

TWDB Report ## Final – Hydrostratigraphy of the Gulf Coast Aquifer from the Brazos River to the Rio Grande

API number	NAD27 latitude	NAD27 longitude	Dip section/ position	Strike section/ position*	Company	Lease	County	Lithology and water qual data	Paleo data
420070006700	28.1800	-96.9625			Union Producing Co.	Tatton	Aransas	X	
421753258400	28.5689	-97.5848			Morris Cannon	Jack Grant	Goliad	X	
421753156200					Mirada Management, I	Tomlinson-Tolbert Ga	Goliad	X	
					Cockburn	Scott	Wharton	X	
424810138700	29.2818	-96.4509			Sunray Dx Oil	Wallace	Wharton	X	
423910020500	28.4210	-97.0489			Quintana Pet. Corp.	Williams	Refugio	X	
423550502600	27.6166	-97.8490			Humble O&R Co. King		Nueces	X	
423113301740	28.3777	-98.3501					McMullen	X	
422973382800					Finger Oil & Gas	Braly	Live Oak	X	
421313586800	27.6478	-98.7441					Duval	X	
422153226400	26.2572	-98.5590			Starr County Expl Co	Guerra	Hidalgo	X	
422490149400	27.7235	-98.2276			Whalen	Lundell's Inc.	Jim Wells	X	
422473218400	27.1704	-98.6075			Mestena, Inc.	Portero	Jim Hogg	X	
					Arco Oil & Gas Co	Sharman	Dewitt	X	
420073073100	28.1979	-96.8822			Conoco	St. Charles	Aransas	X	
420253206500	28.4355	-97.9480			Mueller Engineering	Brooks	Bee	X	
420610019500	26.1180	-97.7589			Standard Oil Co Op T	Moothart	Cameron	X	X
425052973000					Jonnell Gas Co	Lopez Heirs	Zapata	X	
423650033900					Union Prod Co	Schroeder	Nueces	X	
422610021700	26.9094	-97.5933			Humble O&R	Chas M. Armstrong	Kenedy	X	
422730058500	27.3715	-97.4261			Humble Oil & Refinin		Kleberg	X	
422730055400	27.5098	-97.3607			Humble O&R Co, King		Kleberg	X	
422610047900	27.2392	-97.6567			Mobil Oil Co, State	Well 1	Kenedy	X	
422610039400	26.9768	-97.8345			Humble O&R Co	Mrs. Sprita K. East	Kenedy	X	X
422610039300	26.9768	-97.8345			Humble O&R Co	Mrs. S. M. East	Kenedy	X	X
422610034100	27.1362	-97.7150			Humble O&R Co, John		Kenedy	X	X
422730084500	27.3263	-97.7249			Cities Service Pet.	Quackenbush	Kleberg	X	
422730122500	27.2859	-97.8555			Humble O&R Co, King		Kleberg	X	
422730194400	27.4053	-97.7601			Lone Star Prod. Co.	Bessio H. Muil	Kleberg	X	X
422973439700	28.3897	-98.3022			Lindholm Oil Inc	Babin	Live oak	X	
422730179500	27.3455	-97.9272			Humble O&R Co, King		Kleberg	X	
422730211600	27.4769	-97.2752					Kleberg	X	
423113187600	28.2674	-98.4498			Pintex Operating Co	Rivers	McMullen	X	
423113216100	28.2051	-98.3775			Arco Oil & Gas Co	D.W. Rhode	McMullen	X	

TWDB Report ## Final – Hydrostratigraphy of the Gulf Coast Aquifer from the Brazos River to the Rio Grande

API number	NAD27 latitude	NAD27 longitude	Dip section/ position	Strike section/ position*	Company	Lease	County	Lithology and water qual data	Paleo data
423550611200	27.8576	-97.3680			Forest Oil Corp & Mo		Nueces	X	X
423550622500	27.6670	-97.4988			Socony Mobil et al	Russell	Nueces	X	
423550651700					Cherryville Corp	Burton Dunn, et al	Nueces	X	
423553130900	27.8315	-97.1637			Adobe O&G Corp (MCMO)	Fordyce Unit (State)	Nueces	X	
423553000900	27.8741	-97.8884			Kirkpatrick O&G & Na	Annie Pegmund	Nueces	X	
424090224200	27.9314	-97.1976			Tenneco Oil Co	McC Campbell	San Patricio	X	X
424090368200	27.9458	-97.7403			Mikton Oil Co	Masiran	San Patricio	X	
424093191400	27.9678	-97.5147			Southern Royalty Inc		San Patricio	X	
424273185800	26.3615	-98.7612			Txo Prod Corp	Wardner	Starr	X	
424270428500	26.3045	-98.6363			Clark Fuel Prod Co	Laborde	Starr	X	
					Jennings Exploration	Henderson et al	San Patricio	X	
424273225000	26.4715	-98.8152			Wright Bros. Energy,	Doyno	Starr	X	
424273272000	26.3538	-98.6301			Neuhaus Properties	Farias	Starr	X	
424273350800	26.3761	-98.5432			Dan A. Hughes, Co.	Morse	Starr	X	
424690019000	28.7863	-96.7166			Flaitz & Mitchell	Keeran Ranch	Victoria	X	
424690018900					Rodney Delange et al	McCan	Victoria	X	
424693253300	28.9138	-96.9854			Cummins & Walker Oil	McCan	Victoria	X	
424690149700	28.6157	-97.0773			Mrs. James R. Doughe	Marbach	Victoria	X	
424693289200	28.6997	-97.1088			Klotzman	A Salinas	Victoria	X	
424690314900	28.8605	-96.8267					Victoria	X	
424693268500	28.7848	-97.1029			Cpx Petroleum Inc.	Engel	Victoria	X	
424793319300	27.5279	-98.8967			Galatia Investments	Garza et al	Webb	X	
424793403100	27.2799	-98.9987					Webb	X	
424890043200	26.4618	-97.6597			Sun Oil Co	Scott Ethyl K et al	Willacy	X	
424890008300	26.4999	-97.3869			Humble O&R Co.	Sauz Ranch - Nopal	Willacy	X	
424890005800	26.4618	-97.6597			H.L. Hunt	Hearne	Willacy	X	
424893094000	26.5731	-97.8627			Rio-Tex, Inc.	Garcia Ranch	Willacy	X	
424890064200	26.4622	-97.9350			Pan American	Rio Farms	Willacy	X	
426020005200	27.7071	-97.1322					Nueces	X	
426020005200	27.7071	-97.1322			Southland Royalto Co	State Tract 886 Must	Nueces	X	
420070085800	28.2632	-96.8832			Continental Oil Co	St Charles Ranch	Aransas	X	
420610019500	26.1180	-97.7589			Standard Oil of Texas	Moothart	Cameron	X	X
424890026500	26.5772	-97.4589			Pan American	Rodriquez	Willacy	X	

TWDB Report ## Final – Hydrostratigraphy of the Gulf Coast Aquifer from the Brazos River to the Rio Grande

API number	NAD27 latitude	NAD27 longitude	Dip section/ position	Strike section/ position*	Company	Lease	County	Lithology and water qual data	Paleo data
424273230600	26.5619	-98.5912			Paul Cameron Jr	Cameron	Starr	X	
423550660100	27.7290	-97.5899			Ramada O&G Co (F.E.	Noting	Nueces	X	
422733209000	27.6092	-97.9300			Union Pacific	Wardner	Kleberg	X	
423913213600	28.3485	-97.0462			Gruy Petro Managemen	Tatton	Refugio	X	
421310967600	27.3861	-98.3131					Duval	X	
428135738000					Doran Energy Corp	Serna	Duval	X	
421313678800	27.5851	-98.2502			Genesis Pet. Corp	Ortiz Gas Unit	Duval	X	
422490179100	27.7067	-98.0487			Russell Brown Operat	Wh Farmer	Jim Wells	X	
422153276800	26.3854	-98.3708			Coastal O&G Corp.	Garcia	Hidalgo	X	
422150181000	26.5329	-98.3415			Southwestern O&R Co	Alexander	Hidalgo	X	
422610016400					Sinclair	Garcia	Kenedy	X	
422970217000	28.2271	-98.0063			Kirksmith et al	Freeman	Live Oak	X	
424093257200	28.1068	-97.3799			Marathon Oil Co	Welder	San Patricio	X	
424090256100					Warren & Shelly	Locke	San Patricio	X	
					Killam Oil Co	Killam Hurd Bruni "7	Webb	X	
425050271900	26.8812	-98.9662			The Texas Company	Hartman	Zapata	X	
421310848000	27.6866	-98.3783			The Texas Company	Gravis	Duval	X	
423550080700	27.8918	-97.6755			Standard Oil & Gas C	Kerr	Nueces	X	
424793867300	27.3483	-98.8672			Killam Oil Co	Killam Hurd Bruni "7	Duval	X	
					Sam H. Harper	Stahlman	Waller	X	
421230001700	29.2544	-97.1160			Mobil Oil Co.	Boyd	Dewitt	X	
422850000700	29.5891	-97.0733			Fidelity Oil & Royal	Olsovsky	Lavaca	X	
422970153300	28.2749	-97.9132			Haas Brothers	Range	Live Oak	X	

13 Appendix B Listing of geophysical logs stratigraphic contacts

See Table 5-2 for a definition of the column headers.

UWI/API	Dip Section/ Position		Strike Section/ Position		Stratigraphic Contacts (ft, msl)									
					Approx. Ground Level	Beaumont	Lissie	Willis	Upper Goliad	Lower Goliad	Upper Lagarto	Middle Lagarto	Lower Lagarto	Oakville
424770023900	8	1			320	-	-	-	-	-	-	-	-	-15
424773062500	8	2												
424770029400	8	3			214	-	-	147	-	-	-188	-390	-740	-1090
NOAPI_18624	8	4			195	-	-	51	-	-	-375	-674	-1045	-1420
420150023000	8	5			179	-	131	-16	-101	-207	-588	-969	-1364	-1795
424730024300	8	6			145	-	113	-53	-153	-268	-708	-1116	-1531	-1988
424730031800	8	7	D"	1	191	-	-24	-242	-401	-538	-996	-1473	-2066	-2578
421570000100	8	8			146	-	-153	-364	-644	-917	-1395	-1829	-2577	-3174
421570102600	8	9			97	-	-187	-411	-740	-1135	-1629	-2041	-2838	-3430
421573198300	8	10			91	61	-243	-456	-857	-1297	-1803	-2306	-3118	-3786
421570089400	8	11			73	-36	-341	-512	-1080	-1555	-2190	-2771	-3554	-4465
421570245900	8	12	E"	3	59	-112	-434	-609	-1216	-1778	-2445	-3131	-3960	-4912
420390145200	8	13			42	-357	-765	-1052	-2115	-2820	-3550	-4172	-5122	-6424
420390422400	8	14			34	-458	-929	-1264	-2418	-3264	-4074	-4770	-5866	-7605
420390427700	8	15			5	-708	-1225	-1698	-2883	-3776	-4836	-5957	-7228	-
420390429100	8	16			5	-708	-1255	-1784	-3104	-4020	-5075	-6252	-7634	-
427060002200	8	17	G"	1	0	-833	-1382	-1984	-3296	-4259	-5511	-7094	-9419	-
420150001700	9	1			361	-	-	-	-	-	-	-	-307	-
420153053900	9	2			272	-	-	-	-	-	-	-	-735	-
420150066300	9	3			283	-	-	30	-	-86	-582	-918	-1437	-1943
420150026200	9	4	D"	4	192	-	99	-188	-255	-490	-1026	-1374	-1938	-2480
420150068300	9	5			140	120	-42	-347	-657	-1002	-1486	-1828	-2380	-3048
420153073800	9	6			128	80	-135	-427	-749	-1153	-1583	-1972	-2592	-3391
421573175200	9	7			117	11	-229	-494	-805	-1237	-1689	-2114	-2796	-3569
421573180500	9	8			96	-47	-274	-539	-1024	-1505	-2012	-2567	-3358	-4330
421570167400	9	9	E"	5	65	-165	-406	-701	-1549	-2072	-2657	-3409	-4384	-5440
420390271500	9	10			57	-269	-543	-850	-1742	-2513	-3146	-3849	-4840	-6097
420390286500	9	11			41	-419	-773	-1110	-1982	-2877	-3596	-4300	-5296	-6609
NOAPI_18912	9	12			30	-539	-926	-1293	-2282	-3191	-3942	-4703	-5684	-7108
420390389800	9	13	F"	5	30	-621	-1056	-1447	-2489	-3487	-4217	-5010	-6044	-7511
420393035000	9	14			12	-663	-1157	-1653	-2734	-3737	-4565	-5613	-6728	-8746
420393211000	9	15			15	-749	-1271	-1801	-2918	-4054	-5004	-6230	-7452	-10090

TWDB Report ## Final – Hydrostratigraphy of the Gulf Coast Aquifer from the Brazos River to the Rio Grande

UWI/API	Dip Section/ Position		Strike Section/ Position		Stratigraphic Contacts (ft, msl)									
					Approx. Ground Level	Beaumont	Lissie	Willis	Upper Goliad	Lower Goliad	Upper Lagarto	Middle Lagarto	Lower Lagarto	Oakville
420390481100	9	16	G"	2	5	-813	-1353	-1916	-3683	-4642	-5871	-7375	-9671	-
427064036000	9	17												
421493208800	10	1												
421493132900	10	2			351	-	-	-	-	-	-	-	-	124
420893153100	10	3			291	-	-	227	-	143	-288	-507	-786	-1061
420890005700	10	4			205	-	-	163	-	-9	-396	-626	-953	-1254
420890009000	10	5			313	-	-	17	-	-224	-631	-933	-1291	-1652
420893124600	10	6	D"	6	213	-	103	-98	-219	-506	-915	-1249	-1791	-2243
NOAPI 18620	10	7			175	-	-21	-245	-444	-795	-1240	-1674	-2298	-2927
424810121800	10	8			154	-	-46	-296	-507	-891	-1326	-1717	-2468	-3104
424810120500	10	9			136	-	-95	-351	-559	-945	-1386	-1780	-2645	-3305
424813403300	10	10			101	29	-201	-472	-1034	-1572	-2125	-2495	-3424	-4291
424813344200	10	11			106	72	-163	-450	-898	-1429	-1911	-2286	-3171	-3907
424813294400	10	12	E"	7	86	-117	-383	-676	-1530	-2079	-2686	-3244	-4080	-5169
424810256200	10	13			73	-198	-468	-756	-1679	-2356	-2946	-3432	-4316	-5520
NOAPI 18639	10	14			55	-340	-687	-988	-2098	-2778	-3440	-4097	-5064	-6410
423210067000	10	15			35	-495	-943	-1262	-2467	-3258	-3980	-4874	-5853	-7271
NOAPI 18891	10	16	F"	7	29	-585	-1056	-1384	-2795	-3566	-4329	-5363	-6356	-8480
423210082400	10	17			10	-671	-1225	-1679	-3349	-4139	-5166	-6427	-	-
427043007300	10	18	G"	4	0	-770	-1401	-1996	-3934	-4838	-5894	-7307	-	-
427043000500	10	19			0	-952	-1642	-2474	-4442	-5428	-	-	-	-
427040007100	10	20			0	-889	-1588	-2241	-4287	-5182	-6529	-	-	-
427040007000	10	21			0	-1098	-2096	-3628	-7604	-9950	-	-	-	-
427044002600	10	22			0	-	-	-5021	-	-	-	-	-	-
421493204900	11	1			294	-	-	-	-	-	-	-	49	-208
420893164500	11	2			363	-	-	-	-	-	-	191	-272	-587
420893145600	11	3			354	-	-	-	97	-	304	-40	-503	-894
420893163900	11	4			340	-	-	246	-	-	9	-367	-908	-1399
420893173400	11	5			254	-	-	-8	-	-153	-473	-933	-1483	-2110
420893215800	11	6			170	-	21	-194	-359	-641	-1098	-1505	-2070	-2768
420893059200	11	7	D"	8	211	-	105	-82	-158	-446	-800	-1256	-1771	-2350
420890075900	11	8			156	-	-14	-259	-478	-807	-1247	-1684	-2381	-2964
424813369000	11	9			141	102	-109	-325	-753	-1223	-1651	-2176	-	-
420893198100	11	10			152	135	-69	-313	-650	-1084	-1511	-2009	-	-
424813336100	11	11			127	67	-156	-359	-877	-1376	-1804	-2389	-3111	-3727
424813147700	11	12			100	-14	-280	-515	-1136	-1709	-2277	-2985	-3640	-4354
424810357500	11	13	E"	8	90	-107	-365	-605	-1415	-1993	-2618	-3360	-4050	-5020

TWDB Report ## Final – Hydrostratigraphy of the Gulf Coast Aquifer from the Brazos River to the Rio Grande

UWI/API	Dip Section/ Position		Strike Section/ Position		Stratigraphic Contacts (ft, msl)									
					Approx. Ground Level	Beaumont	Lissie	Willis	Upper Goliad	Lower Goliad	Upper Lagarto	Middle Lagarto	Lower Lagarto	Oakville
NOAPI 18827	11	14			48	-234	-542	-808	-1763	-2428	-3127	-3915	-4644	-5536
NOAPI 18844	11	15			45	-379	-736	-1034	-2166	-2957	-3618	-4473	-5205	-6237
423210268900	11	16			35	-427	-805	-1126	-2293	-3094	-3843	-4665	-5434	-6719
423210114700	11	17	F"	8	35	-465	-867	-1193	-2382	-3188	-3968	-4799	-5644	-7046
423210253900	11	18			8	-547	-983	-1384	-2660	-3532	-4434	-5322	-6312	-
426040001200	11	19			0	-618	-1087	-1534	-2957	-3906	-5144	-6212	-7434	-
427040000700	11	20	G"	6	0	-611	-1076	-1555	-3124	-3986	-5194	-6668	-8167	-
421490032700	12	1			409	-	-	-	-	-	-	-	-	-
421493262000	12	2			276	-	-	-	-	-	-	75.488	-247.69	-446
NOAPI 18602	12	3			256	-	-	-	-	-	-7.4887	-426.74	-786.23	-1169.0
422853272900	12	4			203	-	-	-	-	-88.74	-452.94	-866.56	-1234.7	-1582
422853117200	12	5			256	-	-	5.6903	-115.6	-367.8	-680.04	-1145.8	-1566.6	-2054
422850032600	12	6	D"	10	199	-	197	-99	-183	-456	-792	-1249	-1713	-2289
420893160400	12	7			150	-	25.056	-221.6	-487.4	-899.7	-1356.7	-1847.4	-2405.3	-3041.3
NOAPI 18743	12	8												
424810169500	12	9			85	58.23808	-167.4	-408.2	-846.5	-1395	-1887.7	-2404.4	-2986.4	-3797.5
424810177000	12	10	E"	11	73	-161	-420	-669	-1474	-1995	-2512	-3122	-3844	-4778
422393247200	12	11			66	-235.064	-523.7	-779.1	-1631	-2156	-2777.8	-3375.3	-4136.2	-5050.6
423210217100	12	12			48	-303.3377	-630.7	-869.3	-1802	-2387	-3070.1	-3736.6	-4408.3	-5404.3
423210229500	12	13			27	-355.5113	-732.7	-968.3	-2105	-2878	-3598.9	-4406.7	-5298.6	-6385.5
423210267200	12	14			30	-411.5046	-773.5	-1013	-2123	-3066	-3826.7	-4600.5	-5559.7	-6638.8
423213171600	12	15			17	-483.9385	-857.2	-1094	-2252	-	-	-	-	-
423210251400	12	16			5	-536.112	-969.6	-1186	-2468	-3228	-4102.8	-4755.8	-5530.6	-
426043004100	12	17			0	-536.112	-1014	-1283	-2616	-3494	-4460.7	-	-	-
427043021000	12	18	G"	7	0	-560	-1058	-1466	-2736	-	-	-	-	-
427044023000	12	19			0	-572.2322	-1106	-1568	-3027	-	-5892.5	-	-	-
427044030000	12	20												
422853026800	13	1			441	-	-	-	-	-	-	-	-	84.72
422850035800	13	2			246	-	-	-	-	189.55	-94.038	-400.31	-729.27	-1119.3
422850050900	13	3	D"	13	171	-	-	60	25	-256	-585	-970	-1434	-1939
422853176200	13	4			119	-	53.426	-131.7	-408	-804.8	-1186.6	-1643.3	-2062.6	-2617.7
424693243200	13	5			95	-	-154.7	-305.8	-774.9	-1202	-1644.1	-2085.5	-	-
422390004700	13	6			84	74.2915	-192.2	-368.6	-888.1	-1331	-1759.8	-2190.2	-2631.6	-3259.4
422390155600	13	7			67	-45.1579	-319.2	-519.8	-1218	-1598	-2062.6	-2511.8	-3028.4	-3794.3
422390192100	13	8	E"	14	45	-161	-391	-639	-1524	-1958	-2467	-3051	-3665	-4587
422390337800	13	9			4	-199.3285	-534.9	-776.9	-1875	-	-	-	-	-
422390319800	13	10			25	-259.2837	-615.6	-852.5	-1969	-2670	-3364.1	-3896.8	-4612.2	-5668.1

TWDB Report ## Final – Hydrostratigraphy of the Gulf Coast Aquifer from the Brazos River to the Rio Grande

UWI/API	Dip		Strike		Stratigraphic Contacts (ft, msl)									
	Section/ Position	Position	Section/ Position	Position	Approx. Ground Level	Beaumont	Lissie	Willis	Upper Goliad	Lower Goliad	Upper Lagarto	Middle Lagarto	Lower Lagarto	Oakville
420570085200	13	11	F"	14	8	-345	-674	-943	-2176	-3000	-3745	-4343	-5085	-
420573090300	13	12			0	-449.2458	-761.8	-1110	-2341	-3273	-4097.5	-4756.5	-5566.3	-6462.7
NOAPI 18788	13	13			0	-474.4485	-792	-1220	-2440	-3371	-4342.8	-5173.3	-5968.9	-6968.6
427033000600	13	14	G"	10	0	-480	-842	-1437	-2831	-3842	-5143	-6513	-8603	-13101
421770042400	14	1												
421230087000	14	2			271	-	-	-	-	-	-	-	-	-624
421230029000	14	3			239	-	-	-	-	38	-247	-675	-1124	-1582
421233187900	14	4	D"	15	216	-	-	-	158	-125	-506	-950	-1395	-1989
424693155300	14	5			134	-	-	-	-293	-599	-1095	-1541	-2015	-2789
424690093400	14	6			66	-	54	10	-760	-1147	-1609	-1978	-2388	-3162
NOAPI 993	14	7			59	51	-102	-285	-1032	-1505	-1973	-2354	-2775	-3647
424690162400	14	8			82	24	-241	-495	-1182	-1782	-2273	-2625	-3040	-3877
NOAPI 990	14	9	E"	16	68	28	-269	-564	-	-	-	-	-	-
424693189700	14	10			56	4	-281	-607	-1536	-2169	-2799	-3205	-3704	-4577
420570132300	14	11			4	-66	-444	-757	-1993	-2923	-3559	-4098	-4730	-5943
420570122100	14	12			0	-226	-565	-1119	-2441	-3378	-4129	-5069	-6076	-7774
427033031900	14	13	G"	13	0	-350	-722	-1333	-2726	-3774	-4979	-6184	-	-
427034001000	14	14			0	-454	-815	-1091	-2846	-4005	-5483	-7332	-10019	-
422550023600	15	1												
421230033700	15	2			416	-	-	-	-	-	-	-	-	215
421230036200	15	3			319	-	-	-	-	-	96	-380	-813	-1270
421750043400	15	4	D"	17	288	-	-	-	-	114	-251	-754	-1192	-1769
421753010500	15	5			220	-	-	-	6	-255	-582	-1122	-1540	-2126
421753166400	15	6			117	-	114	-	-327	-661	-1075	-1589	-2065	-2669
421753171900	15	7			111	-	12	-117	-643	-1003	-1435	-1922	-2427	-3122
424690143800	15	8			106	-	-57	-277	-964	-1351	-1808	-2292	-2835	-3609
423910002300	15	9	E"	17	78	-	-146	-425	-1275	-1722	-2294	-2853	-3461	-4322
423913146600	15	10			51	-19	-250	-540	-1561	-2018	-2615	-3154	-3743	-4707
423910008600	15	11	F"	17	15	-232	-527	-839	-2211	-2814	-3535	-3970	-4675	-5954
420570118500	15	12			5	-274	-595	-1023	-2508	-3339	-4247	-4845	-5616	-6685
427034014000	15	13	G"	14	0	-326	-641	-1208	-2844	-3915	-5118	-6278	-8154	-
424930153600	16	1												
422550063400	16	2												
422553024600	16	3			249	-	-	-	-	-	-	-	-	-337
422553134600	16	4			307	-	-	-	-	-	195	-39	-388	-965
421750145600	16	5	D'	1	190	-	-	-	-	-	-90	-564	-1054	-1640
421753335000	16	6			213	-	-	-	-	-229	-697	-1152	-1551	-2198

TWDB Report ## Final – Hydrostratigraphy of the Gulf Coast Aquifer from the Brazos River to the Rio Grande

UWI/API	Dip		Strike		Stratigraphic Contacts (ft, msl)									
	Section/ Position	Position	Section/ Position	Position	Approx. Ground Level	Beaumont	Lissie	Willis	Upper Goliad	Lower Goliad	Upper Lagarto	Middle Lagarto	Lower Lagarto	Oakville
421753263600	16	7			215	-	-	-	-332	-613	-1077	-1546	-	-
421753216500	16	8			123	-	-	-	-771	-1158	-1640	-2161	-2678	-3435
421753194500	16	9	E',E"	1,19	86	-	23	-	-1101	-1504	-2106	-2621	-3242	-4084
423913211800	16	10			67	-	-78	-374	-1404	-1966	-2551	-3161	-3756	-4615
423913158800	16	11			53	15	-200	-515	-1597	-2138	-2710	-3232	-3855	-4748
420070035400	16	12			23	-145	-334	-725	-1826	-2561	-3176	-3673	-4288	-5333
420073066000	16	13			1	-259	-520	-939	-2082	-3082	-3900	-4598	-5632	-7586
427030000200	16	14	G',G"	1,15	0	-375	-764	-1341	-2879	-3987	-4891	-5998	-7223	-10271
424930174700	17	1												
422970001100	17	2												
420253155700	17	3			466	-	-	-	-	432	-	-106	-351	-731
420250030500	17	4			385	-	-	-	-	354	243	-210	-557	-1202
420253149300	17	5	D'	3	334	-	-	-	-	269	146	-323	-842	-1522
420253258400	17	6			223	-	-	-	7	-230	-676	-1145	-1544	-2182
420253048700	17	7			144	-	96	-	-488	-844	-1255	-1744	-2239	-2977
420250243000	17	8	E'	2	91	-	-55	-260	-1141	-1572	-2106	-2538	-2999	-3814
423913207400	17	9			43	-	-136	-324	-1412	-1817	-2425	-2769	-3198	-3951
423910365900	17	10			29	-27	-191	-387	-1544	-2059	-2648	-3042	-3492	-4424
423910372200	17	11	F',F"	1,19	23	-95	-277	-480	-1722	-2299	-2953	-3355	-3889	-4948
420070033100	17	12			0	-203	-507	-732	-2210	-3183	-3945	-4403	-4993	-6148
420070454000	17	13			1	-330	-635	-926	-2566	-3526	-4308	-4885	-5653	-6795
427033021500	17	14	G'	2	0	-350	-671	-1225	-2894	-4010	-4983	-6089	-6952	-8581
422970004300	18	1												
422970082400	18	2												
422970138700	18	3			230	-	-	-	-	-	-	-	2	-397
422973327600	18	4	D'	6	192	-	-	-	-	134	-54	-471	-974	-1603
420253181600	18	5			231	-	-	-	-253	-505	-822	-1296	-1785	-2477
420253191200	18	6			214	-	171	-	-462	-729	-1189	-1607	-2096	-2767
420250202600	18	7			166	-	46	-51	-835	-1166	-1622	-2071	-2540	-3328
424090034400	18	8	E'	4	104	82	-83	-293	-1358	-1777	-2248	-2713	-3222	-3987
424093225200	18	9			60	-	-120	-382	-1433	-1909	-2408	-2919	-3502	-4561
424093243800	18	10			50	32	-143	-461	-1488	-1969	-	-	-	-
424090256200	18	11			36	-17	-180	-483	-1564	-2126	-2724	-3409	-3900	-4819
424093228400	18	12	F'	3										
420073080400	18	13			14	-217	-509	-880	-2249	-3099	-	-	-	-
427023023300	18	14	G'	3	0	-339	-638	-1146	-2902	-3952	-4968	-6019	-6820	-7993
423110117300	19	1												

TWDB Report ## Final – Hydrostratigraphy of the Gulf Coast Aquifer from the Brazos River to the Rio Grande

UWI/API	Dip		Strike		Stratigraphic Contacts (ft, msl)									
	Section/ Position	Position	Section/ Position	Position	Approx. Ground Level	Beaumont	Lissie	Willis	Upper Goliad	Lower Goliad	Upper Lagarto	Middle Lagarto	Lower Lagarto	Oakville
422973265600	19	2			366	-	-	-	-	-	-	-	295	59
422973033000	19	3			402	-	-	-	-	-	-	324	-80	-414
422970260400	19	4	D'	8	352	-	-	-	-	271	244	-145	-706	-1173
422973354100	19	5			226	-	-	-	77	-88	-331	-770	-1388	-1918
422973351100	19	6			110	-	-	-	-491	-753	-1037	-1444	-2088	-2628
422493198500	19	7			93	-	105	-	-684	-1010	-1419	-1848	-2449	-3016
424093171600	19	8			101	87	-31	-160	-1055	-1546	-2060	-2594	-3165	-3905
424093188300	19	9	E'	5	94	-8	-199	-407	-1524	-2048	-2585	-3096	-3616	-4474
423553024900	19	10			61	-105	-295	-512	-1641	-2144	-2670	-3188	-3752	-4713
423553127000	19	11			22	-174	-388	-618	-1748	-2328	-2955	-3582	-4111	-5056
423550612200	19	12	F'	4	0	-217	-518	-800	-2308	-2969	-3635	-4279	-4874	-6041
426020004000	19	13	G'	4	0	-357	-774	-1209	-2872	-3595	-4428	-5131	-5801	-7091
427020000300	19	14			0	-378	-947	-1358	-3124	-3926	-4850	-5567	-6214	-7639
427024001200	19	15			0	-541	-1358	-1839	-3830	-4682	-5665	-6426	-7091	-
423110183400	20	1												
423113177900	20	2												
423113137300	20	3			446	-	-	-	-	-	-	-	-	374
421313825400	20	4	D'	10	512	-	-	-	-	377	124	-239	-655	-1194
421310107500	20	5			413	-	-	-	218	38	-259	-709	-1007	-1465
422493172400	20	6			295	-	-	-	-582	-921	-1200	-1735	-2063	-2681
422493019900	20	7			230	-	161	-	-816	-1150	-1431	-1921	-2225	-2904
422493145000	20	8			173	-	55	-64	-890	-1337	-1642	-2092	-2502	-3250
423553085900	20	9			139	112	-62	-226	-941	-1397	-1760	-2262	-2709	-3454
423550033900	20	10			97	31	-174	-410	-1663	-2177	-2663	-3212	-3666	-4423
423553266600	20	11	E'	6	80	-10	-276	-524	-1932	-2550	-3096	-3624	-4118	-5034
423550099200	20	12			54	-142	-393	-666	-2043	-2650	-3186	-3628	-4065	-4959
423553130800	20	13			22	-147	-410	-728	-2016	-2590	-3144	-	-	-
423550318200	20	14	F'	6	15	-296	-608	-911	-2280	-2972	-3627	-4277	-4998	-6149
423553170400	20	15			0	-316	-657	-990	-2390	-3209	-4005	-4596	-5226	-6329
427020001500	20	16			0	-364	-743	-1151	-2741	-3745	-4612	-5332	-6056	-7925
421310545000	21	1												
421310350100	21	2			586	-	-	-	-	-	-	-	315	38
421313760200	21	3			387	-	-	-	-	-12	-363	-851	-1406	-1894
422493205300	21	4			284	-	202	-	-553	-945	-1340	-1827	-2342	-2804
422493192300	21	5			201	-	-14	-103	-1188	-1572	-1982	-2383	-2889	-3392
422730000300	21	6			140	-	-143	-319	-1385	-1805	-2286	-2744	-3231	-3730
422730031600	21	7	E'	8	95	68	-224	-426	-1590	-2092	-2726	-3299	-3792	-4443

TWDB Report ## Final – Hydrostratigraphy of the Gulf Coast Aquifer from the Brazos River to the Rio Grande

UWI/API	Dip		Strike		Stratigraphic Contacts (ft, msl)									
	Section/ Position	Section/ Position	Section/ Position	Section/ Position	Approx. Ground Level	Beaumont	Lissie	Willis	Upper Goliad	Lower Goliad	Upper Lagarto	Middle Lagarto	Lower Lagarto	Oakville
423550408200	21	8			48	-119	-438	-833	-2339	-2943	-3635	-4136	-4729	-5565
422730053700	21	9			33	-143	-500	-854	-2422	-3179	-3866	-4442	-5052	-5975
422730054200	21	10	F'	7	16	-188	-519	-797	-2388	-3137	-3782	-4365	-4955	-5857
422730200100	21	11	G'	7	0	-381	-635	-1056	-3117	-4019	-4989	-5702	-6337	-7447
426020006500	21	12			0	-410	-699	-1147	-3203	-4112	-5074	-5815	-6457	-7499
427024026400	21	13			0	-523	-825	-1387	-3506	-4513	-5363	-6034	-6732	-8137
424790108500	22	1												
421313619300	22	2			719	-	-	-	-	-	-	-	537	54
421313519700	22	3	D'	13	586	-	-	-	-	546	346	32	-453	-1006
421310782600	22	4			480	-	-	-	289	-13	-373	-730	-1310	-1785
421313726100	22	5			425	-	-	-	-72	-557	-1024	-1374	-1910	-2461
421313234100	22	6			265	-	258	-	-480	-898	-1374	-1803	-2361	-2977
422493086800	22	7			182	-	100	44	-931	-1385	-1904	-2433	-3018	-3706
422733233600	22	8			97	21	-86	-289	-1414	-1965	-2715	-3218	-3849	-4599
422730108500	22	9			43	-191	-461	-881	-2604	-3291	-3965	-4443	-4970	-5745
422730088100	22	10			0	-321	-569	-817	-2196	-3015	-3640	-4157	-4685	-5621
422730088300	22	11	F'	8	0	-461	-720	-1133	-2444	-3316	-4030	-4673	-5439	-6671
426010000200	22	12	G,G'	1,9	0	-670	-1101	-1626	-3217	-4101	-4927	-5599	-6302	-7605
424793381200	23	1			858	-	-	-	-	777	-	-	-	-
424793451300	23	2			794	-	-	-	-	726	-	-	-	477
421311018900	23	3	D	2	672	-	-	-	-	602	-	494	113	-356
421310996700	23	4			548	-	-	-	291	153	42	-328	-789	-1282
422473177300	23	5			479	-	-	-	105	-69	-463	-989	-1508	-2051
421313634000	23	6			424	-	-	-	-104	-362	-965	-1420	-1886	-2377
421310980400	23	7			352	-	-	-	-320	-639	-1231	-1667	-2130	-2718
422490337500	23	8			177	-	-	-	-700	-1074	-1629	-2158	-2683	-3260
422490351400	23	9	E	2	131	-	101	-	-931	-1338	-1985	-2482	-3083	-3706
422730124200	23	10			75	-	-20	-140	-1414	-1862	-2520	-3057	-3694	-4594
422610014200	23	11			45	-54	-166	-357	-1610	-2122	-2738	-3210	-	-
422610035300	23	12			34	-117	-352	-636	-2002	-2785	-3569	-4100	-4713	-5718
422610010000	23	13	F,F'	1,9	16	-214	-513	-921	-2254	-3179	-3903	-4501	-5213	-6371
422610018700	23	14	G	2	0	-282	-588	-1041	-2508	-3591	-4462	-5272	-5819	-7049
427010000200	23	15	G	3	0	-325	-678	-1197	-3350	-4527	-5551	-6260	-7042	-8335
424793526800	24	1												
424793868300	24	2			881	-	-	-	-	747	-	-	-	-
422470014000	24	3			751	-	-	-	-	683	-	-	581	321
422470035400	24	4	D	3	559	-	-	-	-	512	-	328	22	-366

TWDB Report ## Final – Hydrostratigraphy of the Gulf Coast Aquifer from the Brazos River to the Rio Grande

UWI/API	Dip		Strike		Stratigraphic Contacts (ft, msl)									
	Section/ Position	Section/ Position	Section/ Position	Section/ Position	Approx. Ground Level	Beaumont	Lissie	Willis	Upper Goliad	Lower Goliad	Upper Lagarto	Middle Lagarto	Lower Lagarto	Oakville
422473156500	24	5			476	-	-	-	-	343	226	-192	-607	-1088
422470031300	24	6			437	-	-	-	301	156	-209	-670	-1135	-1676
420470043500	24	7			309	-	-	-	-152	-424	-995	-1482	-1992	-2555
420470011700	24	8			156	-	-	-	-498	-845	-1471	-1958	-2657	-3257
420470023000	24	9	E	4	97	-	46	-45	-850	-1301	-1939	-2514	-3213	-3911
422610016800	24	10			50	-	-48	-321	-1335	-1996	-2627	-3255	-3955	-4928
422610017800	24	11			37	-81	-188	-551	-1653	-2373	-3055	-3636	-4355	-5458
422610037300	24	12			23	-120	-268	-662	-1787	-2608	-3327	-3955	-4627	-5819
422613017400	24	13	F	2	18	-202	-465	-872	-2107	-3110	-3823	-4480	-5173	-6355
422613112700	24	14			5	-231	-519	-938	-2260	-3456	-4382	-4958	-5576	-6827
422610020100	24	15			5	-256	-582	-979	-2396	-3762	-4757	-5391	-6114	-7428
427010000100	24	16	G	5	0	-329	-788	-1280	-3299	-4778	-5946	-6566	-7401	-8866
427013003300	24	17			0	-362	-812	-1344	-3530	-5010	-6266	-7038	-7855	-9323
427014003000	24	18												
425053098400	25	1												
422473194000	25	2												
422473169500	25	3			750	-	-	-	-	681.38	-	-	-	421
422473187800	25	4			629	-	-	-	-	538.94	-	-	246	-227
422473174900	25	5	D	4	545	-	-	-	-	439	-	410	18	-481
422473199500	25	6			478	-	-	-	-	216.02	92.527	-140.46	-580.75	-1148.1
422473225400	25	7			442	-	-	-	-	42.598	-135.47	-439.46	-876.44	-1480.3
422470261000	25	8			418	-	-	-	273.02	-21.47	-309.57	-626.01	-1113.9	-1715.5
420473155200	25	9			329	-	-	-	54	-325.5	-731.98	-1136.8	-1693.4	-2240.3
420473206500	25	10			243	-	-	-	-	-	-1152.8	-1568.5	-2182.3	-2728.4
420470069400	25	11			239	-	-	-	-358.5	-865.6	-1353	-1799.4	-2451.2	-3113.2
420473001700	25	12			159	-	137.86	-	-533.3	-1071	-1625	-2174.1	-2836.1	-3472.5
420470124900	25	13	E	5	115	-	75	-59	-776	-1317	-1977	-2710	-3396	-4068
420470126700	25	14			67	40.12526	-43.88	-253.4	-1057	-1624	-2352	-3114.4	-3760.2	-4514.8
422610022300	25	15			25	-31.96005	-183.7	-575.3	-1590	-2313	-3168.5	-3896.9	-4532.6	-5486.2
422610021900	25	16			15	-125.9659	-335.7	-778	-1991	-2848	-3697.9	-4546.2	-5246.1	-6271.4
422610034000	25	17	F	3	10	-175	-362	-853	-2078	-3028	-	-	-	-
427013000100	25	18	G	6	0	-406	-890	-1510	-4038	-5389	-6629	-	-	-
422473148400	26	1												
422470152900	26	2			727	-	-	-	-	703	-	-	-	523
422473139400	26	3	D	5	553	-	-	-	-	451	-	-	279	-230
422470237100	26	4			430	-	-	-	-	300	220	57	-152	-687
422470245900	26	5			326	-	-	-	-	106	-75	-285	-630	-1194

TWDB Report ## Final – Hydrostratigraphy of the Gulf Coast Aquifer from the Brazos River to the Rio Grande

UWI/API	Dip		Strike		Stratigraphic Contacts (ft, msl)									
	Section/ Position	Position	Section/ Position	Position	Approx. Ground Level	Beaumont	Lissie	Willis	Upper Goliad	Lower Goliad	Upper Lagarto	Middle Lagarto	Lower Lagarto	Oakville
420473204100	26	6			247	-	-	-	68	-175	-553	-886	-1366	-1966
420473163400	26	7			286	-	-	-	-67	-316	-802	-1297	-1835	-2406
420473163900	26	8			170	-	-	-	-178	-515	-1049	-1671	-2262	-2835
420473066200	26	9	E	6	98	-	-	-	-437	-1005	-1606	-2253	-2928	-3808
422610024800	26	10			47	-	16	-20	-1055	-1776	-2435	-3056	-3753	-4698
422610025000	26	11			27	-	-175	-550	-1768	-2351	-3064	-3752	-4428	-5371
422610021000	26	12	F	4	20	-191	-429	-940	-2242	-3177	-3929	-4595	-5237	-6443
422610026400	26	13			9	-413	-666	-1233	-2607	-3635	-4512	-5179	-5876	-7472
422610029100	26	14			1	-506	-805	-1417	-2813	-3888	-4816	-5490	-6198	-8001
425050228800	27	1												
425050274200	27	2												
422470225800	27	3												
422473227500	27	4	D	7	507	-	-	-	-	449	-	-	63	-435
422470237600	27	5			432	-	-	-	-	295	121	-101	-536	-1121
422470249800	27	6			256	-	-	-	-	21	-314	-844	-1318	-1889
422150000200	27	7			207	-	-	-	-	-261	-770	-1326	-1883	-2534
422150005400	27	8			142	-	-	-	-116	-638	-1204	-1776	-2393	-3217
422150181400	27	9	E	8	88	-	-	-	-378	-1116	-1743	-2380	-3076	-4219
422613004700	27	10			47	-	-12	-	-1061	-1802	-2453	-3086	-3827	-4929
422610036100	27	11			24	-12	-155	-564	-1766	-2557	-3275	-3881	-4568	-5817
422610027200	27	12			20	-66	-226	-629	-1905	-2769	-3547	-4152	-4812	-5974
422610027800	27	13	F	5	17	-103	-284	-718	-1972	-2863	-3731	-4312	-4949	-6158
422610027700	27	14			25	-158	-323	-779	-2104	-3046	-3876	-4778	-6051	-7489
422610028900	27	15			20	-216	-415	-857	-2148	-3104	-3837	-4749	-6040	-7437
422610029400	27	16			0	-284	-498	-1022	-2410	-3468	-4152	-5293	-7030	-8494
427004000100	27	17												
425050297300	28	1												
424270185900	28	2												
424273084000	28	3												
424270165700	28	4	D	8	512	-	-	-	-	443	-	-	240	-26
424270103600	28	5			378	-	-	-	-	308	-	-109	-546	-1095
422150021800	28	6			182	-	-	-	-	145	-331	-829	-1289	-1948
422153142400	28	7			127	-	-	-	-	-51	-544	-1070	-1719	-2534
422150008100	28	8			85	-	-	-	-	-329	-877	-1490	-2173	-3011
422150010100	28	9	E	10	66	-	-	-	-220	-786	-1332	-1947	-2749	-3682
422150194900	28	10			52	-	-	-	-466	-1066	-1622	-2290	-3046	-4139
424893061000	28	11			47	-	-	-	-686	-1333	-1959	-2610	-3300	-4424

TWDB Report ## Final – Hydrostratigraphy of the Gulf Coast Aquifer from the Brazos River to the Rio Grande

UWI/API	Dip		Strike		Stratigraphic Contacts (ft, msl)									
	Section/ Position	Position	Section/ Position	Position	Approx. Ground Level	Beaumont	Lissie	Willis	Upper Goliad	Lower Goliad	Upper Lagarto	Middle Lagarto	Lower Lagarto	Oakville
424890049800	28	12			37	-	-22	-	-1247	-1920	-2737	-3355	-4106	-5218
424890046900	28	13			29	-	-184	-539	-1679	-2450	-3340	-4012	-4642	-5688
424890005900	28	14			20	-184	-567	-937	-2207	-3041	-3946	-4553	-5243	-6358
424890066100	28	15	F	7	15	-350	-911	-1354	-2680	-3671	-4555	-5211	-5836	-7375
424890008500	28	16			5	-537	-1133	-1711	-3208	-4203	-5053	-5881	-6682	-9024
424890064100	28	17	G	8	0	-809	-1447	-2077	-3811	-4970	-5970	-6949	-7994	-
427003006000	28	18												
424273128800	29	1												
424273165300	29	2												
424273178300	29	3	D	9	351	-	-	-	-	303	-	-	-	-174
424270471700	29	4			432	-	-	-	-	267	-	-	65	-397
422150067500	29	5			300	-	-	-	-	224	75	-248	-513	-1239
422150080200	29	6			284	-	-	-	-	130	-167	-625	-1107	-2082
422150073600	29	7			162	-	-	-	-	-223	-715	-1304	-1869	-2951
422153117400	29	8	E	11	89	-	-	-	-323	-948	-1606	-2355	-3089	-4204
422150109200	29	9			59	-	-	-	-843	-1561	-2343	-3107	-3736	-4936
424890054800	29	10			42	20	-49	-	-1393	-2236	-3026	-3817	-4440	-5732
424890053800	29	11			33	-119	-180	-617	-1773	-2601	-3502	-4307	-4949	-6188
424890063800	29	12			22	-355	-646	-1131	-2361	-3368	-4329	-4976	-5564	-6996
424890004900	29	13	F	8	19	-511	-959	-1455	-2804	-3882	-4838	-5479	-6047	-7587
420610001700	29	14			6	-774	-1474	-2010	-	-	-	-	-	-
420610002200	29	15			0	-1046	-1795	-2447	-	-	-	-	-	-
420610002900	29	16	G	9	1	-1157	-1957	-2629	-4889	-6052	-7198	-8315	-9481	-
427003001000	29	17	G	10	0	-1542	-2593	-3320	-	-	-	-	-	-
424273296400	30	1												
424273268600	30	2												
424273267200	30	3	D	11	228	-	-	-	-	180	-	-	-	-344
422153002800	30	4			128	-	-	-	-	-59	-166	-499	-842	-1429
422153105900	30	5			145	-	126	-	-27	-333	-508	-988	-1497	-2358
422150158100	30	6			149	103	-20	-182	-764	-1319	-1698	-2346	-2953	-4043
422150186000	30	7			119	-14	-171	-422	-1096	-1776	-2280	-2935	-3659	-4834
422153090100	30	8	E	14	80	-103	-303	-560	-1327	-2104	-2705	-3441	-4237	-5397
422150119900	30	9			77	-253	-538	-797	-1607	-2469	-3168	-4051	-4775	-6010
422150117000	30	10			71	-331	-674	-1024	-1879	-2832	-3557	-4479	-5209	-6462
422150116100	30	11			59	-422	-778	-1186	-2093	-3104	-3855	-4781	-5514	-6808
420610009700	30	12			50	-530	-937	-1377	-2477	-3541	-4341	-5225	-5929	-7184
NOAPI 974	30	13			40	-590	-1031	-1510	-2728	-3885	-4723	-5532	-6178	-7450

TWDB Report ## Final – Hydrostratigraphy of the Gulf Coast Aquifer from the Brazos River to the Rio Grande

UWI/API	Dip Section/ Position		Strike Section/ Position		Stratigraphic Contacts (ft, msl)									
					Approx. Ground Level	Beaumont	Lissie	Willis	Upper Goliad	Lower Goliad	Upper Lagarto	Middle Lagarto	Lower Lagarto	Oakville
420610009400	30	14			37	-642	-1056	-1588	-2851	-4108	-5021	-5695	-6284	-7655
420613001600	30	15	F	9	30	-658	-1091	-1644	-3049	-4311	-5268	-5974	-6541	-8307
420613046300	30	16			13	-686	-1171	-1789	-3340	-4767	-5763	-6534	-7158	-9230
420613004000	30	17			9	-712	-1214	-1892	-3532	-5073	-6162	-7011	-7721	-10090
420613050000	30	18			9	-810	-1335	-2048	-3878	-5653	-6820	-8223	-	-
420613046400	30	19			3	-992	-1601	-2430	-4639	-6544	-7781	-9474	-	-
426000000200	30	20	G	11	0	-1848	-2974	-3735	-6587	-8685	-10579	-12099	-13389	-
422470237200			D	6	456	-	-	-	-	439	-	-	375	-181
424273232200			D	10	270	-	-	-	-	264	-	-	215	-364
421750192800			D'	2	321	-	-	-	-	243	106	-328	-882	-1458
420253003100			D'	4	338	-	-	-	-	237	123	-340	-882	-1609
420250166500			D'	5	349	-	-	-	-	260	147	-271	-820	-1469
422970216900			D'	7	181	-	-	-	-	-	-43	-488	-1048	-1689
422973268100			D'	9	252	-	-	-	-	-	277	-111	-643	-1105
421313789500			D'	11	488	-	-	-	-	-	328	-3	-396	-912
421313772000			D'	12	692	-	-	-	-	563	357	60	-439	-882
421313398000			D'	14	642	-	-	-	-	-	380	49	-453	-1000
424733043100			D''	2	121	-	-48	-349	-391	-553	-1068	-1492	-2129	-2571
420153023100			D''	3	151	-	-	-	-	-532	-1012	-1436	-2014	-2535
NOAPI 18786			D''	5	192	-	-	-	-	-476	-894	-1235	-1791	-2271
NOAPI 18752			D''	7	190	-	129	-123	-205	-427	-817	-1186	-1701	-2240
420890057200			D''	9	210	-	173	-65	-160	-479	-812	-1239	-1745	-2346
422850030800			D''	11	194	-	-	-132	-199	-450	-769	-1283	-1750	-2313
422853146400			D''	12	192	-	-	4	-69	-336	-635	-1065	-1522	-1961
421233162200			D''	14	180	-	-	77	-31	-310	-734	-1206	-1631	-2132
421230082400			D''	16	266	-	-	-	-	74	-366	-821	-1279	-1870
421753159300			D''	18	252	-	-	-	-	245	-192	-727	-1171	-1764
421770028700			D''	19	261	-	-	-	-	-	-94	-622	-1080	-1646
421313586900			D ₂ D'	1,15	671	-	-	-	-	633	-	277	-145	-644
420473167100			E	3	98	-	-	-	-	-	-1959	-2488	-3115	-3802
422150007700			E	7	82	-	46	-136	-580	-1299	-1985	-2619	-3318	-4239
422150008300			E	9	70	-	-	-	-274	-842	-1534	-2144	-2998	-4021
422150102400			E	12	79	-	11	-	-318	-973	-1622	-2267	-3118	-4261
422150104100			E	13	77	58	-103	-171	-766	-1452	-2031	-2670	-3478	-4730
422150203900			E	15	73	-191	-481	-717	-1529	-2439	-3047	-3743	-4475	-5820
420253002700			E'	3	72	-	-88	-248	-1246	-1669	-2189	-2664	-3153	-3918
423553269800			E'	7	109	27	-223	-456	-1667	-2171	-2691	-3184	-3633	-4381

TWDB Report ## Final – Hydrostratigraphy of the Gulf Coast Aquifer from the Brazos River to the Rio Grande

UWI/API	Dip Section/ Position		Strike Section/ Position		Stratigraphic Contacts (ft, msl)									
					Approx. Ground Level	Beaumont	Lissie	Willis	Upper Goliad	Lower Goliad	Upper Lagarto	Middle Lagarto	Lower Lagarto	Oakville
422730050000			E'	9	110	-	-155	-358	-1429	-1960	-2656	-3187	-3739	-4401
421573151300			E"	1	67	-82	-420	-614	-1047	-1578	-2201	-2835	-3728	-4804
420390001500			E"	2	56	-53	-392	-642	-1007	-1573	-2225	-3018	-4036	-5324
421573191300			E"	4	75	-174	-426	-673	-1581	-2102	-2844	-3855	-4727	-5688
424813335000			E"	6	72	-161	-413	-683	-1571	-2068	-2659	-3406	-4461	-5572
424810280200			E"	9	74	-126	-378	-614	-1518	-1969	-2615	-3169	-4079	-5131
424810189100			E"	10	88	-139	-398	-640	-1490	-2009	-2504	-3085	-	-
422390081600			E"	12	50	-176	-448	-676	-1490	-1974	-2492	-3061	-3748	-4718
422390193600			E"	13	17	-185	-412	-639	-1508	-2029	-2504	-3057	-3688	-4655
NOAPI 992			E"	15	52	-88	-372	-658	-	-	-	-	-	-
423913025600			E"	18	87	-	-107	-305	-1207	-1654	-2245	-2824	-3448	-4313
422490282400			E,E'	1,10	132	-	-84	-260	-1139	-1687	-2390	-2867	-3484	-4063
424890006300			F	6	15	-213	-486	-940	-2079	-3055	-3881	-4482	-5134	-6334
420610012400			F	10	33	-731	-1153	-1703	-3178	-4562	-5609	-6298	-6898	-8734
420610012500			F	11	34	-757	-	-	-	-	-	-	-	-
424090395200			F'	2	21	-90	-248	-425	-1685	-2298	-2965	-3375	-3970	-4971
423550629100			F'	5	26	-220	-501	-697	-1949	-2550	-3185	-3650	-4291	-5239
420390448100			F''	1	6	-659	-1085	-1435	-2525	-3614	-4345	-5091	-6053	-7451
420390426500			F''	2	18	-699	-1109	-1407	-2494	-3627	-4413	-5154	-6223	-7605
420390446700			F''	3	20	-664	-1093	-1480	-2948	-4474	-5409	-6019	-7211	-8667
420390388800			F''	4	20	-629	-1049	-1458	-2503	-3526	-4255	-5043	-6154	-7857
420390406900			F''	6	27	-584	-1032	-1404	-2498	-3404	-4142	-5096	-6090	-7666
423210112000			F''	9	16	-515	-891	-1181	-2401	-3142	-3896	-4648	-5503	-7005
423210211900			F''	10	39	-422	-780	-1013	-2341	-3092	-3857	-4549	-5377	-6851
423210204300			F''	11	5	-401	-740	-980	-2316	-3027	-3860	-4578	-5438	-6804
423213099600			F''	12	10	-374	-733	-982	-2276	-2990	-3734	-4475	-5307	-6710
423210237100			F''	13	0	-353	-724	-970	-2241	-2961	-3720	-4360	-5134	-6634
420570087200			F''	15	0	-332	-674	-961	-2171	-3005	-3762	-4205	-5063	-6605
420573087600			F''	16	10	-301	-655	-951	-2216	-3013	-3795	-4242	-5032	-6608
420070000600			F''	18	15	-163	-431	-705	-2012	-2608	-3360	-3768	-4346	-5376
426013011700			G	4	0	-328	-737	-1206	-2931	-4060	-	-	-	-
427003000400			G	7	0	-739	-1370	-1990	-3762	-5040	-6161	-	-	-
423550657700			G'	5	4	-307	-676	-1130	-2774	-3464	-4152	-4924	-5629	-6573
422730056500			G'	6	0	-321	-691	-1128	-2939	-3650	-4358	-5119	-5788	-6749
422730177800			G'	8	1	-339	-760	-1218	-2918	-3848	-4769	-5554	-6181	-7221
422610006000			G'	10	0	-326	-771	-1209	-2835	-3690	-4613	-5374	-5951	-6934
426043002400			G''	3	0	-758	-1365	-1984	-3886	-4724	-5887	-7368	-9670	-

TWDB Report ## Final – Hydrostratigraphy of the Gulf Coast Aquifer from the Brazos River to the Rio Grande

UWI/API	Dip Section/ Position		Strike Section/ Position		Stratigraphic Contacts (ft, msl)									
					Approx. Ground Level	Beaumont	Lissie	Willis	Upper Goliad	Lower Goliad	Upper Lagarto	Middle Lagarto	Lower Lagarto	Oakville
426040000600			G"	5	0	-647	-1116	-1724	-3654	-4516	-5658	-7007	-	-
427043019500			G"	8	0	-579	-1001	-1577	-2821	-3781	-5178	-6375	-8569	-13193
427033020800			G"	9	0	-585	-952	-1577	-2876	-3844	-5203	-6536	-8879	-13151
427033031200			G"	11	0	-548	-915	-1503	-2861	-3773	-5092	-6386	-8775	-13222
427033023100			G"	12	0	-430	-787	-1437	-2789	-3749	-5075	-6445	-8488	-
420250047400					336	-	-	-	-	-	-	-	-	-226
420250160200					346	-	-	-	-	-	-	-	-	-1585.7
420253227800					232	-	-	-	-	-	-	-	-	-1956.1
420573090500					20	-	-	-	-	-	-	-	-	-5665.3
420610000900					25	-	-	-	-	-	-	-	-6544.8	-7866.4
420613039800					29	-	-	-	-	-	-	-	-6555.7	-7658.8
421233002000					354	-	-	-	-	-	-	-	-	-799.25
421313626300					475	-	-	-	-	-	-	-	-	-1352.5
421313695800					643	-	-	-	-	-	-	-	357.45	47.208
421753155300					212	-	-	-	-	-	-	-	-	-1913.8
422390191700					15	-	-375.4	-726.1	-	-	-	-	-	-
422390199200					36	-	-426.8	-824.2	-	-	-	-	-	-
422390318800					25	-	-478.3	-	-	-	-	-	-	-5308.7
422470020700					684	-	-	-	-	-	-	496.11	-118.52	-513.63
422470054800					677	-	-	-	-	-	-	-	-	475.26
422470221500					708	-	-	-	-	-	-	-	-	526.63
422490179100					182	-	-	-	-	-	-	-2225.8	-	-
422610009200					5	-	-	-	-	-	-	-	-	-6621.6
422610021700					10	-	-	-780	-	-	-	-	-	-
422730003600					140	-	-	-	-	-	-	-	-	-3785.6
422730054800					15	-	-	-	-	-	-	-	-	-5962.2
422730122000					37	-	-	-	-	-	-	-	-	-6050.8
422733229300					25	-	-	-	-	-	-	-	-	-6089.4
422850044600					101	-	62.041	-154.2	-	-	-	-	-	-
422973000200					222	-	-	-	-	-	-	-73.003	-	-1292
422973030100					267	-	-	-	-	-	-	-	-	-2331.7
422973251900					139	-	-	-	-	-	-	-655.77	-	-
422973360000					492	-	-	-	-	-	-	-	-	-473.15
422973382900					234	-	-	-	-	-	-	-	-	-219.09
423210008700					59	-	-	-	-	-	-	-	-	-5807.7
423210011600					60	-	-	-	-	-	-	-	-	-5428.1
423210107500					15	-447.4657	-881.4	-1142	-2173	-2964	-3745.2	-4429.8	-5230.2	-6753.7

TWDB Report ## Final – Hydrostratigraphy of the Gulf Coast Aquifer from the Brazos River to the Rio Grande

UWI/API	Dip Section/ Position		Strike Section/ Position		Stratigraphic Contacts (ft, msl)									
					Approx. Ground Level	Beaumont	Lissie	Willis	Upper Goliad	Lower Goliad	Upper Lagarto	Middle Lagarto	Lower Lagarto	Oakville
423210216200					72	-	-	-	-	-	-	-	-	-6838
423550611200					0	-	-	-	-	-	-	-	-	-5205.2
423910011000					41	-	-	-	-	-2279	-2843.6	-3273.2	-3899.2	-5007
423910198800					43	-	-	-	-	-	-	-	-	-
424093191400					63	-	-	-	-	-	-	-	-	-4571.8
424270050900					295	-	-	-	-	185.72	-	-322.36	-774.68	-1369.5
424273041200					379	-	-	-	-	134.16	-	-129.25	-456.07	-965.54
424273120400					325	-	-	-	-	290.96	-	-	-	200.73
424273230600					457	-	-	-	-	270.04	-	-	41.476	-412.17
424273272000					259	-	-	-	-	182.69	-	-	-33.862	-322.59
424273278100					254	-	-	-	-	188.7	-	-	68.398	-196.27
424273350800					324	-	-	-	-	-	-	-	-448.91	-1170.7
424690260000					37	-47.13529	-296.3	-473.4	-1574	-2236	-2925.3	-3311.5	-3808.9	-4750.9
424693342100					180	-	-	-	-	-	-	-	-	-2272.3
424693343100					151	-	-	-	-	-	-	-	-	-2352.7
424770027200					284	-	-	-	-	-	-	-422.41	-758.25	-1101.3
424890008300					0	-482.4413	-715.6	-1112	-2938	-4174	-4959.3	-5981.6	-7182.8	-8962.1

14 Appendix C Estimated total sand thickness (ft) at each geophysical log location

API	Dip Section	Dip Position	Strike Section	Strike Position	Beaumont	Lissie	Willis	Upper Goliad	Lower Goliad	Upper Lagarto	Middle Lagarto	Lower Lagarto	Oakville
424770023900	8	1			0	0	0	0	0	0	0	0	271
424773062500	8	2			0	0	0	0	0	0	0	0	0
424770029400	8	3			0	0	0	0	0	0	190	240	225
NOAPI_18624	8	4			0	0	0	0	0	137	193	216	199
420150023000	8	5			0	0	75	22	54	173	216	243	226
424730024300	8	6			0	0	68	55	87	214	211	262	229
424730031800	8	7	D"	1	0	214	63	65	69	202	245	325	317
421570000100	8	8			0	297	170	229	181	303	199	473	369
421570102600	8	9			55	206	214	246	268	232	201	426	339
421573198300	8	10			29	191	168	304	279	217	231	422	367
421570089400	8	11			86	281	169	457	243	354	261	341	562
421570245900	8	12	E"	3	123	282	165	534	312	353	238	297	458
420390145200	8	13			340	291	231	661	483	342	227	544	609
420390422400	8	14			327	305	256	570	483	457	234	715	841
420390427700	8	15			377	379	240	675	380	544	525	892	635
420390429100	8	16			497	342	262	793	416	633	769	998	777
427060002200	8	17	G"	1	530	421	205	721	490	683	1038	1548	13
420150001700	9	1			0	0	0	0	0	0	66	240	341
420153053900	9	2			0	0	0	0	0	132	143	233	344
420150066300	9	3			0	0	195	0	50	248	85	286	298
420150026200	9	4	D"	4	0	89	212	71	135	227	54	228	276
420150068300	9	5			29	135	282	237	205	230	161	331	303
420153073800	9	6			47	191	258	211	216	190	137	278	359
421573175200	9	7			107	219	231	217	273	183	134	218	340
421573180500	9	8			140	203	224	383	265	261	322	316	462
421570167400	9	9	E"	5	179	171	208	576	247	305	275	460	546
420390271500	9	10			214	127	265	475	269	305	254	556	672
420390286500	9	11			311	192	216	607	226	394	185	358	761
NOAPI_18912	9	12			280	219	229	529	461	500	171	354	873
420390389800	9	13	F"	5	332	299	269	432	242	517	231	514	943

TWDB Report ## Final – Hydrostratigraphy of the Gulf Coast Aquifer from the Brazos River to the Rio Grande

API	Dip Section	Dip Position	Strike Section	Strike Position	Beaumont	Lissie	Willis	Upper Goliad	Lower Goliad	Upper Lagarto	Middle Lagarto	Lower Lagarto	Oakville
420393035000	9	14			377	296	315	571	427	553	528	712	1297
420393211000	9	15			418	256	302	572	455	537	729	868	1488
420390481100	9	16	G"	2	443	373	270	991	494	643	1039	1538	14
427064036000	9	17			0	0	0	0	0	0	0	0	0
421493208800	10	1			0	0	0	0	0	0	0	0	0
421493132900	10	2			0	0	0	0	0	0	0	0	209
420893153100	10	3			0	0	0	0	0	305	101	175	123
420890005700	10	4			0	0	0	0	96	263	102	154	159
420890009000	10	5			0	0	267	0	164	273	201	209	328
420893124600	10	6	D"	6	0	78	177	94	204	320	193	380	255
NOAPI_18620	10	7			0	101	188	156	273	212	193	238	317
424810121800	10	8			0	126	180	93	251	171	137	416	403
424810120500	10	9			0	144	250	203	345	180	196	427	418
424813403300	10	10			37	166	209	444	311	254	161	407	501
424813344200	10	11			31	185	245	362	323	260	158	325	391
424813294400	10	12	E"	7	78	192	209	699	221	361	315	467	671
424810256200	10	13			152	179	210	627	226	248	180	397	643
NOAPI_18639	10	14			294	240	224	605	256	186	245	247	696
423210067000	10	15			327	259	177	468	345	391	334	237	960
NOAPI_18891	10	16	F"	7	464	319	209	748	256	377	611	570	1528
423210082400	10	17			467	319	252	705	333	728	734	170	648
427043007300	10	18	G"	4	464	343	233	897	413	662	663	867	15
427043000500	10	19			0	0	0	0	0	0	0	0	0
427040007100	10	20			0	0	0	0	0	0	0	0	0
427040007000	10	21			0	0	0	0	0	0	0	0	0
427044002600	10	22			0	0	0	0	0	0	0	0	0
421493204900	11	1			0	0	0	0	0	0	0	135	175
420893164500	11	2			0	0	0	0	0	0	70	183	159
420893145600	11	3			0	0	0	0	0	56	136	179	159
420893163900	11	4			0	0	65	0	0	153	144	234	197
420893173400	11	5			0	0	210	0	131	192	162	250	280
420893215800	11	6			0	108	168	100	163	212	165	223	334

TWDB Report ## Final – Hydrostratigraphy of the Gulf Coast Aquifer from the Brazos River to the Rio Grande

API	Dip Section	Dip Position	Strike Section	Strike Position	Beaumont	Lissie	Willis	Upper Goliad	Lower Goliad	Upper Lagarto	Middle Lagarto	Lower Lagarto	Oakville
420893059200	11	7	D"	8	0	73	165	41	221	156	228	226	271
420890075900	11	8			0	153	157	171	212	160	136	324	315
424813369000	11	9			0	238	153	339	252	207	339	341	423
420893198100	11	10			0	177	83	271	167	190	297	352	360
424813336100	11	11			58	197	159	416	319	223	383	332	448
424813147700	11	12			68	175	146	361	277	221	296	315	389
424810357500	11	13	E"	8	64	130	194	534	276	236	304	350	499
NOAPI_18827	11	14			73	190	157	442	307	243	253	372	417
NOAPI_18844	11	15			166	208	146	554	378	19	142	372	331
423210268900	11	16			260	253	182	593	384	228	146	339	477
423210114700	11	17	F"	8	317	281	217	609	426	347	188	384	567
423210253900	11	18			363	258	205	513	512	582	510	644	733
426040001200	11	19			353	232	191	497	463	950	660	890	1145
427040000700	11	20	G"	6	352	216	189	538	427	929	822	1074	1204
421490032700	12	1			0	0	0	0	0	0	0	0	0
421493262000	12	2			0	0	0	0	0	0	103	225	49
NOAPI_18602	12	3			0	0	0	0	0	127	256	173	140
422853272900	12	4			0	0	0	113	64	185	148	130	124
422853117200	12	5			0	0	171	80	135	152	163	143	180
422850032600	12	6	D"	10	0	0	197	73	159	118	138	152	230
420893160400	12	7			0	89	182	171	283	209	186	208	360
NOAPI_18743	12	8			51	111	220	280	249	198	236	204	458
424810169500	12	9			24	186	190	322	309	257	234	269	469
424810177000	12	10	E"	11	158	146	150	380	251	227	256	391	370
422393247200	12	11			194	207	179	518	248	199	283	348	342
423210217100	12	12			220	224	149	525	410	233	279	244	424
423210229500	12	13			219	196	147	376	283	365	408	439	598
423210267200	12	14			223	193	145	491	355	402	328	459	551
423213171600	12	15			298	247	189	644	346	435	296	527	631
423210251400	12	16			242	211	108	537	420	607	409	644	1586
426043004100	12	17			288	239	122	488	481	747	720	1037	1776
427043021000	12	18	G"	7	321	249	174	437	522	1032	826	1283	1960

TWDB Report ## Final – Hydrostratigraphy of the Gulf Coast Aquifer from the Brazos River to the Rio Grande

API	Dip Section	Dip Position	Strike Section	Strike Position	Beaumont	Lissie	Willis	Upper Goliad	Lower Goliad	Upper Lagarto	Middle Lagarto	Lower Lagarto	Oakville
427044023000	12	19			0	0	0	0	0	0	0	0	0
427044030000	12	20			0	0	0	0	0	0	0	0	0
422853026800	13	1			0	0	0	0	0	0	0	0	194
422850035800	13	2			0	0	0	0	54	181	139	167	190
422850050900	13	3	D"	13	0	0	0	118	161	242	137	201	221
422853176200	13	4			0	48	121	225	240	167	246	246	236
424693243200	13	5			0	158	102	299	190	67	156	232	224
422390004700	13	6			38	140	127	376	300	129	178	109	175
422390155600	13	7			84	209	135	421	171	93	88	52	395
422390192100	13	8	E"	14	149	143	203	594	231	236	174	172	482
422390337800	13	9			156	207	195	562	219	221	79	229	274
422390319800	13	10			157	173	120	555	395	189	103	129	216
420570085200	13	11	F"	14	160	225	206	602	554	208	145	183	472
420573090300	13	12			303	240	111	577	610	400	89	589	373
NOAPI_18788	13	13			255	154	226	533	457	506	562	464	414
427033000600	13	14	G"	10	288	199	293	482	511	897	1034	1366	1795
421770042400	14	1			0	0	0	0	0	0	0	0	0
421230087000	14	2			0	0	0	0	0	0	0	207	284
421230029000	14	3			0	0	0	0	0	272	181	220	214
421233187900	14	4	D"	15	0	0	0	0	266	220	137	159	237
424693155300	14	5			0	0	0	282	237	338	234	177	360
424690093400	14	6			0	16	29	568	228	250	203	175	377
NOAPI_993	14	7			26	85	130	523	203	181	153	181	459
424690162400	14	8			55	157	169	452	229	149	116	191	495
NOAPI_990	14	9	E"	16	69	156	179	535	267	176	105	237	511
424693189700	14	10			40	174	202	763	264	184	33	298	452
420570132300	14	11			53	280	188	813	327	277	105	351	530
420570122100	14	12			152	224	138	563	695	385	320	765	695
427033031900	14	13	G"	13	226	236	305	555	641	670	646	1174	979
427034001000	14	14			0	0	0	0	0	0	0	0	0
422550023600	15	1			0	0	0	0	0	0	0	0	0
421230033700	15	2			0	0	0	0	0	0	0	0	126

TWDB Report ## Final – Hydrostratigraphy of the Gulf Coast Aquifer from the Brazos River to the Rio Grande

API	Dip Section	Dip Position	Strike Section	Strike Position	Beaumont	Lissie	Willis	Upper Goliad	Lower Goliad	Upper Lagarto	Middle Lagarto	Lower Lagarto	Oakville
421230036200	15	3			0	0	0	0	0	0	352	222	241
421750043400	15	4	D"	17	0	0	0	0	0	406	251	304	215
421753010500	15	5			0	0	0	143	153	233	244	292	146
421753166400	15	6			0	16	0	302	185	232	222	275	217
421753171900	15	7			0	64	58	363	182	273	219	279	310
424690143800	15	8			0	100	108	490	216	219	218	304	442
423910002300	15	9	E"	17	80	72	135	620	180	220	332	331	461
423913146600	15	10			53	151	139	611	151	255	256	331	524
423910008600	15	11	F"	17	167	180	186	718	138	206	220	385	586
420570118500	15	12			189	148	193	760	500	269	123	382	500
427034014000	15	13	G"	14	0	0	0	0	0	0	0	0	0
424930153600	16	1			0	0	0	0	0	0	0	0	0
422550063400	16	2			0	0	0	0	0	0	0	0	0
422553024600	16	3			0	0	0	0	0	0	0	0	247
422553134600	16	4			0	0	0	0	0	0	221	221	198
421750145600	16	5	D'	1	0	0	0	0	0	189	298	296	163
421753335000	16	6			0	0	0	0	121	453	259	230	164
421753263600	16	7			0	0	0	0	527	245	263	192	171
421753216500	16	8			0	0	0	562	173	177	257	182	383
421753194500	16	9	E',E"	1,19	0	44	23	777	230	288	288	209	700
423913211800	16	10			0	88	135	881	148	254	224	212	561
423913158800	16	11			35	112	141	786	113	196	221	261	542
420070035400	16	12			113	117	139	752	204	266	196	246	585
420073066000	16	13			182	198	176	229	494	465	79	198	1020
427030000200	16	14	G',G"	1,15	264	204	147	509	651	364	487	410	1674
424930174700	17	1			0	0	0	0	0	0	0	0	0
422970001100	17	2			0	0	0	0	0	0	0	0	0
420253155700	17	3			0	0	0	0	0	0	0	0	496
420250030500	17	4			0	0	0	0	0	0	0	467	239
420253149300	17	5	D'	3	0	0	0	0	0	139	283	330	175
420253258400	17	6			0	0	0	119	220	258	197	192	161
420253048700	17	7			0	36	0	452	227	188	243	193	318

TWDB Report ## Final – Hydrostratigraphy of the Gulf Coast Aquifer from the Brazos River to the Rio Grande

API	Dip Section	Dip Position	Strike Section	Strike Position	Beaumont	Lissie	Willis	Upper Goliad	Lower Goliad	Upper Lagarto	Middle Lagarto	Lower Lagarto	Oakville
420250243000	17	8	E'	2	0	100	87	658	280	205	329	105	621
423913207400	17	9			0	132	113	733	217	298	46	202	228
423910365900	17	10			43	125	128	705	51	103	169	246	603
423910372200	17	11	F',F''	1,19	80	140	65	816	167	69	109	291	594
420070033100	17	12			142	244	146	791	223	176	125	227	670
420070454000	17	13			238	209	97	771	478	229	184	286	745
427033021500	17	14	G'	2	252	118	4	647	699	257	672	309	965
422970004300	18	1			0	0	0	0	0	0	0	0	0
422970082400	18	2			0	0	0	0	0	0	0	0	0
422970138700	18	3			0	0	0	0	0	0	0	0	454
422973327600	18	4	D'	6	0	0	0	0	113	0	418	337	292
420253181600	18	5			0	0	0	357	194	224	179	315	218
420253191200	18	6			0	35	0	463	144	199	213	175	200
420250202600	18	7			0	79	42	579	95	148	213	188	289
424090034400	18	8	E'	4	19	107	138	775	142	153	246	128	476
424093225200	18	9			0	139	192	689	184	173	313	97	968
424093243800	18	10			22	134	223	591	188	210	246	207	635
424090256200	18	11			36	165	190	701	186	198	235	199	503
424093228400	18	12	F'	3	125	214	165	773	287	133	118	257	749
420073080400	18	13			174	205	88	586	462	167	162	275	764
427023023300	18	14	G'	3	249	131	44	700	617	268	612	300	723
423110117300	19	1			0	0	0	0	0	0	0	0	0
422973265600	19	2			0	0	0	0	0	0	0	0	114
422973033000	19	3			0	0	0	0	0	0	0	136	165
422970260400	19	4	D'	8	0	0	0	0	0	0	237	365	142
422973354100	19	5			0	0	0	0	216	171	267	410	277
422973351100	19	6			0	0	0	468	155	166	179	324	193
422493198500	19	7			0	0	0	593	154	240	215	267	230
424093171600	19	8			12	43	60	670	161	279	236	74	309
424093188300	19	9	E'	5	53	122	166	692	207	279	228	184	556
423553024900	19	10			91	128	137	608	187	155	214	218	583
423553127000	19	11			126	170	178	718	232	124	237	246	532

TWDB Report ## Final – Hydrostratigraphy of the Gulf Coast Aquifer from the Brazos River to the Rio Grande

API	Dip Section	Dip Position	Strike Section	Strike Position	Beaumont	Lissie	Willis	Upper Goliad	Lower Goliad	Upper Lagarto	Middle Lagarto	Lower Lagarto	Oakville
423550612200	19	12	F'	4	152	296	278	1170	205	71	109	296	767
426020004000	19	13	G'	4	264	267	172	858	360	160	307	323	709
427020000300	19	14			281	313	123	783	449	302	345	315	800
427024001200	19	15			0	0	0	0	0	0	0	0	0
423110183400	20	1			0	0	0	0	0	0	0	0	0
423113177900	20	2			0	0	0	0	0	0	0	0	0
423113137300	20	3			0	0	0	0	0	0	0	0	28
421313825400	20	4	D'	10	0	0	0	0	113	0	231	334	212
421310107500	20	5			0	0	0	139	119	197	153	151	181
422493172400	20	6			0	0	0	575	217	199	41	72	248
422493019900	20	7			0	42	55	518	261	185	135	126	252
422493145000	20	8			0	73	57	486	284	232	73	59	299
423553085900	20	9			13	96	91	548	159	219	202	132	339
423550033900	20	10			25	135	149	797	180	259	66	39	388
423553266600	20	11	E'	6	40	202	159	821	117	276	107	269	516
423550099200	20	12			88	176	162	861	227	281	115	336	515
423553130800	20	13			100	144	200	656	184	118	209	236	566
423550318200	20	14	F'	6	215	117	110	432	326	44	104	297	567
423553170400	20	15			225	207	170	727	425	50	133	272	546
427020001500	20	16			253	236	198	713	590	397	262	356	920
421310545000	21	1			0	0	0	0	0	0	0	0	0
421310350100	21	2			0	0	0	0	0	0	0	0	232
421313760200	21	3			0	0	0	99	170	196	154	180	224
422493205300	21	4			0	0	0	507	161	228	167	188	225
422493192300	21	5			0	75	42	542	122	215	236	233	197
422730000300	21	6			25	74	134	522	158	273	187	260	194
422730031600	21	7	E'	8	7	78	155	550	131	258	193	114	279
423550408200	21	8			57	205	168	765	10	339	203	376	612
422730053700	21	9			66	184	173	943	153	226	222	240	523
422730054200	21	10	F'	7	103	19	106	1011	36	183	189	193	411
422730200100	21	11	G'	7	206	72	60	1267	440	274	258	365	513
426020006500	21	12			224	70	142	1304	534	270	260	341	496

TWDB Report ## Final – Hydrostratigraphy of the Gulf Coast Aquifer from the Brazos River to the Rio Grande

API	Dip Section	Dip Position	Strike Section	Strike Position	Beaumont	Lissie	Willis	Upper Goliad	Lower Goliad	Upper Lagarto	Middle Lagarto	Lower Lagarto	Oakville
427024026400	21	13			0	146	281	0	0	0	1643	342	694
424790108500	22	1			0	0	0	0	0	0	0	0	0
421313619300	22	2			0	0	0	0	0	0	0	0	165
421313519700	22	3	D'	13	0	0	0	0	0	0	0	196	262
421310782600	22	4			0	0	0	0	331	74	128	66	216
421313726100	22	5			0	0	0	393	331	176	140	93	247
421313234100	22	6			0	0	0	557	159	233	189	143	256
422493086800	22	7			0	18	45	635	42	230	239	234	240
422733233600	22	8			9	13	113	566	137	183	226	370	344
422730108500	22	9			21	58	192	714	193	312	275	368	415
422730088100	22	10			63	113	92	876	326	214	227	353	564
422730088300	22	11	F'	8	320	229	161	938	508	276	200	472	622
426010000200	22	12	G,G'	1,9	298	41	231	1028	394	197	177	390	618
424793381200	23	1			0	0	0	0	0	0	0	0	0
424793451300	23	2			0	0	0	0	0	0	0	0	139
421311018900	23	3	D	2	0	0	0	0	0	0	0	362	305
421310996700	23	4			0	0	0	0	234	58	140	162	254
422473177300	23	5			0	0	0	236	165	251	236	149	273
421313634000	23	6			0	0	0	460	161	266	206	128	230
421310980400	23	7			0	0	0	526	182	326	228	145	272
422490337500	23	8			0	0	0	559	174	165	200	264	265
422490351400	23	9	E	2	0	1	48	578	137	190	242	380	291
422730124200	23	10			5	0	45	789	134	266	226	390	451
422610014200	23	11			0	20	162	965	239	282	146	506	543
422610035300	23	12			26	93	175	975	328	368	261	243	569
422610010000	23	13	F,F'	1,9	80	161	170	709	289	288	147	434	561
422610018700	23	14	G	2	140	177	210	826	517	374	280	302	616
427010000200	23	15	G	3	150	230	282	1150	621	577	295	385	678
424793526800	24	1			0	0	0	0	0	0	0	0	0
424793868300	24	2			0	0	0	0	0	0	0	0	186
422470014000	24	3			0	0	0	0	0	0	0	97	170
422470035400	24	4	D	3	0	0	0	0	0	0	114	156	206

TWDB Report ## Final – Hydrostratigraphy of the Gulf Coast Aquifer from the Brazos River to the Rio Grande

API	Dip Section	Dip Position	Strike Section	Strike Position	Beaumont	Lissie	Willis	Upper Goliad	Lower Goliad	Upper Lagarto	Middle Lagarto	Lower Lagarto	Oakville
422473156500	24	5			0	0	0	0	107	113	204	124	249
422470031300	24	6			0	0	0	0	228	331	155	226	272
420470043500	24	7			0	0	0	315	125	301	297	189	293
420470011700	24	8			0	0	0	368	212	240	152	443	305
420470023000	24	9	E	4	0	1	23	641	218	256	173	441	304
422610016800	24	10			30	11	172	769	317	341	328	345	469
422610017800	24	11			25	20	197	881	371	292	230	497	506
422610037300	24	12			55	41	203	863	419	351	293	414	615
422613017400	24	13	F	2	115	117	329	874	493	338	295	395	656
422613112700	24	14			112	161	295	785	619	362	274	313	700
422610020100	24	15			112	167	297	861	895	621	268	359	768
427010000100	24	16	G	5	120	272	244	1028	939	721	273	417	829
427013003300	24	17			127	282	253	1087	936	753	378	406	827
427014003000	24	18			0	0	0	0	0	0	0	0	0
425053098400	25	1			0	0	0	0	0	0	0	0	0
422473194000	25	2			0	0	0	0	0	0	0	0	0
422473169500	25	3			0	0	0	0	0	0	0	0	193
422473187800	25	4			0	0	0	0	0	0	0	249	278
422473174900	25	5	D	4	0	0	0	0	0	0	66	215	200
422473199500	25	6			0	0	0	0	0	0	273	260	239
422473225400	25	7			0	0	0	0	232	161	143	299	282
422470261000	25	8			0	0	0	0	363	122	137	340	292
420473155200	25	9			0	0	0	202	284	252	243	274	295
420473206500	25	10			0	0	0	276	246	295	219	276	323
420470069400	25	11			0	0	0	321	305	242	238	333	362
420473001700	25	12			0	2	16	416	271	276	256	293	377
420470124900	25	13	E	5	0	5	0	689	250	359	410	400	298
420470126700	25	14			0	28	136	625	334	253	473	346	304
422610022300	25	15			26	46	257	785	345	501	414	352	497
422610021900	25	16			86	66	333	914	437	402	379	455	624
422610034000	25	17	F	3	130	81	334	852	503	369	318	479	703
427013000100	25	18	G	6	128	333	311	1268	906	721	23	506	805

TWDB Report ## Final – Hydrostratigraphy of the Gulf Coast Aquifer from the Brazos River to the Rio Grande

API	Dip Section	Dip Position	Strike Section	Strike Position	Beaumont	Lissie	Willis	Upper Goliad	Lower Goliad	Upper Lagarto	Middle Lagarto	Lower Lagarto	Oakville
422473148400	26	1			0	0	0	0	0	0	0	0	0
422470152900	26	2			0	0	0	0	0	0	0	0	0
422473139400	26	3	D	5	0	0	0	0	0	0	0	0	305
422470237100	26	4			0	0	0	0	0	0	209	112	218
422470245900	26	5			0	0	0	0	183	175	102	162	320
420473204100	26	6			0	0	0	148	148	238	166	196	365
420473163400	26	7			0	0	0	179	226	221	256	355	271
420473163900	26	8			0	0	0	373	245	299	347	324	368
420473066200	26	9	E	6	0	0	0	376	400	310	334	481	294
422610024800	26	10			0	11	24	972	578	380	312	412	271
422610025000	26	11			40	33	275	926	266	481	378	371	431
422610021000	26	12	F	4	119	63	462	1023	447	406	301	378	762
422610026400	26	13			193	159	379	1141	500	506	264	295	927
422610029100	26	14			126	72	357	590	542	511	313	352	1009
425050228800	27	1			0	0	0	0	0	0	0	0	0
425050274200	27	2			0	0	0	0	0	0	0	0	0
422470225800	27	3			0	0	0	0	0	0	0	0	0
422473227500	27	4	D	7	0	0	0	0	0	0	0	255	229
422470237600	27	5			0	0	0	0	0	0	309	334	237
422470249800	27	6			0	0	0	0	164	270	311	240	281
422150000200	27	7			0	0	0	0	314	334	389	311	372
422150005400	27	8			0	0	0	298	328	361	309	350	543
422150181400	27	9	E	8	0	37	0	238	575	451	300	308	571
422613004700	27	10			0	9	14	705	584	418	316	391	454
422610036100	27	11			22	23	270	945	549	445	337	360	653
422610027200	27	12			37	2	165	845	525	446	218	384	389
422610027800	27	13	F	5	59	68	259	892	494	503	279	365	619
422610027700	27	14			98	155	236	917	506	495	598	707	796
422610028900	27	15			121	134	210	806	424	419	575	686	795
422610029400	27	16			129	74	43	764	148	434	860	869	807
427004000100	27	17			0	0	0	0	0	0	0	0	0
425050297300	28	1			0	0	0	0	0	0	0	0	0

TWDB Report ## Final – Hydrostratigraphy of the Gulf Coast Aquifer from the Brazos River to the Rio Grande

API	Dip Section	Dip Position	Strike Section	Strike Position	Beaumont	Lissie	Willis	Upper Goliad	Lower Goliad	Upper Lagarto	Middle Lagarto	Lower Lagarto	Oakville
424270185900	28	2			0	0	0	0	0	0	0	0	0
424273084000	28	3			0	0	0	0	0	0	0	0	0
424270165700	28	4	D	8	0	0	0	0	0	0	0	0	253
424270103600	28	5			0	0	0	0	0	0	199	300	357
422150021800	28	6			0	0	0	0	46	256	239	263	331
422153142400	28	7			0	0	0	0	150	232	215	364	376
422150008100	28	8			0	0	0	94	173	300	264	418	396
422150010100	28	9	E	10	0	0	0	154	457	471	413	473	529
422150194900	28	10			0	0	0	308	467	436	424	370	590
424893061000	28	11			0	0	0	514	491	445	352	342	564
424890049800	28	12			0	20	47	776	464	428	328	385	538
424890046900	28	13			48	32	132	755	487	481	261	339	451
424890005900	28	14			86	226	205	818	434	490	247	338	486
424890066100	28	15	F	7	168	369	272	844	409	507	268	322	689
424890008500	28	16			187	241	359	906	368	517	359	368	1124
424890064100	28	17	G	8	271	39	250	725	364	345	463	416	647
427003006000	28	18			430	315	66	0	0	0	3503	511	13
424273128800	29	1			0	0	0	0	0	0	0	0	0
424273165300	29	2			0	0	0	0	0	0	0	0	0
424273178300	29	3	D	9	0	0	0	0	0	0	0	69	286
424270471700	29	4			0	0	0	0	0	0	131	113	248
422150067500	29	5			0	0	0	0	0	140	190	101	313
422150080200	29	6			0	0	0	0	142	196	234	226	381
422150073600	29	7			0	0	0	57	201	296	302	302	411
422153117400	29	8	E	11	0	0	0	272	440	429	309	430	520
422150109200	29	9			0	0	0	591	474	518	389	313	574
424890054800	29	10			14	26	125	672	527	490	356	300	600
424890053800	29	11			61	16	138	585	519	545	227	346	529
424890063800	29	12			177	187	255	735	628	497	224	294	578
424890004900	29	13	F	8	252	286	315	757	658	394	181	173	658
420610001700	29	14			349	467	420	882	469	589	338	216	763
420610002200	29	15			560	347	177	1479	362	490	502	387	235

TWDB Report ## Final – Hydrostratigraphy of the Gulf Coast Aquifer from the Brazos River to the Rio Grande

API	Dip Section	Dip Position	Strike Section	Strike Position	Beaumont	Lissie	Willis	Upper Goliad	Lower Goliad	Upper Lagarto	Middle Lagarto	Lower Lagarto	Oakville
420610002900	29	16	G	9	601	425	18	1314	243	374	526	434	94
427003001000	29	17	G	10	777	403	58	780	622	535	767	486	12
424273296400	30	1			0	0	0	0	0	0	0	0	0
424273268600	30	2			0	0	0	0	0	0	0	0	173
424273267200	30	3	D	11	0	0	0	0	0	0	0	127	161
422153002800	30	4			0	0	0	0	0	160	124	169	328
422153105900	30	5			0	33	0	73	233	121	206	218	456
422150158100	30	6			25	76	104	348	175	90	126	282	508
422150186000	30	7			61	114	131	410	296	242	212	392	569
422153090100	30	8	E	14	99	131	105	215	413	315	293	442	579
422150119900	30	9			127	226	150	624	459	430	418	420	583
422150117000	30	10			320	252	163	584	552	481	368	382	544
422150116100	30	11			329	319	242	744	523	468	349	366	544
420610009700	30	12			452	298	245	608	559	367	430	305	551
NOAPI 974	30	13			413	283	284	691	680	447	383	262	545
420610009400	30	14			458	269	343	698	660	505	290	229	591
420613001600	30	15	F	9	417	248	376	676	647	426	264	198	752
420613046300	30	16			380	296	309	647	530	582	298	196	910
420613004000	30	17			423	290	356	879	595	679	352	250	1049
420613050000	30	18			460	234	239	1046	861	599	627	404	240
420613046400	30	19			570	178	141	1194	857	617	745	704	12
426000000200	30	20	G	11	1005	143	2	1238	891	799	846	460	12
422470237200			D	6	0	0	0	0	0	0	133	16	168
424273232200			D	10	0	0	0	0	0	0	0	39	288
421750192800			D'	2	0	0	0	0	0	151	199	245	158
420253003100			D'	4	0	0	0	0	107	85	206	232	174
420250166500			D'	5	0	0	0	0	90	0	353	260	202
422970216900			D'	7	0	0	0	0	150	47	108	364	151
422973268100			D'	9	0	0	0	0	0	0	132	375	43
421313789500			D'	11	0	0	0	0	0	0	0	0	627
421313772000			D'	12	0	0	0	0	0	0	0	296	240
421313398000			D'	14	0	0	0	0	122	0	123	115	247

TWDB Report ## Final – Hydrostratigraphy of the Gulf Coast Aquifer from the Brazos River to the Rio Grande

API	Dip Section	Dip Position	Strike Section	Strike Position	Beaumont	Lissie	Willis	Upper Goliad	Lower Goliad	Upper Lagarto	Middle Lagarto	Lower Lagarto	Oakville
424733043100			D"	2	0	166	134	28	127	253	275	237	307
420153023100			D"	3	0	125	186	52	105	232	139	247	295
NOAPI_18786			D"	5	255	154	226	533	457	506	562	464	414
NOAPI_18752			D"	7	0	44	176	58	166	205	166	241	283
420890057200			D"	9	0	31	224	57	208	153	209	204	277
422850030800			D"	11	0	0	243	64	130	202	210	80	124
422853146400			D"	12	0	0	122	74	173	135	149	147	177
421233162200			D"	14	0	50	25	111	218	231	176	127	230
421230082400			D"	16	0	0	0	0	0	326	103	218	282
421753159300			D"	18	0	0	0	0	0	383	348	390	182
421770028700			D"	19	0	0	0	0	0	0	596	314	185
421313586900			D,D'	1,15	0	0	0	0	27	0	0	161	251
420473167100			E	3	0	0	20	624	180	204	168	385	322
422150007700			E	7	0	14	0	393	507	392	348	383	414
422150008300			E	9	0	0	0	186	338	385	358	462	498
422150102400			E	12	0	47	0	231	418	410	273	489	517
422150104100			E	13	0	126	29	359	457	400	294	491	585
422150203900			E	15	190	228	152	0	0	0	1552	397	635
420253002700			E'	3	0	115	93	728	171	193	240	141	448
423553269800			E'	7	26	132	165	608	198	239	150	143	309
422730050000			E'	9	13	39	144	574	126	300	300	148	288
421573151300			E''	1	100	209	147	328	370	460	140	384	273
420390001500			E''	2	0	0	0	0	0	0	0	0	0
421573191300			E''	4	177	142	203	740	229	344	355	448	506
424813335000			E''	6	180	198	155	458	266	250	314	475	572
424810280200			E''	9	92	168	190	636	331	266	199	442	538
424810189100			E''	10	159	177	166	543	220	212	252	407	350
422390081600			E''	12	165	211	168	535	201	170	225	237	458
422390193600			E''	13	152	173	169	580	231	212	182	210	443
NOAPI_992			E''	15	106	169	230	477	305	206	94	154	547
423913025600			E''	18	0	120	112	698	224	272	246	387	490
422490282400			E,E'	1,10	13	10	130	548	96	224	210	292	255

TWDB Report ## Final – Hydrostratigraphy of the Gulf Coast Aquifer from the Brazos River to the Rio Grande

API	Dip Section	Dip Position	Strike Section	Strike Position	Beaumont	Lissie	Willis	Upper Goliad	Lower Goliad	Upper Lagarto	Middle Lagarto	Lower Lagarto	Oakville
424890006300			F	6	83	94	194	575	479	480	284	401	623
420610012400			F	10	444	276	417	761	388	746	297	214	797
420610012500			F	11	566	394	469	1085	598	631	388	299	625
424090395200			F'	2	72	155	99	790	210	189	120	285	606
423550629100			F'	5	155	171	138	687	212	104	165	265	549
420390448100			F''	1	0	0	0	0	0	0	0	0	0
420390426500			F''	2	352	249	223	461	661	442	303	700	642
420390446700			F''	3	441	294	262	895	467	559	172	879	852
420390388800			F''	4	342	303	344	595	373	483	215	651	1036
420390406900			F''	6	392	251	258	603	364	543	407	617	1161
423210112000			F''	9	359	320	262	655	415	377	267	447	711
423210211900			F''	10	278	246	143	677	328	299	159	345	579
423210204300			F''	11	198	187	148	660	294	460	248	386	598
423213099600			F''	12	185	178	46	570	319	379	261	424	657
423210237100			F''	13	181	220	114	568	380	394	138	324	636
420570087200			F''	15	194	176	144	569	465	259	92	357	586
420573087600			F''	16	210	238	181	483	421	491	188	305	643
420070000600			F''	18	118	141	100	787	178	282	183	233	569
426013011700			G	4	137	262	118	874	655	672	292	369	696
427003000400			G	7	255	195	114	184	681	153	577	583	441
423550657700			G'	5	227	243	234	968	373	19	223	327	475
422730056500			G'	6	227	235	178	950	494	156	190	262	465
422730177800			G'	8	184	11	24	1143	485	263	368	397	504
422610006000			G'	10	174	146	176	1033	405	286	230	340	497
426043002400			G''	3	426	380	240	1061	409	585	707	1420	16
426040000600			G''	5	344	243	286	696	353	889	580	327	840
427043019500			G''	8	336	225	291	429	502	1145	853	1567	2359
427033020800			G''	9	0	0	0	0	0	0	0	0	0
427033031200			G''	11	0	0	0	0	0	0	0	0	0
427033023100			G''	12	261	207	348	501	505	856	962	1398	1302
420250047400					0	0	0	0	0	0	0	0	233
420250160200					0	0	0	0	93	75	226	246	174

TWDB Report ## Final – Hydrostratigraphy of the Gulf Coast Aquifer from the Brazos River to the Rio Grande

API	Dip Section	Dip Position	Strike Section	Strike Position	Beaumont	Lissie	Willis	Upper Goliad	Lower Goliad	Upper Lagarto	Middle Lagarto	Lower Lagarto	Oakville
420253227800					0	0	0	173	225	159	139	241	82
420573090500					124	209	160	724	243	142	24	173	578
420610000900					269	229	288	734	699	438	246	400	556
420613039800					412	257	315	739	740	460	299	321	485
421233002000					0	0	0	0	0	0	0	219	422
421313626300					0	0	0	0	240	0	236	258	94
421313695800					0	0	0	0	0	0	0	0	300
421753155300					0	0	0	0	104	407	192	247	128
422390191700					141	125	214	491	189	236	188	209	450
422390199200					174	130	250	479	245	235	181	221	409
422390318800					152	183	261	557	397	191	73	163	244
422470020700					0	0	0	0	0	0	0	326	241
422470054800					0	0	0	0	0	0	0	0	132
422470221500					0	0	0	0	0	0	0	0	0
422490179100					0	108	40	339	176	211	220	372	193
422610009200					127	179	216	784	472	346	252	331	528
422610021700					84	104	359	725	512	348	309	498	697
422730003600					22	25	93	621	108	235	266	157	197
422730054800					199	108	100	498	295	85	153	290	479
422730122000					7	34	181	772	228	290	268	394	831
422733229300					10	71	149	794	300	252	272	362	912
422850044600					0	32	137	159	229	151	229	260	227
422973000200					0	0	0	0	0	0	0	261	702
422973030100					0	0	0	0	214	247	157	363	390
422973251900					0	0	0	279	172	195	2	603	151
422973360000					0	0	0	0	0	0	0	98	463
422973382900					0	0	0	0	0	0	0	0	163
423210008700					218	201	174	565	332	196	149	320	333
423210011600					241	211	191	660	336	220	113	365	384
423210107500					349	246	157	555	298	467	269	639	986
423210216200					347	222	173	510	324	545	252	516	528
423550611200					86	205	209	838	292	128	242	267	505

TWDB Report ## Final – Hydrostratigraphy of the Gulf Coast Aquifer from the Brazos River to the Rio Grande

API	Dip Section	Dip Position	Strike Section	Strike Position	Beaumont	Lissie	Willis	Upper Goliad	Lower Goliad	Upper Lagarto	Middle Lagarto	Lower Lagarto	Oakville
423910011000					98	213	173	726	166	237	98	345	538
423910198800					68	60	131	803	159	208	189	211	555
424093191400					65	113	159	506	195	248	183	201	478
424270050900					0	0	0	0	0	245	210	284	306
424273041200					0	0	0	0	0	91	228	226	261
424273120400					0	0	0	0	0	0	0	0	73
424273230600					0	0	0	0	0	0	163	132	182
424273272000					0	0	0	0	0	0	0	121	159
424273278100					0	0	0	0	0	0	0	0	155
424273350800					0	0	0	0	0	0	155	222	382
424690260000					63	167	134	793	327	281	27	216	424
424693342100					0	0	0	412	241	324	291	204	116
424693343100					0	52	0	419	195	227	175	202	83
424770027200					0	0	0	0	0	0	0	553	244
424890008300					92	87	224	1151	385	548	481	562	948

15 Appendix D TWDB comments on draft hydrostratigraphy report and responses

We have completed our review of the submitted report entitled “Hydrostratigraphy of the Gulf Coast Aquifer from the Brazos River to the Rio Grande” prepared by Young and others (2009). We present our comments in two sections: “General comments” presents the overall review comments for the report and “Specific comments” discusses these comments in much greater detail.

15.1 General comments

The authors have generally done a good job in developing the hydrogeologic framework of the Gulf Coast Aquifer extending from the Brazos River in the north to the Rio Grande in the south. This hydrogeological framework information presented for 10 geologic units extending from the Chicot to the Jasper aquifers was developed using both chronostratigraphic and lithostratigraphic information using about 900 geophysical logs. The concept of using both chronostratigraphy and lithostratigraphy in developing the hydrogeologic framework is laudable. Although the information provided on tops and bottoms of the different geologic units, sand percentages, depositional facies, and fresh water content are very useful, they need to be cleaned-up to make it consistent with the published information and ensure consistencies between the different datasets provided.

The draft report contains several inconsistencies with regard to thickness information and subcrop outline for the different geologic units. For example, outline of the Catahoula subcrop should coincide with the western extent of the Jasper Aquifer (SWAP data) and/or top of the Jackson Aquifer in areas but the presented outline and structure/framework data provided do not match. This outline needs to be further clarified and appropriately addressed. Many of the subcrop areas also cross-cut each other, which they should not, if these formations were deposited during different time periods. Also, the aquifers arbitrarily thicken in the outcrop areas compared to sections in the shallow down-dip areas which need to be clarified further. Many of the thickness maps show part of the areas that abruptly thicken or thin that appears geologically inconsistent and need to be examined. A thorough editorial review of the report is also warranted to address issues with references to figures, typos, and explanation of terms (for example, paleotopographic/depositional features) introduced in the different sections.

15.1.1 Response to specific questions contained in the general comments

Comment: The draft report contains several inconsistencies with regard to thickness information and subcrop outline for the different geologic units. For example, outline of the Catahoula subcrop should coincide with the western extent of the Jasper Aquifer (SWAP data) and/or top of the Jackson Aquifer in areas but the presented outline and structure/framework data provided do not match. This outline needs to be further clarified and appropriately addressed.

Response: As we discussed in a meeting with TWDB on December 15, 2009, there are no inconsistencies in the subcrop outlines despite the appearance of inconsistencies in some of our figures. In our dataset, the Catahoula outcrop coincides with top of the Jackson

Aquifer and a portion of the Catahoula outcrop (as defined by the SWAP data) is part of the Jasper Aquifer. To improve the clarity of the discussion regarding the subcrop outlines, Section 7 has been revised to provide a better explanation of the Catahoula outcrop and Figure 7-22 has been revised to show the western extent of the Jasper Aquifer defined by the SWAP data.

Comment: Many of the subcrop areas also cross-cut each other, which they should not, if these formations were deposited during different time periods.

Response: As we discussed in a meeting with TWDB on December 15, 2009, the subcrop areas will cross-cut outcrop areas. To clarify this point, we have added Figure 7-21 and have defined the term “outcrop” and “subcrop” in the report.

Comment: Also, the aquifers arbitrarily thicken in the outcrop areas compared to sections in the shallow downdip areas which need to be clarified further. Many of the thickness maps show part of the areas that abruptly thicken or thin that appears geologically inconsistent and need to be examined.

Response: The large changes in thicknesses near the outcrop of the Oakville and the Lagarto formations are attributed to relatively steep dips of these two formations, the relatively large land surface elevation changes near the outcrop of these two formations, and the relatively small-sized length intervals used to plot thickness changes near the outcrop. We have added several sentences in Section 7.2 to discuss these issues. In reviewing our geological surfaces, we discovered and corrected a problem with our surfaces in the up-dip portion of dip section 12.

Comment: A thorough editorial review of the report is also warranted to address issues with references to figures, typos, and explanation of terms (for example, paleotopographic/depositional features) introduced in the different sections.

Response: We have reviewed the report, corrected several inappropriate references to figures, added definitions to a few key geologic terms, and simplified the geological discussion where appropriate.

15.2 Specific Comments

1. Base of Oakville Formation lies below the base of Catahoula Formation in the south-east corner and the east corner of the aquifer. Given that the Oakville Formation lies above the Catahoula Formation stratigraphically, this alteration to the stratigraphic sequence needs to be addressed.

Response: In the draft report, the Oakville Formation was accidentally truncated near its southeast and eastern boundaries. This truncation led to the cited alteration in the stratigraphic sequence. We have corrected the truncation problem and fixed the stratigraphic sequence.

2. The Oakville_Thickness raster has one cell with a 6,623 feet value which is inconsistent with the difference between the bases of Lower Lagarto and Oakville. Please revise all Oakville thickness raster surfaces.

Response: The problem with the one cell with a 6,623 feet value has been corrected. In addition, all Oakville surfaces and thicknesses have been appropriately modified. As we discussed in our December 15, 2009 meeting, this problem was caused by using slightly different boundaries to crop the different formations at the Rio Grande.

3. Please provide the DEM used to calculate thicknesses in the outcrop areas and specify the source of the DEM. In many cases, the transition to outcrop in thickness surfaces indicates a thickening of the formations while the cross-sections indicate otherwise.

Response: We have added the DEM in the geodatabase

4. The MiddleLagarto_Thickness raster is inconsistent with the difference between the bases of upper Lagarto and middle Lagarto. Please revise all middle Lagarto thickness raster surfaces.

Response: We have revised all middle Lagarto thickness raster surfaces. This inconsistency was caused by the problem identified in comment # 2 with cropping the formation surfaces at the Rio Grande.

5. The LowerGoliad_Thickness raster is inconsistent with the difference between the bases of Upper Goliad and Lower Goliad. Please revise all Lower Goliad thickness raster surfaces.

Response: We have revised all lower Goliad thickness raster surfaces. This inconsistency was caused by the problem identified in comment # 2 with cropping the formation surfaces at the Rio Grande.

6. The Willis_Thickness raster is inconsistent with the difference between the bases of Lissie and Willis. Please revise all Willis thickness raster surfaces.

Response: We have revised all Willis thickness raster surfaces. This inconsistency was caused by the problem identified in comment # 2 with cropping the different formation surfaces at the Rio Grande.

7. We could not verify the Beaumont_Thickness raster because the top surface raster (DEM?) is missing from the deliverables.

Response: The DEM has been included in the geodatabase per comment #3.

8. Please explain abrupt thickening and thinning of the aquifers. For example, see thin areas in the northwestern and central parts of the Oakville Formation (Figure 7-2). Also note missing section along the coast in the northwest along Brazoria and Matagorda Counties.

Response: The missing section of the Oakville Formation has been addressed in our response to comment #1. The thickening and thinning of the aquifers primarily occurs with the Oakville and Lagarto Formations near outcrops. The large relative changes in the aquifer thickness occur because of the steep dips associated with these two formations and the greatest changes in land surface elevations occurs across the outcrops of these two formations. Several sentences were added to Section 7.2 to explain why relatively large changes in the formation thicknesses occur near the outcrop of the Oakville and Lagarto Formations.

9. Please label all cross-sections with east-west and appropriately label the section line. Currently, they are labeled as “...*near* dip section X...” in the captions and not on the figures.

Response: “East” and “west” labels were added to the cross-sections. Also the caption “near dip section X” was added to the figures.

10. Please rephrase the following sentence in paragraph 1, page 30: “This major Pliocene extrabasinal river for deltaic and continental margin progradation offshore from Houston.”

Response: We have rephrased the sentence.

11. Please update Section 4.0 to include sections discussing the Oakville and Lagarto.

Response: We have expanded Section 4.0 to include the Oakville and Lagarto.

12. Section 7.1, second paragraph, page 57: Please correct spelling of Pliestocene to Pleistocene.

Response: We have corrected the spelling of Pleistocene.

13. Section 7.2, first paragraph, page 58: Please correct reference citing Namlin, 2006 to Hamlin, 2006 or update Reference Section with this reference.

Response: We have updated the reference to Hamlin, 2006.

14. Section 7.2, fourth and fifth paragraph, page 58: Text references counties and features such as Luncker fault zone and salt domes on Figure 7.2. However Figure 7.2 does not identify counties or these features. Please update figure with county names and/or label features for consistency with text and figure.

Response: We have removed the reference to Figure 7.2. Figure 7.2 and several other figures have been updated to include county names.

15. Figure 7.1: Please correct spelling of Burkville to Burkeville and Catahoul to Catahoula.

Response: We have corrected the spelling of Burkeville and Catahoula in Figure 7-1.

16. Figure 7.5: Please include county, Karnes?, in upper x axis.

Response: We have added Karnes in the upper X axis.

17. Figure 7-21: Please schedule a meeting to discuss overlap, zero thickness, and implementation of the correlation of subcrop to outcrop. Need to discuss Upper Catahoula and how that correlates to Gulf Coast Aquifer boundaries.

Response: On December 15, 2009, we met with the TWDB to explain the correlation of subcrop and outcrop and how the Upper Catahoula correlates to the Gulf Coast Aquifer boundaries. As a result of this meeting, we have modified Figure 7-22, added Figure 7-21, and provided additional explanatory text in Section 7.0.

18. Table 8-2, Page 85, Definition column for FD: Please correct spelling of lagonnal to lagoonal.

Response: Table 8-2 has been changed per the comment.

19. Section 9.1.1, page 91: Please correct spelling of Aransas County from Arnasas.

Response: The suggested change was made.

20. The geodatabase is missing the core deliverables of this project. Please add top and/or bottom raster surfaces to the geodatabase for every formation and aquifer unit.

Response: The bottom raster surfaces were added to the geodatabase.

21. Well_Stratigraphy_Only has no usable data for many attributes. Please revise this feature class.

Response: We have revised the feature class so there are no attributes with no useable data.

22. Geologic_Unit_Thickness feature dataset is empty. Please provide feature classes if applicable, or remove it from the geodatabase.

Response: We have revised the feature class so there are no attributes with no useable data.

23. Lissie_Sand_Thickness has negative values. Please revise the top and bottom surfaces used to derive the sand thickness. Consequently revise the Lissie_Sand_Thickness and Lissie_Percent_Sand surfaces.

Response: The negative values near the Rio Grande are a result of the inconsistent cropping of different formations, which has been discussed in our response to comment #2. We have corrected the problem and have revised the surfaces and sand thicknesses appropriately.

24. Willis_Sand_Thickness has negative values. Please revise the top and bottom surfaces used to derive the sand thickness. Consequently revise the Willis_Sand_Thickness and Willis_Percent_Sand surfaces.

Response: The negative values occur near the Rio Grande are a result of the inconsistent cropping of different formations, which has been discussed in our response to comment #2. We have corrected the problem and have revised the surfaces and sand thicknesses appropriately.

25. Contours from Middle_Lagarto_Base_Elevation_Contours do not match contours in Figure 7-12. Please revise.

Response: The wrong surfaces were plotted in Figure 7-12. We have corrected the problem.

26. According to the August 24, 2009 meeting, URS agreed to provide TDS concentration lines for 1000, 3000, and >3000 mg/L for each aquifer. Please provide the actual water quality data that was used to generate water quality maps in the report.

Response: The actual water quality data used to categorize groundwater TDS concentrations as 1000, 3000, and >3000 mg/L for each aquifer is provided in the geodatabase.

27. All raster datasets do not cover the southern tip of the state in Cameron County. Please revise.

Response: The raster datasets have been revised to cover the southern tip of Cameron County.

28. Metadata for the geodatabase is largely incomplete. Metadata needs to contain information regarding the source of the data and how it was processed to obtain the final product. Simply copying a title statement three times does not qualify it as metadata.

Response: The metadata has been revised and contains information regarding the source of the data and how it was processed to obtain the final product.

29. Please provide a rationale for including Figure 10-1. This figure has not been referred to or discussed in the text.

Response: Figure 10-1 is referenced in the text in Section 10.1. The sentence is “Figure 10-1 illustrates how the relationships between concentration and specific conductivity can vary among different salts and is concentration dependent.”

30. Please rework Table 10-2. We assume that the authors are presenting data on relationships between specific conductivity and total dissolved solids. As is, the table is difficult to follow. Some discussions on how the data in the table was derived will be helpful.

Response: Table 10-2 has been simplified and additional explanation has been added to the report to address the comment.

31. Please ensure that all shapefiles used in generating figures in the report (for example, water quality concentrations, bottom and tops of the aquifers and confining units, thickness, sand percentages) are included in the updated geodatabase.

Response: We have included the shapefiles to generate the figures in the geodatabase.